Attributes of the [4Fe4S] Cofactor Coordinated by UvrC, a DNA Repair Enzyme

Thesis by
Rebekah Miriam Brawer Silva

In Partial Fulfillment of the Requirements for the
Degree of
Doctor of Philosophy

CALIFORNIA INSTITUTE OF TECHNOLOGY
Pasadena, California

2020
Defended May 19, 2020

Rebekah Miriam Brawer Silva
ORCID: 0000-0002-9144-4939

To my family,
who were my first teachers

"The first principle is that you must not fool yourself—and you are the easiest person to fool. So you have to be very careful about that. After you've not fooled yourself, it's easy not to fool other scientists. You just have to be honest in a conventional way after that...I'm talking about a specific, extra type of integrity that is not lying, but bending over backwards to show how you're maybe wrong, that you ought to do when acting as a scientist. And this is our responsibility as scientists, certainly to other scientists, and I think to laymen."

Richard Phillips Feynman
Commencement Address
California Institute of Technology
June 14, 1974

ACKNOWLEDGEMENTS

As I reflect on graduate school, I often meditate on how important so many mentors, colleagues, friends, and family have been to me. Just how significant the human factor in science is the biggest surprise, as scientists are often depicted as solitary creatures experimenting alone in a lab. This depiction does not reflect the reality of the experience of an experimentalist, and I am glad science can be such a collaborative and enriching endeavor. I have benefitted from so many who have provided encouragement, teaching, brainstorming, questioning, critiquing, and time during my days at Caltech. I cannot possibly detail comprehensively how many people were a part of enabling me to complete my doctoral studies. I am particularly grateful for everything I have learned in graduate school, and included here is my best attempt to describe the ways in which I have learned through the people around me as I have completed my doctoral degree.

I have learned the most from my advisor, Professor Jacqueline Barton, primarily how to be a fearless and creative scientist. I came to Caltech knowing that I wanted to study proteins with metal centers, but truthfully, inorganic chemistry was not my strongest subject in college. Going into the field of bioinorganic chemistry scared me a little, but I am so grateful I took that leap. In the Barton group, I have had the opportunity to study a very fascinating enzyme, and I am so proud of everything we have accomplished while studying UvrC. At all phases of the UvrC project, I had to find a way to "push back the frontiers" by being daring and imaginative, and I could not have learned or accomplished everything I did without Jackie's guidance. I am also grateful that Jackie involves her students in project design, grant writing, and review writing. She also gives her trainees many opportunities to present their research, on campus and at conferences. Jackie supported me when I went to the Steenbock Symposium in 2018 at UW Madison, and she nominated me to present at Seminar Day in 2019. I had a fabulous time presenting at both seminars, and preparing for them had a much larger influence on me than I could have ever predicted. I have learned so much from Jackie through participating on these writing projects, and I know I will use her writing insights in the future. I will take everything I have learned from Jackie about science, project design, writing, and academia with me wherever I go!

I am also most appreciative for my thesis committee - Professors Harry Gray, Dianne Newman, and Douglas Rees. I could not ask for a better committee chair

than Harry, who has been so supportive of my teaching and research. I am forever grateful that Harry champions both endeavors. He has provided so much guidance on oxygen-sensitive proteins, spectroscopy, teaching Ch101, and navigating graduate school. I have also benefitted and learned from great conversations with Doug about metalloproteins, protein expression, and life as a scientist. I especially appreciate that he opened up his lab so that I could pursue anaerobic purification of UvrC using Rees group equipment. Dianne has been a wonderful resource during graduate school, and I greatly appreciate her guidance while I pivoted my project toward exclusively anaerobic methods. With Dianne's influence, I love bacteria even more now. Her enthusiasm is contagious, and she has built a wonderful, interdisciplinary community at Caltech for those who love microbes. My committee truly has been the Dream Team!

My time in graduate school would not have been the same without the incredible administrative assistants in the Barton lab. Elizabeth Garcia has been with the group since 2017, and she has made the lab so much fun! She is the master of efficiency, and I have learned so much about streamlining work from her. We have also had so much fun talking about her adorable nephew, her majestic cat, life, music, and the newest, fun snacks that we find. Elizabeth even mailed me fun snacks while I was writing my thesis during the quarantine, and they were such an encouragement while I typed my tome. I am also appreciative of Elizabeth's predecessors, Elisha Okawa and Maureen Renta, and all the hard work that they put into the group.

In the Barton group, I have had wonderful opportunities to work along side fantastic young scientists who have been part of my development as a scientist, mentor, and teacher. I have learned so much from every person with whom I have overlapped. My current labmates are Dr. Adela Nano, Dr. Miguel Pinto, Dr. Md Kausar Raza, and (soon to be Dr.!) Stephanie Threatt. The group is so warm and friendly, and I appreciate the insights they have shared on research, careers, and academia. I especially enjoy when they teach me new techniques in lab and when I can reciprocate. The group has been especially collaborative as we have cleaned out lab space, and I am thankful for their strong committment to laboratory safety.

Numerous former labmates had major influences on me during graduate school. My first collaborators were Dr. Michael Grodick and Dr. Andy Zhou. Mike began the UvrC project with me, and he taught me everything he knew about protein purification, spectroscopy, electrochemistry, data analysis, and navigating graduate school while we were building the foundations of the UvrC project. Dr. Andy Zhou studied UvrC and the nucleotide excision repair pathway *in vivo*, and I appreciate

his insights on connections between my *in vitro* data and his *in vivo* data. Andy's perspective on synthetic biology and the future of the biological sciences were also a source of inspiration for me. I also had a opportunity to work with Siobhán MacArdle when she joined the group. We studied Topoisomerase 1 together, and training her for the first six months she was in the group was a highlight of graduate school. During long purification days working in the cold room and waiting for protein to elute, we found time to treat ourselves with boba, frozen yogurt, and other fun snacks. Those long days were incredibly rewarding, and I am so glad for our time working together! I was the mentor for two undergraduate students, Jianing (Jenny) He and Sirus Han. I think perhaps Jenny and Sirus taught me more than I could teach them, and their seemingly never-ending curiosity and enthusiasm was infectious. Jenny is in medical school and Sirus is in graduate school, and I hope I was able to contribute to them accomplishing their goals.

Other members of Subgroup 2 (the protein people!) include Dr. Theodore Zwang, Professor Edmund Tse, Dr. Phillip Bartels, Professor Natalie Muren, Dr. Elizabeth O'Brien, Dr. Anna Arnold, and Dr. Helen Segal. Ted, Ed, and Phil were particularly important in teaching me new techniques and providing expert guidance during the challenging period when I was realizing that UvrC was sensitive under aerobic conditions. Natalie and Liz were excellent writing partners, and I should be so fortunate to work with such good writers in the future. Natalie was our fearless leader while we wrote the NIH grant, and Liz co-wrote two long reviews with me. Liz also motivated me to learn how to use Illustrator!

Many other labmates also contributed profoundly to my experience in graduate school. Dr. Kelsey Boyle continues to be a positive force in my life, and I feel like have known her forever. We became friends quickly at the beginning of graduate school, and she has been a cherished source of support and feedback, both in research and in teaching. I am so glad that we crossed paths, and I'm sure we will again in Minnesota! Dr. Kathryn Schaefer was also such a wonderful labmate, a great teacher in the lab, and I appreciate our continuing friendship. Dr. Adam Boynton was another great labmate who never had an unkind word to say. I still enjoy talking with him about sports, food, and traveling. I have also been fortunate to overlap with many postdoctoral scholars who have joined the group and have contributed what I call "postdoc magic." I could fill an entire memoir with all that I have learned from them. These postdocs include Dr. Lionel Marcélis, Dr. Levi Ekanger, Dr. Yingxin Deng, Dr. Sandra König, Dr. Nirit Kantor-Uriel, and Dr. Aoshu Zhong.

Former colleagues also include Professor Alexis Komor, Professor Ariel Furst, and Dr. Alyson Weidmann, and it is exciting to see their careers unfold. Visiting colleagues included Professor Michael Hill, Professor Eric Stemp, Professor Eylon Yavin, Professor Frank Crespilho, Professor Pernilla Wittung-Stafshede, and Viktoria Urland. I have benefited from discussions about careers at PUIs with Mike Hill. I similarly benefited from conversations with Eylon about science and from a seminar by Pernilla about being a woman in science. Frank contributed expertise in graphite electrochemistry to the group, and many of us have utilized the methods he developed with Phil. I have also overlapped with other undergraduate students, in and outside of the Barton group, and I enjoyed being a resource for them outside of their research projects. These undergraduates include Sebastian Bedoya, Andy Dorfeuille, Stephanie Gu, Qixuan (Alice) Jin, and Brenda Wu as well as Divya Kolli, Michelle Le, Maryann Morales, and Elizabeth Park.

Outside of the Barton group, I have been fortunate to work with many great scientists at Caltech. The Rees group has been a fantastic resource for me and a huge influence on my work. My project could not have progressed without them. Ailiena Maggiolo has been particularly generous with her time, and she is an awesome teacher in the lab. She is such a talented scientist, and I look forward to hearing about everything she accomplishes in graduate school! Dr. Renee Arias, Dr. Belinda Wenke, Dr. Trixia Buscagen, and Dr. Rebeccah Warmack have also been welcoming and helpful while I have used equipment in the Rees Group. I have additionally benefitted from the insights of and discussions with members of the Newman group, especially Professor Megan Bergkessel, Dr. Scott Saunders, and Dr. Nathan Glaser. Megan had plenty of postdoc magic while at Caltech, and I look forward to seeing her accomplishments as a professor. I have also enjoyed seeing Maiko Obana from the Tirrell group in lab, and I have enjoyed my conversations with her about science, people, safety, and music.

My project also greatly benefitted from the expertise of scientists who oversee core facilities. Dr. Paul Oyala oversees the EPR Facility, and he has not only assisted me in acquiring data, but has helped me understand much more about the spectra I collected. He has vast knowledge about EPR and EPR of metalloproteins, and my lab has been so grateful for his wide-ranging expertise. Dr. Mona Shahgholi oversees the Multi User Mass Spectrometry Laboratory, and she has always been so helpful to me. I greatly enjoy our conversations about data, DNA, and careers in science. Dr. Bruce Brunschwig oversees the Molecular Materials Research Center, and I had the opportunity to work with him while I have been the Graduate

Laboratory Assistant for the Asylum MFP-3D Bio AFM instrument. I appreciate his careful management of the instruments in the the MMRC and his great sense of humor. Dr. Korhan Sahin has been a GLA on the instrument with me, and I appreciate his tireless work to maintain and update the instrument. I have constantly used the instruments in the Center for Molecular Medicine, and I appreciate everything the new director, Professor Mikhail Shapiro, and the new manager, Dina Malounda, have done to update the center and help instrument caretakers fulfill our duties. The scientists who oversee safety operations on campus have taught me so much about how to carry out experiments safely and efficiently, and they have been a huge support for me, especially while I have been safety officer. I always enjoy conversations with Dr. Haick Issaian; he has great stories about his time in graduate school generating his own radionuclides that always make me laugh. Dr. André Jefferson has also been a helpful resource about radiation safety. As safety officer, I have had a chance to work with Dr. Nathan Siladke and Mark Gatchalian and his safety team. They have all been wonderful, and I appreciate how their careful work creates a safe environment for experimentalists.

Prior to Ch101, I was a teaching assistant during my first year for Dr. Jeffrey Mendez. I enjoyed my role as a "demo TA", and appreciated the opportunity to be creative in designing demonstrations for students during lectures. I was fortunate to meet many wonderful young teachers who became dear friends. The first quarter of my first year, I met Dr. Tonia Ahmed. She was so professional with students and had superior content mastery. I even went to her NMR office hours! I remember the day I decided that she was likely a great person because of she was such a great teaching assistant. I was (of course!) correct, and she has become a significant person in my life. We shared an apartment for four years, and some of my best days of graduate school were spent with her. We cooked together, watched movies, imagined the day we would own pets, and still talk all the time. During the second and third terms of my first year, I had so much fun teaching with Dr. Antoinette Blom, Dr. Kelsey Boyle, and Dr. Sarah Del Ciello. We were a great team! I remember the night that I texted Kelsey furiously as I panicked at the thought of being unable to perform the data analysis my students were expected to complete. The issue turned out to be a typo, but I will never forget how Kelsey's very calm demeanor helped ease us toward identifying the issue (not me!). I also appreciate the undergraduate TAs who also served with us; I worked directly with Rebekah Kitto, Katja Luxem, and Katherine Fisher. I was a TA during my second year for Professor Nathan Lewis. Dr. Bryan Hunter (Gray group alum!) was the head TA for the course, and he is

really wise beyond his years about both teaching and science. Another Gray group alum, Dr. Morgan Cable, has also been so kind to me, and she has given me great insights on life in the sciences.

Advancing through graduate school would have not been possible without the wonderful administrative support in the CCE Division. While she worked in the Division, Agnes Tong was such a huge resource for graduate students in her role as a Graduate Option Program Manager for Chemistry. She was so kind to me on my visit weekend, and her kindness has continued throughout graduate school. We miss her in the CCE Division, but I know she is doing great work at the Caltech Y. I enjoy visiting Agnes in her office at The Y, catching up with her, and getting meals with her. Alison Ross is the current Graduate Option Program Manager for Chemistry, and she has been a huge support especially during my final year as a graduate student. I really enjoy our conversations and her encouragement whenever I see her. Agnes, Alison, and three other administrators in the Division, Silva Virgil, Amy Woodall-Ojeda, and Anne Penney, were all particularly supportive of Ch101 and helped with many aspects of this teaching project. Agnes guided Kelsey and me on the course approval process, Silva manages the Ch101 website, and Alison, Amy, and Anne all assisted with Division-wide announcements.

None of us in the Division could do our experiments without those who manage Division procurement, the CCE stockroom, grants, and other areas that help facilitate research. Joseph Drew, Armando Villasenor, and Gregory Rolette operate the stockroom, and I always enjoy visiting and chatting with them. I call Joe "The Sheriff" of the Division, and he is always of great assistance for graduate students and postdocs when we need equipment repaired and attention from Facilities. Steven Gould and Elisa Brink were always more than helpful when I had issues with various vendors, and I enjoyed stopping by their office and talking to them. I have uniquely had the opportunity to work with two grant managers, Rosine Sarafian and Raquel Rodriguez. Rosine helped me so much when I submitted an NIH fellowship, and Raquel was a wealth of helpful information during the first year I was an instrument caretaker for the Center for Molecular Medicine (formerly the Center for the Chemistry of Cellular Signaling). Other administrators in the Division have been so helpful, including Patricia Anderson, Margarita Davis, Kristy Nguyen, and Phoebe Ray. I always enjoy talking to Margarita and Pat whenever I can, and I appreciate the help from Kristy and Phoebe in scheduling meetings with Dianne and Doug. I am grateful for assistance from Verrinia Amatulli-Kelly, Rebecca Fox, and Richard Jackson as well. Through Elizabeth, the Barton group has also gotten to know Penny

Neder-Muro, who works in Caltech Archives. Our group lunches have been so much fun! I have enjoyed working alongside the custodial staff at Caltech, particularly Jose, Juan, Ralph, and Sergio, who are always so friendly and take pride in their work.

In addition to research, I highly value effective teaching, and I could not imagine my time at Caltech without the Center for Teaching, Learning, and Outreach (CTLO). Dr. Cassandra Horii leads an amazing team at the CTLO, and I am grateful for all the opportunities and support they provide for me and my colleagues. I had an amazing time at the 2017 POD Conference in Montréal. What an adventure! I am especially grateful for the mentorship of Dr. Jennifer Weaver. Everyone needs a Jenn in their lives during graduate school, and she has made graduate school so much more enjoyable and meaningful. Jenn and the CTLO guided me, Kelsey, and Olivia Wilkins as we served as student leaders of the Caltech Project for Effective Teaching. My experience as a co-director planning seminars, leading journal club discussions, and advising peers about their teaching projects were invaluable experiences, and I could not have asked for better co-directors than Kelsey and Olivia. They have both taught me so much about effective teaching. Additional members of the CTLO team have included Leslie Rico, Mitch Aiken, Dr. Kathryn Cahalan, Ellie Race-Moore, Tina Zelaya, Holly Ferguson, Dr. Melissa Dabiri, Daniel Thomas, Daniel Martin, Harrison Parker, Julius Su, and James Maloney. Leslie spoils me so much whenever I visit the CTLO, and Mitch, Kitty, and Ellie are always so warm and friendly. I will miss the CTLO so much!

While in my third year of graduate school, Kelsey and I decided to take on a passion project and create a new class in the CCE Division for graduate students and postdocs who wanted to design and lead their own elective courses. This type of course is not unprecedented at Caltech, however, the structure and oversight Kelsey and I built into the Ch101 program is novel. We had so much support from the founding faculty mentors, Professors Harry Gray, Mitchio Okurmura, Brian Stoltz, David Tirrell. Harry was an incredible cheerleader, and Mitchio worked with Kelsey and me on course approval and structure. Brian and Dave provided important insights on the structure of the program as well. Dave additionally served as the faculty mentor for the course I co-taught with Kelsey, and Brian, along with Professor Dennis Dougherty, continues to be a huge advocate for Ch101. After Kelsey graduated, Olivia partnered with me in co-facilitating the program, and once again, I could not have had better colleagues and friends to work alongside. I am also appreciative for the other graduate students and postdocs who have participated

in the program, particularly Professor Allegra Liberman-Martin and Dr. Samuel Ho.

Well beyond the realms of research and teaching, I have received extended support from all corners of campus. Dr. Felicia Hunt was so helpful during a particularly challenging period, and she was part of the network of support that saw me through that time. The team at the Caltech library has always been so supportive, and I very much appreciate the extra support from Dr. Donna Wrublewski and Dr. Katherine Johnson during thesis writing. The Caltech Y directed by Dr. Athena Castro is another wonderful resource for the Caltech community, and their community service program at the Union Station Adult Center organized by Liz Jackman has provided much-needed perspective in the midst of research. The Registrar's office is yet another place on campus where I have received support. Teresita Legaspi and Gloria Brewster are always delightful, and I enjoy visiting, chatting, and eating candy they leave out for students. I received emergency assistance twice during graduate school from The Caltech Store the first time my hard drive failed and from the CCE Division the second time my hard drive failed. Roy Estrada (the Caltech Store) and Suresha Guptha (CCE Division) are lifesavers! I have a great relationship with healthcare providers at The Caltech Health Clinic and in the Caltech network. I have seen Alice Sogomonian, Dr. Ken Randomski, Grace Ho, and my allergist Dr. Kevin Farnam, and they have helped me recover from various health challenges that have arisen during graduate school. When my insurance changes, I will miss them greatly. Dr. Norman Lavin (Lyme specialist) and Dr. Roger Katz (allergist) are two other doctors who have helped me through major medical issues, and I would not be functioning today without them.

The amount of help I have had during graduate school has been matched by the number of friendships I have made. During my first year, I met several people who became important to me during graduate school - Dr. Catriona Blunt, Dr. Samuel Ho, and Dr. Jessica Sampson. I appreciate Catie's direct feedback on my NSF fellowship application, and for great meals and conversations with Sam and Jess on science, academia, and life. I am fortunate I had many opportunities to meet graduate students and postdoctoral scholars outside of the CCE Division. I have enjoyed learning how different Divisions organize their academic programs and approach their research. I have met most of my friends outside of CCE through the Graduate Christian Fellowship, Missio Community Church, and the Caltech Christian Fellowship, and I never imagined I would be surrounded by so many brothers, sisters, and complete saints during graduate school. These communities are constant sources

of encouragement for me, and they have stood beside me through all the peaks and valleys of graduate school. I will cherish my many long, philosophical, and silly conversations with my crew, and I am grateful that those conversations are ongoing, in person and on the GCFam chat. I have attempted to include here a sweet memory or two about each person. Dr. Jamie Rankin was one of my first friends at Caltech, and she is a constant ray of sunshine. Her sunny personality reaches from Princeton all the way to Pasadena. I instantly knew I would like Dr. Voon Hui Lai when she introduced herself at her first GCF lunch. I am so glad we spent time getting Sunday lunches together and had quite the adventure when we traveled to Kansas City for Jonas' wedding. We ate our weight's worth in amazing BBQ! Voon is half a world away, and I am so glad I can talk to her all the time through the internet! I appreciate Dr. Kimberley Mac Donald's thoughtfulness, and I know I will visit her and Nora one day soon. I greatly enjoyed the year I co-led Grad Group with Albert Wandui. He is such a kind soul and has a calming spirit, and working with him could not have come at a better time. I particularly remember the night when Albert and the Grad Group - Mark Zhang, Liz and Ken Jenkins, Michelle Cua, Ying Shi Teh, Mikhail Polyakov, and Voon - visited me while I was working late in the lab and brought me Mark Zhang's amazing creme bruleé. The data I collected that night is in my paper!

I am already missing my brunch life with Dr. Kirsti Pajunen. Rachel Gelhar is so thoughtful, and I appreciate her gluten-free baking. Heidi Klumpe has a delightful and whimsical personality, and in few words, she says so many insightful things. I always enjoy seeing Robbie and Ashley Polski. They are full of surprises and keep me laughing. Widianto Moestopo and Andrew Ylitalo are absolutely delightful, and I wish we had more chances to spend time together. Rebekah Loving has been so generous with her time and expertise in computational biology; I cannot believe she is only in her first year. Maria Camarca and Tanner Harms are two other first years who always brighten my day. Dr. Gerard Salter is the newest addition, and he continues the tradition of awesome postdocs who have been part of the GCF. Lena Maxey and Julie Cho are honorary GCF members, and they are so fun to be around. (Soon to be Dr.!) Rachel Ford has kept me laughing during thesis writing by telling me great jokes and funny stories, and she is a whiz at data analysis, particularly sigmoidal curves. I do not get to see enough of Liz Holman, but I belly laugh when I do. Amy Torrens is always so hospitable, and I hope she is enjoying her new life abroad. Missio friends include Dr. Karissa Archer, Amber Height, Elise Hegnauer, Katie Lemon, Dr. Juli Wu-Bonin, and Frances Tang. They are a great encouragement to me, and I am so happy to have the Missio family in my life. My newest

friends are Dr. Howard Hui and Estrella Sainburg, whom I met through Voon. She is always bringing people together! There are many GCF alums - Professor Brandon and Laura Henderson and their twins, Dr. Justin Su, Dr. Yong-Sheng Soh and Li Ling Quek, Drs. Jonas and Aba Lippuner (and Mr. Spock), Dr. Charles Cao, and Yuka Sakazaki, Dr. John and Odelia Pang, Professor Josh Brake, Dr. Kat Saad, Dr. Julie Hofstra, and Dr. Christopher and Courtney Frick - whom I am grateful to know and hope to see again in the future. I have encountered great mentors through GCF and Missio. Professor Wilfred Iwan is such a treasure, and I thank him for passing on so much wisdom to us. Len and Amy Tang have had a humongous influence on me, and we have had some key conversations that have shaped me as an adult. I am also grateful for Janet Atkins and her mentorship, Jeff Stills and the SAFE planning committee, and for the time that Janna Louie, Jeff and Lisa Liou, Lisa Corujo, Christopher Spolar, Lydia Lockhart, Dolly Spadaro, and Sally Alway have put into the group. I am also grateful for the many, long talks with Dr. Deborah Smith and for the teaching of Greg Waybright.

While at Caltech, I have been fortunate to live in a beautiful city that is full of resources. Many fun times have been spent at the Athenaeum, Trader Joe's, and Sprouts, eating at so many delicious restaurants, and simply walking outside. I have also lived in luxury for a graduate student. I shared an affordable, spacious apartment with Tonia, and I know what a rarity that is in LA county. Just before Tonia graduated, Kim introduced me to Tom and Norma Heaton. Tom and Norma were looking for a house-sitter while they traveled on his sabbatical, and ever since, I have been beyond blessed to call their beautiful home my home. While they have been away, I have been the guardian of the Heaton house! Since they have been back, they have been so thoughtful and kind while I have been working on finishing graduate school. They are the embodiment of generosity, and I appreciate all the times they include me in their lives.

I have lived a very eventful and full life while at Caltech, and I think the novella I have written here is a testament to how many people I have met and places I have been. The story is no different for life prior to Caltech. I began my undergraduate studies at Riverside Community College, and took my first chemistry course from Dr. John Georgakakos. He gave me the perfect, first introduction to chemistry. I am glad he told me early on that I should think about graduate school, even though I was not entirely sure what he meant. He and the other professors I had at RCC are a huge reason why I value effective teaching. I greatly appreciate my organic chemistry professor, Dr. Bernier, my biology professor, Dr. Herrick,

and my calculus professor, Dr. Somasundaram (Dr. Soma), as well. Dr. Bernier is a constant source of support, Dr. Herrick first introduced me to the NSF-REU program at UC Riverside that would give me my first research experience in Professor Linda Walling's lab, and Dr. Soma recommended me for my first teaching experience. Linda, Missy, and Fran gave me an incredible introduction to research, and my amazing experiences in Walling World have helped me push through some challenging times that would follow. I still cannot believe Missy mentored me so masterfully the summer after her first year of graduate school! After transferring to Stanford, I joined Professor Chaitan Khosla's group, and working for him under the mentorship of (now Professor!) Satoshi Yuzawa singularly prepared me for the rigors of graduate research. I appreciate the training I received from the rest of the Khosla lab, particularly from Professor Lou Charkoudian, who gave me the idea to create my own course to teach in graduate school. In my coursework at Stanford, almost by chance, I took Professor Ed Solomon's inorganic class. Before that Spring 2011 term, I had already accepted I was a very average inorganic student. But through his class, and the efforts of the very talented TA that term, Ryan Hadt (now a professor here!), changed my perspective so radically, that I decided I wanted to study metalloproteins in graduate school. Ed's class is another reason why I value effective teaching so highly. Professor Joan Licata and Professor Sarah Heilshorn are two other instructors who were particularly influential, and Professors Stephen Fried (chemistry) and Professor David Sher (math) were as well when they were teaching assistants.

I have made many friends along the way at Stanford, including Aubrey, Marie, Sara, Lena, Guez, Juliann, Andy, Weikang, and the members of the Kimball Study and the Mars Mark Study. Aubrey has been such a good friend at Stanford and at Caltech. I am so happy I can talk to Marie more frequently now, and I always enjoy catching up with Lena and Sara. Visiting Juliann in NY and Andy and Marie in Boston in 2017 was a highlight of graduate school. Thanks for letting me couch surf! I am so glad to be back in touch with Weikang as well! I am incredibly grateful that Sara and her cousin Bobby introduced me to Dr. Larry and Vicki Sullivan. I lived with the Sullivans for my last quarter at Stanford, and much like the Heatons, they are the embodiment of generosity. In my own life, I will find some way to pay forward the compassion they have for students. My dear friends from Riverside are Jessica, Caitlin, Margeen, Heather, and Wailun (in order of appearance!). I have known Jessica since middle school, Caitlin since high school, and Margeen, Heather, and Wailun since RCC. They have seen me through many phases of my

academic journey, from my high school illness, to my early years as a chemist, to my panic prior to transferring to Stanford that hilarious day at IKEA. Jessica, Caitlin, and Wailun often check in on me, Margeen and Heather keep me company over the internet as I work, and it is difficult to find the words for how much they mean to me. Though not often enough, Brian and Marie Starkey, Alex, Richard, their adorable daughter Ellie, Al, Loris, and Sam are always a joy to so. I am also so grateful for my high school guidance counselor, Mr. Hoopai, who still wishes me happy birthday every year and is a great supporter of my parents and brother. My high school teachers and mentors, Ms. Cunningham, Mr. Figeroa, Mr. Moore, Mr. Bushman, and Mr. Sutton, Travis Osbourne, Sam and Stacey Boone, Holly Rodriguez, Marry McInteer, and Renee McAlexander were also hugely influential. UCR professors, Andrew Chang and Carol Lovatt, were colleagues of my mother when I was young, and they were also quite influential during my formative years.

To my family, I could not accomplish what I have without your support. Harriet Brookman has been so wonderfully generous to me and my brother, and we are grateful for all of her support of our family. Life has been a sweeter since we reconnected with the Brawer side, and I hope to see Harriet, Mark, Deb, their children, and the Faber side (Zenie and Leah!) more in the future. My parents' friends have also been like family to me, and Gail Lacey, Mona Obetz, and Shirley Roper have been particularly generous with us. My Dad's colleagues at work, particularly Judge Theodore Piatt and Dr. Linda Bosserman, were a huge reason I applied to Stanford, and I thank Linda especially for her encouragement. Uncle Keshi has known my Dad since college, and he has been so nice to my brother and me. My immediate family - my mother Deborah, my father David, my brother David Louis, my grandmother Genesha, and my great uncle Louis - were my first teachers, and as time marches forward, I realize more and more how blessed I was to grow up in the Silva house. Both of my parents are college educated, and I did not know what a privilege that was until I got to high school. I still did not really understand the magnitude of the great start my family gave me until graduate school. For example, when I was two or three, I remember playing with letter magnets with Uncle Louie. When I was three, I started learning to read with my Dad, and my Mom and Grandmother are lifelong grammarians who made sure I knew the structure of the English language. While I know how I learned to read, I am not sure how my brother learned how to read. I think perhaps I helped teach him when I began reading to him at six days old, in preparation for college (I was a serious child). We are almost 7 years apart, so when he was born, he became my first student. I do not know if he wanted to

be my first pupil, but poetically, he teaches me new things all the time now. He has most recently been my guide through learning new software, and many phone calls with him have helped me write and format my thesis. Completing my thesis has been a most difficult task, but at along last, I am done! Thank you to all who have invested in me and taught me more than I could have ever imagined.

ABSTRACT

Protein-bound iron sulfur clusters are critical in cells and allow proteins to carry out many essential functions as electron carriers, catalysts for challenging organic reactions, and sensors of cellular environments. A wide range of protein families are known to coordinate iron sulfur clusters, and a growing category includes proteins involved in maintenance of the genome. Within the last three decades, iron sulfur clusters have been demonstrated to be important for enzymes that function in DNA repair, DNA replication, and transcription pathways. To date, iron sulfur clusters in the cubane [4Fe4S] geometry with all cysteine ligands have been exclusively reported for DNA repair and replication enzymes. In contrast to enzymes where the cofactor is necessary for active site chemistry or directly-linked to protein function, the [4Fe4S] cluster in the overwhelming majority of repair and replication enzymes is not involved in the catalytic modification of DNA substrates. Rather, the role of the cofactor appears to vary in function from protein to protein, and has been demonstrated to be important for protein stability, in the assembly of multisubunit proteins, and for substrate recognition, among other roles. Through investigations of the redox chemistry of the cofactor, our group has found that these enzymes participate in DNA-mediated charge transport chemistry, the process through which electrons rapidly migrate through well-stacked, duplex DNA. Long-range, DNA-mediated redox signaling provides a means of rapid communication among DNA-processing proteins for organizing repair and replication activities across the nucleus.

Notably, the first observations of the [4Fe4S] cofactor associated with repair and replications enzymes has consistently occurred well after the first biochemical studies of these enzymes. In some cases, the demonstration of a [4Fe4S] center has taken place decades later after initial work. Some proteins have required use of anaerobic methods in order to detect the cofactor, perhaps explaining why in some cases the metal center had eluded observation. Analysis of protein sequences might be expected to help accelerate identification of new iron sulfur centers in repair and replication enzymes. However, even with the abundance of sequencing data available in the post-genomic era, prediction of a metal center based on sequences alone has been challenging. This is in large part because the spacing of the coordinating cysteine residues can be quite irregular, leading to a weak bioinformatic signature.

Identifying proteins with overlooked [4Fe4S] cofactors poses an exciting challenge, and there are some elegant examples in the literature where data from genetics

assays has been used in combination with careful sequence analysis to predict and discover iron sulfur centers in repair and replication enzymes. Described here is the evolution of our studies on one well-known repair enzyme from *Escherichia coli*, UvrC. UvrC is part of the nucleotide excision repair pathway in the Bacteria domain which is responsible for addressing the wide class of bulky, helix-distorting lesions that can form after exposure to sources such as ultraviolet light, cigarette smoke, chemotherapeutics, and protein-DNA crosslinks. UvrC, an excision nuclease with two distinct active sites that incise the phosphodiester backbone on either side of the site of damage, has been historically challenging to study. Given how essential UvrC is in repairing damaged substrates, new insight has been greatly needed.

Through integration of several key reports from the literature regarding the sequence of UvrC and evidence that pointed to a cofactor from genetics assays, our group predicted that UvrC is a [4Fe4S] protein. Development of a new overexpression system and an anaerobic purification method allowed for isolation of UvrC in holo form. We used spectroscopic techniques to confirm that the cluster type was [4Fe4S], and a combination of spectroscopy and chromatography to demonstrate that the UvrC-bound cofactor is susceptible to oxidative degradation. We also found that loss of the cofactor, either through aerobic degradation or mutation of coordinating cysteines, is associated with aggregation of apoprotein. Importantly, in its holo form with the cofactor bound, UvrC forms high affinity complexes with duplexed DNA substrates; the apparent dissociation constants to well-matched and damaged duplex substrates are 100 ± 20 nM and 80 ± 30 nM, respectively. This high affinity DNA binding contrasts reports made for isolated protein lacking the cofactor. Moreover, using DNA electrochemistry, we find that the cluster coordinated by UvrC is redox-active and participates in DNA-mediated charge transport chemistry with DNA-bound midpoint potential of 90 mV vs. NHE.

The work detailed in this dissertation has highlighted how critical the [4Fe4S] center is for UvrC, where the cofactor has been implicated in protein stabilization, substrate binding, and redox signaling on DNA. Handling an apo form of UvrC may have led to the previous challenges catalogued by researchers. Through the development of entirely new methods to study UvrC under anaerobic conditions, many opportunities are now available to study UvrC and the NER pathway anew *in vitro* and *in vivo*. Such work will contribute additional insight on how iron sulfur clusters are essential for enzymes that maintain genomic integrity.

PUBLISHED CONTENT AND CONTRIBUTIONS

E. O'Brien, R. M. B. Silva, and J. K. Barton (2016). "Redox Signaling through DNA." *Israel Journal of Chemistry* **56**, 9-10, 705– 723.
DOI: 10.1002/ijch.201600022.
R.M.B.S. participated in writing the review.

J. K. Barton, R. M. B. Silva, and E. O'Brien (2019). "Redox Chemistry in the Genome: Emergence of the [4Fe4S] Cofactor in Repair and Replication." In: *Annual Review of Biochemistry* **88**, 163-190.
DOI: 10.1146/annurev-biochem-013118-110644.
R.M.B.S. participated in writing the review.

R. M. B. Silva, M. A. Grodick, and J. K. Barton (2020). "UvrC Coordinates an O_2-Sensitive [4Fe4S] Cofactor." In: *Journal of the American Chemical Society*, in press.
DOI: 10.1021/jacs.0c01671.
R.M.B.S. developed anaerobic methods, designed experiments, performed data analysis, and wrote the manuscript. M.A.G. contributed to plasmid design, initial method development, and aerobic studies.

TABLE OF CONTENTS

LIST OF ILLUSTRATIONS

LIST OF TABLES

Chapter 1

REDOX CHEMISTRY IN THE GENOME*,†

Iron sulfur clusters are modular, tunable metal cofactors found in all domains of life that are often agents of redox chemistry in biology, operating over a wide and tunable range of physiological potentials, from approximately -500 mV vs. NHE to 300 mV vs. NHE (NHE = normal hydrogen electrode) [8, 92, 116]. Common cofactor geometries include the rhomboid [2Fe2S] cluster and the cubane [3Fe4S] and [4Fe4S] clusters (**Figure 1.1**, *Top*), though more complex geometries are also well-known and studied. These cofactors commonly mediate redox reactions in nitrogen fixation, photosynthesis, and respiration [3, 94, 126], often acting in a chain of metal cofactors within an otherwise insulating protein matrix [52, 141]. Iron sulfur centers in transcription factors can also mediate responses to changes in cellular environment through chemical transformations of the center [27, 67, 91]. Iron sulfur centers undergo electron transfer at a range of redox potentials that varies depending on the local protein environment and solvent exposure (**Figure 1.1**, *Middle*) [33, 57]. One of the most common geometries is the [4Fe4S] cluster, which is found in the $[4Fe4S]^{2+}$ resting state. High potential [4Fe4S] clusters, like those in high potential iron (HiPIP) proteins, can be oxidized to the $[4Fe4S]^{3+}$ state and lower potential clusters, like those in ferredoxins, can be reduced to the $[4Fe4S]^{+}$ state [53]. Thirty years ago, these [4Fe4S] clusters were found also to be associated with a protein involved in DNA repair [28], and over time, more and more proteins involved in DNA processing were found to contain [4Fe4S] clusters.

After decades of progress, it is now understood that the incorporation of [FeS] metal centers occurs through a highly regulated and coordinated series of metabolically expensive steps by a network of iron sulfur cluster biogenesis proteins [5, 17, 43, 72, 100, 110, 118, 120, 122, 123, 137], some of which in eukaryotes are essential for cluster delivery to repair and replication enzymes (**Figure 1.1**, *Bottom*). At present, specialized biogenesis components have not been identified for [4Fe4S] repair proteins in prokaryotes, though, prokaryotic biogenesis has been

*Adapted from E. O'Brien, R. M. B. Silva, and J. K. Barton (2016). "Redox Signaling through DNA." *Israel Journal of Chemistry* **56**, 9-10, 705–723. DOI: 10.1002/ijch.201600022.

†Adapted from J. K. Barton, R. M. B. Silva, and E. O'Brien (2019). "Redox Chemistry in the Genome: Emergence of the [4Fe4S] Cofactor in Repair and Replication." *Annual Review of Biochemistry* **88**, 163-190. DOI: 10.1146/annurev-biochem-013118-110644.

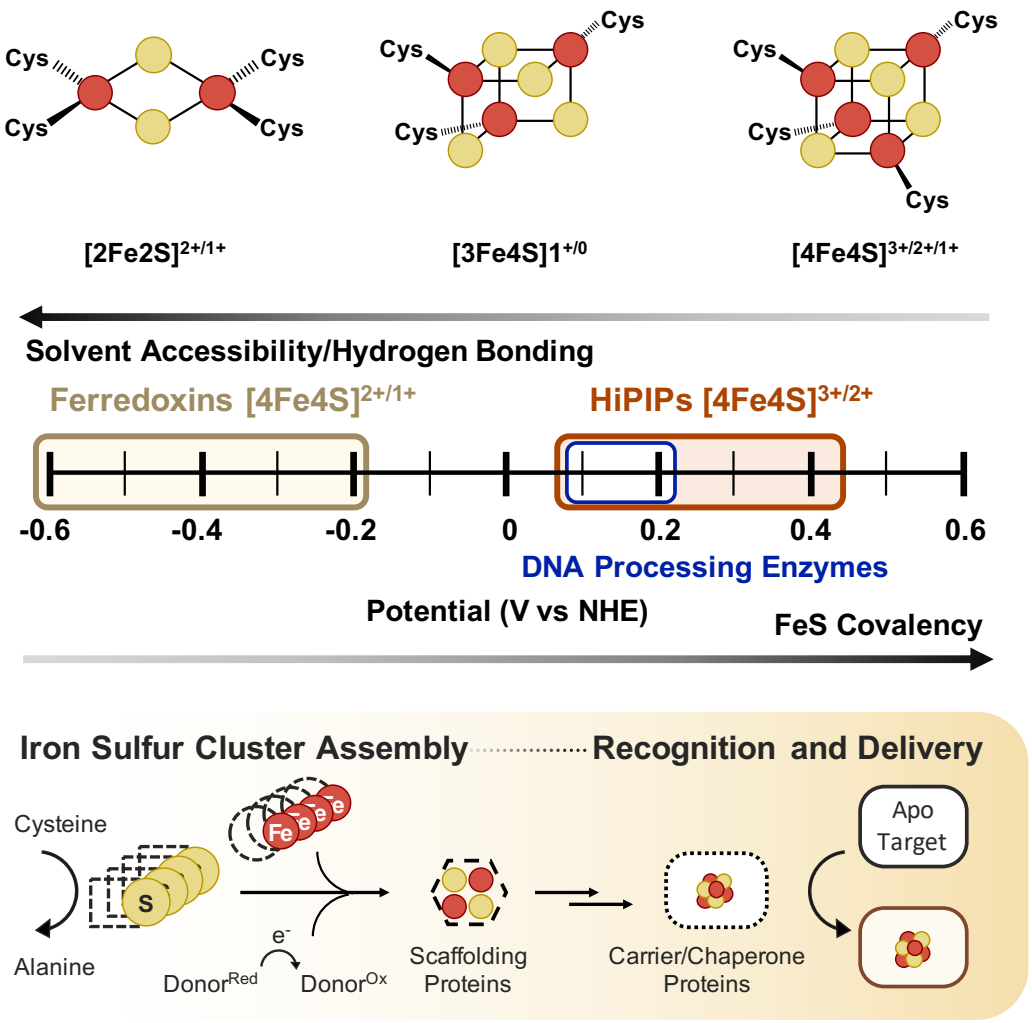

Figure 1.1 Iron sulfur clusters in DNA processing enzymes.[6, 17, 43, 118, 120] (*Top*) Iron sulfur cofactors can be found in [2Fe2S], [3Fe4S], and [4Fe4S] geometries, though more complex geometries are well-known. Iron in shown in red and sulfur in yellow. Common redox states are shown. (*Middle*) The potential of the [4Fe4S] cluster cofactor is tunable over a wide range of physiological redox potential values. Ferredoxins access the $[4Fe4S]^{2+/1+}$ couple, upon reduction from the resting $[4Fe4S]^{2+}$ state (light brown). High potential iron proteins (HiPIPs) access the $[4Fe4S]^{3+/2+}$ couple upon oxidation to the $[4Fe4S]^{3+}$ state from the resting $[4Fe4S]^{2+}$ state (dark brown). DNA-processing enzymes with [4Fe4S] cofactors have DNA-bound redox potentials that fall within the HiPIP $[4Fe4S]^{3+/2+}$ potential range, at ~65–150 mV versus the Normal Hydrogen Electrode (NHE) (blue). The solvent accessibility and hydrogen bonding/electrostatic environment of the cluster all contribute to tuning the redox potential of the cofactor. (*Bottom*) Reactive iron and sulfide species are assembled on protein scaffolds, and mature clusters are delivered to apoprotien targets, often with the aid of carrier and chaperone proteins.

linked to pathogenesis and antibiotic resistance [38]. Mechanisms of protein target recognition by biogenesis machinery have been brought to the forefront recently [120], and interestingly, bioinformatic signatures of the coordinating cysteines in repair and replication proteins are surprisingly weak [140].

1.1 IRON SULFUR CLUSTERS IN DNA PROCESSING ENZYMES

Following these remarkable discoveries, several questions arose about the nature of the [4Fe4S] cluster in nucleic acid processing enzymes. Creation and incorporation of iron-sulfur clusters into proteins is a metabolically expensive task requiring the engagement of several protein systems. Placing an iron-containing cofactor in a DNA-binding protein could additionally place the bound nucleic acid at risk of damage. A labile ferrous iron from the cofactor could react with hydrogen peroxide in the cellular environment; this Fenton chemistry creates reactive oxygen species which could damage nearby DNA bases [65, 66]. Why then does Nature spend the requisite energy incorporating a redox-active inorganic cofactor into a DNA-processing enzyme? What were their roles? Were they structural factors or perhaps ancestral relics? As described here, we are finding that these [4Fe4S] clusters carry out redox reactions in DNA-processing proteins, serving as redox switches to regulate protein binding to the DNA polyanion.

The surprising discovery of a [4Fe4S] cluster in the base excision repair (BER) glycosylase Endonuclease III (EndoIII) from *Escherichia coli* (*E. coli*) in 1989 [28] soon led to the discovery of [4Fe4S] clusters in MutY (an EndoIII paralog) and Uracil DNA Glycosylase in *Archaeoglobus fulgidus* (AfUDG) [55, 59]. Over the following decades, nucleic acid processing enzymes across many pathways were shown to contain [4Fe4S] cofactors (**Table 1.1** [5, 9, 30, 43, 60, 61, 76, 140, 143, 148, 149]. In most cases, discovery of the [4Fe4S] cluster occurred years after the first isolation of the gene products [43]. As predictive tools and protein isolation methods become more and more sophisticated, we and others expect that even more [4Fe4S] clusters will be observed in essential DNA processing enzymes [43, 121].

Table 1.1 DNA Processing Enzymes Coordinating a [4Fe4S] Cluster

[4Fe4S Proteins]					
Bacteria	**Archaea**	**Eukarya**	**Pathway**	**Enzyme Family**	**Refs.**
EndoIII; MutY; UDG (Family 4)		Ntg2, NTHL1; Myh1, MUTYH	Base excision repair	Glycosylases	[5, 30]
DinG	XPD	Rad3, XPD; FANCJ; RTEL1; ChlR1	Many repair pathways	SF2 $5' \rightarrow 3'$ helicases	[43, 143]
AddAB (Gram-positive)		Dna2	Replication-coupled repair	Helicase-nucleases with $5' \rightarrow 3'$ nuclease activity	[80, 143]
PhrB (Class FeS-BCPs)			Photoreactivation DNA repair	(6-4) photolyase	[148]
Spore photoproduct lyase			Direct repair of UV damage (spore photoproduct)	Radical SAM enzyme	[9, 76]
Cas4			CRISPR adaptive immunity	$5' \rightarrow 3'$ exonuclease	[149]
	RNA polymerase (RpoD)	RNA polymerase II (Rpb3)	Transcription	Template-directed RNA polymerase	[60]
		DNA primase	Replication	*De novo* synthesis of RNA primers	[5]
		Pol α	Replication	Extension of RNA primers	[5]
		Pol ϵ	Replication	Leading strand polymerase	[5]
		Pol δ	Replication	Lagging strand polymerase	[5]
		Pol ζ	Replication	Translesion polyermase	[5]

Proteins separated by a semicolon are homologs or paralogs from the same protein family. Proteins separated by commas in the Eukarya column are from yeast (left) and humans (right). See text for abbreviations and additional references.

The question of what role the [4Fe4S] clusters played, however, was less straightforward to answer, as early studies demonstrated that the clusters were isolated in the electron paramagnetic resonance (EPR) silent $[4Fe4S]^{2+}$ state and were resistant to powerful chemical oxidants and reductants [13, 28, 59]. Moreover, the spectroscopic signature of coordinating cysteines was unchanged upon binding a damaged substrate, leading to the initial conclusion that the cluster had a structural role [28, 42, 131]. MutY, however, could be denatured and refolded in the apo form, challenging this early conclusion [114]. A substrate-sensing role was proposed for the cluster in light of this result, but a general, chemical function for the cofactor eluded observation.

1.2 CHARACTERIZING THE FUNDAMENTAL PROPERTIES OF DNA-MEDIATED CHARGE TRANSPORT CHEMISTRY

At the same time that these proteins involved in DNA processing were being found to contain [4Fe4S] clusters, experiments were being conducted to characterize DNA charge transport chemistry (DNA CT), where electrons rapidly migrate through well-stacked duplex DNA [46]. The native substrate of these [4Fe4S] enzymes, double stranded DNA (dsDNA), was initially predicted to conduct charge in the dry, solid state [36], as the π-stacked DNA bases resemble the structure of graphite, a conductive material (**Figure 1.2**). To assess whether DNA conducted charge in biologically relevant aqueous conditions, new platforms were developed to examine this chemistry. Two important characteristics of this chemistry emerged: (i) DNA CT can occur over long molecular distances with shallow distance dependence, and (ii) DNA CT is exquisitely sensitive to perturbations in π-stacking of the bases.

A range of studies using DNA-bound electron donors and acceptors were used to characterize DNA CT chemistry. In an early photophysical study, a DNA oligomer was prepared containing a tethered luminescent ruthenium complex (donor) intercalated at one end of the duplex and a rhodium complex that acts as an oxidizing quencher (acceptor) at the other end of the duplex. While the tethered, DNA-bound ruthenium complex luminesced in the absence of the rhodium complex, in its presence, the luminescence was quenched by electron transfer occurring *through* the π-stacked dsDNA duplex, and remarkably over a distance > 40 Å [97]. In a subsequent experiment using the base analog 2-aminopurine, a base analog as the luminescent donor, with guanine serving as the electron acceptor, electron transfer quenching was also evident, but was attenuated in the presence of a single base mismatch (a lesion that perturbs π-stacking) intervening between the bound donor and

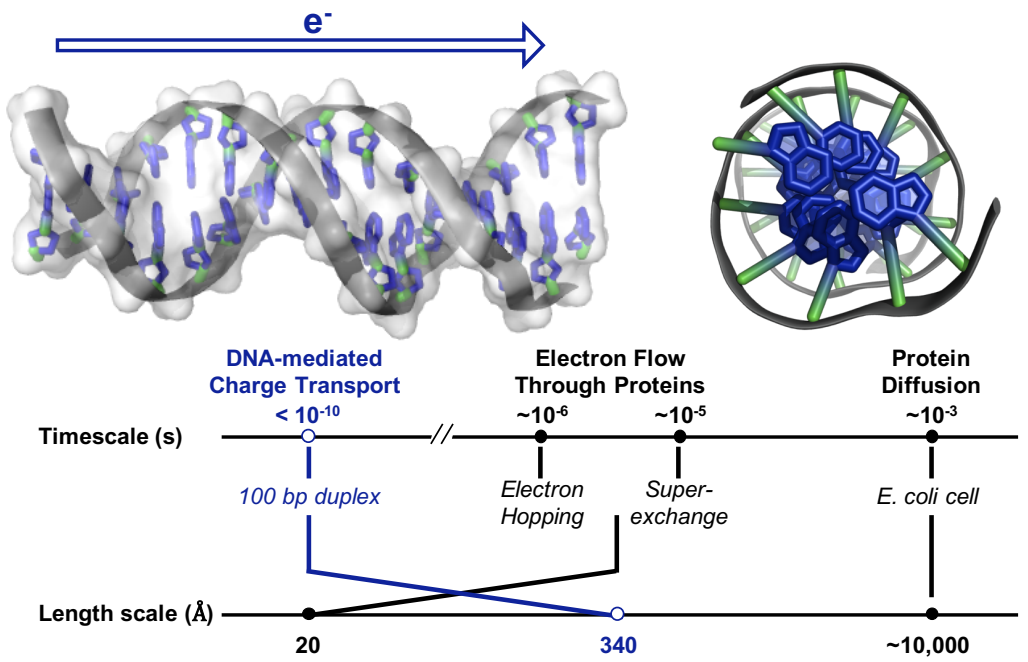

Figure 1.2 DNA charge transport (DNA CT) chemistry [48, 52, 93, 101, 141]. The structure of DNA facilitates long-range, rapid electron transfer. (*Top left*) Side view of DNA. The aromatic bases at the center of the DNA helix are oriented so that the π-orbitals of adjacent bases overlap with one another in the duplex. This structural property suggests that charge could pass through the π-stacked base pairs of DNA. (*Top right*) View down the helical axis of aromatic base pairs (blue) stacked in 3.4-Å layers at the center of DNA. (*Bottom*) Timescale and length scale of various electron transfer pathways through biomolecules (Protein Data Bank ID 3BSE).

acceptor [74]. Long-range CT through a 63 bp (base pair) duplex DNA substrate has also been observed with DNA-intercalating photooxidants, where the DNA-bound photooxidant can promote oxidative damage at guanine residues from a distance. A covalent rhodium photooxidant at one end of a DNA duplex, for example, oxidizes guanine bases at the 5′- guanine of a guanine doublet, the site of low oxidation potential, through DNA CT, generating 7,8-dihydro-8-oxo-2′-deoxyguanosine lesions 200 Å from the site of intercalation [101]. DNA CT chemistry through well-stacked RNA/DNA hybrids has also been observed [106, 108]. Experiments monitoring base-base CT utilizing 2-aminopurine furthermore showed that these DNA CT reactions can occur on the picosecond timescale, gated by the motions of the bases [107], and moving 10 times the single-step tunneling distance through protein in a miniscule fraction of the time [48, 52, 112, 141]

Again, however, perturbations in base stacking, as occur with base mismatches

or kinks in the DNA, turn off this long-range CT chemistry. In fact, proteins that bind and kink the DNA, such as TATA-binding protein, can be used to turn off DNA CT. In contrast, proteins that bind DNA without affecting DNA base stacking, as with histones, do not alter DNA CT [15, 102, 115].

We also explored DNA CT in the ground state using DNA electrochemistry. Here, as with the photophysical studies, we observe long-range CT as long as the DNA is well-stacked. Indeed, ground state CT through DNA was observed over 100 base pairs to a tethered, intercalating redox probe, Nile blue, using multiplexed DNA-modified gold electrodes, but a single base mismatch in the 100-mer was sufficient to attenuate the redox signal severely [129]. Duplex DNA with well-stacked bases is thus a strikingly effective mediator of charge transport, but what proteins serve as the electron donors and acceptors? In order to utilize DNA CT for long-range redox reactions, electron donors and acceptors must both possess a redox-active center capable of one-electron transfer reactions and bind duplex DNA such that their redox centers are coupled into the π-stacked bases. Repair and replication enzymes bearing the [4Fe4S] meet all of these criteria and were thus examined in the context of DNA CT chemistry, described in the next section.

1.3 MEASURING REDOX POTENTIALS OF [4FE4S] ENZYMES BOUND TO DNA

For our early electrochemistry studies, we had used proteins to modulate DNA CT to a small DNA-bound redox probe [15], but we considered that DNA electrochemistry could be used also to examine DNA CT to a redox cofactor *within* a DNA-bound protein. Could a DNA-binding protein containing a redox cofactor carry out DNA CT chemistry? If so, DNA CT experiments could be used to characterize the redox centers of DNA-binding proteins and to determine their DNA-bound potentials.

1.3.1 DNA-Mediated Electrochemistry

DNA-modified Au electrodes have become a useful platform for assessing whether a DNA-processing [4Fe4S] enzyme is redox-active in solution under physiologically relevant conditions (**Figure 3.8**). Gold surfaces are functionalized with alkanethiol-modified DNA duplexes through formation of a thiol-gold bond. Duplex DNA bound to the surface is then characterized, with respect to density, surface thickness, and ability to be cut by restriction enzymes. In this platform, the DNA, functionalized onto an electrode surface, is biologically accessible; restriction enzymes, for example, can cut the DNA on the electrode with sequence specificity, just as in

solution. Once assembled, the Au surface is used as the working electrode in a three-electrode cell, often with an Ag/AgCl gel tip as the reference electrode and a platinum wire as the auxiliary electrode [111, 128, 129]. DNA-bound redox potentials of [4Fe4S] proteins can be measured with this method, where charge flows to (cathodic peak) and from (anodic peak) the electrode through the DNA to the cluster, reversibly oxidizing $[4Fe4S]^{2+}$ to $[4Fe4S]^{3+}$, then re-reducing $[4Fe4S]^{3+}$ to $[4Fe4S]^{2+}$ in the process. Electrochemical studies on these platforms have been central to the prediction and discovery of redox signaling between DNA-bound [4Fe4S] enzymes across different repair pathways [6, 104, 132].

We first examined MutY, EndoIII, and AfUDG, three base excision repair proteins found to contain [4Fe4S] clusters [13]. Earlier studies using strong chemical oxidants and reductants had suggested that the clusters were redox-inactive at physiological potentials [28], but these studies had been conducted in the *absence* of DNA. It was reasonable to consider that binding the DNA polyanion might change the potential of the cluster within the protein. Our studies showed first that a reversible signal was detectable at ~80 mV versus NHE, within the physiological window, for each of these proteins bound to the DNA-modified electrode [33, 92]. The potentials were consistent with those found for the clusters in HiPIP proteins and were at equal potentials for all of the repair proteins examined. Moreover, the presence of an abasic site on the DNA intervening between the bound protein and the electrode surface served to attenuate the signal from the cluster. This result established two important points: (i) we were measuring the *DNA-bound* potential of the protein and (ii) we were observing DNA-mediated CT between the electrode and the cluster within the protein. Many repair and replication proteins have now been studied using this DNA electrochemistry platform, and in each case we have observed reversible, redox signals in the physiological potential range, near ~80 mV vs. NHE, corresponding to cycling between the $[4Fe4S]^{2+}$ and $[4Fe4S]^{3+}$ oxidation states [6, 13, 35, 96, 104, 130, 132].

It is noteworthy that the most recent generation of DNA-modified electrodes utilizes a multiplexed chip so several experimental conditions can be examined in parallel (**Figure 3.8**) [111, 128, 129]. Patterned, silicon chips with sixteen independently addressable Au electrodes uniform in area can be physically divided into four quadrants and used to monitor the redox activity of a single protein on as many as four different DNA substrates on the same surface. The platform can also be used to compare CT efficiency of WT and mutant protein on the same chip. All of the experiments described can moreover be carried out anaerobically.

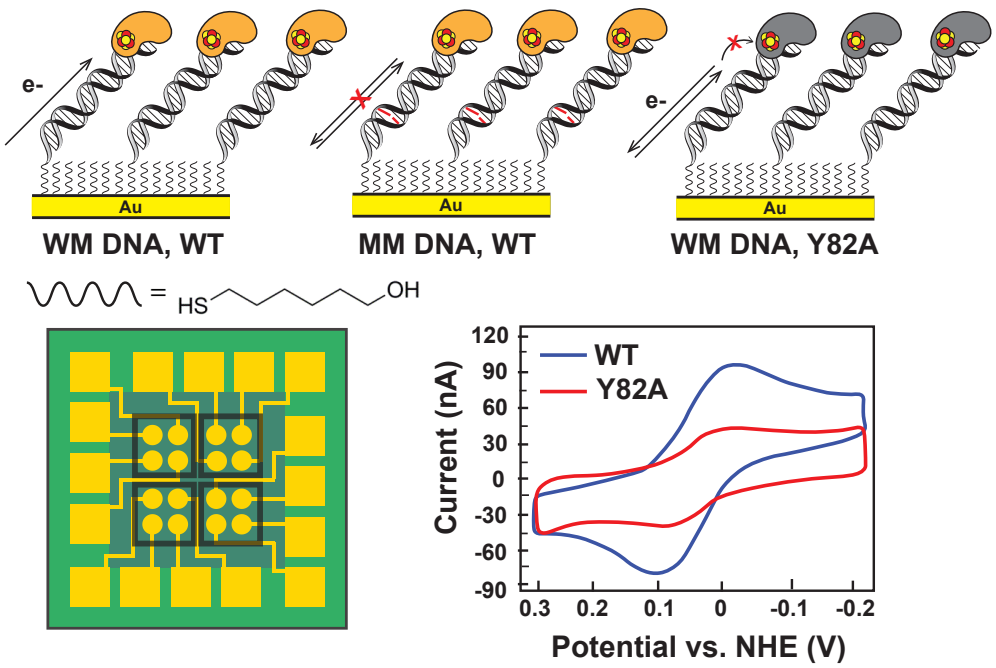

Figure 1.3 Measuring the redox potential of DNA-bound [4Fe4S] enzymes [13, 16, 111, 128, 129]. (*Top*) DNA electrochemistry on Au electrodes, where well-matched (WM) DNA duplexes containing a tethered alkanethiol are attached to a gold electrode passivated with β-mercaptohexanol, which can be used to assess redox signals from DNA-bound, [4Fe4S] proteins. Signals are attenuated when base lesions, such as mismatches (MM, shown in red) in the duplex, are present, or when the redox pathway within the [4Fe4S] protein, as for EndoIII Y82A (shown in gray), is deficient in charge transport (CT). (*Bottom left*) A multiplexed chip platform has now been adapted to measure [4Fe4S] protein signals on 16 separate DNA-modified electrodes, with replicates on a single surface. (*Bottom right*) Cyclic voltammetry scanning can be used to measure the DNA-mediated redox signal from CT-proficient proteins (such as WT EndoIII, blue) and CT-deficient mutant proteins (EndoIII Y82A, red).

1.3.2 Graphite Electrochemistry to Compare DNA-bound and DNA-free Potentials of [4Fe4S] Cluster Proteins

We became interested in monitoring directly the shift in potential for [4Fe4S] repair proteins bound to DNA versus free, and that required measuring the protein potential both in the absence and presence of DNA. DNA electrochemistry on Au electrode surfaces is amenable to measuring physiological potentials ranging from -200 mV to +500 mV vs. NHE [6, 7, 35, 51, 54, 88, 96, 104, 111, 130, 132]. However, scanning beyond this range is necessary to observe a redox signal from a protein in the absence of DNA, which has a higher (more reductive) midpoint potential due

to the absence of the DNA polyanion [7, 35, 51, 54, 132]. In order to measure the DNA-free and DNA-bound redox potentials of EndoIII, highly oriented pyrolytic graphite (HOPG) electrodes were used [51]. Bare surfaces or surfaces modified with pyrene-functionalized duplex DNA (which creates a DNA monolayer through π-stacking between pyrene and graphite) facilitated direct comparison of DNA-free and DNA-bound EndoIII [4Fe4S] cluster redox potentials. A negative shift of approximately 200 mV was observed for the DNA-bound EndoIII relative to DNA-free EndoIII. Given that protein binding does not lead to a large conformational change in the protein or DNA, this shift in redox potential for the [4Fe4S] cluster thermodynamically reflects a roughly 1000-fold tighter DNA binding affinity for the oxidized $[4Fe4S]^{3+}$ state, relative to the reduced $[4Fe4S]^{2+}$ state (**Figure 1.4**, Left). Oxidation of the $[4Fe4S]^{2+}$ cluster to the $[4Fe4S]^{3+}$ state thus should serve as a redox switch for DNA binding.

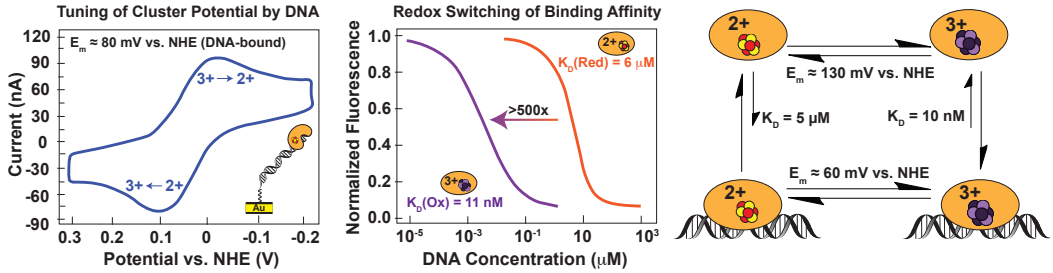

Figure 1.4 DNA binding shifts the potential of [4Fe4S] cluster enzymes. (*Left*) Tuning of cluster potential by DNA. EndoIII has a redox potential of approximately 80 mV vs NHE for the $[4Fe4S]^{3+/2+}$ couple measured on a DNA-modified Au electrode [13]. On graphite electrodes, the DNA-bound potential is ~60 mV vs NHE, which is a negative shift from the ~130 mV vs NHE potential for this couple when the protein is not bound to DNA [7, 51]. (*Middle*) Redox switching of binding affinity. This shift in potential corresponds thermodynamically to a stabilization of the oxidized $[4Fe4S]^{3+}$ state upon binding the DNA polyanion. Microscale thermophoresis on electrochemically oxidized and native reduced EndoIII indicates that a > 500-fold increase in DNA-binding affinity is associated with the conversion from $[4Fe4S]^{2+}$ to the $[4Fe4S]^{3+}$ state, consistent with this negative shift in potential [132]. (*Right*) A thermodynamic cycle for oxidized and reduced protein associating and dissociating with DNA is shown.

1.3.3 Spectroscopic Observation of [4Fe4S] Cluster Redox Activity in DNA-Processing Proteins

Electrochemical observations of the [4Fe4S] cluster in DNA-processing enzymes was also complemented by spectroscopic analysis. EPR spectroscopy requires chemical or electrochemical conversion of the resting, diamagnetic $[4Fe4S]^{2+}$ enzymes to the paramagnetic oxidized $[4Fe4S]^{3+}$ or reduced $[4Fe4S]^{+}$ redox states, and thus was used to establish the resting state for the DNA-bound repair protein as $[4Fe4S]^{2+}$ [7, 75, 117, 138]. We also demonstrated that the DNA-bound protein can be oxidized photochemically, from a distance, using DNA CT from a distantly tethered intercalating photooxidant [6]. Importantly, we were also able to demonstrate spectroscopically that the cluster could be oxidized by guanine radicals, generated using flash-quench experiments monitored by transient absorption spectroscopy [144]. Indeed, these studies highlight how the oxidized $[4Fe4S]^{3+}$ cluster could be generated within the cell *from a distance* using DNA CT from guanine radicals formed under conditions of oxidative stress, and in so doing, activating the DNA repair machinery.

1.3.4 A Shift in Cluster Potential Reflects a Redox Switch in DNA Binding

While we had seen several examples of DNA binding yielding a shift in redox potential for the clusters within the repair proteins, from which one can infer a difference in DNA binding affinity for the protein with a $[4Fe4S]^{3+}$ cluster versus a $[4Fe4S]^{2+}$ cluster, we were not at first able to measure this difference directly. In the absence of DNA, the $[4Fe4S]^{3+}$ cluster degrades oxidatively to a $[3Fe4S]^{+}$ cluster, which affects protein binding. As a result, binding affinities for the $[4Fe4S]^{3+/2+}$ clusters needed to be determined anaerobically.

Recently we found that microscale thermophoresis could be used under anaerobic conditions to carry out the DNA binding experiments for the [4Fe4S] proteins in the two oxidation states [132]. EndoIII containing the $[4Fe4S]^{3+}$ cluster was first generated on DNA-modified electrodes and then, under strictly anaerobic conditions, the thermophoresis experiments were conducted. Consistent with the shift in potential associated with DNA binding, oxidized EndoIII with the $[4Fe4S]^{3+}$ cluster was indeed found to bind >500 times more tightly to dsDNA than the reduced EndoIII with the $[4Fe4S]^{2+}$cluster (**Figure 1.4**, Middle). This difference in binding affinity is understandable based simply on electrostatic considerations, assuming that a conformational change in the protein does not occur upon cluster oxidation. In fact, calculations of the potential energy change for the $[4Fe4S]^{2+}$ cluster versus

the $[4Fe4S]^{3+}$ state, based on the distance of the cluster from the DNA polyanion and the intervening protein dielectric, well reflect the change in binding affinity that we see. It is interesting in that context that we find similar shifts in potential for all of the DNA repair proteins examined, and, for proteins with reported crystal structures, the clusters generally appear to be ~ 20 Å from the DNA polyanionic backbone. Based upon the measurements for EndoIII, then, we can consider that binding of these repair proteins to the DNA polyanion serves to tune the potential of the cluster by altering the electrostatic environment, activating the cluster toward oxidation, and lowering the $[4Fe4S]^{3+/2+}$ couple into a physiologically accessible potential range. Additional binding affinity measurements of other repair proteins in reduced and oxidized states are needed to continue examining the role of the cluster in the context of each protein.

1.4 DNA REPAIR ENZYMES COORDINATING [4FE4S] CENTERS

Thousands of DNA damage sites are generated by endogenous and exogenous agents in each cell daily [26]. An arsenal of DNA repair pathways has evolved to address the structurally and chemically diverse lesions, though a comprehensive understanding of how repair pathways efficiently identify and remove damaged bases has remained elusive [25, 50, 87]. In the case of the repair proteins that contain [4Fe4S] clusters, what they share is a low copy number within the cell and a moderate specificity in binding their target lesion versus unmodified DNA. But with few players and not a high specificity in targeting, how do they effectively find all the lesions within the cell and on a timescale appropriate to the organism?

We have considered that DNA charge transport chemistry might provide a first step in localizing repair proteins that contain these clusters in the vicinity of lesions, essentially redistributing the proteins to regions of damage, irrespective of the actual lesion characteristics as long as the damage interferes with DNA CT. We had actually found earlier that many common base lesions interfere with DNA CT [12]. Moreover, the fact that these proteins share a similar redox potential means that essentially they can work together, transferring electrons from one to another to carry out a first scan of the genome.

We have, by now, found many types of DNA repair proteins containing [4Fe4S] clusters that are involved in redox signaling on DNA, and we have probed how these redox signaling networks work in coordination utilizing DNA CT through their [4Fe4S] clusters. We have also found CT deficiencies in mutated proteins strongly linked to disease. In the context of redox signaling, included below, is an overview

of the major repair protein families that coordinate a [4Fe4S] cluster, the damaged substrates they repair, and illustrations of how they may utilize redox signaling to maintain genomic integrity (**Figure 1.5**).

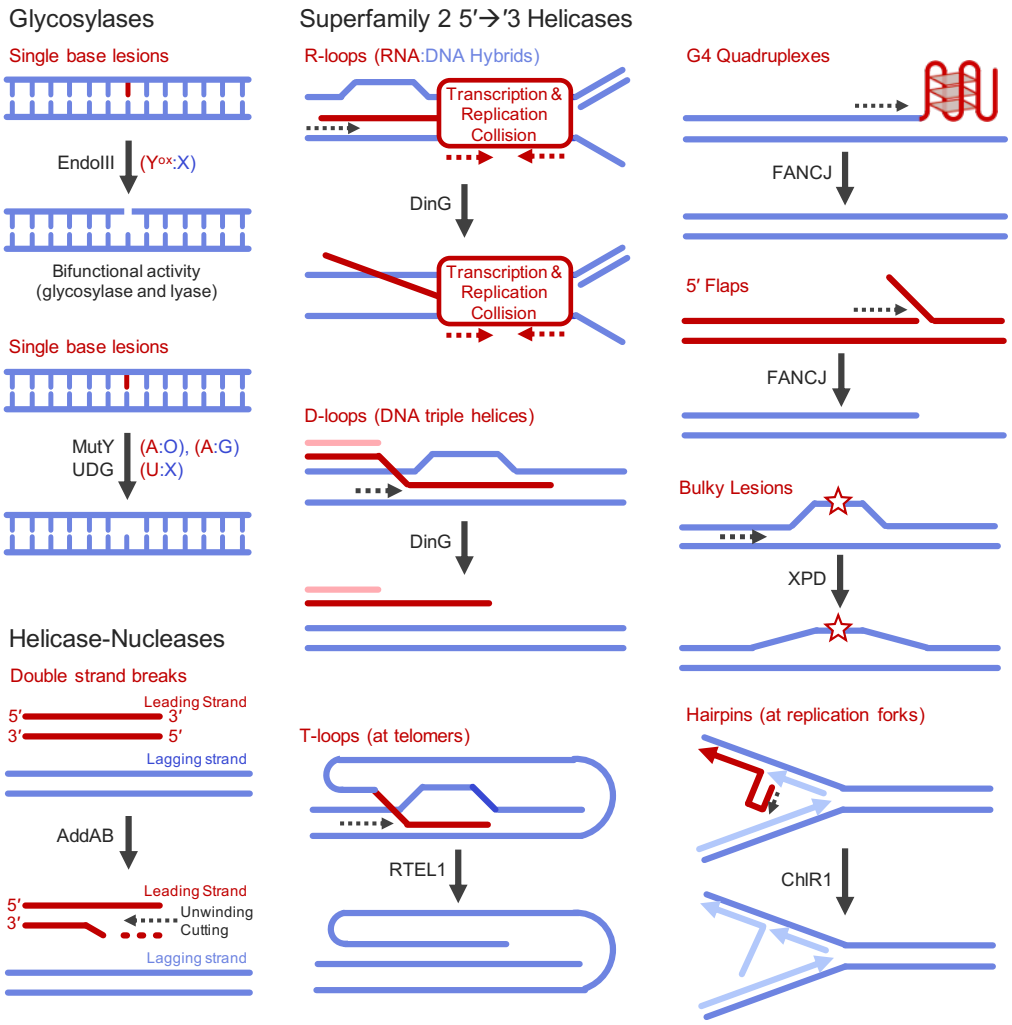

Figure 1.5 Reactions and substrates for DNA repair enzymes containing [4Fe4S] clusters. (*Top Left*) Glycosylases remove several single-base lesions caused by endogenous and exogenous agents [12, 30, 83]. (*Right*) Superfamily 2 5′→3′ helicases participate in several pathways and are involved in unwinding very diverse substrates. The substrate specificity overlaps for many of the helicases (e.g., FANCJ and RTEL1), although genome location (e.g., telomeres) and cell cycle phase (e.g., replication in the S phase) appear to be factors in activity [18, 19, 125, 143]. (*Bottom Left*) The helicase-nuclease AddAB processes double-strand breaks [80, 140].

1.4.1 Glycosylases

Glycosylases are key players in BER, a highly conserved pathway responsible for recognizing and removing single-base lesions generated by spontaneous deamination, alkylating agents, and oxidative stress, among other sources of damage (**Figure 1.5**, Top Left) [30, 58]. For EndoIII, MutY, and AfUDG, biochemical studies have very elegantly demonstrated that mutations at coordinating cysteines or in the cluster binding domain can affect protein expression, enzymatic function, and DNA binding, even though the cluster is located remotely from the glycosylase active site and there is not a large conformational change associated with the binding to DNA [31, 37, 83, 131]. Specific to mammalian BER, a connection has been established between the glycosylases NTHL1 and and multiple cancers, most notably MUTYH-associated polyposis (MAP). These syndromes are characterized by increased risk of aggressive, early-onset colorectal cancer [26, 30, 139].

As described above, several BER glycosylases were demonstrated to participate in DNA-mediated CT chemistry [13]. Further examination of the available structures of EndoIII in the free and DNA-bound forms revealed a few highly conserved aromatic residues between the cluster and the DNA, which could provide a CT pathway through the protein [14, 52, 119, 141]. Informed by these crystal structures, several key mutants of EndoIII have been generated and characterized, including a CT deficient/enzymatically proficient mutant Y82A and charge-flipped mutants to explore the electrostatics near the cluster [14, 51, 119]. Unique to the HiPIP-like [4Fe4S] repair proteins, the DNA polyanion is the governing factor that shifts the potential and stabilizes the cluster in the $[4Fe4S]^{3+}$ state [7, 51, 57], so that only variations in the intensity of the redox signal is observed for different mutants bound to the DNA electrode, as a function of their proficiency in carrying out DNA CT; the DNA-bound potential is the same for all of the EndoIII mutants. Furthermore, redox sensing of base stack perturbations on DNA-modified gold electrodes containing a lesion has been observed, even when that lesion is not a substrate for the glycosylase [13, 119].

1.4.2 Superfamily 2 (SF2) $5' \rightarrow 3'$ Helicases

SF2 helicases were the second family of enzymes discovered to coordinate a [4Fe4S] cluster [124]. SF2 helicases are NTP-dependent proteins that directionally translocate and unwind duplexes [143]. Distinct from the glycosylase family, the helicases are involved in several repair pathways (**Figure 1.5**, Right). These pathways respond to stress from multiple sources, and there are many examples of extensive crosstalk

and cooperativity among a complex network of repair pathways that include SF2 helicases with [4Fe4S] clusters [43]. As might be expected, mutations in SF2 helicases containing [4Fe4S] cluster are associated with a host of genetic disorders and cancers and are being targeted for cancer therapies [18, 135].

A common theme with SF2 helicases is the multifunctional nature of their activities within the cell (**Figure 1.5**, Right). In bacteria, DinG resolves R-loops, RNA:DNA hybrids, formed at collisions between replication and transcription machinery; DinG has also been shown to be active on D-loops (displacement loops, triple stranded DNA) [117, 136]. Notably, mutation of the ligating cysteines of DinG results in an increased susceptibility to proteolytic degradation *in vitro* [117]. A new, well-conserved bacterial protein YoaA was identified in a genetics screen to be involved in coordinating repair and replication machinery at blocked replication forks. Based on sequence similarity to DinG, YoaA was predicted also to be a [4Fe4S] protein [20].

The first archaeal/eukaryotic SF2 helicase discovered, XPD, is part of the transcription factor IIH (TFIIH) complex and is involved in both nucleotide excision repair (NER) and transcription initiation [124]. In NER, helicase activity is critical for removing damaged oligomers, and helicase activity can be disrupted by mutating cysteines that coordinate the [4Fe4S] cluster, even though the [4Fe4S] cluster does not participate directly in catalyzing substrate unwinding [43, 117]. In contrast, only the association of XPD with TFIIH is needed to initiate transcription, which is thought to aid assembly of other proteins with TFIIH. Many other facets of XPD have also been studied, including a role for XPD in preventing oxidative damage in the mitochondria [62].

Both XPD and DinG can participate in DNA CT chemistry with a shared DNA-bound redox potential of approximately 80 mV vs. NHE [54, 96]. Further probing of the CT activity found that upon addition of ATP, the signal for XPD and DinG quite stunningly increased without any shift in the midpoint potential. Helicase activity thus increases the electrochemical signal through better coupling of the cluster to the π-stacked DNA bases, essentially signaling helicase activity through DNA CT. The increased coupling upon co-factor binding appears to be an important feature of the SF2 helicase family that helps coordinate repair and replication, signaling from a distance that the helicase is active.

Another eukaryotic SF2 helicase, FANCJ has a role in several pathways. Compromised FANCJ function, which can result from mutations in the cluster binding domain, has been linked to several cancers, and FANCJ upregulation has been found

in many tumor types [19]. FANCJ is known to act on many substrates, including duplex substrates, D-loops, and G4 quadruplexes (89). FANCJ association with numerous other proteins, including BRCA1, can depend on the timing of the damage response and the type of lesions generated. Furthermore, FANCJ activity has been observed to alleviate replication stress through resolution of stalled replication forks, particularly at telomers rich in G4 quadruplexes. Two other SF2 helicases that coordinate a [4Fe4S] cluster, RTEL1 and Chlr1, resolve several different types of structures in the process of facilitating replication [11, 135]. Both RTEL1 and Chlr1 have been also found to associate with various replication proteins. Mutations in these enzymes are similarly associated with an array of diseases [5, 11, 43, 56]. Electrochemical studies of these proteins have not yet been conducted, but studying these proteins in the context of redox signaling will likely illuminate how these multifunctional enzymes coordinate their activities.

1.4.3 Helicase-Nucleases

In 2009, the first helicase-nuclease containing a [4Fe4S] cluster identified was AddB, part of the AddAB heterodimer found in gram positive bacteria and some proteobacteria [80, 145]. Helicase-nuclease activity is involved in double strand break (DSB) repair, which can be caused by a number of factors, including collapsed replication forks (**Figure 1.5**, Bottom Left). Located in the C-terminal nuclease domain of AddB, the cluster was found to be essential for binding of DNA substrates, but not essential for complexation with AddA or for maintaining structure, though a stabilizing role of the cluster was suggested. The crystal structure of the AddAB in complex with a DNA substrate revealed a DNA binding loop supported by the cluster domain, providing explanation of why mutating coordinating cysteines abolished substrates binding [125]. A homologous [4Fe4S] helicase-nuclease, Dna2, was later found in eukaryotes (*vide infra*).

1.4.4 Monitoring Redox Signaling Among [4Fe4S] Repair Proteins

Given the multitude of these clusters, their similarity in redox potential, and their diversity in lesions targeted, we became interested in examining how the proteins might cooperate in searching for DNA lesions. To study cooperative, redox communication between [4Fe4S] proteins, a series of *in vitro* and *in vivo* assays were developed to monitor signaling networks. *In vitro*, atomic force microscopy (AFM) has facilitated visualization of [4Fe4S] repair protein distribution on well matched (WM) DNA versus duplex DNA containing a single base mismatch (MM) [14, 54, 119, 130, 132].

Though strands containing a single, engineered C:A mismatch are not native substrates for any of the repair enzymes studied, preferential binding to the 3.8 kb long MM strands, expressed as a binding density ratio of 1.5 (**Figure 1.6**, Top Left) has been seen for all CT-proficient repair proteins. Mixtures of [4Fe4S] proteins from different repair pathways, and, remarkably, mixtures of cluster proteins from distinct organisms also signal cooperatively one to another, localizing to damaged strands.

Two factors have been found to affect the efficiency of the damage search: (i) the CT proficiency of a protein and (ii) the extent to which the protein population is oxidized [132]. Mixing CT-proficient and CT-deficient proteins (*eg.* EndoIII and Y82A) impairs localization to MM strands; the binding density ratio is 1. Protein samples that are 99% oxidized generated anaerobically using DNA electrochemistry also do not redistribute to MM strands, likely due to the >500-fold increase in binding affinity. Redistribution of oxidized EndoIII, however, can be restored with addition of reduced DinG. The same phenomenon was seen in the reciprocal experiment with oxidized DinG and reduced EndoIII. These data underscore that long-range redox signaling between [4Fe4S] enzymes is dependent on the shared DNA-bound redox potential and CT proficiency of the protein.

Complementary genetics assays were developed using strains of *E. coli* engineered to depend sensitively on the repair activity of MutY or DinG for growth [14, 54]. For example, to examine DinG repair activity of R-loops *in vivo*, a strain was used in which an essential and highly-expressed ribosomal gene was inverted, which causes collisions between transcription and replication machinery, formation of R-loops at those collisions, and requires DinG repair of R-loops for cell survival [54]. Putative redox signaling networks can be disrupted by genetically knocking out a signaling partner [14, 54]. Limited growth in the knocked out strains therefore points to diminished repair activity occurring, owing to limited availability of signaling partners (**Figure 1.6**, Top Right). Complementation plasmids for EndoIII, which include WT enzyme, Y82A, and D138A have been used to monitor how rescue with wild type and EndoIII mutants can restore survival. With this genetic approach, evidence of signaling among BER enzymes and DinG has been found to be necessary for repair activity and growth of cells. Rescue with the CT-competent but enzymatically deficient D138A, but not the CT-deficient but enzymatically competent Y82A, restores growth in EndoIII knockouts. These data demonstrate that CT proficiency and not enzymatic activity is needed for redox signaling and efficient repair activity in other pathways.

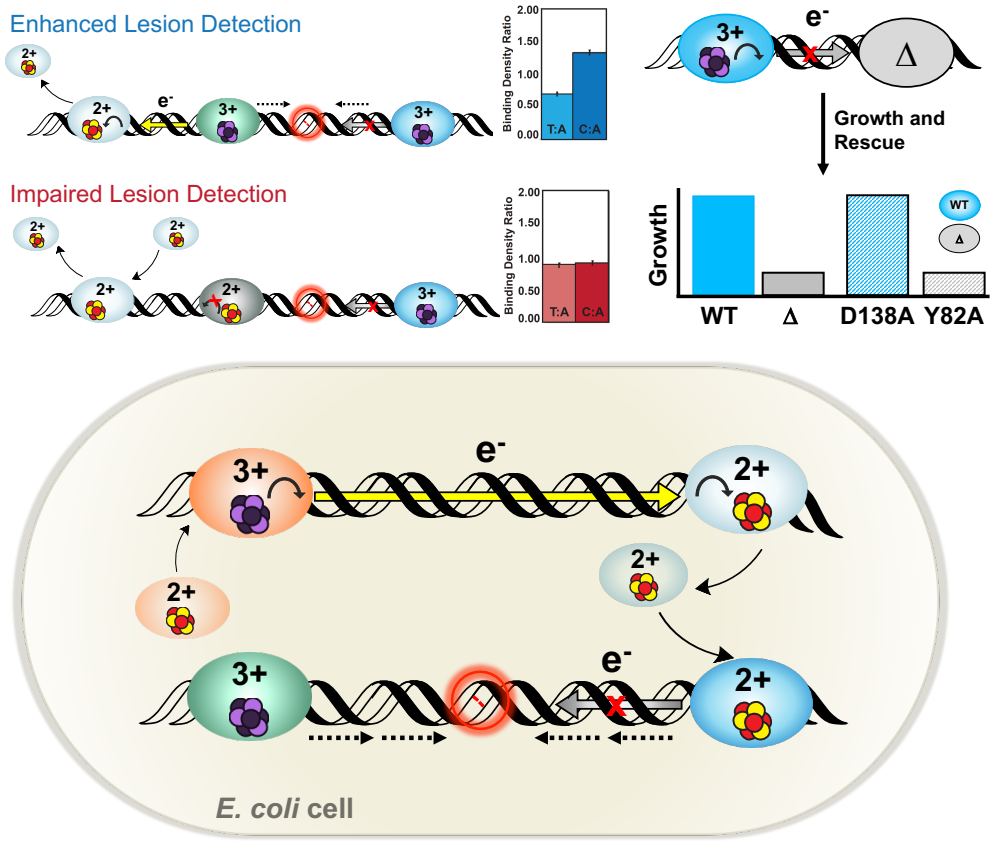

Figure 1.6 DNA-mediated redox signaling among DNA repair enzymes containing [4Fe4S] clusters. (*Top Left*) The atomic force microscopy (AFM) redistribution assay. A greater binding density of [4Fe4S] repair proteins is found on 3.8-kb duplex strands containing an engineered C:A MM compared to the WM strand, even though the MM is not a substrate for [4Fe4S] repair proteins (blue bar graph). If the protein is deficient in DNA CT, the binding density is the same for MM and WM strands (red bar graph) [14, 54, 119, 130, 132]. (*Top Right*) Genetics assays for detection of DNA-mediated redox signaling among *E. coli* [4Fe4S] repair proteins [14, 54]. Rescue plasmids expressing CT-proficient (D138A) or CT-deficient (Y82A) variants of EndoIII are introduced to Δ*nth* (EndoIII knockout) *E. coli* strains (Δ, gray) that report on the repair activity of a putative signaling partner to evaluate if the parent phenotype (blue) can be rescued (bar graph). Rescue can be achieved only with a CT-proficient enzyme (light blue bar vs light gray bar), indicating that DNA-mediated redox signaling is necessary for efficient repair. (*Bottom*) A model for DNA-mediated redox signaling network among repair proteins [5, 46]. DNA binding activates the native $[4Fe4S]^{2+}$ state toward oxidation, leading to a > 500-fold increase in DNA-binding affinity in the $[4Fe4S]^{3+}$ state. Oxidized proteins remain bound and diffuse along the DNA until another $[4Fe4S]^{2+}$ protein bound at a distal site can reduce the oxidized protein, effectively scanning the intervening DNA for lesions through DNA CT. On damaged strands, redox signaling is disrupted and any nearby oxidized proteins remain bound. Thus, DNA CT allows repair proteins to scan large sections of the genome and redistribute to areas containing damage.

1.4.5 A Model for Scanning the Genome Utilizing DNA CT Chemistry

To describe how DNA-mediated CT chemistry could be utilized for more efficient lesion detection, we developed a model for redox signaling among a network of [4Fe4S] repair proteins (**Figure 1.6,**, Bottom) [14, 16, 54, 119, 130, 132]. Upon association of freely-diffusing protein in the $[4Fe4S]^{2+}$ state onto duplex DNA, the protein is activated toward oxidation and can reduce a distally bound protein from the $[4Fe4S]^{3+}$ state to the more weakly binding $[4Fe4S]^{2+}$ state. Alternatively, guanine radicals ($G^{\bullet+}$), a product of oxidative stress, can generate the $[4Fe4S]^{3+}$ species by DNA CT over long molecular distances [12, 101, 144]. Iterations of this CT can occur across the genome, providing a rapid CT scan for the integrity of the genome, and redistributing the repair proteins in the vicinity of lesions. In these regions, if there is a lesion that attenuates CT, redox signaling between the cluster proteins is interrupted. Both proteins in the tightly-binding $[4Fe4S]^{3+}$ state persist on the DNA and can localize by facilitated diffusion to the precise site of damage. Thus DNA CT aids in the first step of repair proteins finding and localizing in the vicinity of lesions.

1.4.6 Diseases and Cancers Related to Mutations in [4Fe4S] Proteins

Mutations linking cancer with compromised repair activity by human [4Fe4S] proteins have been reported [5, 88]. Investigations into the redox chemistry of mutant proteins has helped illuminate how impaired redox signaling capacity could contribute to disease. For example, Y82 in EndoIII from *E. coli* parallels in structural position of Y166 in MUTYH. As discussed, the Y82A mutant is CT-deficient, and this parallel Y166S mutation has been known to be associated with MAP colorectal cancers [23, 49]. Within the context of DNA CT chemistry, a mutation which compromises the CT proficiency of one repair protein could understandably lead to compromised crosstalk of [4Fe4S] repair pathways across the genome.

Perhaps more directly, a novel MUTYH germline variant, C306W, was recently found in a patient with colonic polyposis and a family history of early-onset colon cancer [88]. Mutation of C306, a [4Fe4S] cluster-ligating cysteine, does not fully abolish cluster loading or DNA-bound redox activity, but is destabilizing, leading to rapid oxidative degradation of the [4Fe4S] cluster to the $[3Fe\text{-}4S]^{+1}$ species on a DNA electrode, which has not been seen for the WT enzyme. Degradation of the cluster results in diminished binding to DNA substrates and enzymatic function. The C306W mutant is a powerful example of how cluster degradation disrupts enzymatic activity and redox signaling, emphasizing the critical role of the cluster in

preventing onset of disease. Moreover, this degradation occurs only with oxidation, underscoring the important role of the cluster in carrying out redox chemistry.

Mutations in XPD have also been linked to disease, in particular, to three distinct but related disorders with extreme photosensitivity: trichothiodystrophy (TTD), Cockayne syndrome (CS), and xeroderma pigmentosum (XP) [18, 43]. Crystal structures of XPD have helped illuminate how common mutations in different domains of XPD lead to specific disorders [39, 142]. For example, the L325V mutation (from *Sulfolobus acidocaldarius*, L461 in human XPD), specifically associated with XP and TTD, is CT-deficient relative to the WT enzyme, with diminished ability to distinguish well-matched versus mismatched strands in our AFM assay [130]. Another mutation, G34R (also from *S. acidocaldarius*, G47R in human XPD), is associated with loss of ATP binding and helicase activity. Consistent with these data, the G34R mutant did not exhibit enhanced electronic coupling upon addition of ATP on DNA-modified electrodes [96]. Thus, these disease-relevant mutations not only impair enzymatic activity, but also diminish redox signaling capacity.

The study of the redox chemistry and cooperative signaling between disease-relevant mutants has exemplified intimate connections between cluster stability, enzymatic activity, redox activity, and CT proficiency [43]. Mutations in other [4Fe4S] proteins may also affect enzymatic or redox signaling activity, and we expect that many heretofore uncharacterized clinically relevant mutations will be linked to compromised redox signaling. The cluster within these proteins thus represents an intriguing new therapeutic target.

1.4.7 Redox-Mediated Catalysis by [4Fe4S] Radical SAM Enzymes

For all of the proteins described thus far, the [4Fe4S] cluster has been involved in redox chemistry but not directly in the enzymatic reaction carried out by the protein. This contrasts the more than 100,000 known radical *S*-adenosyl-L-methionine (SAM) enzymes [79, 84]. Radical SAM enzymes, some of which repair or modify nucleic acid substrates, employ the tunable, versatile [4Fe4S] cluster cofactor to catalyze essential biochemical reactions in multiple metabolic pathways [1, 9, 76, 79, 86, 127]. It is important to note that these proteins, unlike those that carry out redox signaling, contain ferredoxin-like clusters coordinated by three cysteines, which cycle between the $[4Fe4S]^{+}$ and $[4Fe4S]^{2+}$ states during activity. The primary reaction catalyzed by the redox function of the cluster is the generation of a 5′-deoxyadenosyl (5′-dA•) radical, a powerful, aliphatic oxidant which then cat-

alyzes further biochemical reactions. For radical SAM proteins that act on nucleic acids, comparison of the redox potentials of the $[4Fe4S]^{2+/1+}$ couple in the presence and absence of substrates will be interesting to consider regarding the chemistry driving catalysis.

1.5 EUKARYOTIC DNA POLYMERASES COORDINATING [4FE4S] CENTERS

Diverse, specialized replication enzymes, many of which contain [4Fe4S] clusters, duplicate large eukaryotic genomes with high fidelity [44, 93]. DNA primase, B-family polymerases α (Pol α), δ (Pol δ), and ε (Pol ε), the helicase-nuclease Dna2, and the translesion DNA polymerase ζ (Pol ζ) all contain a [4Fe4S] cofactor [75, 99, 113, 138]. These multisubunit enzymes, along with the replicative helicase (CMG), processivity factors such as proliferating cell nuclear antigen (PCNA), replication factor c (RFC), and single-stranded binding protein Replication Protein A (RPA), work together to coordinate replication [4, 24, 71, 85, 98, 146]. Before polymerases can synthesize new DNA, replication origin sites in the genome must be recognized and licensed before more factors, including DNA Pol ε, can form the pre-initiation complex [34, 40, 68]. Once active, the replicative helicase complex then unwinds AT-rich DNA at origin sites, initiating bidirectional replication on the two parent strands of genomic DNA, a process which is spatiotemporally regulated through kinase phosphorylation [78, 95, 109]. After annealing and origin firing, polymerases then begin DNA synthesis.

1.5.1 DNA Polymerase-α-Primase Begins Replication through Coordinated Binding and Dissociation Events

DNA polymerase-α-primase (pol-prim) is the heterotetrameric complex responsible for synthesizing an RNA-DNA primer which begins DNA synthesis on a template [22]. Primase consists of an RNA polymerase subunit p48 and a regulatory subunit p58, and synthesizes a 8-14 nt (nucleotides) RNA primer on ssDNA [2, 41, 77]. Polymerase α consists of a catalytic subunit p180 and an auxiliary subunit p70 and synthesizes a ~10-30 nt DNA segment downstream of the RNA primer. The C-terminal domain of the primase auxiliary subunit (p58C), and putatively the C-terminal domain of the Pol α catalytic subunit (p180), coordinate [4Fe4S] cofactors [75, 99, 138]. To synthesize RNA/DNA primers, primase first binds ssDNA and two nucleotide triphosphates (NTPs). After substrate binding and synthesis of a phosphodiester bond between NTPs, primase is converted to the active form. Pri-

mase then rapidly elongates the primer, and finally truncates synthesis, handing off the template to Pol α [2, 41, 99, 103]. After this transfer step, Pol α binds the RNA/DNA template and deoxynucleotide triphosphates (dNTPs), polymerizing ~10-30 dNTPs downstream of the RNA primer. After this sequence is completed, DNA polymerases ε and δ can take over replication.

Primase and Pol α contain [4Fe4S] clusters, but are otherwise structurally and functionally distinct from Pol δ and Pol ε [22, 77]. Primase and Pol α are heterodimers containing catalytic and regulatory subunits. These low-fidelity enzymes lack a proofreading exonuclease domain and have error rates of ~10^{-2} and ~10^{-5}-10^{-4} respectively, and unlike Pol ε and Pol δ, Pol α and primase also do not interact with PCNA [2, 22, 41, 77]. Primase [4Fe4S] cluster assembly and fidelity are, moreover, negatively affected by oxidative stress conditions in the cell [81], suggesting cluster sensitivity to the redox environment.

The [4Fe4S] cluster of DNA primase was recently discovered to function as a redox switch, regulating DNA binding and signaling [104]. The [4Fe4S] domain of primase, p58C, can independently bind DNA [81, 134]. On a DNA-modified electrode, this protein was anaerobically oxidized and re-reduced using bulk electrolysis. Subsequent CV scans showed that the oxidized $[4Fe4S]^{3+}$ protein was bound to the DNA electrode with the cluster signal evident, while the reduced $[4Fe4S]^{2+}$ form could not be detected; the reduced form was only loosely associated [104]. As we had seen with the repair proteins, the oxidation state of the cluster governed DNA binding, providing a redox switch for binding. This electrochemically controlled switch is likely mediated by conserved tyrosines that facilitate electron transfer between the cluster and the DNA binding interface (**Figure 1.7**, Left) [81, 104, 134]. Mutation of these tyrosines to phenylalanine or leucine attenuates redox activity on DNA electrodes and compromises primase initiation on ssDNA but not catalytic activity. Primase truncation is gated by DNA CT *in vitro*; a single base mismatch in a nascent primer abrogates truncation.

In a proposed model of primase-polymerase α handoff (**Figure 1.7**, Left), oxidized, tightly bound $[4Fe4S]^{3+}$ primase, coupled into the RNA/DNA duplex, synthesizes the RNA primer. When a reduced $[4Fe4S]^{2+}$ polymerase α cluster contacts the RNA/DNA duplex, polymerase α is oxidized by primase with DNA CT through the nascent RNA/DNA helix. Our results with human DNA primase indicated that a mismatch formed in the growing DNA/RNA hybrid inhibited the handoff, consistent with the idea that DNA CT facilitated this rapid, long range signaling. Through CT, polymerase α becomes tightly bound in the $[4Fe4S]^{3+}$form, and primase is reduced

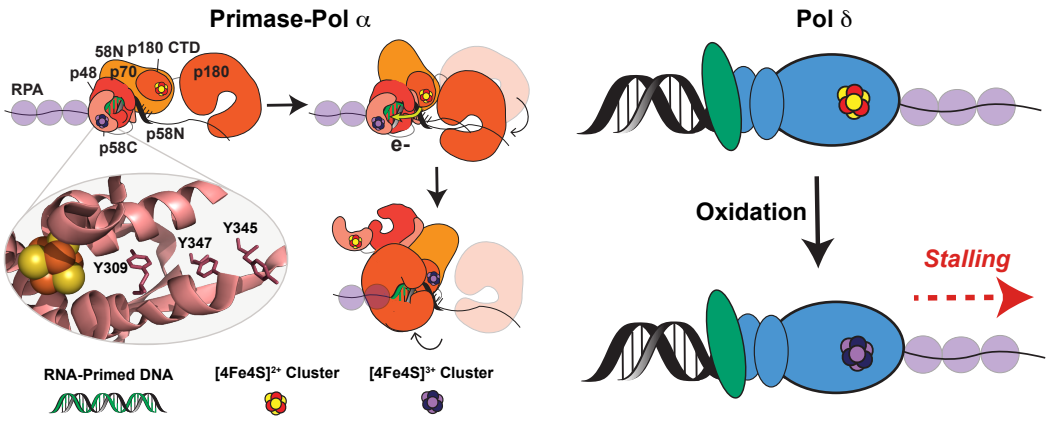

Figure 1.7 Models for redox-mediated regulation of Primase-Pol α and Pol δ activity during replication. (*Left*) Primase in the oxidized 3+ state (purple and blue) is bound to the RNA/DNA primer during primer synthesis, and when the RNA primer reaches appropriate length, Pol α, which is in the 2+ state (red and yellow), can be oxidized by Primase through DNA charge transport through the RNA:DNA hybrid segment (green and black strand). Reduced Primase then dissociates and the handoff is completed when Pol α continues synthesizing DNA. Shown are three conserved tyrosine residues positioned between the cluster and p58C DNA-binding domain (Protein Data Bank ID 3L9Q) [104, 134]. (*Right*) In complex with PCNA, Pol δ accomplishes lagging strand synthesis during replication. When replication stress occurs, stalling of Pol δ can occur by transfer of an electron from the $[4Fe4S]^{2+}$ cluster (red and yellow) to an acceptor (ex. guanine radicals, another [4Fe4S] protein) or by direct oxidation of the Pol δ when in complex with DNA. In the 3+ state (purple and blue), Pol δ stalls until damage resolution [6].

to the $[4Fe4S]^{2+}$ form. Primase dissociates from the substrate, allowing polymerase α to bind and synthesize DNA on the template. Redox switching driven by [4Fe4S] cofactors thus may coordinate these binding and dissociation events.

We recently observed that the redox-driven DNA binding switch is conserved in yeast as well as human primase [105]. On DNA electrodes, oxidized $[4Fe4S]^{3+}$ p58C is tightly bound, whereas reduced $[4Fe4S]^{2+}$ p58C is loosely associated with DNA in yeast and human systems. Yeast and human redox switches, moreover, are mediated by conserved tyrosines positioned between the p58C DNA binding interface and [4Fe4S] cluster. Remarkably the tyrosines are positioned differently, but mediate the same chemistry in yeast and human primase. Mutations at Y397 in yeast primase moreover cause partial loss of redox signaling and lead to oxidative degradation to a $[3Fe4S]^{+}$ species on DNA. This effect is severe enough to cause lethality in yeast for the p58C Y397L mutation, underscoring the importance of this redox signaling chemistry in essential replication processes.

1.5.2 DNA Polymerases ε and δ Divide Labor between Leading and Lagging Strands

Pol ε and Pol δ are the larger, high-fidelity polymerases responsible for DNA synthesis on the leading and lagging strands, with proofreading $3'\rightarrow5'$ exonuclease domains and mutation rates of ~10^{-6}-10^{-5} and ~10^{-6}-10^{-4}, respectively [22, 45]. PCNA binding moreover enhances the intrinsic processivity of both enzymes. The high intrinsic polymerase fidelity (with aide in overall replication fidelity from mismatch repair machinery) is necessary for these enzymes, as their products remain in the daughter DNA copy. Pol-prim products, on the other hand, are removed during Okazaki Fragment maturation.

The division of replicative labor has been extensively debated and investigated [73, 82, 89, 90]. Studies monitoring ribonucleotide or mispaired base incorporation in an RnaseH knockout cell line by error-prone Pol ε or Pol δ mutants has illuminated the distribution of DNA synthesis. A Pol ε variant, *pol2*M644G, causes ribonucleotide incorporation on the leading strand [82, 90]. A low-fidelity polymerase δ variant, *pol3*L612M, conversely causes an increase in replication errors, localized on the lagging strand [89]. Although Pol δ can replicate the leading strand templates under certain conditions, Pol ε putatively synthesizes the leading strand and Pol δ, the lagging strand under normal conditions [73].

The four-subunit Pol ε holoenzyme has a large polymerase subunit, Pol2, which contains two [4Fe4S] clusters. The first cluster, located within the active polymerase domain, is essential for polymerase activity but dispensable for exonuclease activity [69]. The second [4Fe4S] cluster is ligated in the Pol2 C-terminal domain, further from the active polymerase site, and is stabilized by coordination with Dpb2 [103]. The Dpb2 subunit of Pol ε is associated with the C-terminus of Pol2 and is essential for replisome assembly and checkpoint activation [22]. The noncatalytic Dpb3 and Dpb4 subunits likely enhance polymerase ε processivity. Characterizing the putative [4Fe4S] clusters in polymerase ε will illuminate new roles for DNA-mediated redox signaling in replication in the context of a complex, multisubunit enzyme.

The three-subunit Pol δ coordinates a [4Fe4S] cluster in the Pol3 subunit catalytic domain. Pol δ auxiliary subunit Pol31 associates with Pol3 to stabilize the cluster [99] and the subunit, Pol32 [22, 45]. After replication factor C loads PCNA onto DNA, Pol δ coordinates with PCNA to extend the Okazaki fragments begun by pol-prim [133, 147]. PCNA binding greatly enhances Pol δ processivity, and biochemical evidence suggests that a conformational switch may occur during polymerase δ PCNA binding and activity [45]. Pol δ moreover is uniquely capable

of strand displacement synthesis [22], consistent with its role in Okazaki fragment maturation, interacting with protein partners like Dna2. Pol δ is additionally stabilized in the presence of stalled forks during replication stress and may play a role in response to changes in the environment [32].

Pol δ has been demonstrated electrochemically to be redox-active on DNA, with a midpoint potential near 100 mV vs. NHE in the presence of PCNA (**Figure 1.7**, Right) [6]. With PCNA bound, Pol δ already binds very tightly to DNA, so it is difficult to consider the cluster oxidation to function as a redox switch for binding. Instead what we observe is that oxidation to the $[4Fe4S]^{3+}$ state slows polymerase activity *in vitro*, an effect which can be electrochemically reversed by reducing the protein back to the $[4Fe4S]^{2+}$ state. These results inspired a model where PCNA-bound, reduced $[4Fe4S]^{2+}$ Pol δ processively synthesizes DNA. Under oxidizing conditions, the cluster is converted to the $[4Fe4S]^{3+}$ form, inducing tighter DNA binding, so tight as to stall activity. Pol δ then remains stalled in the oxidized form, consistent with the stalling of Pol δ found under conditions of oxidative stress [10]. While repair proteins then may be activated with cluster oxidation under conditions of oxidative stress, replication would be inhibited. However, the polymerase can be re-reduced and restored to the processive form after DNA damage resolution, potentially through long range signaling using DNA CT from repair proteins (**Figure 1.8**). Thus here the cluster may function as a redox switch to stall replication under conditions of oxidative stress. Clearly, this signaling needs still to be established, though the electrochemistry and biochemistry show that this long range signaling is possible.

1.6 MORE [4FE4S] PROTEINS IN DNA PROCESSING

In addition to the primary replicative eukaryotic DNA polymerases, several other enzymes have now been discovered to contain [4Fe4S] cofactors [61, 113, 148]. Dna2 is a [4Fe4S] helicase-nuclease enzyme important in double strand break repair, Okazaki fragment maturation, and processing stalled replication forks [150]. The cluster in Dna2 is located in the nuclease domain, approximately 10 Å from the bound ssDNA substrate. The 5′-flap endonuclease activity is primarily associated with processing of long flaps during Okazaki fragment maturation [22]. Dna2 also plays a role in preventing regression of stalled replication forks, however, and the enzyme has weak ATP-dependent helicase activity [21, 63]. Dna2 function, especially helicase and nuclease coordination, is still unclear; [4Fe4S] redox signaling may be

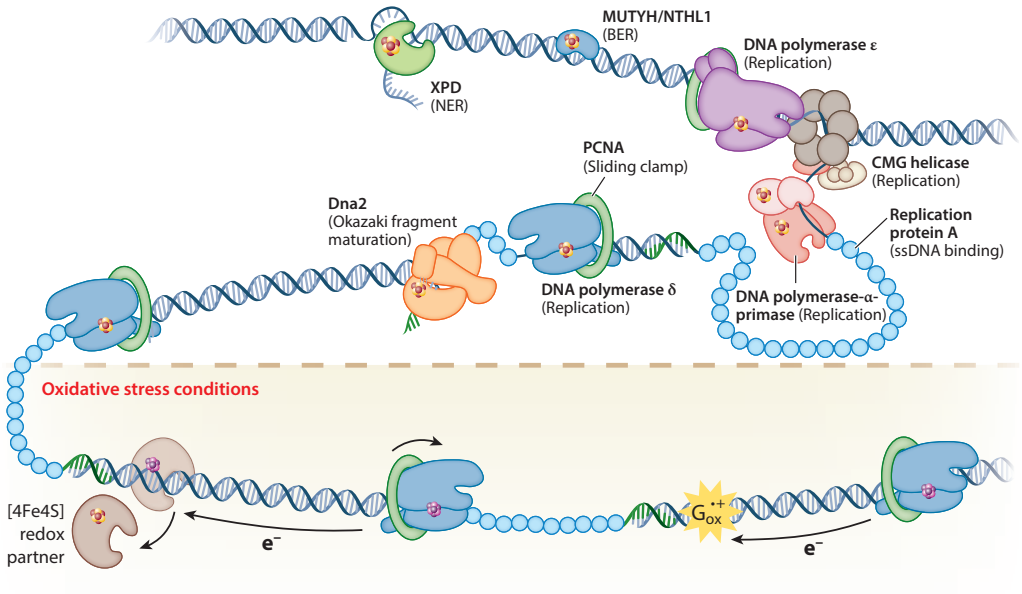

Figure 1.8 [4Fe4S] enzymes in eukaryotic repair and replication. B-family polymerases, DNA primase, Dna2 helicase-nuclease, and BER/NER enzymes such as NTHL1, MUTYH, and XPD all coordinate a [4Fe4S] cluster cofactor. Several of these proteins have been demonstrated to participate in DNA-mediated redox signaling; characterization of their redox roles is ongoing. Under oxidative stress conditions, Pol δ may be converted to the $[4Fe4S]^{3+}$ state as a means to stall synthesis under poor cellular conditions. Pol δ can be reversibly oxidized and reduced through DNA charge transport, which may regulate polymerase activity on the lagging strand [5, 6, 88, 104]. Additional abbreviations: CMG, Cdc45/Mcm2–7/GINS; PCNA, proliferating cell nuclear antigen.

important for regulating the multiple cellular roles for Dna2 and its interaction with other [4Fe4S] enzymes, such as Pol δ.

The translesion polymerase Pol ζ also contains a [4Fe4S] cluster, coordinated in the Rev3 catalytic subunit [85, 99], which is homologous to other B-family polymerase catalytic subunits. This enzyme also contains a subunit Rev7, and two subunits found in Pol δ, Pol31 and Pol32, but lacks an exonuclease domain. Interacting with PCNA and many other replication factors, Pol ζ catalyzes mutagenic polymerase activity in the presence of lesions that stall replication fork progression [85]. Additionally, RNA polymerase II, which synthesizes RNA during transcription, has been demonstrated to contain a [4Fe4S] cluster in methanogens [61, 70, 85]. Finally, Cas4 and PhrB have also been observed to coordinate [4Fe4S] clusters in some species of bacteria [148, 149]. Cas4 is an exonuclease part CRISPR (clustered regularly interspaced short palindromic repeats) adaptive immunity while PhrB, part of a class of iron-sulfur bacterial cryptochromes and photolyases (Fes BCPs),

is a photolyase that directly repairs (6-4) photoproducts that arise following UV damage. These proteins may use redox signaling on DNA to coordinate activity in cells, and investigation of their [4Fe4S] redox properties will illuminate important biochemical features of the proteins and their pathways.

1.7 IDENTIFYING NEW [4FE4S] CENTERS IN DNA PROCESSING ENZYMES

Several have noted that given how many new [FeS] proteins have been identified in the past three decades that carry out essential cellular functions, many more [FeS] proteins would be reasonably expected to be discovered across all domains of life [29, 43, 121]. To underscore this point, the [4Fe4S] cofactor for the overwhelming majority of DNA repair and replication enzymes has been discovered years to decades after initial characterization of the gene or gene product. Moreover, even for a well-studied model organism like *E. coli*, a large percentage of gene functions are still uncharacterized or poorly annotated [64]. New [FeS] enzymes from entirely new protein families may also await discovery within this group of genes without known function (known as the y-ome) [47].

Informed by trends in previous discoveries, our group hypothesized that other DNA repair enzymes also likely coordinated [4Fe4S] centers that had not been observed. Focusing on *E. coli*, we noted that glycosylases (EndoIII and MutY) and SF2 helicases (DinG and likely YoaA), enzymes in major repair pathways, are known to coordinate [4Fe4S] clusters. However, a [4Fe4S] center in a protein from another major pathway, NER, had not yet been identified in prokaryotes. This is in contrast to archaeal and eukaryotic organisms (see discussion of XPD above). Our group made the observation that the sequence of a bacterial NER enzyme, UvrC, contained four atypically-spaced cysteine residues of unknown function in an N-terminal region that had already been characterized in the literature as cysteine-rich. The residues - C154, C166, C174, and C178 - were not spaced suitably to coordinate a metal like zinc (common in proteins that bind to DNA), but were reminiscent of the spacing found in the other bacterial [4Fe4S] repair proteins. During my thesis work, I have focused on UvrC and described here is the evolution of my research on this enzyme. Chapter 2 includes a summary of early observations of the [4Fe4S] center and my demonstration that the [4Fe4S] center was prone to degradation in an aerobic environment. Chapter 3 details my development of anaerobic methods to study UvrC under stable conditions, which enabled broad characterization of UvrC

as a metalloprotein. In Chapter 4, I describe ongoing efforts to generate stable, apo species of UvrC. Finally, in Chapter 5, I provide a summary of my thesis work and perspective on new research opportunities to investigate UvrC and the bacterial NER pathway anew in the context of the [4Fe4S] cofactor.

References

[1] B. P. Anton, L. Saleh, J. S. Benner, E. A. Raleigh, S. Kasif, and R. J. Roberts. RimO, a MiaB-like enzyme, methylthiolates the universally conserved Asp88 residue of ribosomal protein S12 in Escherichia coli. *Proceedings of the National Academy of Sciences*, 105(6):1826–1831, 2008. ISSN 0027-8424. doi: 10.1073/pnas.0708608105. URL http://www.pnas.org/cgi/doi/10.1073/pnas.0708608105.

[2] B. Arezi and R. D. Kuchta. Eukaryotic DNA primase. *Trends in Biochemical Sciences*, 25(11):572–576, 2000. ISSN 09680004. doi: 10.1016/S0968-0004(00)01680-7.

[3] D. I. Arnon, F. R. Whatley, and M. B. Allen. Triphosphopyridine nucleotide as a catalyst of photosynthetic phosphorylation. *Nature*, 180(4578):182–185, 1957. ISSN 00280836. doi: 10.1038/180182a0.

[4] A. G. Baranovskiy, N. D. Babayeva, Y. Zhang, J. Gu, Y. Suwa, Y. I. Pavlov, and T. H. Tahirov. Mechanism of Concerted RNA-DNA Primer Synthesis by the Human Primosome. *Journal of Biological Chemistry*, 291(19):10006–10020, 2016. ISSN 1083351X. doi: 10.1074/jbc.M116.717405.

[5] P. L. Bartels, E. O'Brien, and J. K. Barton. DNA signaling by iron-sulfur cluster proteins. In T. A. Rouault, editor, *Biochemistry, Biosynthesis and Human Diseases: Biochemistry, Biosynthesis, and Human Diseases*, volume 2, pages 405–423. De Gruyter, Berlin, Boston, 2017. ISBN 9783110479850. doi: 10.1515/9783110479850-015.

[6] P. L. Bartels, J. L. Stodola, P. M. Burgers, and J. K. Barton. A Redox Role for the [4Fe4S] Cluster of Yeast DNA Polymerase δ. *Journal of the American Chemical Society*, 139(50):18339–18348, 2017. ISSN 15205126. doi: 10.1021/jacs.7b10284.

[7] P. L. Bartels, A. Zhou, A. R. Arnold, N. N. Nuñez, F. N. Crespilho, S. S. David, and J. K. Barton. Electrochemistry of the [4Fe4S] Cluster in Base Excision Repair Proteins: Tuning the Redox Potential with DNA. *Langmuir*, 33(10):2523–2530, mar 2017. ISSN 15205827. doi: 10.1021/acs.langmuir.6b04581. URL http://dx.doi.org/10.1021/acs.langmuir.6b04581.

[8] H. Beinert, R. H. Holm, and E. Münck. Iron-sulfur clusters: Nature's modular, multipurpose structures. *Science*, 277(5326):653–659, 1997. ISSN 00368075. doi: 10.1126/science.277.5326.653.

[9] A. Benjdia, K. Heil, T. R. M. Barends, T. Carell, and I. Schlichting. Structural insights into recognition and repair of UV-DNA damage by Spore Photoproduct Lyase, a radical SAM enzyme. *Nucleic Acids Research*, 40(18): 9308–9318, 2012. ISSN 03051048. doi: 10.1093/nar/gks603.

[10] M. Berti and A. Vindigni. Replication stress: Getting back on track. *Nature Structural and Molecular Biology*, 23(2):103–109, 2016. ISSN 15459985. doi: 10.1038/nsmb.3163.

[11] S. K. Bharti, I. Khan, T. Banerjee, J. A. Sommers, Y. Wu, and R. M. Brosh. Molecular functions and cellular roles of the ChlR1 (DDX11) helicase defective in the rare cohesinopathy Warsaw breakage syndrome. *Cellular and Molecular Life Sciences*, 71(14):2625–2639, 2014. ISSN 14209071. doi: 10.1007/s00018-014-1569-4.

[12] A. K. Boal and J. K. Barton. Electrochemical detection of lesions in DNA. *Bioconjugate Chemistry*, 16(2):312–321, 2005. ISSN 10431802. doi: 10.1021/bc0497362.

[13] A. K. Boal, E. Yavin, O. A. Lukianova, V. L. O'Shea, S. S. David, and J. K. Barton. DNA-bound redox activity of DNA repair glycosylases containing [4Fe-4S] clusters. *Biochemistry*, 44(23):8397–8407, 2005. ISSN 00062960. doi: 10.1021/bi047494n. URL http://pubs.acs.org/doi/abs/10.1021/bi047494n.

[14] A. K. Boal, J. C. Genereux, P. A. Sontz, J. A. Gralnick, D. K. Newman, and J. K. Barton. Redox signaling between DNA repair proteins for efficient lesion detection. *Proceedings of the National Academy of Sciences*, 106(36): 15237–15242, sep 2009. ISSN 0027-8424. doi: 10.1073/pnas.0908059106. URL http://www.pnas.org/cgi/doi/10.1073/pnas.0908059106.

[15] E. M. Boon, J. E. Salas, and J. K. Barton. An electrical probe of protein-DNA interactions on DNA-modified surfaces. *Nature Biotechnology*, 20(3): 282–286, 2002. ISSN 10870156. doi: 10.1038/nbt0302-282.

[16] E. M. Boon, A. L. Livingston, N. H. Chmiel, S. S. David, and J. K. Barton. DNA-mediated charge transport for DNA repair. *Proceedings of the National Academy of Sciences*, 100(22):12543–12547, 2003. ISSN 0027-8424. doi: 10.1073/pnas.2035257100. URL http://www.pnas.org/cgi/doi/10.1073/pnas.2035257100.

[17] J. J. Braymer and R. Lill. Iron–sulfur cluster biogenesis and trafficking in mitochondria. *Journal of Biological Chemistry*, 292(31):12754–12763, 2017. ISSN 1083351X. doi: 10.1074/jbc.R117.787101.

[18] R. M. Brosh. DNA helicases involved in DNA repair and their roles in cancer. *Nature Reviews Cancer*, 13(8):542–558, 2013. ISSN 1474175X. doi: 10.1038/nrc3560.

[19] R. M. Brosh and S. B. Cantor. Molecular and cellular functions of the FANCJ DNA helicase defective in cancer and in Fanconi anemia. *Frontiers in Genetics*, 5:372, 2014. ISSN 16648021. doi: 10.3389/fgene.2014.00372.

[20] L. T. Brown, V. A. Sutera, S. Zhou, C. S. Weitzel, Y. Cheng, and S. T. Lovett. Connecting Replication and Repair: YoaA, a Helicase-Related Protein, Promotes Azidothymidine Tolerance through Association with Chi, an Accessory Clamp Loader Protein. *PLoS Genetics*, 11(11):e1005651, 2015. ISSN 15537404. doi: 10.1371/journal.pgen.1005651.

[21] M. E. Budd, W. C. Choe, and J. L. Campbell. The nuclease activity of the yeast Dna2 protein, which is related to the RecB-like nucleases, is essential in vivo. *Journal of Biological Chemistry*, 275(22):16518–16529, 2000. ISSN 00219258. doi: 10.1074/jbc.M909511199.

[22] P. M. Burgers and T. A. Kunkel. Eukaryotic DNA Replication Fork. *Annual Review of Biochemistry*, 86(1):417–438, 2017. ISSN 0066-4154. doi: 10.1146/annurev-biochem-061516-044709. URL http://www.annualreviews.org/doi/10.1146/annurev-biochem-061516-044709.

[23] J. P. Cheadle and J. R. Sampson. MUTYH-associated polyposis-From defect in base excision repair to clinical genetic testing. *DNA Repair*, 6(3):274–279, 2007. ISSN 15687864. doi: 10.1016/j.dnarep.2006.11.001.

[24] O. Chilkova, B.-H. Jonsson, and E. Johansson. The Quaternary Structure of DNA Polymerase ϵ from Saccharomyces cerevisiae. *Journal of Biological Chemistry*, 278(16):14082–14086, 2003. ISSN 0021-9258. doi: 10.1074/jbc.M211818200. URL http://www.jbc.org/lookup/doi/10.1074/jbc.M211818200.

[25] M. Christmann and B. Kaina. Transcriptional regulation of human DNA repair genes following genotoxic stress: Trigger mechanisms, inducible responses and genotoxic adaptation. *Nucleic Acids Research*, 41(18):8403–8420, 2013. ISSN 03051048. doi: 10.1093/nar/gkt635.

[26] A. Ciccia and S. J. Elledge. The DNA Damage Response: Making It Safe to Play with Knives. *Molecular Cell*, 40(2):179–204, 2010. ISSN 10972765. doi: 10.1016/j.molcel.2010.09.019.

[27] J. C. Crack, J. Green, A. J. Thomson, and N. E. Brun. Iron-sulfur clusters as biological sensors: The chemistry of reactions with molecular oxygen and nitric oxide. *Accounts of Chemical Research*, 47(10):3196–3205, 2014. ISSN 15204898. doi: 10.1021/ar5002507.

[28] R. P. Cunningham, H. Asahara, J. F. Bank, C. P. Scholes, J. C. Salerno, K. Surerus, E. Miinck, J. McCracken, J. Peisach, and M. H. Emptage.

Endonuclease III Is an Iron-Sulfur Protein. *Biochemistry*, 28(10):4450–4455, may 1989. ISSN 15204995. doi: 10.1021/bi00436a049. URL http://dx.doi.org/10.1021/bi00436a049.

[29] A. Cvetkovic, A. L. Menon, M. P. Thorgersen, J. W. Scott, F. L. Poole, F. E. Jenney, W. A. Lancaster, J. L. Praissman, S. Shanmukh, B. J. Vaccaro, S. A. Trauger, E. Kalisiak, J. V. Apon, G. Siuzdak, S. M. Yannone, J. A. Tainer, and M. W. Adams. Microbial metalloproteomes are largely uncharacterized. *Nature*, 466(7307):779–782, 2010. ISSN 00280836. doi: 10.1038/nature09265.

[30] S. S. David and S. D. Williams. Chemistry of Glycosylases and Endonucleases Involved in Base-Excision Repair. *Chemical Reviews*, 98(3):1221–1262, 1998. ISSN 0009-2665. doi: 10.1021/cr980321h. URL http://pubs.acs.org/doi/abs/10.1021/cr980321h.

[31] S. S. David, V. L. O'Shea, and S. Kundu. Base-excision repair of oxidative DNA damage. *Nature*, 447(7147):941–950, 2007. ISSN 14764687. doi: 10.1038/nature05978.

[32] G. De Piccoli, Y. Katou, T. Itoh, R. Nakato, K. Shirahige, and K. Labib. Replisome Stability at Defective DNA Replication Forks Is Independent of S Phase Checkpoint Kinases. *Molecular Cell*, 45(5):696–704, 2012. ISSN 10972765. doi: 10.1016/j.molcel.2012.01.007.

[33] A. Dey, F. E. Jenney, M. W. Adams, E. Babini, Y. Takahashi, K. Fukuyama, K. O. Hodgson, B. Hedman, and E. I. Solomon. Solvent tuning of electrochemical potentials in the active sites of HiPIP versus ferredoxin. *Science*, 318 (5855):1464–1468, 2007. ISSN 00368075. doi: 10.1126/science.1147753.

[34] B. P. Duncker, I. N. Chesnokov, and B. J. McConkey. The origin recognition complex protein family. *Genome Biology*, 10(3):214, 2009. ISSN 1465-6906. doi: 10.1186/gb-2009-10-3-214. URL http://genomebiology.biomedcentral.com/articles/10.1186/gb-2009-10-3-214.

[35] L. A. Ekanger, P. H. Oyala, A. Moradian, M. J. Sweredoski, and J. K. Barton. Nitric Oxide Modulates Endonuclease III Redox Activity by a 800 mV Negative Shift upon [Fe4S4] Cluster Nitrosylation. *Journal of the American Chemical Society*, 140(37):11800–11810, sep 2018. ISSN 0002-7863. doi: 10.1021/jacs.8b07362. URL https://doi.org/10.1021/jacs.8b07362.

[36] D. D. Eley and D. I. Spivey. Semiconductivity of organic substances. IX. Nucleic acid in the dry state. *Transactions of the Faraday Society*, 58:411–415, 1962. ISSN 0014-7672. doi: 10.1039/tf9625800411.

[37] L. M. Engstrom, O. A. Partington, and S. S. David. An iron-sulfur cluster loop motif in the archaeoglobus fulgidus uracil-DNA glycosylase mediates efficient uracil recognition and removal. *Biochemistry*, 51(25):5187–5197, 2012. ISSN 00062960. doi: 10.1021/bi3000462.

[38] B. Ezraty, A. Vergnes, M. Banzhaf, Y. Duverger, A. Huguenot, A. R. Brochado, S. Y. Su, L. Espinosa, L. Loiseau, B. Py, A. Typas, and F. Barras. Fe-S cluster biosynthesis controls uptake of aminoglycosides in a ROS-less death pathway. *Science*, 340(6140):1583–1587, 2013. ISSN 10959203. doi: 10.1126/science.1238328.

[39] L. Fan, J. O. Fuss, Q. J. Cheng, A. S. Arvai, M. Hammel, V. A. Roberts, P. K. Cooper, and J. A. Tainer. XPD Helicase Structures and Activities: Insights into the Cancer and Aging Phenotypes from XPD Mutations. *Cell*, 133(5): 789–800, 2008. ISSN 00928674. doi: 10.1016/j.cell.2008.04.030.

[40] M. Fragkos, O. Ganier, P. Coulombe, and M. Méchali. DNA replication origin activation in space and time. *Nature Reviews Molecular Cell Biology*, 16(6):360–374, 2015. ISSN 14710080. doi: 10.1038/nrm4002.

[41] D. N. Frick and C. C. Richardson. DNA primases. *Annual Review of Biochemistry*, 70:39–80, 2001. ISSN 0066-4154. doi: 10.1146/annurev.biochem.70.1.39. URL http://www.ncbi.nlm.nih.gov/pubmed/11395402.

[42] W. Fu, S. O'Handley, R. P. Cunningham, and M. K. Johnson. The role of the iron-sulfur cluster in Escherichia coli endonuclease III. A resonance Raman study. *Journal of Biological Chemistry*, 267(23):16135–16137, 1992. ISSN 00219258.

[43] J. O. Fuss, C. L. Tsai, J. P. Ishida, and J. A. Tainer. Emerging critical roles of Fe-S clusters in DNA replication and repair. *Biochimica et Biophysica Acta - Molecular Cell Research*, 1853(6):1253–1271, 2015. ISSN 18792596. doi: 10.1016/j.bbamcr.2015.01.018. URL http://dx.doi.org/10.1016/j.bbamcr.2015.01.018.

[44] R. A. Ganai and E. Johansson. DNA Replication - A Matter of Fidelity. *Molecular Cell*, 62(5):745–755, jun 2016. ISSN 1097-2765. doi: 10.1016/j.molcel.2016.05.003. URL http://dx.doi.org/10.1016/j.molcel.2016.05.003.

[45] P. Garg and P. M. J. Burgers. DNA polymerases that propagate the eukaryotic DNA replication fork. *Critical Reviews in Biochemistry and Molecular Biology*, 40(2):115–128, 2005. ISSN 10409238. doi: 10.1080/10409230590935433.

[46] J. C. Genereux and J. K. Barton. Mechanisms for DNA charge transport. *Chemical Reviews*, 110(3):1642–1662, 2010. ISSN 00092665. doi: 10.1021/cr900228f. URL http://pubs.acs.org/doi/abs/10.1021/cr900228f.

[47] S. Ghatak, Z. A. King, A. Sastry, and B. O. Palsson. The y-ome defines the 35experimental evidence of function. *Nucleic Acids Research*, 47(5): 2446–2454, 2019. ISSN 13624962. doi: 10.1093/nar/gkz030.

[48] B. Giese, M. Graber, and M. Cordes. Electron transfer in peptides and proteins. *Current Opinion in Chemical Biology*, 12(6):755–759, 2008. ISSN 13675931. doi: 10.1016/j.cbpa.2008.08.026.

[49] M. P. Golinelli, N. H. Chmiel, and S. S. David. Site-directed mutagenesis of the cysteine ligands to the [4Fe-4S] cluster of Escherichia coli MutY. *Biochemistry*, 38(22):6997–7007, jun 1999. ISSN 00062960. doi: 10.1021/bi982300n. URL https://doi.org/10.1021/bi982300n.

[50] J. Gorman and E. C. Greene. Visualizing one-dimensional diffusion of proteins along DNA. *Nature Structural and Molecular Biology*, 15(8):768–774, 2008. ISSN 15459993. doi: 10.1038/nsmb.1441.

[51] A. A. Gorodetsky, A. K. Boal, and J. K. Barton. Direct Electrochemistry of Endonuclease III in the Presence and Absence of DNA. *Journal of the American Chemical Society*, 128(37):12082–12083, sep 2006. ISSN 0002-7863. doi: 10.1021/ja064784d. URL http://dx.doi.org/10.1021/ja064784dhttp://pubs.acs.org/doi/abs/10.1021/ja064784d.

[52] H. B. Gray and J. R. Winkler. Electron flow through metalloproteins. *Biochimica et Biophysica Acta - Bioenergetics*, 1797(9):1563–1572, 2010. ISSN 00052728. doi: 10.1016/j.bbabio.2010.05.001.

[53] H. B. Gray, E. I. Stiefel, J. S. Valentine, and I. Bertini. *Bioinorganic Chemistry*. University Books, 2006. ISBN 1891389432.

[54] M. A. Grodick, H. M. Segal, T. J. Zwang, and J. K. Barton. DNA-mediated signaling by proteins with 4Fe-4S clusters is necessary for genomic integrity. *Journal of the American Chemical Society*, 136(17):6470–6478, 2014. ISSN 15205126. doi: 10.1021/ja501973c.

[55] Y. Guan, R. C. Manuel, A. S. Arvai, S. S. Parikh, C. D. Mol, J. H. Miller, R. S. Lloyd, and J. A. Tainer. MutY catalytic core, mutant and bound adenine structures define specificity for DNA repair enzyme superfamily. *Nature Structural Biology*, 5(12):1058–1064, 1998. ISSN 10728368. doi: 10.1038/4168.

[56] M. Guo, K. Hundseth, H. Ding, V. Vidhyasagar, A. Inoue, C. H. Nguyen, R. Zain, J. S. Lee, and Y. Wu. A distinct triplex DNA unwinding activity of ChlR1 helicase. *Journal of Biological Chemistry*, 290(8):5174–5189, 2015. ISSN 1083351X. doi: 10.1074/jbc.M114.634923.

[57] Y. Ha, A. R. Arnold, N. N. Nuñez, P. L. Bartels, A. Zhou, S. S. David, J. K. Barton, B. Hedman, K. O. Hodgson, and E. I. Solomon. Sulfur K-Edge XAS Studies of the Effect of DNA Binding on the [Fe4S4] Site in EndoIII and MutY. *Journal of the American Chemical Society*, 139(33):11434–11442, 2017. ISSN 15205126. doi: 10.1021/jacs.7b03966.

[58] D. B. Hall, R. E. Holmlin, and J. K. Barton. Oxidative DNA damage through long-range electron transfer. *Nature*, 382(6593):731–735, aug 1996. ISSN 0028-0836. doi: 10.1038/382731a0. URL http://www.nature.com/doifinder/10.1038/382731a0.

[59] J. A. Hinks, M. C. Evans, Y. De Miguel, A. A. Sartori, J. Jiricny, and L. H. Pearl. An iron-sulfur cluster in the Family 4 uracil-DNA glycosylases. *Journal of Biological Chemistry*, 277(19):16936–16940, 2002. ISSN 00219258. doi: 10.1074/jbc.M200668200.

[60] A. Hirata and K. S. Murakami. Archaeal RNA polymerase. *Current Opinion in Structural Biology*, 19(6):724–731, 2009. ISSN 0959440X. doi: 10.1016/j.sbi.2009.10.006.

[61] A. Hirata, B. J. Klein, and K. S. Murakami. The X-ray crystal structure of RNA polymerase from Archaea. *Nature*, 451(7180):851–854, 2008. ISSN 14764687. doi: 10.1038/nature06530.

[62] B. V. Houten, J. Kuper, and C. Kisker. Role of XPD in cellular functions: To TFIIH and beyond. *DNA Repair*, 44:136–142, 2016. ISSN 15687856. doi: 10.1016/j.dnarep.2016.05.019.

[63] J. Hu, L. Sun, F. Shen, Y. Chen, Y. Hua, Y. Liu, M. Zhang, Y. Hu, Q. Wang, W. Xu, F. Sun, J. Ji, J. M. Murray, A. M. Carr, and D. Kong. The intra-S phase checkpoint targets Dna2 to prevent stalled replication forks from reversing. *Cell*, 149(6):1221–1232, 2012. ISSN 00928674. doi: 10.1016/j.cell.2012.04.030.

[64] P. Hu, S. C. Janga, M. Babu, J. J. Díaz-Mejía, G. Butland, W. Yang, O. Pogoutse, X. Guo, S. Phanse, P. Wong, S. Chandran, C. Christopoulos, A. Nazarians-Armavil, N. K. Nasseri, G. Musso, M. Ali, N. Nazemof, V. Eroukova, A. Golshani, A. Paccanaro, J. F. Greenblatt, G. Moreno-Hagelsieb, and A. Emili. Global functional atlas of Escherichia coli encompassing previously uncharacterized proteins. *PLoS Biology*, 7(4):0929–0947, 2009. ISSN 15457885. doi: 10.1371/journal.pbio.1000096.

[65] J. A. Imlay. Iron-sulphur clusters and the problem with oxygen. *Molecular Microbiology*, 59(4):1073–1082, 2006. ISSN 0950382X. doi: 10.1111/j.1365-2958.2006.05028.x.

[66] J. A. Imlay. The molecular mechanisms andphysiological consequences of oxidativestress: lessons from a model bacterium. *Nature Reviews Microbiology*, 11(7):443–454, may 2013. doi: 10.1038/nrmicro3032. URL http://dx.doi.org/10.1038/nrmicro3032.

[67] J. A. Imlay. Transcription Factors That Defend Bacteria Against Reactive Oxygen Species. *Annual Review of Microbiology*, 69(1):93–108, 2015. ISSN 0066-4227. doi: 10.1146/annurev-micro-091014-104322.

[68] L. M. Iyer, D. D. Leipe, E. V. Koonin, and L. Aravind. Evolutionary history and higher order classification of AAA+ ATPases. *Journal of Structural Biology*, 146(1-2):11–31, 2004. ISSN 10478477. doi: 10.1016/j.jsb.2003.10.010.

[69] R. Jain, E. S. Vanamee, B. G. Dzikovski, A. Buku, R. E. Johnson, L. Prakash, S. Prakash, and A. K. Aggarwal. An iron-sulfur cluster in the polymerase domain of yeast DNA polymerase ϵ. *Journal of Molecular Biology*, 426(2):301–308, 2014. ISSN 00222836. doi: 10.1016/j.jmb.2013.10.015.

[70] M. E. Jennings, F. H. Lessner, E. A. Karr, and D. J. Lessner. The [4Fe-4S] clusters of Rpo3 are key determinants in the post Rpo3/Rpo11 heterodimer formation of RNA polymerase in Methanosarcina acetivorans. *MicrobiologyOpen*, 6(1):e00399, 2017. ISSN 20458827. doi: 10.1002/mbo3.399.

[71] E. Johansson, J. Majka, and P. M. J. Burgers. Structure of DNA Polymerase δ from Saccharomyces cerevisiae. *Journal of Biological Chemistry*, 276(47):43824–43828, 2001. ISSN 0021-9258. doi: 10.1074/jbc.M108842200. URL http://www.jbc.org/lookup/doi/10.1074/jbc.M108842200.

[72] D. C. Johnson, D. R. Dean, A. D. Smith, and M. K. Johnson. Structure, Function, and Formation of Biological Iron-Sulfur Clusters. *Annual Review of Biochemistry*, 74(1):247–281, 2005. ISSN 0066-4154. doi: 10.1146/annurev.biochem.74.082803.133518. URL http://www.annualreviews.org/doi/10.1146/annurev.biochem.74.082803.133518.

[73] R. E. Johnson, R. Klassen, L. Prakash, and S. Prakash. A Major Role of DNA Polymerase δ in Replication of Both the Leading and Lagging DNA Strands. *Molecular Cell*, 2015. ISSN 10974164. doi: 10.1016/j.molcel.2015.05.038.

[74] S. O. Kelley and J. K. Barton. Electron transfer between bases in double helical DNA. *Science*, 283(5400):375–381, 1999. ISSN 00368075. doi: 10.1126/science.283.5400.375.

[75] S. Klinge, J. Hirst, J. D. Maman, T. Krude, and L. Pellegrini. An iron-sulfur domain of the eukaryotic primase is essential for RNA primer synthesis. *Nature Structural and Molecular Biology*, 14(9):875–877, 2007. ISSN 15459993. doi: 10.1038/nsmb1288.

[76] A. C. Kneuttinger, K. Heil, G. Kashiwazaki, and T. Carell. The radical SAM enzyme spore photoproduct lyase employs a tyrosyl radical for DNA repair. *Chemical Communications*, 49(7):722–724, 2013. ISSN 13597345. doi: 10.1039/c2cc37735g.

[77] R. D. Kuchta and G. Stengel. Mechanism and evolution of DNA primases. *Biochimica et Biophysica Acta - Proteins and Proteomics*, 1804(5):1180–1189, 2010. ISSN 15709639. doi: 10.1016/j.bbapap.2009.06.011.

[78] K. Labib and A. Gambus. A key role for the GINS complex at DNA replication forks. *Trends in Cell Biology*, 17(6):271–278, 2007. ISSN 09628924. doi: 10.1016/j.tcb.2007.04.002.

[79] N. D. Lanz and S. J. Booker. Auxiliary iron-sulfur cofactors in radical SAM enzymes. *Biochimica et Biophysica Acta - Molecular Cell Research*, 1853 (6):1316–1334, 2015. ISSN 18792596. doi: 10.1016/j.bbamcr.2015.01.002.

[80] J. S. Lenhart, J. W. Schroeder, B. W. Walsh, and L. A. Simmons. DNA Repair and Genome Maintenance in Bacillus subtilis. *Microbiology and Molecular Biology Reviews*, 76(3):530–564, 2012. ISSN 1092-2172. doi: 10.1128/MMBR.05020-11. URL `http://mmbr.asm.org/cgi/doi/10.1128/MMBR.05020-11`.

[81] L. Liu and M. Huang. Essential role of the iron-sulfur cluster binding domain of the primase regulatory subunit Pri2 in DNA replication initiation. *Protein and Cell*, 6(3):194–210, 2015. ISSN 16748018. doi: 10.1007/s13238-015-0134-8.

[82] S. A. Lujan, J. S. Williams, A. R. Clausen, A. B. Clark, and T. A. Kunkel. Ribonucleotides are signals for mismatch repair of leading-strand replication errors. *Molecular Cell*, 50(3):437–443, 2013. ISSN 10972765. doi: 10.1016/j.molcel.2013.03.017.

[83] O. A. Lukianova and S. S. David. A role for iron-sulfur clusters in DNA repair. *Current Opinion in Chemical Biology*, 9(2):145–151, 2005. ISSN 13675931. doi: 10.1016/j.cbpa.2005.02.006.

[84] S. J. Maiocco, T. L. Grove, S. J. Booker, and S. J. Elliott. Electrochemical Resolution of the [4Fe-4S] Centers of the AdoMet Radical Enzyme BtrN: Evidence of Proton Coupling and an Unusual, Low-Potential Auxiliary Cluster. *Journal of the American Chemical Society*, 137(27):8664–8667, 2015. ISSN 15205126. doi: 10.1021/jacs.5b03384.

[85] A. V. Makarova and P. M. Burgers. Eukaryotic DNA polymerase ζ. *DNA Repair*, 29:47–55, 2015. ISSN 15687856. doi: 10.1016/j.dnarep.2015.02.012.

[86] A. Marquet, D. Florentin, O. Ploux, and B. T. S. Bui. In vivo formation of C-S bonds in biotin. An example of radical chemistry under reducing conditions. *Journal of Physical Organic Chemistry*, 11(8/9):529–535, 1998. ISSN 08943230.

[87] C. G. Marsden, J. A. Dragon, S. S. Wallace, and J. B. Sweasy. Base Excision Repair Variants in Cancer. *Methods in Enzymology*, 591:119–157, 2017. ISSN 15577988. doi: 10.1016/bs.mie.2017.03.003.

[88] K. J. McDonnell, J. A. Chemler, P. L. Bartels, E. O'Brien, M. L. Marvin, J. Ortega, R. H. Stern, L. Raskin, G. M. Li, D. H. Sherman, J. K. Barton, and S. B. Gruber. A human MUTYH variant linking colonic polyposis to redox degradation of the [4Fe4S]2+cluster. *Nature Chemistry*, 10(8): 873–880, 2018. ISSN 17554349. doi: 10.1038/s41557-018-0068-x. URL https://www.nature.com/articles/s41557-018-0068-x.

[89] S. A. McElhinny, C. M. Stith, P. M. Burgers, and T. A. Kunkel. Inefficient proofreading and biased error rates during inaccurate DNA synthesis by a mutant derivative of Saccharomyces cerevisiae DNA polymerase. *Journal of Biological Chemistry*, 2007. ISSN 00219258. doi: 10.1074/jbc.M609591200.

[90] S. A. McElhinny, D. Kumar, A. B. Clark, D. L. Watt, B. E. Watts, E. B. Lundström, E. Johansson, A. Chabes, and T. A. Kunkel. Genome instability due to ribonucleotide incorporation into DNA. *Nature Chemical Biology*, 6 (10):774–781, 2010. ISSN 15524469. doi: 10.1038/nchembio.424.

[91] E. L. Mettert and P. J. Kiley. Fe-S proteins that regulate gene expression. *Biochimica et Biophysica Acta - Molecular Cell Research*, 1853(6, SI):1284–1293, jun 2015. ISSN 0167-4889. doi: 10.1016/j.bbamcr.2014.11.018.

[92] J. Meyer. Iron-sulfur protein folds, iron-sulfur chemistry, and evolution. *Journal of Biological Inorganic Chemistry*, 13(2):157–170, 2008. ISSN 09498257. doi: 10.1007/s00775-007-0318-7.

[93] U. Moran, R. Phillips, and R. Milo. SnapShot: Key numbers in biology. *Cell*, 141(7):1262, 2010. ISSN 00928674. doi: 10.1016/j.cell.2010.06.019.

[94] L. E. Mortenson, R. C. Valentine, and J. E. Carnahan. An electron transport factor from Clostridium pasteurianum. *Biochemical and Biophysical Research Communications*, 7(6):448–452, 1962. ISSN 10902104. doi: 10.1016/0006-291X(62)90333-9.

[95] S. E. Moyer, P. W. Lewis, and M. R. Botchan. Isolation of the Cdc45/Mcm2-7/GINS (CMG) complex, a candidate for the eukaryotic DNA replication fork helicase. *Proceedings of the National Academy of Sciences*, 103(27): 10236–10241, 2006. ISSN 0027-8424. doi: 10.1073/pnas.0602400103. URL http://www.pnas.org/cgi/doi/10.1073/pnas.0602400103.

[96] T. P. Mui, J. O. Fuss, J. P. Ishida, J. A. Tainer, and J. K. Barton. ATP-stimulated, DNA-mediated redox signaling by XPD, a DNA repair and transcription helicase. *Journal of the American Chemical Society*, 133(41): 16378–16381, 2011. ISSN 00027863. doi: 10.1021/ja207222t.

[97] C. J. Murphy, M. R. Arkin, Y. Jenkins, N. D. Ghatlia, S. H. Bossmann, N. J. Turro, and J. K. Barton. Long-range photoinduced electron transfer through a DNA helix. *Science*, 262(5136):1025–1029, 1993. ISSN 00368075. doi: 10.1126/science.7802858.

[98] J. R. Nelson, C. W. Lawrence, and D. C. Hinkle. Thymine-thymine dimer bypass by yeast DNA polymerase ζ. *Science*, 272(5268):1646–1649, 1996. ISSN 00368075. doi: 10.1126/science.272.5268.1646.

[99] D. J. A. Netz, C. M. Stith, M. Stümpfig, G. Köpf, D. Vogel, H. M. Genau, J. L. Stodola, R. Lill, P. M. J. Burgers, and A. J. Pierik. Eukaryotic DNA polymerases require an iron-sulfur cluster for the formation of active complexes. *Nature Chemical Biology*, 8(1):125–132, 2012. ISSN 1552-4450. doi: 10.1038/nchembio.721. URL http://www.nature.com/doifinder/10.1038/nchembio.721.

[100] D. J. A. Netz, J. Mascarenhas, O. Stehling, A. J. Pierik, and R. Lill. Maturation of cytosolic and nuclear iron-sulfur proteins. *Trends in Cell Biology*, 24(5): 303–312, 2014. ISSN 18793088. doi: 10.1016/j.tcb.2013.11.005.

[101] M. E. Núñez, D. B. Hall, and J. K. Barton. Long- range oxidative damange to DNA: effects of distance and sequence. *Chem. Biol.*, 6:85–97, 1999. URL http://www.sciencedirect.com/science?_ob=MImg&_imagekey=B6VRP-3WF782V-5-1&_cdi=6240&_user=1010281&_coverDate=02%2F28%2F1999&_sk=%23TOC%236240%231999%23999939997%2394771%23FLP%23display%23Volume_6,_Issue_2,_Pages_63-125_(February_1999)%23tagged%23Volume%23.

[102] M. E. Núñez, K. T. Noyes, and J. K. Barton. Oxidative charge transport through DNA in nucleosome core particles. *Chemistry and Biology*, 9(4): 403–415, 2002. ISSN 10745521. doi: 10.1016/S1074-5521(02)00121-7.

[103] R. Núñez-Ramírez, S. Klinge, L. Sauguet, R. Melero, M. A. Recuero-Checa, M. Kilkenny, R. L. Perera, B. García-Alvarez, R. J. Hall, E. Nogales, L. Pellegrini, and O. Llorca. Flexible tethering of primase and DNA Pol α in the eukaryotic primosome. *Nucleic Acids Research*, 39(18):8187–8199, 2011. ISSN 03051048. doi: 10.1093/nar/gkr534.

[104] E. O'Brien, M. E. Holt, M. K. Thompson, L. E. Salay, A. C. Ehlinger, W. J. Chazin, and J. K. Barton. The [4Fe4S] cluster of human DNA primase functions as a redox switch using DNA charge transport. *Science*, 355(6327): eaag1789, feb 2017. URL http://science.sciencemag.org/content/355/6327/eaag1789.abstract.

[105] E. O'Brien, L. E. Salay, E. A. Epum, K. L. Friedman, W. J. Chazin, and J. K. Barton. Yeast require redox switching in DNA primase. *Proceedings of the National Academy of Sciences of the United States of America*, 115(52): 13186–13191, 2018. ISSN 10916490. doi: 10.1073/pnas.1810715115.

[106] D. T. Odom and J. K. Barton. Long-Range Oxidative Damage in DNA/RNA Duplexes. *Biochemistry*, 40(30):8727–8737, jul 2001. ISSN 0006-2960. doi: 10.1021/bi0102961. URL https://doi.org/10.1021/bi0102961.

[107] M. A. O'Neill and J. K. Barton. 2-Aminopurine: A Probe of Structural Dynamics and Charge Transfer in DNA and DNA:RNA Hybrids. *Journal of the American Chemical Society*, 124(44):13053–13066, nov 2002. ISSN 0002-7863. doi: 10.1021/ja0208198. URL https://doi.org/10.1021/ja0208198.

[108] M. A. O'Neill, H. C. Becker, C. Wan, J. K. Barton, and A. H. Zewail. Ultrafast Dynamics in DNA-Mediated Electron Transfer: Base Gating and the Role of Temperature. *Angewandte Chemie - International Edition*, 42 (47):5896–5900, 2003. ISSN 14337851. doi: 10.1002/anie.200352831.

[109] M. Pacek, A. V. Tutter, Y. Kubota, H. Takisawa, and J. C. Walter. Localization of MCM2-7, Cdc45, and GINS to the site of DNA unwinding during eukaryotic DNA replication. *Molecular Cell*, 21(4):581–587, 2006. ISSN 10972765. doi: 10.1016/j.molcel.2006.01.030.

[110] V. D. Paul and R. Lill. Biogenesis of cytosolic and nuclear iron-sulfur proteins and their role in genome stability. *Biochimica et Biophysica Acta - Molecular Cell Research*, 1853(6):1528–1539, 2015. ISSN 18792596. doi: 10.1016/j.bbamcr.2014.12.018.

[111] C. G. Pheeney, A. R. Arnold, M. A. Grodick, and J. K. Barton. Multiplexed electrochemistry of DNA-bound metalloproteins. *Journal of the American Chemical Society*, 135(32):11869–11878, 2013. ISSN 00027863. doi: 10.1021/ja4041779.

[112] R. Phillips, J. Kondev, and J. Theriot. *Physical Biology of the Cell*. Garland Science, Taylor and Francis Group, London, 1 edition, 2008. ISBN 0815341636. doi: 10.1119/1.3459039. URL http://aapt.scitation.org/doi/10.1119/1.3459039.

[113] S. Pokharel and J. L. Campbell. Cross talk between the nuclease and helicase activities of Dna2: Role of an essential iron-sulfur cluster domain. *Nucleic Acids Research*, 40(16):7821–7830, 2012. ISSN 03051048. doi: 10.1093/nar/gks534.

[114] S. L. Porello, M. J. Cannon, and S. S. David. A Substrate Recognition Role for the [4Fe-4S] 2 + Cluster of the DNA Repair. *Biochemistry*, 37(18): 6465–6475, 1998.

[115] S. R. Rajski, B. A. Jackson, and J. K. Barton. DNA repair: Models for damage and mismatch recognition. *Mutation Research - Fundamental and Molecular Mechanisms of Mutagenesis*, 447(1):49–72, 2000. ISSN 00275107. doi: 10.1016/S0027-5107(99)00195-5.

[116] D. C. Rees and J. B. Howard. The interface between the biological and inorganic worlds: Iron-sulfur metalloclusters. *Science*, 300(5621):929–931, 2003. ISSN 00368075. doi: 10.1126/science.1083075.

[117] B. Ren, X. Duan, and H. Ding. Redox control of the DNA damage-inducible protein DinG helicase activity via its iron-sulfur cluster. *J. Biol. Chem.*, 284 (8):4829, 2009. ISSN 00219258. doi: 10.1074/jbc.M807943200.

[118] B. Roche, L. Aussel, B. Ezraty, P. Mandin, B. Py, and F. Barras. Iron/sulfur proteins biogenesis in prokaryotes: Formation, regulation and diversity. *Biochimica et Biophysica Acta - Bioenergetics*, 1827(3):455–469, 2013. ISSN 00052728. doi: 10.1016/j.bbabio.2012.12.010.

[119] C. A. Romano, P. A. Sontz, and J. K. Barton. Mutants of the base excision repair glycosylase, endonuclease III: DNA charge transport as a first step in lesion detection. *Biochemistry*, 50(27):6133–6145, jul 2011. ISSN 00062960. doi: 10.1021/bi2003179. URL http://dx.doi.org/10.1021/bi2003179.

[120] T. A. Rouault. Mammalian iron-sulphur proteins: novel insights into biogenesis and function. *Nature Reviews Molecular Cell Biology*, 16(1):45–55, jan 2015. ISSN 1471-0072. URL http://dx.doi.org/10.1038/nrm3909http://10.0.4.14/nrm3909.

[121] T. A. Rouault. Iron-sulfur proteins hiding in plain sight. *Nature Chemical Biology*, 11(7):442–445, 2015. ISSN 15524469. doi: 10.1038/nchembio.1843.

[122] T. A. Rouault and N. Maio. Biogenesis and functions of mammalian iron-sulfur proteins in the regulation of iron homeostasis and pivotal metabolic pathways. *Journal of Biological Chemistry*, 292(31):12744–12753, 2017. ISSN 1083351X. doi: 10.1074/jbc.R117.789537.

[123] L. M. Rubio and P. W. Ludden. Biosynthesis of the Cofactor of Nitrogenase. *Annual Review of Microbiology*, 62:93–111, 2008. ISSN 0066-4227. doi: 10.1146/annurev.micro.62.081307.162737. URL http://www.ncbi.nlm.nih.gov/pubmed/18429691.

[124] J. Rudolf, V. Makrantoni, W. J. Ingledew, M. J. R. Stark, and M. F. White. The DNA Repair Helicases XPD and FancJ Have Essential Iron-Sulfur Domains. *Molecular Cell*, 23(6):801–808, 2006. ISSN 10972765. doi: 10.1016/j.molcel.2006.07.019.

[125] K. Saikrishnan, J. T. Yeeles, N. S. Gilhooly, W. W. Krajewski, M. S. Dillingham, and D. B. Wigley. Insights into Chi recognition from the structure of an AddAB-type helicase-nuclease complex. *EMBO Journal*, 31(6):1568–1578, 2012. ISSN 02614189. doi: 10.1038/emboj.2012.9.

[126] R. H. Sands and H. Beinert. Studies on mitochondria and submitochondrial particles by paramagnetic resonance (EPR) spectroscopy. *Biochemical and Biophysical Research Communications*, 3(1):47–52, 1960. ISSN 10902104. doi: 10.1016/0006-291X(60)90101-7. URL http://www.sciencedirect.com/science/article/pii/0006291X60901005.

[127] E. L. Schwalm, T. L. Grove, S. J. Booker, and A. K. Boal. Crystallographic capture of a radical S-adenosylmethionine enzyme in the act of modifying tRNA. *Science*, 352(6283):309–312, 2016. ISSN 10959203. doi: 10.1126/science.aad5367.

[128] J. D. Slinker, N. B. Muren, A. A. Gorodetsky, and J. K. Barton. Multiplexed DNA-modified electrodes. *Journal of the American Chemical Society*, 132 (8):2769–2774, 2010. ISSN 00027863. doi: 10.1021/ja909915m.

[129] J. D. Slinker, N. B. Muren, S. E. Renfrew, and J. K. Barton. DNA charge transport over 34 nm. *Nature Chemistry*, 3(3):228–233, 2011. doi: http://www.nature.com/nchem/journal/v3/n3/abs/nchem.982.html#supplementary-information. URL http://dx.doi.org/10.1038/nchem.982.

[130] P. A. Sontz, T. P. Mui, J. O. Fuss, J. A. Tainer, and J. K. Barton. DNA charge transport as a first step in coordinating the detection of lesions by repair proteins. *Proceedings of the National Academy of Sciences*, 109(6): 1856–1861, 2012. ISSN 0027-8424. doi: 10.1073/pnas.1120063109. URL http://www.pnas.org/cgi/doi/10.1073/pnas.1120063109.

[131] M. M. Thayer, H. Ahern, D. Xing, R. P. Cunningham, and J. a. Tainer. Novel DNA binding motifs in the DNA repair enzyme endonuclease III crystal structure. *The EMBO journal*, 14(16):4108–20, 1995. ISSN 0261-4189. URL http://www.pubmedcentral.nih.gov/articlerender.fcgi?artid=394490&tool=pmcentrez&rendertype=abstract.

[132] E. C. M. Tse, T. J. Zwang, and J. K. Barton. The Oxidation State of [4Fe4S] Clusters Modulates the DNA-Binding Affinity of DNA Repair Proteins. *Journal of the American Chemical Society*, 139(36):12784–12792, sep 2017. ISSN 0002-7863. doi: 10.1021/jacs.7b07230. URL http://dx.doi.org/10.1021/jacs.7b07230.

[133] T. Tsurimoto and B. Stillman. Replication factors required for SV40 DNA replication in vitro. I. DNA structure-specific recognition of a primer-template junction by eukaryotic DNA polymerases and their accessory proteins. *Journal of Biological Chemistry*, 266(3):1950–1960, 1991. ISSN 00219258.

[134] S. Vaithiyalingam, E. M. Warren, B. F. Eichman, and W. J. Chazin. Insights into eukaryotic DNA priming from the structure and functional interactions of the 4Fe-4S cluster domain of human DNA primase. *Proceedings of the National Academy of Sciences*, 107(31):13684–13689, 2010. ISSN 0027-8424. doi: 10.1073/pnas.1002009107. URL http://www.pnas.org/cgi/doi/10.1073/pnas.1002009107.

[135] J. B. Vannier, G. Sarek, and S. J. Boulton. RTEL1: Functions of a disease-associated helicase. *Trends in Cell Biology*, 24(7):416–425, 2014. ISSN 18793088. doi: 10.1016/j.tcb.2014.01.004.

[136] O. N. Voloshin, F. Vanevski, P. P. Khil, and R. D. Camerini-Otero. Characterization of the DNA damage-inducible helicase DinG from Escherichia coli. *Journal of Biological Chemistry*, 278(30):28284–28293, 2003. ISSN 00219258. doi: 10.1074/jbc.M301188200.

[137] F. Wayne Outten. Recent advances in the Suf Fe-S cluster biogenesis pathway: Beyond the Proteobacteria. *Biochimica et Biophysica Acta - Molecular Cell Research*, 1853(6):1464–1469, 2015. ISSN 18792596. doi: 10.1016/j.bbamcr.2014.11.001.

[138] B. E. Weiner, H. Huang, B. M. Dattilo, M. J. Nilges, E. Fanning, and W. J. Chazin. An iron-sulfur cluster in the C-terminal domain of the p58 subunit of human DNA primase. *Journal of Biological Chemistry*, 282(46):33444–33451, 2007. ISSN 00219258. doi: 10.1074/jbc.M705826200.

[139] R. D. Weren, M. J. Ligtenberg, A. Geurts van Kessel, R. M. De Voer, N. Hoogerbrugge, and R. P. Kuiper. NTHL1 and MUTYH polyposis syndromes: two sides of the same coin? *Journal of Pathology*, 244(2):135–142, 2018. ISSN 10969896. doi: 10.1002/path.5002.

[140] M. F. White and M. S. Dillingham. Iron-sulphur clusters in nucleic acid processing enzymes. *Current Opinion in Structural Biology*, 22(1):94–100, 2012. ISSN 0959440X. doi: 10.1016/j.sbi.2011.11.004.

[141] J. R. Winkler and H. B. Gray. Electron flow through metalloproteins. *Chemical Reviews*, 114(7):3369–3380, apr 2014. ISSN 15206890. doi: 10.1021/cr4004715. URL http://pubs.acs.org/doi/abs/10.1021/cr4004715.

[142] S. C. Wolski, J. Kuper, P. Hänzelmann, J. J. Truglio, D. L. Croteau, B. Van Houten, and C. Kisker. Crystal structure of the FeS cluster-containing nucleotide excision repair helicase XPD. *PLoS Biology*, 6(6):1332–1342, 2008. ISSN 15449173. doi: 10.1371/journal.pbio.0060149.

[143] Y. Wu and R. M. Brosh. DNA helicase and helicase-nuclease enzymes with a conserved iron-sulfur cluster. *Nucleic Acids Research*, 40(10):4247–4260, 2012. ISSN 03051048. doi: 10.1093/nar/gks039.

[144] E. Yavin, A. K. Boal, E. D. A. Stemp, E. M. Boon, A. L. Livingston, V. L. O'Shea, S. S. David, and J. K. Barton. Protein-DNA charge transport: Redox activation of a DNA repair protein by guanine radical. *Proceedings of the National Academy of Sciences*, 102(10):3546–3551, 2005. ISSN 0027-8424. doi: 10.1073/pnas.0409410102. URL http://www.pnas.org/cgi/doi/10.1073/pnas.0409410102.

[145] J. T. P. Yeeles, R. Cammack, and M. S. Dillingham. An iron-sulfur cluster is essential for the binding of broken DNA by AddAB-type helicase-nucleases. *Journal of Biological Chemistry*, 284(12):7746–7755, 2009. ISSN 00219258. doi: 10.1074/jbc.M808526200.

[146] J. T. P. Yeeles, T. D. Deegan, A. Janska, A. Early, and J. F. X. Diffley. Regulated eukaryotic DNA replication origin firing with purified proteins. *Nature*, 519 (7544):431–435, 2015. ISSN 14764687. doi: 10.1038/nature14285.

[147] A. Yuzhakov, Z. Kelman, J. Hurwitz, and M. O'Donnell. Multiple competition reactions for RPA order the assembly of the DNA polymerase delta holoenzyme. *EMBO Journal*, 18(21):6189–6199, 1999. ISSN 02614189. doi: 10.1093/emboj/18.21.6189.

[148] F. Zhang, P. Scheerer, I. Oberpichler, T. Lamparter, and N. Krauss. Crystal structure of a prokaryotic (6-4) photolyase with an Fe-S cluster and a 6,7-dimethyl-8-ribityllumazine antenna chromophore. *Proceedings of the National Academy of Sciences*, 110(18):7217–7222, 2013. ISSN 0027-8424. doi: 10.1073/pnas.1302377110. URL `http://www.pnas.org/cgi/doi/10.1073/pnas.1302377110`.

[149] J. Zhang, T. Kasciukovic, and M. F. White. The CRISPR Associated Protein Cas4 Is a 5′ to 3′ DNA Exonuclease with an Iron-Sulfur Cluster. *PLoS ONE*, 7(10):e47232, 2012. ISSN 19326203. doi: 10.1371/journal.pone.0047232.

[150] C. Zhou, S. Pourmal, and N. P. Pavletich. Dna2 nuclease-helicase structure, mechanism and regulation by Rpa. *eLife*, 4:e09832, 2015. ISSN 2050084X. doi: 10.7554/eLife.09832.

Chapter 2

PREDICTION AND FIRST OBSERVATIONS OF A [4FE4S] CLUSTER COORDINATED BY UVRC*

2.1 INTRODUCTION

Maintaining the integrity of the genome is a universal challenge essential for the survival and proliferation of all species [11, 21, 22, 35, 37]. All organisms require an arsenal of repair mechanisms to confront constant endogenous and exogenous assaults on the genome by sources such as reactive oxygen species (ROS), reactive nitrogen species (RNS), stalled transcription and replication machinery, protein-DNA crosslinks, ribonucleotide incorporation, UV light, carcinogens, and other damaging agents. Unrepaired, chemical modifications of DNA resulting from damage events can have deleterious effects that lead to mutation or cell death. The complex network of pathways responsible for locating, processing, and repairing the diverse classes of DNA damage (lesions) continues to offer exciting opportunities to probe how organisms across kingdoms accomplish the overwhelming task of proofreading and replicating up to 10^9 base pairs (bp) of nuclear DNA.

2.1.1 Bulky DNA Lesions

Major classes of DNA damage that can arise in the cell include mismatches, single base lesions, bulky lesions (localized over multiple bases), and double strand breaks [35, 54, 75]. Bulky lesions are a particularly broad category of structurally and chemically diverse DNA damage types that often lead to distortion of the double helix (kinking) (**Figure 2.1**). A common, exogenous source of damage is UV light, which causes formation of photoproducts at adjacent thymine and cytosine bases (ex. thymine-thymine). Another environmental source that leads to formation of bulky lesions are polycyclic aromatic hydrocarbons (PAH) that are products of incomplete combustion from cigarette smoke, industrial processes, and automobile emissions. Benzo[*a*]pyrene adducted to DNA is one example of a PAH that forms a bulky DNA lesion. Small molecule chemotherapeutics that target DNA for cancer treatment can also form bulky lesions, as exemplified by the covalent adduct of

*Sequence alignments, spectroscopy, and associated text adapted from R. M. B. Silva, M. A. Grodick, and J. K. Barton (2020). "UvrC Coordinates an O_2-Sensitive [4Fe4S] Cofactor." *Journal of the American Chemical Society*, in press. DOI: 10.1021/jacs.0c01671

cisplatin and DNA. Even larger adducts can result from crosslinking agents, such as psoralen, which cause formation of interstand crosslinks. Psoralen is commonly used in a laboratory setting as a model for crosslinks that form from naturally-occurring sources under oxidative or nitrosylative stress. Finally, enzymes that process DNA, like topoisomerases or polymerases, can become covalently trapped on DNA duplexes forming very large adducts (not shown).

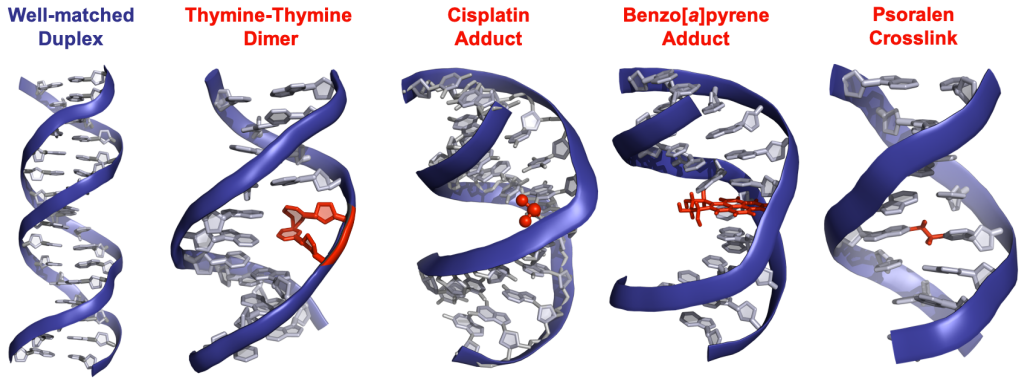

Figure 2.1 Selected examples of bulky DNA lesions. Protein Data Bank ID: 3BSE (well-matched duplex), 1N4E (thymine-thymine dimer), 1AIO (cisplatin adduct), 1JDG (benzo[*a*]pyrene adduct), 20KS (NMR, psoralen-induced crosslink).

2.1.2 Bacterial Nucleotide Excision Repair

As bulky DNA lesions can often block transcription and replication machinery, efficient detection and repair of bulky DNA lesions are vital for cellular homeostasis. The nucleotide excision repair (NER) pathway is the major DNA repair pathway conserved from bacteria to humans primarily responsible for processing bulky lesions [35, 54, 75]. In Bacteria, a remarkably simple network of proteins is involved in processing these lesions **Figure 2.2**). Bacterial NER has been most well-studied in *E. coli*, though the importance of NER for other species, particularly those that are virulent, has been more recently realized [8, 29, 45, 48]. In the classic model of bacterial NER, UvrA and UvrB initiate global genomic repair (GGR) by searching for bulky lesions in a $UvrA_2UvrB_2$ heterodimer complex. Verification of damage is followed by recruitment of the dual-incision endonuclease UvrC (also referred to as an excision nuclease or exinuclease) which then forms the active incision complex with UvrB (under some conditions, the Uvr**C** **Ho**molog, Cho, also incises strands in complex with UvrB). Distinct active sites located at the N and C termini of UvrC carry out incision of the damaged strand 5′ (C-terminal) and 3′ (N-terminal) to the site of damage. The damaged oligomer is unwound by a helicase, UvrD, and patch-

ing is completed by DNA Polymerase 1 and Ligase. Damage detection can also be initiated by transcription machinery, primarily through RNA Polymerase (RNAP) stalled at damaged sites, in a process known as transcription-coupled nucleotide excision repair (TC-NER). Following removal of stalled RNAP by UvrD and other proteins, TC-NER proceeds through the GGR UvrABCD system as shown. Interestingly, while a range of substrates are processed by bacterial NER, the efficiency of the turnover varies, where faster turnover generally occurs for larger lesions [75]. These dynamics, however, are not fully understood.

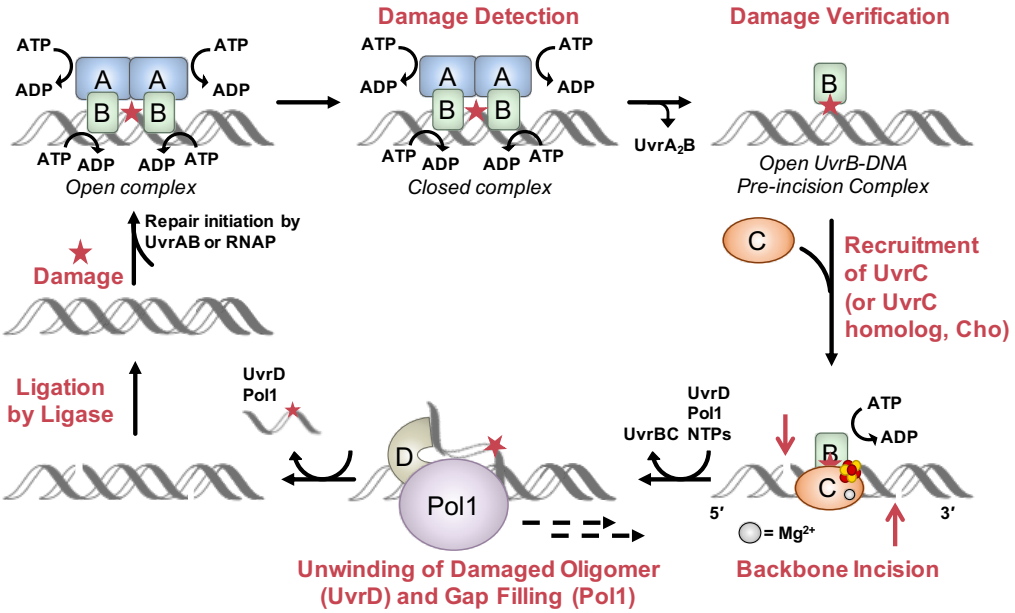

Figure 2.2 Bacterial nucleotide excision repair (NER) [35]. Upon encountering bulky, helix-distorting DNA lesions, NER is initiated by UvrAB or RNAP (top left). Damage detection and verification (top right) is followed by dual incision on the damaged strand from the UvrBC complex (or Cho in some cases, bottom right). Repair is completed by removal of the 12-13 nucleotide damaged oligomer by UvrD, gap filling by Pol1, and sealing of the nicks by ligase (bottom left). ATP is required for many of the steps in NER.

2.1.3 Ongoing Challenges in Bacterial NER Related to UvrC

Though the bacterial NER pathway has been a research focus for nearly four decades, several in the field have noted repeatedly that the UvrABCD system has been non-trivial to investigate, due in large part to the instability of UvrC *in vitro* and the scarcity of UvrC *in vivo* [35, 75]. UvrC has been noted by investigators to be uniquely challenging to purify and handle; UvrC is prone to degradation, aggregation, loss

activity over time (even when stored frozen), and precipitation in solution with itself, UvrA, UvrB, and DNA [59, 73, 75]. Though first isolated in 1981, crystal structures of UvrC or co-crystal structures in complex with a substrate or other NER proteins are also not available, which has limited searches for structural homology (again, in contrast to UvrA, UvrB, and UvrD) [35, 60, 92]. Insight has also been difficult to gain through searches for homology, because UvrC (along with Cho) comprises its own protein family of excision nucleases [35]. *In vivo*, major differences in regulation of UvrC expression and inducibility during the SOS response in comparison to UvrA, UvrB, and UvrD have continued to be perplexing [80]. For example, the expression of UvrC is not inducible by the SOS system, a cellular-wide response to DNA damage present in many bacteria [32]. This again is in contrast to UvrA, UvrB, and UvrD, which are induced during the SOS response [38]. Through early radiolabeling experiments, UvrC has been reported to be expressed between 10-20 copies/cell, though some modern techniques place the copy number up to 300 per cell (or per cell per generation) [40, 71, 80]. Other cellular-wide bacterial physiology studies have reported that UvrC expression may be inducible under some metabolic stress conditions [9, 18, 30]. Again, a range of copy numbers for UvrC were measured, and UvrC was not the main focus of these studies. Furthermore, assembly and regulation of the UvrABC complex, particularly how UvrC is recruited to the damage site *in vivo*, remains an open area of investigation [35]. Overall, efforts toward understanding the mechanisms that underlie the observed instability of UvrC and thus, what factors might stabilize UvrC and facilitate more in-depth study have remained limited. Given how essential UvrC is in removing damaged oligomers, new insight is greatly needed for this enzyme.

2.1.4 A Putative [FeS] Coordination Site in the Sequence of UvrC

Initial examination of UvrC in our group began with the sequence of the protein. Five main regions of UvrC have been identified, which include the N-terminal GIY-YIG endonuclease domain (3′ incision), a cysteine rich region, a UvrBC interacting domain, RNaseH endonuclease domain (5′ incision), and helix-turn-helix motif (**Figure 2.3**) [35, 75]. In the N-terminal cysteine-rich region, four highly-conserved cysteine residues at positions 154, 166, 174, and 178 have been discussed in the literature. The function of the conserved cysteines has remained unknown, but speculated to facilitate interactions between UvrB and UvrC [75]. Because the four cysteines are atypically-spaced, close in proximity, and highly-conserved through the Bacteria domain and up to some archaeal species ($CysX_{6-14}CysX_7CysX_3Cys$

consensus sequence), our group hypothesized that these cysteine residues coordinate a [4Fe4S] cluster. Two putative (LIV)(YF)(RK) tripeptide motifs were also observed, one of which is located N-terminal to the predicted coordination site and the other just after Cys154. Additionally, conserved aromatic and proline residues are also located around Cys154, Cys166, Cys174, and Cys178, one of the few common themes among the sequences of nucleic acid processing enzymes that coordinate the [4Fe4S] cofactor [85]. More moderately-conserved cysteine residues can be found at positions 265, 398, and 413, but these were not hypothesized to participate in Fe coordination because of the absence of other factors suggestive of a [4Fe4S] binding domain.

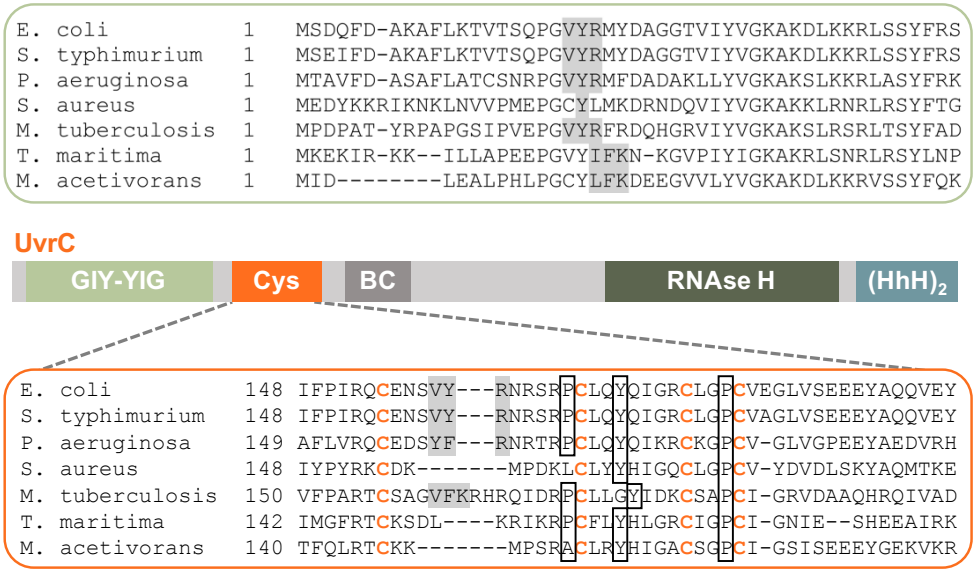

Figure 2.3 Conserved and atypically-spaced cysteine residues in the cys-rich domain of UvrC [35]. Shown is a schematic representation of the GIY-YIG endonuclease (3′ incision, light green), cysteine rich (Cys, orange), UvrBC interacting (BC, purple), RNAse H endonuclease (5′ incision, dark green), and helix-turn-helix ($(HhH)_2$ teal) domains of UvrC (*Middle*). (*Top, Bottom*) Within the N-terminal region, residues 1 to 50 and 148 to 194 are shown. In the cysteine-rich region, Cys154, Cys166, Cys174, and Cys178 (*E. coli* numbering) are highly conserved and atypically-spaced in bacterial and several archaeal species. The UvrC sequence contains additional sequence motifs suggestive of a [4Fe4S] center. Two putative LYR tripeptide motifs (shaded) are located N-terminal (VYR, IFK, or LFK) and between (VYR or VFK) Cys154 Cys166. A highly-conserved aromatic residue (Tyr169) and two conserved proline residues (Pro165 and Pro177) are also located in the vicinity of the conserved cysteine residues.

Our group also noticed additional evidence in the literature consistent with UvrC binding a putative [4Fe4S] cofactor. First, as discussed above, cellular expression of UvrC is highly controlled, and tight regulation of copy number appears to be a common characteristic of repair proteins bearing the [4Fe4S] cofactor. Second, DinG overexpression and Δ*dinG* strains of *E. coli* were inexplicably more sensitive to UV light [84], suggestive of redox signaling between DinG and an unknown protein in NER. We hypothesized that this unknown signaling partner is UvrC. Described here are our initial observations that supported our prediction that UvrC coordinates iron sulfur cluster. Also described are other key observations that informed the refinement of our methods for handling UvrC (detailed in Chapter 3).

2.2 EXPERIMENTAL METHODS

2.2.1 General Procedures

All reagents were used as received and stored according the manufacturer's instructions. All water used was purified on a Milli-Q Reference Ultrapure Water Purification System (≥18.2 MΩ cm). UV-Visible (UV-Vis) spectra of DNA substrates and UvrC were taken on a Cary 100 Bio (Agilent) spectrophotometer using quartz cuvettes (Starna). High performance liquid chromatography (HPLC) was done using HP 1100 (Aglient) system and fast performance liquid chromatography (FPLC) was done using an ÄKTA FPLC™ system (GE Life Sciences). Before use, all solvents and buffers used during purifications were filtered through a 0.22 or 0.45 μm Nalgene™ Rapid-Flow™ filter unit with an SFCA membrane (ThermoFisher Scientific). Glass plates, spacers, and the Owl™ Vertical Electrophoresis System were purchased from ThermoFisher Scientific. Sequencing gel supplies were purchased from National Diagnostics. Anaerobic vinyl chambers (glove bags) were kept at atmospheres of 2-4% H_2 in N_2, with Pd scrubbing towers (Coy Laboratories) and used for experiments requiring anaerobic conditions. When needed, buffers were degassed in an anaerobic chamber by stirring vigorously [43, 63, 88].

2.2.2 Multiple Sequence Alignments

UvrC sequences from *Escherichia coli* (*E. coli*), *Salmonella typhimurium* (*S. typhimurium*), *Pseudomonas aeruginosa* (*P. aeruginosa*), *Staphylococcus aureus* (*S. aureus*), *Mycobacterium tuberculosis* (*M. tuberculosis*), *Thermotoga maritima* (*T. maritima*), and *Methanosarcina acetivorans* (*M. acetivorans*) were aligned using TCoffee (tcoffee.crg.org), and alignments were formatted using BoxShade (ExPasy) [2, 51]. Sequences were placed in decreasing order of taxonomic relationship.

2.2.3 Primers and DNA Substrates.[25, 26, 53]

All oligomers were purchased from Integrated DNA Technologies (IDT) and all plasmids were purchased from Addgene. Dry, single-stranded DNA (ssDNA) oligomers were received on a 1 μmol scale and resuspended in 600 μL in DNA Buffer (5 mM sodium phosphate, 50 mM NaCl, pH 7.0), and 300 μL of this stock was diluted in DNA buffer in a 1:1 ratio before purification. Strands of ssDNA were purified on a reverse phase PLRP-S 300 Å column (Agilent) by HPLC using a linear gradient from 97% 50 mM ammonium acetate in ACN (pH 6.8) to 85% ammonium acetate over a period of 45 min at a flow rate of 2 mL/min. Peaks were collected, dried on a lyophilizer, ethanol precipitated, resuspended in DNA Buffer, quantified by UV-Vis, and stored at -20 °C until use unless otherwise indicated. Sequences of DNA used here are given in (see Appendix A). In DNA Buffer, duplexes were formed by mixing equimolar quantities of complementary strands at ≥ 30 μM, heating to 90°C for 10 minutes, and cooling to 20 °C over a linear gradient for 90 minutes.

Thiol-modified oligonucleotide was resuspended in 10 mM Tris-HCl (pH 8.5, Qiagen) and reduced in 100 nmole batches with an excess of dithiothreitol (DTT, 50 to 100 mgs) to cleave the disulfide protecting group and reveal the thiol moiety [26, 53]. The deprotected oligonucleotide was purified on an Illustra NAP-5 column (GE Life Sciences) and then purified by HPLC as above. Deprotection of the electrochemistry substrate was confirmed on an Autoflex matrix-assisted laser desorption ionization time-of-flight mass spectrometer (Bruker). The thiol-modified strand was quantified by UV-Vis as above, sparged with Ar (1 s of sparging per μL of solution), and sealed with Teflon tape before storing. Duplexes including thiol-modified strands were sparged and sealed with Teflon tape before annealing. Duplexes were also stored at -20 °C until use.

2.2.4 Liquid and Solid Growth Media [25, 26]

Liquid media was prepared by adding 25 g of powered lysogeny broth (Miller, Mo BIO) in 1 L of MilliQ water and sterilizing the solution using the Amsco® Century™ SV-1262 Prevac Steam Sterilizer (Steris) on the Liquid 30 cycle. Solid media was prepared by combining 12.5 g of powered lysogeny broth and 7.5 g of agar (Beckman Dickinson) in 0.5 L of MilliQ and sterilizing the solution by autoclaving. Once agar media had cooled to ~55 °C, ampicillin was added to a final concentration of 50 mg/L, and media was aliquoted into sterile, plastic petri dishes. Ampicillin was added to sterile, liquid media cultures immediately before inoculation.

2.2.5 Amplification of the *uvrC* Gene from Genomic DNA [25, 26]

To isolate the *uvrC* gene (1830 bases), a colony of the MG1665 *E. coli* strain grown on LB/agar plate was resuspended in 100 μL of ddH_2O, and 10 μL was mixed with Gibson Assembly (GA) primers (0.5 μM each, see below for sequences), Expand High Fidelity dNTPs (200 μM; Roche), Expand High Fidelity 10x Buffer (1x, Roche), and Expand High Fidelity Polymerase in a total reaction volume of 50 μL. Temperature cycling is as follows: 1. 5 minutes at 95 °C; 2. 34 cycles of 30 seconds at 95 °C, 1 minute at 55°C, and 4 minutes 72° C; 3. a final elongation for 10 minutes at 72 °C. Amplified products were purified using a PCR purification kit (Qiagen), mixed 1:1 with Ultraclean Gel Dye (MO Bio), resolved at 150 V for 1 hour on a 0.8% agarose gel (Invitrogen) containing 0.5 μg/mL EtBr, visualized with a transilluminator, purified using the gel extraction kit (Qiagen), purified again using the PCR purification kit (Qiagen), and quantified by UV-Vis.

Colony PCR Primer for Gibson Assembly F:
5′-TCGGGATCGAGGAAAACCTGTACTTCCAATCCAATATTATGAGTGATCAGTTTGACGC-3′
Colony PCR Primer for Gibson Assembly R:
5′-TGAAAATCTTCTCTCATCCGCCAAAACAGCCAAGGGATCCTCAATGTTTCAACGACCA
GA-3′

2.2.6 Construction of an Overexpression Plasmid for UvrC [25, 26]

The Gibson assembly method was used for plasmid construction. All plasmid samples were submitted to Laragen (Culver City, CA) for sequencing to confirm integration of the desired gene into the plasmid using the procedures described. In a total volume of 50 μL, 2.5 μg of pBAD plasmid (Addgene 37503), 50 units each of SspI and BamHI, and 10x Cutsmart Buffer (New England Biolabs) were restricted at 37 °C for 16 hours, heat inactivated at 65 °C for 20 min, and held at 4 °C. The restricted plasmid was purified as described. In a total volume of 42.6 μL, 100 ng of restricted plasmid was combined in a 1:1 ratio with the PCR-amplified gene and 2x GA Master Mix (New England Biolabs). The Gibson assembly was completed at 50 °C for 1 hour, diluted three-fold, and 2 μL of diluted samples were transformed into a vial of One Shot® TOP10 Electrocomp™ *E. coli* cells (Invitrogen) using a MicroPulser Electroporation Unit (Bio-Rad) with a 1.8 kV pulse. Cells were recovered by growing in 1 mL of SOC Media (Invitrogen) for 1 hour at 240 rpm at 37 °C. To an LB/Amp plate (50 mg/LB), 250 μL transformed cells were plated and grown at 37 °C overnight. Individual colonies were picked and grown in liquid

cultures overnight as above, miniprepped using a Qiagen kit, and sequenced by Laragen. Samples containing the desired plasmids were transformed into TOP10 cells, grown, cell stocks were made with 25% glycerol, and cells were flash frozen in liquid N_2 before storing -80 °C. See **Figure 2.4** for a promoter map.

2.2.7 Induction Trials [25, 26]

Overnight starter cultures of pBad plasmid containing UvrC from a single colony were grown in Lb/Amp as above. A large 1 L culture was inoculated as above, grown to an OD_{600} of ~0.6, and protein expression was induced by arabinose (10 mg/L). Time points were taken between 0 and 16 hours (0.5 mL), centrifuged at 9000 rpm for 2 min, and stored at -80 °C after discarding the supernatant. For SDS-PAGE gel analysis, these whole cell samples were resuspended in 0.5 mL of Blue Loading Buffer (New England Biolabs), vortexed, heated at 95 °C for 5 minutes, vortexed again, and heated at 95 °C for 5 minutes. Samples were developed at 200 V for 35 min on 7.5% Precast Protein Gels (Bio-Rad) in SDS-PAGE buffer (25 mM Tris, 192 mM glycine, 0.1% SDS, pH 8.3) with High Molecular Weight Dual Color Protein Standards (Bio-Rad). Gels were imaged on the ChemiDoc™ Imaging System (Bio-Rad).

2.2.8 Overexpression of UvrC

A starter culture of One Shot® TOP10 Electrocomp™ *E. coli* Cells (Invitrogen) containing the UvrC overexpression plasmid (encoding the His_6-MBP-UvrC fusion protein) were grown (200 rpm, 37 °C) ~16 hours in LB/Amp (50 mg/L). Large (1 L) cultures LB/Amp (50 mg/L) were inoculated with starter culture, grown (225 rpm, 37 °C) to an OD_{600} of ~0.6, and expression was induced by addition of arabinose to a final concentration of 10 mg/L. Cells were grown for 16 hours (150 rpm, 22 °C), harvested at 5,000 rpm for 20 min, and stored at -80 °C.

2.2.9 Purification of UvrC

2.2.9.1 Purification Buffers and Column Equilibration

The following purification buffers were prepared at a pH of 7.5: Buffer A - Tris-HCl 25 mM, KCl 0.5 M, 10% v/v glycerol, 1 mM DTT; Buffer B - Tris-HCl 25 mM, KCl 0.5 M, 20% v/v glycerol, 0.5 M Imidazole; Buffer C - Tris-HCl 25 mM, KCl 0.5 M, 20% v/v glycerol, 1 mM DTT; Buffer D - Tris-HCl 25 mM, KCl 0.5 M, 20% v/v glycerol, 10 mM maltose monohydrate, 1 mM DTT; Buffer E - Tris-HCl 25 mM, KCl 0.5 M, 20% v/v glycerol. Two stacked HisTrap HP 5 mL columns, three stacked

MBP Trap HP 5 mL columns (GE Healthcare), and a Superdex 200 preparative grade 26/200 size exclusion column (GE Healthcare) were used for purification. In a cold room (4 °C) the night before cell lysis, all columns were equilibrated in water and then in loading buffer. Histrap columns were equilibrated with at least 10 column volumes of Buffer A at a flow rate of 5 mL/min using a peristaltic pump (10 mL per ColVs), the MBP Trap columns were washed with 5 ColVs (15 mL per ColV) of Buffer C ddH_2O (5 mL/min flow rate), and the Superdex column was washed with 1.5 to 2 ColVs (330 mL per ColV) of Buffer E at a flow rate of 1 mL/min overnight (referred to as storage buffer or UvrC buffer). Buffers were also chilled overnight. Additionally, autoclaved polycarbonate centrifuge tubes, a Dounce homogenizer with rods and a 500 mL beaker covered with aluminum foil were also chilled in the cold room overnight.

2.2.9.2 Cell Lysis and Purification [25, 26]

Purification of UvrC should be expected to last between 17-20 hours and should be completed in a single day. Frozen cell pellets were thawed on ice in a cold room and resuspended and homogenized in Buffer A (10g pellet per 100 mL buffer) that was supplemented on the day of the purification with 6-8 tablets of crushed cOmplete™ protease inhibitor cocktail tablets (Roche), DNAse (15 kU, Sigma). Cells were homogenized using a Dounce homogenizer, passed over a 100 μm nylon cell strainer (Corning), and lysed using an Microfluidizer or the other instrument at 25,000 psi over 2-3 cycles. For each cycle, cell lysate was collected on ice. Lysate was loaded into polycarbonate vials and centrifuged on a Sorvall™ RC 6 Plus Centrifuge (ThermoFisherScientific) at 13,000 rpm for 45 minutes at 4 °C. After centrifugation, the supernatant was collected while samples were kept on ice, and the supernatant was filtered over a 0.45 μm membrane. Stacked Histrap columns (GE Life Sciences) were loaded with the cell lysate using a peristaltic pump (GE) at a flow rate of about 3.5 mL/min. During the wash and elution steps, a flow rate of 1.5 mL/min was used. A 4 ColV gradient of Buffer A was used to wash the column, and a gradient from 1 to 100% Buffer B (0 to 0.5 M Imidazole) over 15 ColVs was used to elute the protein. Fractions were collected, pooled, and concentrated using Amicon® filters (30-100 kDa cut off). Stacked MBP Trap columns (GE Life Sciences) were loaded with the sample using a peristaltic pump (GE) at a flow rate of about 0.5 mL/min. During the wash and elution steps, a flow rate of 1.5 mL/min was used. A 4 ColV gradient of Buffer C was used to wash the column, and a gradient from 1 to 100% Buffer D (0 to 10 mM maltose monohydrate) over 10 ColVs was

used to elute the protein. Fractions were again pooled and concentrated to < 10 mLs. Concentrated fractions were loaded onto the Superdex 200 at a flow rate of 1 mL/min using a 10 mL superloop (GE Life Sciences). Samples were eluted with 1 ColV of Buffer E. Soluble fractions were collected, concentrated between 20-30 μM to avoid precipitation upon freezing, then immediately flash frozen in liquid N_2 and stored at -80 °C. Subfractions were taken throughout the purification to assess the purity of the samples by SDS-PAGE as above, combining Blue Loading Buffer (NEB) 1:1 with fractions, pre-heating in sample buffer at 90 °C for 3-5 minutes before resolving on a 4-20% TGX precast gel (Bio-Rad) at 200 V for 35 min along with a High Molecular Weight Dual Color Protein Standers (Biorad). Gels were stained with Bio-Safe™ Coomassie Stain according to the manufacturer's instructions (Biorad). The identity of UvrC was confirmed through peptide mass fingerprinting completed by the Protein/Peptide Micro Analytical Laboratory at Caltech.

2.2.10 UV-Vis and Continuous Wave (CW) Electron Paramagnetic Resonance (EPR) Spectroscopies

2.2.10.1 UV-Vis Spectroscopy [25]

Aliquots of UvrC were thawed on ice in a cold room. The [4Fe4S] cluster concentration was quantified by using the extinction coefficient of the absorption band centered at 410 nm ε = 17,000 $M^{-1}{\cdot}cm^{-1}$ [25, 26] Because of the size of the fusion protein, typically a 10-15x dilution of the thawed protein needed to be made in order to bring the absorption band at 280 nm into the linear region. The total protein concentration was then quantified by using the calculated excitation coefficient (Expasy) of His_6-MBP-UvrC at 280 nm ε = 111,995 $M^{-1}{\cdot}cm^{-1}$. The percent of the [4Fe4S] cofactor incorporated was calculated by dividing the total concentration of [4Fe4S] over the total protein concentration.

2.2.10.2 CW EPR Spectroscopy [25]

EPR samples were prepared in 200 μL volumes at final concentrations of UvrC at 10 μM and ferricyanide at 2 μM or dithionite at 2 μM in UvrC buffer. Prior to mixing, buffer was bubbled with argon and argon was passed over thawed aliquots of protein. UvrC and a chemical oxidant or reductant were mixed on the benchtop in atmosphere. Samples were loaded into clean 4 mm thin-wall precision quartz EPR tubes (Wilmad LabGlass, 715-PW-250MM), capped, and flash frozen in liquid N_2. An EMX X-band spectrometer (Bruker) with an ESR-900 cryogen flow cryostat

(Oxford) and an ITC-503 temperature controller was used to collect X-band CW EPR spectra. Spectra were acquired at 10 K or 50 K at power settings between 0.2-16 mW and a modulation amplitude of 10 gauss using WinEPR software (Bruker) [16].

2.2.11 DNA-modified Gold Electrochemistry on Au Surfaces [25, 26, 53, 66]

A 16-electrode, gold, multiplex chip (4 quadrants with 4 electrodes each) was rinsed and sonicated with acetone three times for five minutes and once with 100% isopropyl alcohol, also for five minutes. The gasket and clamp were washed and sonicated in 50% isopropanol (in water) for five minutes followed by three to five rinses with water. All components were dried using an argon gun. To clear the chip of debris, the chip was cleaned by ozonolysis (UVO Cleaner) for 15 minutes. The chip, gasket, and clamp were assembled and 23 μL duplexed WM electrochemistry substrate at a concentration of 25 μM was added to each quadrant. Monolayers were allowed to form overnight under humid conditions at room temperature. The electrode was then rinsed three times with DNA buffer (5 mM sodium phosphate, 50 mM NaCl, pH 7.0) and then three times with glycerol buffer (DNA buffer with 5% glycerol). The electrode was backfilled with 1 mM of 6-mercaptohexanol (in glycerol buffer) for ~30 minutes. The electrode was rinsed 10 times with DNA buffer. The multiplex chip was equilibrated in electrochemistry buffer at room temperature prior to taking measurements (4 mM spermidine, 25 mM Tris-HCl, pH 7.5, 0.25 M KCl, 20% glycerol). Buffer was removed by pipetting, and 400 μL of 5 μM of UvrC (by cluster) was added to the chip in electrochemistry buffer. A 4% agarose/3 M NaCl gel tip Ag/AgCl reference electrode (MW-2030, RE-6, BASi) was used. The potentiostat, multiplexer, and analysis software were from CH Instruments, Inc. A scan rate of 50-100 mV/s between -0.4 V and 0.2 V (vs. Ag/AgCl) is optimal for cyclic voltammograms. Scan were taken periodically at 0, 1 hr, 2 hrs, and 3 hrs.

Electrochemistry Substrate:
5′-GCGCAGACACGTTGCAGCAC-3′
3′-CGCGTCTGTGCAACGTCGTG-5′-$(CH_2)_6$-SH

2.2.12 Electrophoretic Mobility Shift Assays (EMSA) [16, 61, 62, 78]

2.2.12.1 Radiolabeling and Purification of DNA Substrates.

For 5′ end labeling phosphorylation, 14 μL water, 2 μL T4 PNK buffer (New England Biolabs), 1 μL ssDNA 100 μM stock solution, 2 μl T4 polynucleotide kinase solution, and 1 μL of [γ-^{32}P] ATP (NEG035C005MC, 6000 Ci/mmol, 150 mCi/mL, PerkinElmer) were combined in a 1.7 mL microcentrifuge tube, the tube was clipped, and incubated at 37 °C for 2 hours upon which 80 μL of water was added, the solution was vortexed and purified using a Micro Bio-Spin 6 chromatography column (Biorad) twice according to the manufacturer's instructions. Samples were dried overnight on the speed vac. Samples were resuspended in 10 μL of loading buffer (80% formamide, 10 mM sodium hydroxide, 0.025% xylene cyanol and 0.025% bromophenol blue) and loaded onto a 20% urea denaturing PAGE gel pre-warmed to 50 °C. The gel was run in TBE buffer for ~3 hours at 90 W (0.089M Tris base, 0.089M boric acid, and 2 mM Na_2EDTA, pH 8.3). The gel was exposed to X-ray film (Kodak) in the dark for 30 s, and the X-ray film was developed on Konica Minolta X-ray Developer. The band of ssDNA was excised using the X-ray film as a guide. Excised bands were incubated in 1 mL of 100 mM triethylammonium acetate (TEAA, pH 7.0) at 37 °C overnight. The TEAA supernatant was dried overnight, and the resulting salts were dissolved in 80 μL of ddH_2O and purified using a Micro Bio-Spin column (Biorad). The process was repeated twice. The DNA was again dried on and then resuspended in 50 μL of phosphate buffer. Radiolabeled ssDNA stocks were stored at -20 °C

.

EMSA Substrate:
5′-CCGACTGAACTCTGTACCTGACACGACAAG-3′
3′-GGCTGACTTGAGACATGGACTGTGCTGTTC-5′

2.2.12.2 Annealing Titrations

A 100% yield was assumed following radiolabeling. A solution of or 99:1 cold:radiolabeled 1 μM double-stranded DNA (dsDNA) was generated by heating complementary strands to 95 °C for 10 min and cooling to room temperature over a linear gradient. Titrations from 50%-125% were prepared by varying the complement concentration DNA buffer in order to verify the duplex character of the substrate (and to detect any pipetting errors). Annealing titration samples were run on a 10% TBE

polyacrylamide Native gel (Bio-Rad) in pre-chilled 0.5x TBE buffer at 4 °C for 3 hours at 50 V. Phosphorimaging (GE or Molecular Diagnostics) screens were exposed to samples using the guideline of 300,000 c.p.m. per hour of exposure per sample. Screens are imaged using the Typhoon Imager (GE Healthcare). Images were processed using ImageQuant (GE Healthcare).

2.2.12.3 EMSA Conditions

DNA and protein samples were prepared in 25 mM Tris-Cl (pH 7.5), 20% Glycerol, 100 nM 1% [γ-^{32}P]-dsDNA, 100 mM KCl, and various concentrations of UvrC. Samples were incubated at 4 °C for 2 hours and electrophoresed as above. Some gels were transferred to an Amersham Hybond-N nucleotide blotting paper (GE Healthcare) using a semidry electroblotter (Owl HEP-1) using extra thick cotton blotting paper (Biorad) in transfer buffer (25 mM Tris, HCl, 200 mM glycine, 10% methanol, pH 8.5) for 1 hour at 175 mAmps. Gels were exposed and imaged as above.

2.2.13 UV-Vis Time Courses to Monitor Cofactor Stability

To investigate the stability of UvrC under aerobic conditions, UvrC was incubated at custom Starna cuvettes that were sealed with a screw cap (to prevent evaporation) before heating in a 37 °C water bath. Generally, between 10 μM and 30 μM of UvrC (by cluster) was used. For each time point, the Cary instrument was blanked with buffer at 37 °C. Samples were applied to an equilibrated Superdex 200 column at a flow rate of 1 mL/min in UvrC buffer.

2.2.14 Analysis of Apo Species by Size Exclusion Chromatography

In a cold room, the Superdex 200 Column (GE Healthcare) was pre-equilibrated (1.5 - 2 ColVs) at 1 mL/min in UvrC buffer. Samples were applied and developed also using 1 mL/min flow rate. Selected fractions were pooled and concentrated using Amicon Ultra 10,000 MWCO concentrators. Concentrated fractions were analyzed by SDS-PAGE as above.

2.3 RESULTS AND DISCUSSION

2.3.1 Evidence of a Redox-active [4Fe4S] Cluster Coordinated by UvrC

Initial studies with UvrC under the aerobic conditions described in this section were completed in collaboration with Dr. Michael A. Grodick [25]. As discussed above, we noticed that UvrC has historically been difficult to express and purify

[35, 54, 73, 75], and accordingly, we screened new expression and purification strategies that would yield soluble and pure protein in large enough quantities that a [4Fe4S] metal center could be detected spectroscopically. Included in the screen was a pBAD overexpression plasmid under the control of the L-arabinose promoter with a His_6-Maltose Binding Protein (MBP) affinity/solubility tag encoded N-terminally to UvrC (**Figure 2.4**) [33, 68]. The L-arabinose promoter can be used to prevent leaky expression prior to induction with arabinose, which is an advantage for overexpressing proteins that are potentially toxic to cells prior to induction [28, 56, 67, 72]. Additionally, MBP tags are frequently used to enhance the expression and solubility of target proteins, including for previous overexpression of the C-terminal half of UvrC as well as repair and replication enzymes bearing the [4Fe4S] cluster [6, 10, 36, 41, 64, 89]. A cooler overexpression temperature (22 °C), longer induction time (16 hrs), and an anaerobic purification in buffers that included a high concentration of potassium chloride were also chosen to minimize accumulation of apo, aggregated, or degraded protein [17, 20, 26, 39, 50, 57, 58, 79, 87, 90].

We found that the pBad overexpression system resulted in detectable overexpression of a His_6-MBP-UvrC fusion protein (110 kDa) in whole cell lysate (referred to as UvrC throughout). Cell lysis, purification, and concentration of the UvrC fusion protein using immobilized metal affinity chromatography, MBP affinity chromatograpy, and gel filtration chromatography was performed in the cold room. Our strategy allowed for isolation of the UvrC fusion protein in high purity with a broad and shallow absorption band centered at 410 nm and yellow-tan color characteristic of [4Fe4S] clusters (**Figure 2.4**, Top Left) [19, 24, 42, 69]. Based on the ratio of absorbances at 410 nm and 280 nm, the cofactor was typically 40-60% incorporated.

Initial studies also included assessing the redox activity of UvrC using electron paramagnetic resonance spectroscopy (EPR) and electrochemistry on DNA-modified Au electrodes. We used X-band CW EPR spectroscopy first to assign oxidation states of the [4Fe4S] cluster aided by use of chemical oxidants and reductants. In the 2+ resting state, [4Fe4S] clusters are EPR silent, though some proteins with incompletely incorporated cofactors can be EPR-active under native conditions, often complicating interpretation of spectra of DNA repair and replication enzymes [16, 50, 58]. Indeed, we observed an EPR-active species at $g = 2.01$, which is likely due to a small percentage of the population in the $[3Fe4S]^+$ state (**Figure 2.4**, Top Right). The intensity of the signal decreased with temperature, also consistent with a $[3Fe4S]^+$ species (**Figure 2.4**, Top Right). Because the majority of DNA repair

and replication enzymes are most similar in potential to high potential iron proteins (HiPIPs), which access the 3+/2+ couple, we would expect UvrC to be oxidized by ferricyanide into the EPR-active 3+ state, but we did not observe such a signal for UvrC under the conditions tested (**Figure 2.4**, Middle). Rather, we observed a strong signal appear under reducing conditions in the presence of dithionite, which is more reminiscent of ferredoxin-like clusters.

Chemical oxidation and reduction, however, are harsh methods that can lead to degradation of the cofactor, and many species have been observed by EPR for [4Fe4S] DNA repair and replication proteins upon treatment with oxidants or reductants [13, 50, 55]. In contrast to chemical methods, electrochemical methods using DNA-modified Au surfaces allows for assessment of the DNA-bound redox chemistry of [4Fe4S] proteins under gentler conditions. Efforts to understand the role of electron transfer reactions in DNA repair and replication have only recently begun, as discussed in the previous chapter [1, 3, 27]. Using several complementary techniques, our group has investigated the redox chemistry of glycosylases, SF2 $5'\rightarrow3'$ helicases, primase, and B family replication polymerases that are found in Bacteria, Archaea, and Eukarya. All proteins studied to date have been observed to access the $[4Fe4S]^{3+/2+}$ couple with midpoint potentials of ~200 mV vs. NHE. Binding to DNA polyanions has been shown to tune their midpoint potentials to ~80 mV vs NHE which activates the cluster toward oxidation and would allow these proteins to exchange electrons through long-range signaling through DNA as a first step in lesion detection [1, 3, 27]. A reversible signal occurs at 80 mV vs NHE, indicating that the electron transfer is not damaging for the DNA substrate or the cluster at physiological potentials. Critically, the studies of the redox activity on DNA-modified gold electrodes and other complementary gel-based methods have demonstrated that the [4Fe4S] cluster of repair and replication enzymes can participate in DNA CT chemistry, the transport of charge through the π stack of the duplex. The efficiency of the charge transport is extraordinarily sensitive to disruption of the base stack, a common feature of damaged DNA sites [5]. We have developed models to describe how redox signaling among repair and replication proteins utilize DNA CT chemistry to facilitate repair of damage and faithful replication of the genome on a biologically relevant time scale.

Our group has previously developed a gold electrode platform that can be modified with DNA monolayers which are formed through a thiol-gold bond on surfaces that are accessible to proteins in solution (**Figure 2.4**, Bottom Left) [25, 26, 53]. Generally, the gold electrode serves as the working electrode, while a Ag/AgCl gel

tip and a platinum wire serve as the reference electrode and auxiliary electrodes, respectively. The latest generation of DNA-modified gold electrodes features a multiplex chip with 16 independently addressable electrodes that can be separated into quadrants which allows for up to four different experimental conditions to be assayed in parallel. The platform is often one of the first methods we use to interrogate the DNA-bound redox activity of a [4Fe4S] protein, and the platform can furthermore be adapted for studies that require anaerobic conditions.

Application of UvrC to DNA monolayers on a 16-electrode multiplex chip in buffered solution allowed for observation of a reversible, redox signal centered at a midpoint potential of 85 mV ± 0.03 vs. NHE (**Figure 2.4**, Bottom Left). Our observations of a [4Fe4S] cofactor that exhibited a DNA-bound redox signal offered many opportunities for deeper investigation into the attributes of UvrC in holo form. First, UvrC is not well-known in the bacterial NER literature to form a complex with duplex substrates independently of other NER proteins, so interactions of holo-UvrC with DNA substrates in particular is a major aspect that would need to be characterized further. Second, the presence of a redox-active cofactor opened up avenues to study redox signaling *in vivo* among the BER (EndoIII and MutY), loop repair (DinG), and NER (UvrC) pathways *in vivo* using genetics assays. Dr. Michael A. Grodick and Dr. Andy Zhou completed *in vivo* studies with UvrC (the details of which can be found in their theses) [25, 93]. Redox signaling between UvrC and DinG *in vivo* has already been suggested by the increased UV sensitivity in DinG overexpression and Δ*dinG* strains of *E. coli* [83]. *In vivo* data collected in their thesis work suggest that redox signaling among BER, Loop Repair, and NER indeed may be involved in facilitating growth recovery after challenge of cells with UV-light [25, 93]. My thesis work has focused on the *in vitro* characterization of UvrC, which is detailed in the following sections and chapters.

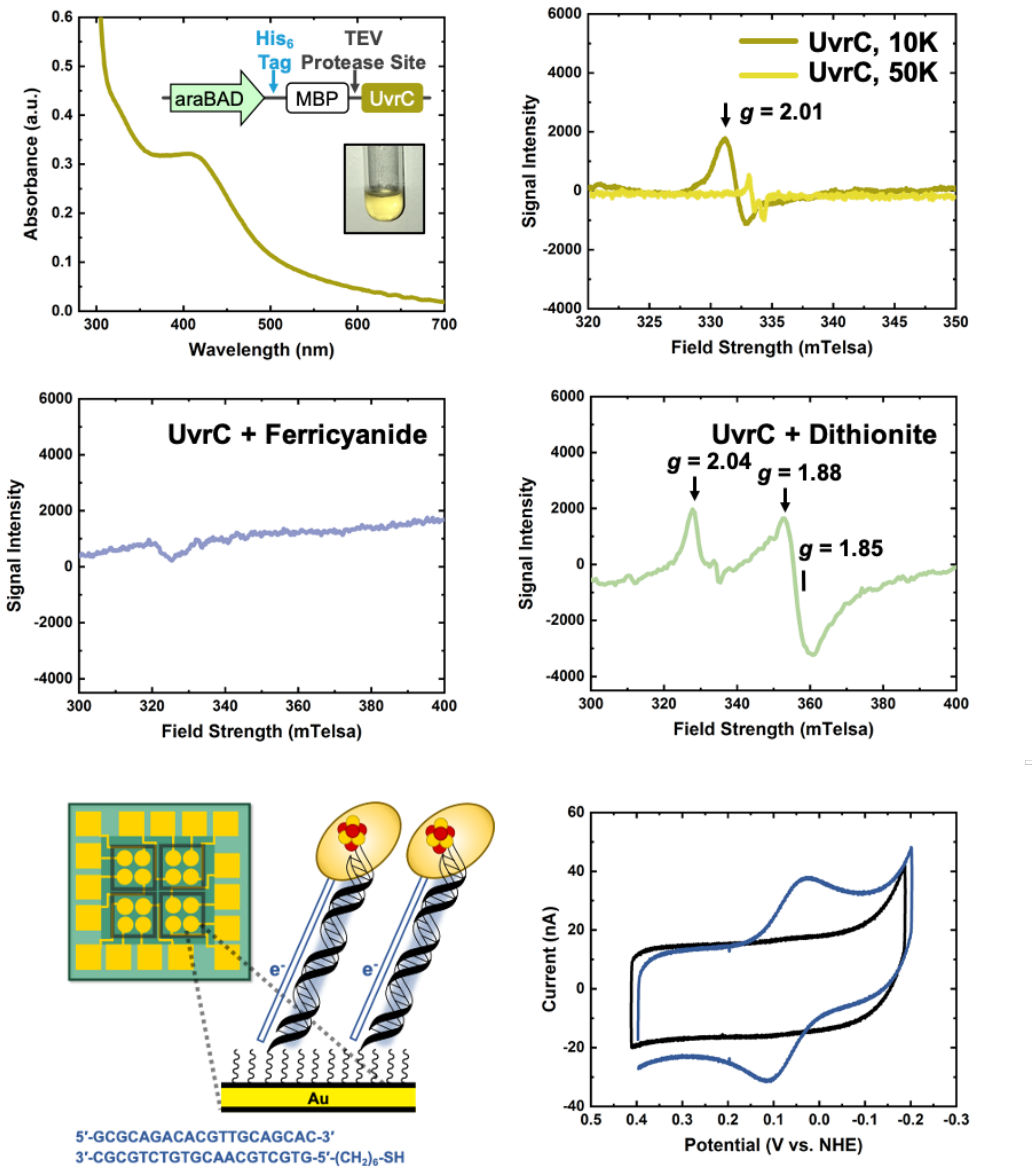

Figure 2.4 First observations of a redox-active [4Fe4S] cofactor coordinated by UvrC. (*Top Left*) Development of a new expression and purification route for UvrC resulted in isolation of a deep yellow protein with a broad and shallow absorption band centered at 410 nm, which is characteristic of [4Fe4S] cluster proteins. (*Top Right and Middle*) X-band CW EPR spectra of purified UvrC (10 μM) was taken for native, purified UvrC (dark yellow), UvrC treated with ferricyanide (2 mM, light purple), and UvrC treated with dithionite (2 mM, light green) at 10K. The signal at g=2.02 for purified protein is attributed to $[3Fe\text{-}4S]^{1+}$ species. (*Bottom*) DNA duplexes in monolayers accessible to proteins are formed on gold through an alkane-thiol linker on multiplex chips with 16 independent electrodes. A midpoint potential of 85 mV ± 0.03 vs. NHE was measured for UvrC (dark blue). UvrC is redox active at physiological potentials when bound to DNA and shares a DNA-bound redox potential with other high potential [4Fe4S] repair proteins.

2.3.2 Optimization of Purification and Storage Conditions for UvrC

2.3.2.1 Modifications to the Purification Sequence

Over the span of several purifications, optimization was necessary in order to improve the workflow for UvrC. The first step taken toward optimizing the purification was improving the Histrap column washing protocol, which occurs after application of the clarified cellular lysate to the column has finished (**Figure 2.5**, Top Left). The wash step was increased from including 1% elution buffer (5 mM imidazole) to 10% elution buffer (50 mM imidazole) in order to address the overlapping peaks that co-eluted. The first peak was later determined to be catalase (a heme protein), which non-specifically bound to the nickel column (protein identification not shown). Increasing the percentage of imidazole used during the column wash step allowed for catalase to elute quickly during from the Histrap column wash, thereby separating this contaminant prior to elution of UvrC peak (see Chapter 3: Appendix A). Over the course of completing multiple purifications of UvrC, we also attempted to increase yields by doubling the volume of Histrap resin (from 5 mL to 10 mL). In doubling the volume of the column, the collected fractions also doubled in volume. This change in volume was not tolerated by the MBP Trap HP columns, even though three MBP Trap HP columns were stacked in series in order to accommodate upstream changes. A large percentage of the UvrC fraction immediately washed off the column (**Figure 2.5**, Top Right, 0-60 mLs), as evidenced by the flow through appearing yellow (not shown). The flow through (FT) and the species that did elute off the column (Fraction 1) were resolved separately using size exclusion chromatography (**Figure 2.5**, Bottom). As can be seen in a comparison of the two chromatograms from the size exclusion column, the majority of the protein that directly washed off the column was soluble UvrC, and the majority of the protein that was retained on the MBP Trap column was in fact aggregated UvrC. Use of the MBP Trap column during purification was therefore eliminated, and a two-column purification with the Histrap and Superdex 200 columns was used for all subsequent purifications (see the Experimental Section of Chapter 3).

2.3.2.2 Storage and Handling Conditions for Increased Stability

Additional observations during the course of carrying out experiments also led to insights on what conditions were necessary to stabilize UvrC. For example, following the final purification step by size exclusion chromatography, protein is often concentrated before freezing at -80 °C to allow for aliquoting of protein at

reasonable working concentrations (in the micromolar range). During a round of purification, UvrC was concentrated above 100 μM (roughly 10 mg/mL for the MBP-UvrC fusion protein), and upon thawing aliquots for subsequent experiments, it was discovered that the protein had completely crashed out of solution (not shown). For this reason, UvrC is concentrated between 20-30 μM (between 2 and 3 mg/mL) before flash freezing and storage at -80 °C (see the Experimental Section above and in Chapter 3). Buffer conditions have also been found to affect UvrC greatly. Great care must be taken when buffer exchanging UvrC into solutions without glycerol (which is optimal for electrochemistry on graphite electrodes [4, 16]). Exchanging UvrC into buffer without glycerol via diafiltration causes UvrC to crash out of solution, forming yellow precipitate, *if* the centrifugation steps are carried out for > than 1-2 minutes. In between short centrifugation steps, UvrC must be mixed by pipetting to avoid precipitation. When buffer exchanging into HEPES buffer via diafiltration (prepared at the same pH and ionic strength as storage buffer), UvrC crashes out immediately, and no methods were found to aid in buffer exchanging. These observations are not surprising, given the wide reports of UvrC instability, and highlight how careful study of UvrC at all steps of handling is absolutely required.

2.3.3 Observation of a UvrC-DNA Complex by EMSA

To continue characterizing UvrC in holo form, we examined how UvrC interacts with radiolabeled, duplexed 30 base pair substrates using electrophoretic mobility shift assays (EMSAs) [16, 61, 62, 78]. UvrC along with the full UvrABC exinuclease has been studied extensively *in vitro* with single stranded DNA (ssDNA), well-matched (WM) dsDNA, damaged duplex substrates, and substrates with nicks, gaps, bubbled regions, and overhangs derived from plasmid DNA and synthetic oligomers [35, 75]. The majority of previous work from chromatographic, optical, and gel-based methods with UvrC from *E. coli* and thermophilic bacteria indicates that UvrC does not form a complex with dsDNA independently of UvrA and UvrB [49, 65, 81, 82, 91]. (It should be noted that UvrC, both truncated and full-length, has been seen to bind to ssDNA or single-stranded regions of nicked, gapped, or bubbled substrates [34, 49, 60, 65, 74].) Thus, it is widely accepted that UvrC requires the action(s) of UvrA and UvrB in order to associate with substrates of duplex character. There have, however, been two reports of UvrC species forming a complex with dsDNA at equilibrium (a tetramer in a gel-based assay) and non-equilibrium (single molecule assays) conditions [31, 70, 86]. It is not clear how these data can be reconciled. What is clear is that UvrC is sensitive to the conditions

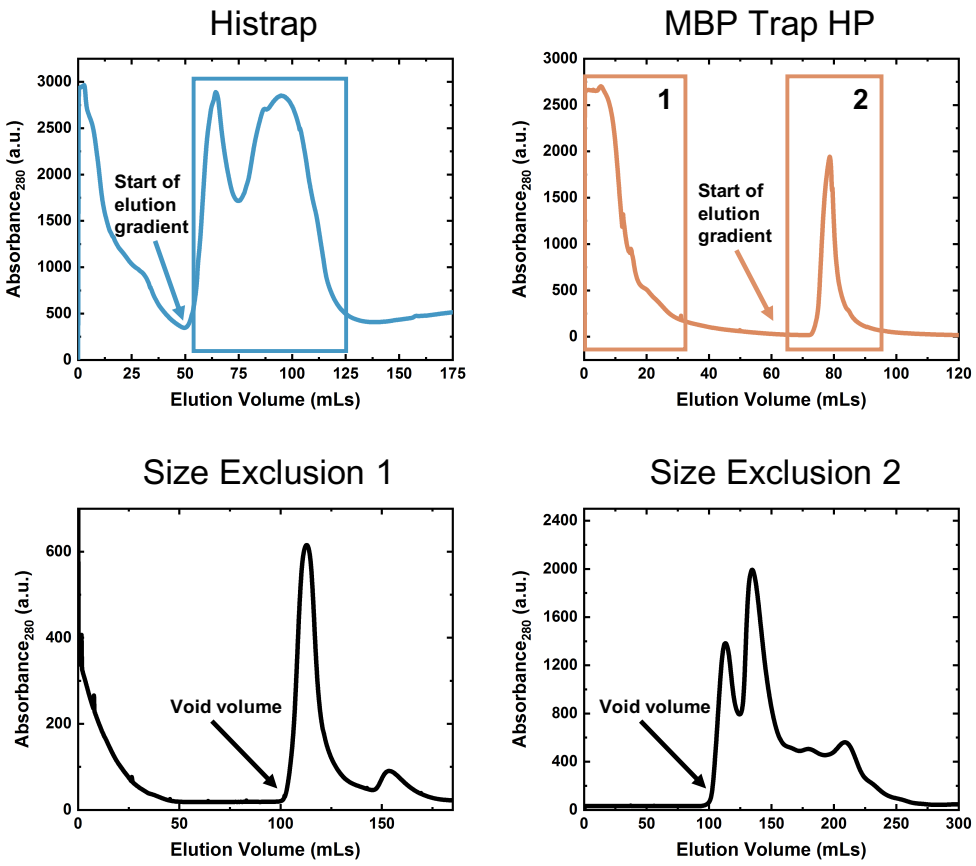

Figure 2.5 Purification Chromatograms for UvrC (reference Mike's thesis). *Top Left* Shown is the chromatogram of the wash and elution steps for the Histrap column. The elution step for the specific chromatogram shown here begins where marked. (*Top Right*) Shown is the chromatogram of the wash and elution steps for the MBP Trap HP column. The elution step for the specific chromatogram shown here begins where marked. (*Bottom Left*) Displayed is the chromatogram from the size exclusion column from the flow through of the MBP Trap HP column, the majority of which is the soluble UvrC. (*Bottom Right*). Displayed is the chromatogram from the size exclusion column from the Fraction 1 (F1) of the MBP Trap HP column, the majority of which is aggregated UvrC species.

under which it is studied, exemplified by reports and our experiences that UvrC is prone to precipitation [52, 73, 94].

Our observations of a DNA-bound redox signal suggested that in holo form, UvrC in fact formed a complex with DNA independently of other NER proteins. We used electrophoretic mobility shift assays (EMSAs or gel shift assays) during our first investigations to study formation of UvrC-DNA complexes. The sequence of the

DNA substrate was taken from the center of the WM sequence of the 3.8 kbp AFM substrate (about the regions that is engineered to include a C:A lesions in the 3.8 kbp MM strand [7]). In order to provide a large enough substrate, a 30 bp duplex was chosen because of a 19 bp DNA footprint for the UvrBC complex that was previously reported [81]. Shown in **Figure 2.6** is a gel from one replicate that demonstrated that relative to other repair proteins on WM DNA, UvrC exhibited high-affinity toward the WM duplex (240 nM) [16, 23, 78]. While all other replicates also showed complexes forming, a consistent pattern and gel quality was difficult to obtain (not shown). While a more optimal system for studying UvrC-DNA complexes required additional development, our initial observations of a UvrC-DNA complex and the redox signal on the DNA-modified gold electrode supported our conclusions that UvrC participates in DNA CT chemistry. This new modality raised other questions about the nature of the UvrC-DNA complex, if UvrC forms similar complexes with other NER substrates, how apo species interacted with DNA duplexes in our hands. More robust methods for interrogating these exciting questions would first need to be developed for UvrC, as the gel pattern and gel quality were highly variable. Over time, the variability seen in gel shift assays and in handling UvrC throughout the course of experiments under aerobic conditions (see previous section) pointed to the source of instability for UvrC, which was investigated and is summarized in the next section.

2.3.4 Degradation of the [4Fe4S] Cofactor in the Presence of O_2

A final, key discovery made during initial studies with UvrC revolved around the stability of the [4Fe4S] cluster. Curiously, across different protein purification cycles, some batches were lighter yellow than others, which could not be easily explained by differences in methods used or by the total protein concentration of the sample. Aliquots of UvrC would also appear to lose color during the course of longer experiments, even when steps were taken to ensure that the protein was kept on ice. The suggestion was made that perhaps the cofactor of UvrC was not stable in atmosphere due to the presence of O_2. To investigate this intriguing possibility, UvrC was incubated at 37 °C (at a physiologically-relevant temperature) in sealed cuvettes in atmosphere, and the absorption band at 410 nm was monitored by UV-Vis. (**Figure 4.3**, Left). Near complete disappearance of the absorption band at 410 nm occurred after incubating at 37 °C after 1 hour, which is a common incubation temperature and time for many activity assays [15, 34, 47, 59, 76]. Complete

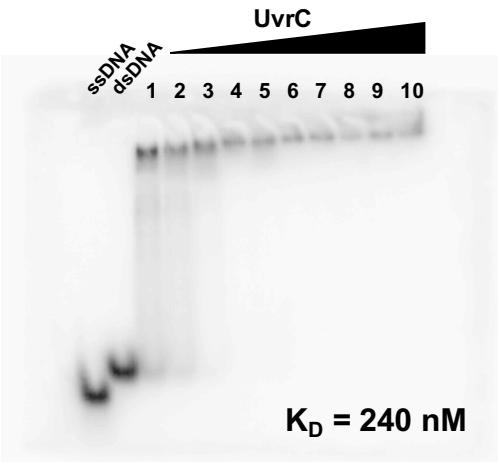

Figure 2.6 First observations of a UvrC-DNA complex. UvrC was incubated with 30 base pair DNA substrates in UvrC buffer (25 mM Tris-HCl, 0.5 M KCl, 20% v/v glycerol). Free and complexed DNA were separated by native gel electrophoresis using a 10% TBE gel and TBE running buffer (recipe) in a cold room at 4 °C. Preliminary data indicated that UvrC forms a complex with WM duplex DNA. Lanes with ssDNA and dsDNA only each contain 100 nM concentration of DNA. Lanes 1-10: 100 nM - 1000 nM UvrC by cluster with a constant duplex concentration of 100 nM. Binding data was fit to a sigmoidal function in Origin.

degradation could be seen after 4 hours (not shown). We emphasize here that in order to detect the oxygen-driven degradation spectroscopically, concentrations of UvrC well above that of what is commonly found in an activity assay needed to be used. Our observations highlight the subtlety of handling a metalloprotein *in vitro* and the importance of carefully monitoring cofactor stability, particularly during early studies with a new metalloprotein.

Because apo and holo forms of metalloproteins can have different oligomeric states, we compared holo- and apo-UvrC by size exclusion chromatography after the 4-hour time point [12, 46]. Apo-UvrC species eluted at the void volume of the column, which corresponds to aggregates that would be > 600 kDa in mass (**Figure 4.3**, Middle). Finally, we verified that the source of degradation was specific to molecular oxygen and not temperature by incubating UvrC at 37 °C in an anaerobic chamber in degassed buffer (**Figure 4.3**, Right). The spectra before and after heating overlap completely, confirming that UvrC undergoes degradation in the presence of molecular oxygen. This result distinguishes UvrC from other repair

proteins in *E. coli* that have been discovered to date which are stable to oxygen, raises even more important questions about UvrC, and suggests the possibility of a multifunctional role for the [4Fe4S] cofactor in NER.

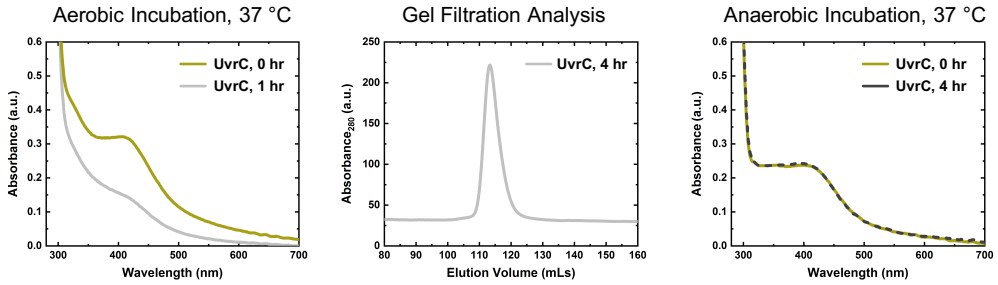

Figure 2.7 Degradation of the UvrC-bound [4Fe4S] cofactor due to molecular oxygen. (*Left*) Aerobic incubation of UvrC at 37 °C results in degradation that is centered at the [4Fe4S] cluster. (*Middle*) Apo species of UvrC elute at the void volume of the Superdex 200 size exclusion column, corresponding to species with molecular weights > 600 kDa. (*Right*) The UvrC-bound [4Fe4S] cluster is stable under anaerobic conditions.

2.4 CONCLUSIONS

The observation of a [4Fe4S] cluster in repair and replication proteins has often occurred many years after the first characterization of the gene and gene products due to several reasons [20, 57, 85]. First, [4Fe4S] clusters, like other metal centers, can be sensitive to expression and purification conditions, which has delayed isolation of protein with intact clusters [14, 57, 77]. Second, prediction of [4Fe4S] coordination sites in nucleic acid processing enzymes has been particularly challenging because the spacing of the coordinating cysteines is atypical across different protein families, leading to a weak bioinformatic signature [85]. As discussed, other indications that a protein may bind an iron-sulfur cluster, such as the LYR sequence motif, are just emerging [44, 57, 77].

The story for UvrC has been consistent with the pattern in the literature. The first biochemical experiments with purified protein were reported in 1981, and many research groups have made significant contributions to the literature on UvrC and bacterial NER. Yet, nearly four decades have passed between the first expression and purification of UvrC and our initial observations of the [4Fe4S] cofactor. The cofactor eluded discovery through serendipitous means possibly because the induction times during overexpression were not long enough to allow

for iron sulfur cluster biogenesis machinery to load the cofactor into nascent protein, the expression vector and purification methods did not allow for UvrC to be isolated at high enough concentrations for the cofactor to be observed by eye, and/or the sensitivity of the cofactor to molecular oxygen caused degradation during the course of harvesting UvrC from overexpression cells. Much remains to be elucidated about many aspects of UvrC, and further studies must be pursued in conjunction with the development of additional anaerobic methods so that more extensive examination of UvrC in holo form can be carried out in a controlled environment.

2.5 ACKNOWLEDGEMENTS

Early studies with UvrC were started in collaboration with Dr. Michael A Grodick and benefited from conversations with Dr. Grodick and Dr. Andy Zhou. We also thank Professor Amie K. Boal for her early insights while she was in the Barton group regarding UvrC and a possible association with a [4Fe4S] cluster. We would especially like to thank Professor Harry B. Gray for suggesting that oxygen may be contributing to the degradation of the [4Fe4S] cofactor.

References

[1] A. R. Arnold, M. A. Grodick, and J. K. Barton. DNA Charge Transport: From Chemical Principles to the Cell. *Cell Chemical Biology*, 23(1):183–197, 2016. ISSN 24519448. doi: 10.1016/j.chembiol.2015.11.010. URL http://dx.doi.org/10.1016/j.chembiol.2015.11.010.

[2] P. Artimo, M. Jonnalagedda, K. Arnold, D. Baratin, G. Csardi, E. De Castro, S. Duvaud, V. Flegel, A. Fortier, E. Gasteiger, A. Grosdidier, C. Hernandez, V. Ioannidis, D. Kuznetsov, R. Liechti, S. Moretti, K. Mostaguir, N. Redaschi, G. Rossier, I. Xenarios, and H. Stockinger. ExPASy: SIB bioinformatics resource portal. *Nucleic Acids Research*, 40(W1):W597–W603, 2012. ISSN 03051048. doi: 10.1093/nar/gks400.

[3] P. L. Bartels, E. O'Brien, and J. K. Barton. DNA signaling by iron-sulfur cluster proteins. In T. A. Rouault, editor, *Biochemistry, Biosynthesis and Human Diseases: Biochemistry, Biosynthesis, and Human Diseases*, volume 2, pages 405–423. De Gruyter, Berlin, Boston, 2017. ISBN 9783110479850. doi: 10.1515/9783110479850-015.

[4] P. L. Bartels, A. Zhou, A. R. Arnold, N. N. Nuñez, F. N. Crespilho, S. S. David, and J. K. Barton. Electrochemistry of the [4Fe4S] Cluster in Base Excision Repair Proteins: Tuning the Redox Potential with DNA. *Langmuir*, 33(10): 2523–2530, Mar 2017. ISSN 15205827. doi: 10.1021/acs.langmuir.6b04581. URL http://dx.doi.org/10.1021/acs.langmuir.6b04581.

[5] A. K. Boal and J. K. Barton. Electrochemical detection of lesions in DNA. *Bioconjugate Chemistry*, 16(2):312–321, 2005. ISSN 10431802. doi: 10.1021/bc0497362.

[6] A. K. Boal, E. Yavin, O. A. Lukianova, V. L. O'Shea, S. S. David, and J. K. Barton. DNA-bound redox activity of DNA repair glycosylases containing [4Fe-4S] clusters. *Biochemistry*, 44(23):8397–8407, 2005. ISSN 00062960. doi: 10.1021/bi047494n. URL http://pubs.acs.org/doi/abs/10.1021/bi047494n.

[7] A. K. Boal, J. C. Genereux, P. A. Sontz, J. A. Gralnick, D. K. Newman, and J. K. Barton. Redox signaling between DNA repair proteins for efficient lesion detection. *Proceedings of the National Academy of Sciences*, 106(36):15237–15242, sep 2009. ISSN 0027-8424. doi: 10.1073/pnas.0908059106. URL http://www.pnas.org/cgi/doi/10.1073/pnas.0908059106.

[8] T. J. Bourret, K. A. Lawrence, J. A. Shaw, T. Lin, S. J. Norris, and F. C. Gherardini. The nucleotide excision repair pathway protects Borrelia burgdorferi from nitrosative stress in Ixodes scapularis ticks. *Frontiers in Microbiology*, 7 (SEP), 2016. ISSN 1664302X. doi: 10.3389/fmicb.2016.01397.

[9] C. W. Brown, V. Sridhara, D. R. Boutz, M. D. Person, E. M. Marcotte, J. E. Barrick, and C. O. Wilke. Large-scale analysis of post-translational modifications in E.coli under glucose-limiting conditions. *BMC Genomics*, 18 (1), 2017. ISSN 14712164. doi: 10.1186/s12864-017-3676-8.

[10] K. Cheng and D. B. Wigley. DNA translocation mechanism of an XPD family helicase. *eLife*, 7:e42400, 2018. ISSN 2050084X. doi: 10.7554/eLife.42400.

[11] A. Ciccia and S. J. Elledge. The DNA Damage Response: Making It Safe to Play with Knives. *Molecular Cell*, 40(2):179–204, 2010. ISSN 10972765. doi: 10.1016/j.molcel.2010.09.019.

[12] J. C. Crack, J. Green, A. J. Thomson, and N. E. Brun. Iron-sulfur clusters as biological sensors: The chemistry of reactions with molecular oxygen and nitric oxide. *Accounts of Chemical Research*, 47(10):3196–3205, 2014. ISSN 15204898. doi: 10.1021/ar5002507.

[13] R. P. Cunningham, H. Asahara, J. F. Bank, C. P. Scholes, J. C. Salerno, K. Surerus, E. Miinck, J. McCracken, J. Peisach, and M. H. Emptage. Endonuclease III Is an Iron-Sulfur Protein. *Biochemistry*, 28(10):4450–4455, May 1989. ISSN 15204995. doi: 10.1021/bi00436a049. URL http://dx.doi.org/10.1021/bi00436a049.

[14] A. Cvetkovic, A. L. Menon, M. P. Thorgersen, J. W. Scott, F. L. Poole, F. E. Jenney, W. A. Lancaster, J. L. Praissman, S. Shanmukh, B. J. Vaccaro, S. A. Trauger, E. Kalisiak, J. V. Apon, G. Siuzdak, S. M. Yannone, J. A. Tainer, and M. W. Adams. Microbial metalloproteomes are largely uncharacterized. *Nature*, 466(7307):779–782, 2010. ISSN 00280836. doi: 10.1038/nature09265.

[15] M. J. DellaVecchia, D. L. Croteau, M. Skorvaga, S. V. Dezhurov, O. I. Lavrik, and B. Van Houten. Analyzing the handoff of DNA from UvrA to UvrB utilizing DNA-protein photoaffinity labeling. *Journal of Biological Chemistry*, 279 (43):45245–45256, 2004. ISSN 00219258. doi: 10.1074/jbc.M408659200.

[16] L. A. Ekanger, P. H. Oyala, A. Moradian, M. J. Sweredoski, and J. K. Barton. Nitric Oxide Modulates Endonuclease III Redox Activity by a 800 mV Negative Shift upon [Fe4S4] Cluster Nitrosylation. *Journal of the American Chemical Society*, 140(37):11800–11810, sep 2018. ISSN 0002-7863. doi: 10.1021/jacs.8b07362. URL https://doi.org/10.1021/jacs.8b07362.

[17] L. Fan, J. O. Fuss, Q. J. Cheng, A. S. Arvai, M. Hammel, V. A. Roberts, P. K. Cooper, and J. A. Tainer. XPD Helicase Structures and Activities: Insights into the Cancer and Aging Phenotypes from XPD Mutations. *Cell*, 133(5): 789–800, 2008. ISSN 00928674. doi: 10.1016/j.cell.2008.04.030.

[18] D. F. Felício, L. d. S. Vidal, R. S. Irineu, A. C. Leitão, W. A. von Kruger, C. d. P. Britto, A. Cardoso, J. S. Cardoso, and C. Lage. Overexpression of Escherichia coli nucleotide excision repair genes after cisplatin-induced damage. *DNA*

Repair, 12(1):63–72, 2013. ISSN 15687864. doi: 10.1016/j.dnarep.2012.10.009.

[19] S. A. Freibert, B. D. Weiler, E. Bill, A. J. Pierik, U. Mühlenhoff, and R. Lill. Biochemical Reconstitution and Spectroscopic Analysis of Iron–Sulfur Proteins. *Methods in Enzymology*, 599:197–226, 2018. ISSN 15577988. doi: 10.1016/bs.mie.2017.11.034.

[20] J. O. Fuss, C. L. Tsai, J. P. Ishida, and J. A. Tainer. Emerging critical roles of Fe-S clusters in DNA replication and repair. *Biochimica et Biophysica Acta - Molecular Cell Research*, 1853(6):1253–1271, 2015. ISSN 18792596. doi: 10.1016/j.bbamcr.2015.01.018. URL http://dx.doi.org/10.1016/j.bbamcr.2015.01.018.

[21] K. S. Gates. An overview of chemical processes that damage cellular DNA: Spontaneous hydrolysis, alkylation, and reactions with radicals. *Chemical Research in Toxicology*, 22(11):1747–1760, 2009. ISSN 0893228X. doi: 10.1021/tx900242k.

[22] G. Giglia-Mari, A. Zotter, and W. Vermeulen. DNA damage response. *Cold Spring Harbor Perspectives in Biology*, 3(1):1–19, 2011. ISSN 19430264. doi: 10.1101/cshperspect.a000745.

[23] D. Graf, J. Wesslowski, H. Ma, P. Scheerer, N. Krauß, I. Oberpichler, F. Zhang, and T. Lamparter. Key amino acids in the bacterial (6-4) photolyase PhrB from Agrobacterium fabrum. *PLoS ONE*, 10(10):e0140955, 2015. ISSN 19326203. doi: 10.1371/journal.pone.0140955.

[24] H. B. Gray, E. I. Stiefel, J. S. Valentine, and I. Bertini. *Bioinorganic Chemistry*. University Books, 2006. ISBN 1891389432.

[25] M. A. Grodick. *DNA-mediated charge transport signaling within the cell*. PhD thesis, California Institute of Technology, 2016. URL https://resolver.caltech.edu/CaltechTHESIS:07192015-214603085.

[26] M. A. Grodick, H. M. Segal, T. J. Zwang, and J. K. Barton. DNA-mediated signaling by proteins with 4Fe-4S clusters is necessary for genomic integrity. *Journal of the American Chemical Society*, 136(17):6470–6478, 2014. ISSN 15205126. doi: 10.1021/ja501973c.

[27] M. A. Grodick, N. B. Muren, and J. K. Barton. DNA charge transport within the cell. *Biochemistry*, 54(4):962–973, 2015. ISSN 15204995. doi: 10.1021/bi501520w.

[28] L. M. Guzman, D. Belin, M. J. Carson, and J. Beckwith. Tight regulation, modulation, and high-level expression by vectors containing the arabinose P(BAD) promoter. *Journal of Bacteriology*, 177(14):4121–4130, 1995. ISSN 00219193. doi: 10.1128/jb.177.14.4121-4130.1995.

[29] P. O. Hardy and G. Chaconas. The nucleotide excision repair system of borrelia burgdorferi is the sole pathway involved in repair of DNA damage by UV light. *Journal of Bacteriology*, 195(10):2220–2231, 2013. ISSN 00219193. doi: 10.1128/JB.00043-13.

[30] J. R. Houser, C. Barnhart, D. R. Boutz, S. M. Carroll, A. Dasgupta, J. K. Michener, B. D. Needham, O. Papoulas, V. Sridhara, D. K. Sydykova, C. J. Marx, M. S. Trent, J. E. Barrick, E. M. Marcotte, and C. O. Wilke. Controlled Measurement and Comparative Analysis of Cellular Components in E. coli Reveals Broad Regulatory Changes in Response to Glucose Starvation. *PLoS Computational Biology*, 11(8):e1004400, 2015. ISSN 15537358. doi: 10.1371/journal.pcbi.1004400.

[31] C. D. Hughes, H. Wang, H. Ghodke, M. Simons, A. Towheed, Y. Peng, B. Van Houten, and N. M. Kad. Real-time single-molecule imaging reveals a direct interaction between UvrC and UvrB on DNA tightropes. *Nucleic Acids Research*, 41(9):4901–4912, 2013. ISSN 03051048. doi: 10.1093/nar/gkt177.

[32] J. A. Imlay. The molecular mechanisms and physiological consequences of oxidative stress: Lessons from a model bacterium. *Nature Reviews Microbiology*, 11(7):443–454, 2013. ISSN 17401526. doi: 10.1038/nrmicro3032.

[33] R. B. Kapust, J. Tözsér, J. D. Fox, D. E. Anderson, S. Cherry, T. D. Copeland, and D. S. Waugh. Tobacco etch virus protease: Mechanism of autolysis and rational design of stable mutants with wild-type catalytic proficiency. *Protein Engineering*, 14(12):993–1000, 2001. ISSN 02692139.

[34] E. Karakas, J. J. Truglio, D. Croteau, B. Rhau, L. Wang, B. Van Houten, and C. Kisker. Structure of the C-terminal half of UvrC reveals an RNase H endonuclease domain with an Argonaute-like catalytic triad. *EMBO Journal*, 26(2):613–622, 2007. ISSN 14602075. doi: 10.1038/sj.emboj.7601497.

[35] C. Kisker, J. Kuper, and B. Van Houten. Prokaryotic nucleotide excision repair. *Cold Spring Harbor Perspectives in Biology*, 5(3):1–18, 2013. ISSN 19430264. doi: 10.1101/cshperspect.a012591.

[36] S. Klinge, J. Hirst, J. D. Maman, T. Krude, and L. Pellegrini. An iron-sulfur domain of the eukaryotic primase is essential for RNA primer synthesis. *Nature Structural and Molecular Biology*, 14(9):875–877, 2007. ISSN 15459993. doi: 10.1038/nsmb1288.

[37] K. N. Kreuzer. DNA damage responses in prokaryotes: Regulating gene expression, modulating growth patterns, and manipulating replication forks. *Cold Spring Harbor Perspectives in Biology*, 5(11):a012674, 2013. ISSN 19430264. doi: 10.1101/cshperspect.a012674.

[38] A. Kuzminov. Recombinational repair of DNA damage in Escherichia coli and bacteriophage lambda. *Microbiology and Molecular Biology*

Reviews : MMBR, 63(4):751–813, 1999. ISSN 1092-2172. URL http://www.ncbi.nlm.nih.gov/pubmed/10585965%0Ahttp://www.pubmedcentral.nih.gov/articlerender.fcgi?artid=PMC98976.

[39] F. H. Lessner, M. E. Jennings, A. Hirata, E. C. Duin, and D. J. Lessner. Subunit D of RNA polymerase from Methanosarcina acetivorans contains two oxygen-labile [4Fe-4S] clusters: Implications for oxidant-dependent regulation of transcription. *Journal of Biological Chemistry*, 287(22):18510–18523, 2012. ISSN 00219258. doi: 10.1074/jbc.M111.331199.

[40] G.-W. Li, D. Burkhardt, C. Gross, and J. Weissman. Quantifying Absolute Protein Synthesis Rates Reveals Principles Underlying Allocation of Cellular Resources. *Cell*, 157(3):624–635, Apr 2014. ISSN 0092-8674. doi: 10.1016/j.cell.2014.02.033. URL https://doi.org/10.1016/j.cell.2014.02.033.

[41] J. J. Lin and A. Sancar. The C-terminal half of UvrC protein is sufficient to reconstitute (A)BC excinuclease. *Proceedings of the National Academy of Sciences of the United States of America*, 88(15):6824–6828, 1991. ISSN 00278424. doi: 10.1073/pnas.88.15.6824.

[42] S. J. Lippard and J. M. Berg. *Principles of Bioinorganic Chemistry*. University Science Books, Mill Valley, CA, 1994. ISBN 0935702725.

[43] Z. Lu, R. Sethu, and J. A. Imlay. Endogenous superoxide is a key effector of the oxygen sensitivity of a model obligate anaerobe. *Proceedings of the National Academy of Sciences of the United States of America*, 115(14):E3266–E3275, 2018. ISSN 10916490. doi: 10.1073/pnas.1800120115.

[44] N. Maio, A. Singh, H. Uhrigshardt, N. Saxena, W. H. Tong, and T. A. Rouault. Cochaperone binding to LYR motifs confers specificity of iron sulfur cluster delivery. *Cell Metabolism*, 19(3):445–457, 2014. ISSN 19327420. doi: 10.1016/j.cmet.2014.01.015.

[45] N. Mazloum, M. A. Stegman, D. L. Croteau, B. Van Houten, N. S. Kwon, Y. Ling, C. Dickinson, A. Venugopal, M. A. Towheed, and C. Nathan. Identification of a chemical that inhibits the mycobacterial UvrABC complex in nucleotide excision repair. *Biochemistry*, 50(8):1329–1335, 2011. ISSN 00062960. doi: 10.1021/bi101674c.

[46] E. L. Mettert and P. J. Kiley. Fe-S proteins that regulate gene expression. *Biochimica et Biophysica Acta - Molecular Cell Research*, 1853(6):1284–1293, 2015. ISSN 18792596. doi: 10.1016/j.bbamcr.2014.11.018.

[47] I. G. Minko, A. J. Kurtz, D. L. Croteau, B. Van Houten, T. M. Harris, and R. S. Lloyd. Initiation of repair of DNA - Polypeptide cross-links by the UvrABC nuclease. *Biochemistry*, 44(8):3000–3009, 2005. ISSN 00062960. doi: 10.1021/bi0478805.

[48] C. Moccia, J. Krebes, S. Kulick, X. Didelot, C. Kraft, C. Bahlawane, and S. Suerbaum. The nucleotide excision repair (NER) system of Helicobacter pylori: Role in mutation prevention and chromosomal import patterns after natural transformation. *BMC Microbiology*, 12, 2012. ISSN 14712180. doi: 10.1186/1471-2180-12-67.

[49] G. F. Moolenaar, M. Bazuine, I. C. Van Knippenberg, R. Visse, and N. Goosen. Characterization of the Escherichia coli damage-independent UvrBC endonuclease activity. *Journal of Biological Chemistry*, 273(52):34896–34903, 1998. ISSN 00219258. doi: 10.1074/jbc.273.52.34896.

[50] D. J. A. Netz, C. M. Stith, M. Stümpfig, G. Köpf, D. Vogel, H. M. Genau, J. L. Stodola, R. Lill, P. M. J. Burgers, and A. J. Pierik. Eukaryotic DNA polymerases require an iron-sulfur cluster for the formation of active complexes. *Nature Chemical Biology*, 8(1):125–132, 2012. ISSN 1552-4450. doi: 10.1038/nchembio.721. URL http://www.nature.com/doifinder/10.1038/nchembio.721.

[51] C. Notredame, D. G. Higgins, and J. Heringa. T-coffee: a novel method for fast and accurate multiple sequence alignment. *Journal of Molecular Biology*, 302(1):205–217, 2000. ISSN 0022-2836. doi: https://doi.org/10.1006/jmbi.2000.4042. URL http://www.sciencedirect.com/science/article/pii/S0022283600940427.

[52] D. K. Orren and A. Sancar. The (A)BC excinuclease of Escherichia coli has only the UvrB and UvrC subunits in the incision complex. *Proceedings of the National Academy of Sciences of the United States of America*, 86(14):5237–5241, 1989. ISSN 00278424. doi: 10.1073/pnas.86.14.5237.

[53] C. G. Pheeney, A. R. Arnold, M. A. Grodick, and J. K. Barton. Multiplexed electrochemistry of DNA-bound metalloproteins. *Journal of the American Chemical Society*, 135(32):11869–11878, 2013. ISSN 00027863. doi: 10.1021/ja4041779.

[54] J. T. Reardon and A. Sancar. Purification and Characterization of Escherichia coli and Human Nucleotide Excision Repair Enzyme Systems. *Methods in Enzymology*, 408:189–213, 2006. ISSN 00766879. doi: 10.1016/S0076-6879(06)08012-8.

[55] B. Ren, X. Duan, and H. Ding. Redox control of the DNA damage-inducible protein DinG helicase activity via its iron-sulfur cluster. *Journal of Biological Chemistry*, 284(8):4829, 2009. ISSN 00219258. doi: 10.1074/jbc.M807943200.

[56] G. L. Rosano and E. A. Ceccarelli. Recombinant protein expression in Escherichia coli: Advances and challenges. *Frontiers in Microbiology*, 5(Apr), 2014. ISSN 1664302X. doi: 10.3389/fmicb.2014.00172.

[57] T. A. Rouault. Iron-sulfur proteins hiding in plain sight. *Nature Chemical Biology*, 11(7):442–445, 2015. ISSN 15524469. doi: 10.1038/nchembio.1843.

[58] J. Rudolf, V. Makrantoni, W. J. Ingledew, M. J. R. Stark, and M. F. White. The DNA Repair Helicases XPD and FancJ Have Essential Iron-Sulfur Domains. *Molecular Cell*, 23(6):801–808, 2006. ISSN 10972765. doi: 10.1016/j.molcel.2006.07.019.

[59] A. Sancar and W. D. Rupp. A novel repair enzyme: UVRABC excision nuclease of Escherichia coli cuts a DNA strand on both sides of the damaged region. *Cell*, 33(1):249–260, 1983. ISSN 00928674. doi: 10.1016/0092-8674(83)90354-9.

[60] A. Sancar, B. M. Kacinski, D. L. Mott, and W. D. Rupp. Identification of the uvrC gene product. *Proceedings of the National Academy of Sciences*, 78 (9):5450 – 5454, sep 1981. ISSN 00278424. doi: 10.1073/pnas.78.9.5450. URL http://www.pnas.org/content/78/9/5450.abstracthttp://ukpmc.ac.uk/articlerender.cgi?tool=pubmed&pubmedid=7029536%5Cnhttp://www.ncbi.nlm.nih.gov/entrez/query.fcgi?cmd=Retrieve&db=PubMed&dopt=Citation&list_uids=7029536.

[61] K. N. Schaefer and J. K. Barton. DNA-mediated oxidation of p53. *Biochemistry*, 53(21):3467–3475, 2014. ISSN 15204995. doi: 10.1021/bi5003184.

[62] K. N. Schaefer, W. M. Geil, M. J. Sweredoski, A. Moradian, S. Hess, and J. K. Barton. Oxidation of p53 through DNA charge transport involves a network of disulfides within the DNA-binding domain. *Biochemistry*, 54(3):932–941, 2015. ISSN 15204995. doi: 10.1021/bi501424v.

[63] M. Senda and T. Senda. Anaerobic crystallization of proteins. *Biophysical Reviews*, 10(2):183–189, 2018. ISSN 18672469. doi: 10.1007/s12551-017-0345-8.

[64] G. D. Shimberg, J. D. Pritts, and S. L. Michel. Iron–Sulfur Clusters in Zinc Finger Proteins. *Methods in Enzymology*, 599:101–137, 2018. ISSN 15577988. doi: 10.1016/bs.mie.2017.09.005.

[65] S. Singh, G. E. Folkers, A. M. Bonvin, R. Boelens, R. Wechselberger, A. Niztayev, and R. Kaptein. Solution structure and DNA-binding properties of the C-terminal domain of UvrC from E. Coli. *EMBO Journal*, 21(22):6257–6266, 2002. ISSN 02614189. doi: 10.1093/emboj/cdf627.

[66] J. D. Slinker, N. B. Muren, A. A. Gorodetsky, and J. K. Barton. Multiplexed DNA-modified electrodes. *Journal of the American Chemical Society*, 132(8):2769–2774, 2010. ISSN 00027863. doi: 10.1021/ja909915m.

[67] H. P. Sørensen and K. K. Mortensen. Advanced genetic strategies for recombinant protein expression in Escherichia coli. *Journal of Biotechnology*, 115 (2):113–128, 2005. ISSN 01681656. doi: 10.1016/j.jbiotec.2004.08.004.

[68] P. Sun, J. E. Tropea, and D. S. Waugh. Enhancing the Solubility of Recombinant Proteins in *Escherichia coli* by Using Hexahistidine-Tagged Maltose-Binding Protein as a Fusion Partner. 705:259–274, 2011. ISSN 10643745. doi: 10.1007/978-1-61737-967-3_16.

[69] W. V. Sweeney and J. C. Rabinowitz. Proteins Containing 4Fe-4S Clusters: An Overview. *Annual Review of Biochemistry*, 49(1):139–161, 1980. ISSN 0066-4154. doi: 10.1146/annurev.bi.49.070180.001035.

[70] M. S. Tang, M. Nazimiec, X. Ye, G. H. Iyer, J. Eveleigh, Y. Zheng, W. Zhou, and Y. Y. Tang. Two Forms of UvrC Protein with Different Double-stranded DNA Binding Affinities. *Journal of Biological Chemistry*, 276(6):3904–3910, 2001. ISSN 00219258. doi: 10.1074/jbc.M008538200.

[71] Y. Taniguchi, P. J. Choi, G.-W. Li, H. Chen, M. Babu, J. Hearn, A. Emili, and X. S. Xie. Quantifying E. coli Proteome and Transcriptome with Single-Molecule Sensitivity in Single Cells. *Science*, 329(5991):533 LP – 538, jul 2010. doi: 10.1126/science.1188308. URL http://science.sciencemag.org/content/329/5991/533.abstract.

[72] K. Terpe. Overview of bacterial expression systems for heterologous protein production: From molecular and biochemical fundamentals to commercial systems. *Applied Microbiology and Biotechnology*, 72(2):211–222, 2006. ISSN 01757598. doi: 10.1007/s00253-006-0465-8.

[73] D. C. Thomas, M. Levy, and A. Sancar. Amplification and purification of UvrA, UvrB, and UvrC proteins of Escherichia coli. *Journal of Biological Chemistry*, 260(17):9875–9883, 1985. ISSN 00219258.

[74] J. J. Truglio, B. Rhau, D. L. Croteau, L. Wang, M. Skorvaga, E. Karakas, M. J. DellaVecchia, H. Wang, B. Van Houten, and C. Kisker. Structural insights into the first incision reaction during nucleotide excision repair. *The EMBO journal*, 24(5):885–894, 2005. ISSN 0261-4189. doi: 10.1038/sj.emboj.7600568.

[75] J. J. Truglio, D. L. Croteau, B. van Houten, and C. Kisker. Prokaryotic Nucleotide Excision Repair: The UvrABC System. *Chemical Reviews*, 106 (2):233–252, Feb 2006. ISSN 00092665. doi: 10.1021/cr040471u. URL http://dx.doi.org/10.1021/cr040471u.

[76] J. J. Truglio, E. Karakas, B. Rhau, H. Wang, M. J. Dellavecchia, B. Van Houten, and C. Kisker. Structural basis for DNA recognition and processing by UvrB. *Nature Structural and Molecular Biology*, 13(4):360–364, 2006. ISSN 15459985. doi: 10.1038/nsmb1072.

[77] C. L. Tsai and J. A. Tainer. Robust Production, Crystallization, Structure Determination, and Analysis of [Fe–S] Proteins: Uncovering Control of Electron Shuttling and Gating in the Respiratory Metabolism of Molybdopterin Guanine Dinucleotide Enzymes. In *Methods in Enzymology*, volume 599, pages 157–196. 2018. ISBN 9780128147177. doi: 10.1016/bs.mie.2017.11.006.

[78] E. C. M. Tse, T. J. Zwang, and J. K. Barton. The Oxidation State of [4Fe4S] Clusters Modulates the DNA-Binding Affinity of DNA Repair Proteins. *Journal of the American Chemical Society*, 139(36):12784–12792, sep 2017. ISSN 0002-7863. doi: 10.1021/jacs.7b07230. URL http://dx.doi.org/10.1021/jacs.7b07230.

[79] S. Vaithiyalingam, E. M. Warren, B. F. Eichman, and W. J. Chazin. Insights into eukaryotic DNA priming from the structure and functional interactions of the 4Fe-4S cluster domain of human DNA primase. *Proceedings of the National Academy of Sciences*, 107(31):13684–13689, 2010. ISSN 0027-8424. doi: 10.1073/pnas.1002009107. URL http://www.pnas.org/cgi/doi/10.1073/pnas.1002009107.

[80] B. Van Houten. Nucleotide excision repair in Escherichia coli. *Microbiological Reviews*, 54(1):18 –51, Mar 1990. URL http://mmbr.asm.org/content/54/1/18.abstract.

[81] B. Van Houten, H. Gamper, A. Sancar, and J. E. Hearst. DNase I footprint of ABC excinuclease. *The Journal of Biological Chemistry*, 262(27):13180–13187, 1987. ISSN 00219258.

[82] R. Visse, M. De Ruijter, G. F. Moolenaar, and P. Van de Putte. Analysis of UvrABC endonuclease reaction intermediates on cisplatin- damaged DNA using mobility shift gel electrophoresis. *Journal of Biological Chemistry*, 267 (10):6736–6742, 1992. ISSN 00219258.

[83] O. N. Voloshin and R. D. Camerini-Otero. The DinG protein from Escherichia coli is a structure-specific helicase. *Journal of Biological Chemistry*, 282(25): 18437–18447, 2007. ISSN 00219258. doi: 10.1074/jbc.M700376200.

[84] O. N. Voloshin, F. Vanevski, P. P. Khil, and R. D. Camerini-Otero. Characterization of the DNA damage-inducible helicase DinG from Escherichia coli. *Journal of Biological Chemistry*, 278(30):28284–28293, 2003. ISSN 00219258. doi: 10.1074/jbc.M301188200.

[85] M. F. White and M. S. Dillingham. Iron-sulphur clusters in nucleic acid processing enzymes. *Current Opinion in Structural Biology*, 22(1):94–100, 2012. ISSN 0959440X. doi: 10.1016/j.sbi.2011.11.004.

[86] N. Wirth, J. Gross, H. M. Roth, C. N. Buechner, C. Kisker, and I. Tessmer. Conservation and divergence in nucleotide excision repair lesion recognition. *Journal of Biological Chemistry*, 291(36):18932–18946, 2016. ISSN 1083351X. doi: 10.1074/jbc.M116.739425.

[87] S. C. Wolski, J. Kuper, P. Hänzelmann, J. J. Truglio, D. L. Croteau, B. Van Houten, and C. Kisker. Crystal structure of the FeS cluster-containing nucleotide excision repair helicase XPD. *PLoS Biology*, 6(6):1332–1342, 2008. ISSN 15449173. doi: 10.1371/journal.pbio.0060149.

[88] A. Yan and P. J. Kiley. Chapter 42 Techniques to Isolate O_2-Sensitive Proteins: [4Fe-4S]-FNR as an Example, 2009. ISSN 00766879.

[89] E. Yavin, A. K. Boal, E. D. Stemp, E. M. Boon, A. L. Livingston, V. L. O'Shea, S. S. David, and J. K. Barton. Protein-DNA charge transport: Redox activation of a DNA repair protein by guanine radical. *Proceedings of the National Academy of Sciences of the United States of America*, 102(10):3546–3551, 2005. ISSN 00278424. doi: 10.1073/pnas.0409410102.

[90] J. T. P. Yeeles, T. D. Deegan, A. Janska, A. Early, and J. F. X. Diffley. Regulated eukaryotic DNA replication origin firing with purified proteins. *Nature*, 519 (7544):431–435, 2015. ISSN 14764687. doi: 10.1038/nature14285.

[91] A. T. Yeung, W. B. Mattes, and L. Grossman. Protein complexes formed during the incision reaction catalyzed by the Escherichia coli UvrABC endonuclease. *Nucleic Acids Research*, 14(6):2567–2582, 1986. ISSN 03051048. doi: 10.1093/nar/14.6.2567.

[92] G. H. Yoakum and L. Grossman. Identification of E. coli *uvrC* protein. *Nature*, 292(5819):171–173, 1981. ISSN 1476-4687. doi: 10.1038/292171a0. URL https://doi.org/10.1038/292171a0.

[93] A. Zhou. *Investigations of DNA-Mediated Redox Signaling Between E. coli DNA Repair Pathways*. PhD thesis, California Institute of Technology, 2019. URL http://resolver.caltech.edu/CaltechTHESIS:11262018-103442842.

[94] Y. Zou, R. Walker, H. Bassett, N. E. Geacintov, and B. Van Houten. Formation of DNA repair intermediates and incision by the ATP-dependent UvrB-UvrC endonuclease. *Journal of Biological Chemistry*, 272(8):4820–4827, 1997. ISSN 00219258. doi: 10.1074/jbc.272.8.4820.

Chapter 3

UVRC COORDINATES AN O_2-SENSITIVE [4FE4S] CLUSTER*

3.1 INTRODUCTION

Proteins that coordinate a metal cofactors often function in cells to maintain homeostasis in the cell, and some even function as sensors of cellular environment [12, 30, 31, 43]. Classic examples include transcription factors, radical SAM enzymes, nitrogenase, hydrogenases, among many others. Metal centers can easily be poisoned by reactive diatomics like O_2 and NO, though some proteins, chiefly transcription factors, utilize changes at the coordination site to regulate responses to stress conditions, iron availability, and the redox state of the cell [12, 30, 31, 43]. As such, many metalloproteins require use of anaerobic methods in order to preserve the integrity of the coordination site and even the protein itself outside of a cellular context [8, 72, 79, 84]. Because air-free techniques have a long history of development by bioinorganic chemists, many robust methods exist that can be readily adapted for other proteins. Appreciation that some [4Fe4S] proteins may require anaerobic handling has begun, and as researchers continue to detect metal centers coordinated by nucleic acid processing enzymes, we expect that use of anaerobic methods will become more and more widespread for repair and replication proteins [20, 63].

Our group has developed several anaerobic methods to examine the DNA-bound redox chemistry, the nature of substrate interactions in reduced (2+) and oxidized (3+) states, and enzymatic activity in reduced and oxidized states of [4Fe4S] repair and replication proteins. However, the enzymes examined to date have not required anaerobic methods during purification in order to isolate protein with stable cofactors. To develop a robust system for purification of UvrC, we utilized the resources on campus for nitrogenase that were made available to us by the Rees lab [72, 84]. The Rees group has developed well-established methods for purifying and studying nitrogenase under strict anaerobic conditions. Detailed here are the anaerobic methodologies that were adapted for UvrC and the first characterization of UvrC as an O_2-sensitive metalloprotein, which serves as a basis for future work

*Experimental Methods, Results and Discussion, and Conclusions adapted from R. M. B. Silva, M. A. Grodick, and J. K. Barton (2020). UvrC Coordinates an O_2-Sensitive [4Fe4S] Cofactor. *Submitted*.

with UvrC in holo form.

3.2 EXPERIMENTAL METHODS

3.2.1 General Procedures

All reagents were used as received and stored according the manufacturer's instructions. All water used was purified on a Milli-Q Reference Ultrapure Water Purification System (≥18.2 MΩ cm). Anaerobic vinyl chambers (glove bags) were kept at atmospheres of (2-4% H_2 in Argon or N_2, ≤ 1 ppm of O_2) with Pd scrubbing towers (Coy Laboratories) and used for experiments requiring anaerobic conditions. Unless specified otherwise, all protein buffers were degassed in an anaerobic chamber by stirring vigorously overnight, protein samples were handled anaerobically, and other solutions of reagents that came in contact with UvrC were prepared anaerobically as well [40, 68, 87]. UV-Vis spectra of UvrC were taken on a Cary 100 Bio (Agilent) spectrophotometer using custom quartz cuvettes (Starna) modified with an airtight screwcap or on a DeNovix DS-C Spectrophotometer using quartz cuvettes (Starna) in the glove bag. DNA concentrations were taken as above aerobically. High performance liquid chromatography (HPLC) was done using HP 1100 (Aglient) system and fast performance liquid chromatography (FPLC) was done using an ÄKTA FPLC™ system (GE Life Sciences) or a NGC™ Chromatography System (Bio-Rad). Before use, all solvents and buffers used during purifications were filtered through a 0.22 or 0.45 μm Nalgene™ Rapid-Flow™ filter unit with an SFCA membrane (ThermoFisher Scientific). Glass plates, spacers, and the Owl™ Vertical Electrophoresis System were purchased from ThermoFisher Scientific. Sequencing gel supplies were purchased from National Diagnostics.

3.2.2 DNA Substrates and Plasmids

Unless specified otherwise below, oligomers and plasmids were treated as detailed in Chapter 2.

3.2.3 Overexpression of UvrC

The MBP-UvrC fusion protein was overexpressed as described in Chapter 2.

3.2.4 Air-free Purification of UvrC

Described is the procedure for purifying UvrC that was adapted from the purification method for nitrogenase [72, 84]. Unless otherwise stated, steps were completed at room temperature. See **Appendix A** at the end of this chapter for additional

description of the methods.

3.2.4.1 Degassing Purification Buffers

The following purification buffers were prepared at a pH of 7.5: Lysis Buffer (25 mM Tris-HCl, 0.5 M KCl, 10% v/v glycerol), Nickel Elution Buffer (25 mM Tris-HCl, 0.5 M KCl, 20% v/v glycerol, 0.5 M Imidazole), and Size Exclusion Buffer (25 mM Tris-HCl, 0.5 M KCl, 20% v/v glycerol). The buffers were placed in separate round bottom flasks with custom glass adapters, connected to a Schlenk line, and degassed using a timer (Eagle Signal) alternating vacuum (7 min) and Ar (2 min) for 12 cycles.

3.2.4.2 Column Equilibration

The day before cell lysis, two stacked HisTrap HP 5 mL columns (GE Healthcare) and a Superdex 200 preparative grade 26/200 size exclusion column (GE Healthcare) were used for purification. Nickel columns were washed with at least 5 column volumes (10 mL, ColVs) of ddH_2O and the Superdex column was washed with 1.5 to 2 ColVs of ddH_2O using an ÄKTA FPLC™ system (GE Life Sciences). Once buffers were degassed, the Superdex 200 was washed with 1.5 to 2 ColV (330 mL) of size exclusion buffer overnight. The next day, the HisTrap columns were washed with >10 ColV of lysis buffer with 1 mM dithiothreitol (DTT). DTT was also added to elution buffer to a final concentration of 1 mM. The Superdex 200 was also equilibrated with an addition 100 mL of degassed size exclusion buffer containing 1 mM DTT.

3.2.4.3 Sterilization of Equipment

A glass stirring rod, a glass beaker, polycarbonate centrifuge tubes, Dounce homogenizer with rods, and two 250 mL wide-mouth screw cap bottles were autoclaved and subsequently placed in a cold room to chill overnight.

3.2.4.4 Anaerobic lysis and chromatography[†]

All following steps were completed in an anaerobic chamber, on a Schlenk line, or in airtight vials. While columns were equilibrating, cell pellets were thawed,

[†]This section is completed in a single day over the course of 15-17 hours. Freezing and storing the concentrated fractions following the Histrap column and completing the purification over a span of two days has never been attempted. Considering the increased stability of UvrC in anaerobic conditions, this may be tolerated.

resuspended in Lysis Buffer (100 mL lysis buffer per 10 g of wet pellet) that was supplemented on the day of the purification with 6-8 tablets of crushed cOmplete™ protease inhibitor cocktail tablets (Roche), DNAse (15 kU, Sigma), and DTT (1 mM), and homogenized on ice using a Dounce homogenizer. The cell slurry was passed over a 100 μm nylon cell strainer (Corning) and lysed using an Emulsiflex-C5 (Avestin) homogenizer at 25,000 psi under a positive pressure of Ar over two cycles. For each cycle, cell lysate was collected on ice. Lysate was loaded into polycarbonate vials and centrifuged on a Sorvall™ RC 6 Plus Centrifuge (ThermoFisherScientific) at 13,000 rpm for 45 minutes at 4 °C.

Using an ÄKTA FPLC™ system (GE Life Sciences), the supernatant was loaded under a positive pressure of Ar at a flow rate of 2.5 mL/min onto the HisTrap column. At a flow rate of 1.5 mL/min, Histrap columns were washed with 4 ColVs of 10 % Elution Buffer and eluted with 10 to 100 % Elution Buffer over 15 ColVs. Fractions were collected under a positive pressure of Ar and concentrated to <10 mLs using an Amicon® Stirred Ultrafiltration Cell over a 30 kDa cutoff filter using the minimum overpressure that allowed for filtration. Concentrated fractions were loaded under a positive pressure of Ar onto the Superdex 200 at a flow rate of 1 mL/min. Samples were eluted with 1 ColV of Size Exclusion Buffer containing 1 mM DTT. Soluble fractions were collected, concentrated between 20-30 μM to avoid precipitation upon freezing, aliquoted in screw cap vials, then immediately flash frozen in liquid N_2 and stored at ≤ -80 °C. Subfractions were taken throughout the purification to assess the purity of the samples by SDS-PAGE as above, combining Blue Loading Buffer (NEB) 1:1 with fractions, and pre-heating in sample buffer at 80 °C for 2 minutes before resolving on a 4-20% TGX precast gel (Bio-Rad) at 200 V for 35 min.

3.2.5 Fe Quantification by the Ferene Assay

The colorimetric ferene assay was performed according to a published procedure in triplicate [16]. Briefly, samples (including a UvrC buffer control) were diluted 1:1 with HNO_3 (21.7% v/v) to a total volume of 200 μL. Samples were heated at 95 °C for 30 min, cooled at 4 °C for at least 10 min, and centrifuged. After centrifugation, 600 μL of ammonium acetate (7.5% w/v), 100 μL of ascorbic acid (12.5% w/v), and 100 μL of 3-(2-pyridyl)-5,6-di(2-furyl)-1,2,4-triazine-5′,5′′,-disulfonate (ferene, 10 mM) were added. Samples were incubated at room temperature for 30 min before absorbance at 593 nm was recorded. Calibration curves were prepared using an Fe standard solution (1001 ± 2 mg/L Fe in 2% v/v HNO_3, TraceCERT Fe standard for

ICP).

3.2.6 Assessment of UvrC Stability

To investigate the stability of UvrC under aerobic conditions, UvrC was thawed on ice in a cold room and then buffer exchanged into aerobic UvrC buffer as described above. UvrC was quantified by UV-Vis as above in Starna cuvettes that were sealed with a screw cap (to prevent evaporation) before heating in a 37 °C water bath. Generally, between 10 μM and 30 μM of UvrC (by cluster) was used. For each time point, the Cary instrument was blanked with buffer at 37 °C. Samples at a concentration of 5 μM were loaded into a Hamilton syringe, injected into a 250 μL superloop on a Bio-Rad NGC, and applied to a Superdex 100/300L analytical size exclusion column (GE Healthcare) at a flow rate of 0.35 mL/min in UvrC buffer. An aliquot of protein was reserved and analyzed by SDS-PAGE as above. Samples that included DNA substrates were treated as above and well-matched (WM) duplexes were added 1:1 with holo-UvrC (ex. 20 μM DNA and 20 μM UvrC by cluster). UvrC samples that included WM dsDNA were measured against buffer that included the same concentration of DNA. For comparison, UvrC was also heated anaerobically in UvrC buffer in a capped microfuge tube on a heat block in the glove bag and assessed as above. UvrC was also buffer exchanged anaerobically into 25 mM Tris-HCl, 0.1 M KCl, and 20% glycerol (v/v) at a pH of 7.5 (activity buffer) and examined by size exclusion chromatography as above. UvrC in low-salt activity buffer was used immediately in downstream assays.

3.2.7 UV-Vis and Continuous Wave (CW) Electron Paramagnetic Resonance (EPR) Spectroscopies

For all assays described below, aliquots of UvrC were thawed on ice in an anaerobic chamber and buffer-exchanged by diafiltration into UvrC buffer (25 mM Tris-HCl, 0.5 M KCl, 20% v/v glycerol) using Amicon Ultra-0.5 mL 10,000 kDa cut off mini filter units (Millipore). The [4Fe4S] cluster concentration was quantified by using the extinction coefficient of the absorption band centered at 410 nm ε = of 17,000 $M^{-1}{\cdot}cm^{-1}$ [23]. Because of the size of the fusion protein, typically a 10-15x dilution of the thawed protein was made to bring the absorption band at 280 nm into the linear region. The total protein concentration was then quantified by using the calculated excitation coefficient (Expasy) of His_6-MBP-UvrC at 280 nm ε = 111,995 $M^{-1}{\cdot}cm^{-1}$. The percent of the [4Fe4S] cofactor incorporated was calculated by dividing the total concentration of [4Fe4S] over the total protein concentration.

EPR samples were prepared in 200 μL volumes at final concentrations of UvrC at 10 μM and ferricyanide at 50 μM of 2 mM dithionite in UvrC buffer. Stocks of ferricyanide and dithionite were prepared in an anaerobic chamber in degassed UvrC buffer. Samples were loaded into clean (soaked in 2% nitric acid, washed with water, washed with ethanol, dried, and cooled) 4 mm thin-wall precision quartz EPR tubes (Wilmad LabGlass, 715-PW-250MM), capped, sealed with parafilm, and flash frozen in liquid N_2. An EMX X-band spectrometer (Bruker) with an ESR-900 cryogen flow cryostat (Oxford) and an ITC-503 temperature controller was used to collect X-band CW EPR spectra. Spectra were acquired at 10 K at power settings between 12-16 mW and a modulation amplitude of 10 Gauss using WinEPR software (Bruker) [16]. Data presented was collected in triplicate.

3.2.8 Molecular Weight Determination [53, 69, 74]

Stock solutions of proteins from the Gel Filtration HMW Calibration Kit (GE Healthcare) were made anaerobically from lyophilized powder in UvrC buffer according the manufacturer's instructions. Standards were flash frozen and stored at -80 °C until use. Once standards were thawed on ice in a glove bag, all subsequent steps were completed at room temperature. Samples were diluted to recommended concentrations, passed through a 0.22 μM syringe filter, loaded into a Hamilton syringe, and injected into a 250 μL superloop. All chromatography was done anaerobically at a flow rate of 0.35 mL/min on a Bio-Rad NGC using a Superdex 100/300L analytical size exclusion column (GE Healthcare) in UvrC buffer. All standards were completed in triplicate. UvrC was thawed on ice in an anaerobic chamber, buffer-exchanged into UvrC buffer, quantified by UV-Vis (by cluster concentration), and 250 μL of UvrC (between concentrations of 5 and 10 μM by cluster for each replicate) was assessed by analytical size exclusion chromatography.

3.2.9 Radiolabeling and Purification of DNA Substrates [16, 66, 67, 80]

For 5′ end labeling phosphorylation, 14 μL water, 2 μL T4 PNK buffer (New England Biolabs), 1 μL ssDNA 100 μM stock solution, 2 μl T4 polynucleotide kinase solution and 1 μL of [γ-^{32}P] ATP (NEG035C005MC, 6000 Ci/mmol, 150 mCi/mL, PerkinElmer) were combined in a 1.7 mL microcentrifuge tube, the tube was clipped, and incubated at 37 °C for 30 min followed by heat inactivation at 65 °C for 20 min. Solutions were cooled, centrifuged, and the volume of the solution was brought up to > 25 μL (or two labeling reactions were combined). Micro Bio-Spin 6 columns (Bio-Rad) were used to purify radiolabeled ssDNA followed by a Monarch

PCR & DNA Cleanup Kit (New England Biolabs) with a modified protocol for short oligomers. Briefly, the filtrate from the Micro Bio-Spin 6 column was combined with 100 μL Monarch DNA Cleanup Binding Buffer and 300 μL ethanol. The resulting solution was loaded into a Monarch DNA Cleanup Column (New England Biolabs) and spun at 16,000 g for 1 min. After discarding the flow-through, 500 μL of a 1:4 solution of Monarch DNA Cleanup Binding Buffer and ethanol were added to the column and spun at 16,000 g for 1 min. This washing procedure was repeated once more and flow-through was discarded each time. The column was spun at 16,000 g for 1 min to remove residual ethanol. Radiolabeled ssDNA stocks were stored at -20 °C.

3.2.10 Annealing Titrations [16, 66, 67, 80]

A 100% yield was assumed following radiolabeling. A solution of or 95:5 cold:radiolabeled between 30 to 40 μM dsDNA was generated by heating complementary strands to 95 °C for 10 min and cooling to room temperature over a linear gradient. Titrations from 75%-125% were prepared by varying the complement concentration DNA buffer in order to verify the duplex character of the substrate (and to detect any pipetting errors). Radioactivity was measured using the LS 6000SC Scintillation Counter (Beckman). DNA was electrophoresed at 50 V for 90-105 minutes at RT using Bio-Rad Mini-PROTEAN 4-20% TGX Precast Gels (Native PAGE) in Tris-Glycine buffer. Phosphorimaging screens (GE Healthcare or Molecular Diagnostics) were exposed according to the guideline that samples with 300,000 counts require 1 hour of exposure. The exposed screens were scanned using the Typhoon FLA 9000 (GE Healthcare). Images were analyzed using Image Lab^{TM} software (Bio-Rad). See text and **Appendix B** for an annealing titration gel.

3.2.11 Electrophoretic Mobility Shift Assays (EMSAs)[16, 66, 67, 80]

Native PAGE running buffer (25 mM Tris, 192 mM glycine, pH 8.3 from Bio-Rad) was degassed overnight in an anaerobic chamber with vigorous stirring. Duplex character of substrates was assessed by an annealing titration (see Supporting Experimental Section), and completely annealed duplexes were used for EMSAs and in activity assays (see below). Radioactivity was detected using an LS 6000SC Scintillation Counter (Beckman). In an anaerobic chamber, 10 nM to 2 μM UvrC (by cluster) was incubated for 30 min at room temperature with 100 nM dsDNA in activity buffer or UvrC buffer. DNA proteins mixtures were electrophoresed at 50 V for 2 hours at room temperature using Mini-PROTEAN TGX 4-20% Precast

Gels (Bio-Rad). Gels were exposed on a phosporimaging screen as described in the Supporting Experimental Section. For each replicate, bands were quantified using Image Lab^{TM} (Bio-Rad) and the fraction of bound DNA was plotted as a function of free UvrC concentration and fit to the Hill function using Origin (OriginLab Corporation). The apparent dissociation constant reported is the free UvrC concentration when half of the DNA substrates are bound. From three independent trials, the apparent dissociation constants were averaged over and are reported with the standard error of the mean. See text and **Appendix B** for the structure of the fluorescein substrate.

WM EMSA Substrate:
^{32}P-5′-CCGACTGAACTCTGTACCTGACACGACAAG-3′
3′-GGCTGACTTGAGACATGGACTGTGCTGTTC-5′
Fluorescein (F) EMSA Substrate:
^{32}P-5′-CCGACTGAACTCTGTACCTGACACGACAAG-3′
3′-GGCTGACTTGAGACATGGACTGTGCTGTTC-5′

3.2.12 Incision Assays [33, 46, 59, 70, 77, 78, 86]

In an anaerobic chamber, UvrC was buffer exchanged into activity buffer. Solutions of $MgCl_2$, ATP, and DTT were prepared in the glove bag in filtered and degassed water (Trials 1 and 2) or in filtered and degassed buffer containing 25 mM Tris-HCl, 0.1 M KCl, 20% v/v glycerol. UvrC was pre-incubated at room temperature with 10 mM $MgCl_2$ and 1 mM DTT. Just before adding 3 μM ^{32}P-dsDNA (WM or F), 10 mM ATP was added to UvrC and samples were incubated at 37 °C for 1 hr and then heat inactivated at 70 °C for >10 min. Radioactivity was quantified using the Beckman LS 6000SC Scintillation Counter (Beckman). Samples were mixed 1:1 with denaturing loading dye (80% formamide, 10 mM sodium hydroxide, 0.025% xylene cyanol, and 0.025% bromophenol blue, in TBE buffer from National Diagnostics [0.089 M Tris base, 0.089 M boric acid, and 2 mM Na_2EDTA at pH 8.3]) and stored at -20 °C until use. A 20% TBE-Urea polyacrylamide sequencing gel was pre-heated to over 50 °C, and then samples were resolved on the pre-heated gel for 120 min at 90 Watts. Gels were exposed on a phosporimaging screen, imaged, and visualized as described.

3.2.13 DNA-Modified Electrochemistry on Au Surfaces [22, 23, 55, 71]

A 16-electrode, gold, multiplex chip (4 quadrants with 4 electrodes each) was rinsed and sonicated with acetone three times for five minutes and once with 100% isopropyl alcohol, also for five minutes. The gasket and clamp were washed and sonicated in 50% isopropanol (in water) for five minutes followed by three to five rinses with water. All components were dried using an argon gun. To clear the chip of debris, the chip was cleaned by ozonolysis (UVO Cleaner) for 15 minutes. The chip, gasket, and clamp were assembled and 23 μL duplexed WM electrochemistry substrate at a concentration of 25 μM (see Supporting Experimental Section) was added to each quadrant. Monolayers were allowed to form overnight under humid conditions at room temperature. The electrode was then rinsed three times with DNA buffer (5 mM sodium phosphate, 50 mM NaCl, pH 7.0) and then three times with glycerol buffer (DNA buffer with 5% glycerol). The electrode was backfilled with 1 mM of 6-mercaptohexanol (in glycerol buffer) for ~30 minutes. The electrode was rinsed 10 times with DNA buffer. In an anaerobic chamber, 400 μL of 5 μM of UvrC (by cluster) was added to the chip in electrochemistry buffer (4 mM spermidine, 25 mM Tris-HCl, pH 7.5, 0.25 M KCl, 20% glycerol). A 4% agarose/3 M NaCl gel tip Ag/AgCl reference electrode (MW-2030, RE-6, BASi) was used. The potentiostat, multiplexer, and analysis software were from CH Instruments, Inc. A scan rate of 50-100 mV/s between -0.4 V and 0.2 V (vs. Ag/AgCl) is optimal for cyclic voltammograms. Scans were taken periodically at 0, 1 hr, 2 hrs, and 3 hrs. Square wave scans were taken after 3 hours, and then scan rates were varied from 10 to 1600 mV/s. A Randles-Sevcik analysis was done by plotting the current vs scan rate and (scan rate)$^{1/2}$. Data presented is representative of three independent trials.

Electrochemistry Substrate:
5′-CCGACTGAACTCTGTACCTGACACGACAAG-3′
3′-GGCTGACTTGAGACATGGACTGTGCTGTTC-5′-$(CH_2)_6$-SH

3.3 RESULTS AND DISCUSSION

3.3.1 An Anaerobic Environment Stabilizes the [4Fe4S] Cofactor and UvrC

Anaerobic cell lysis and purification methods used for nitrogenase in the Rees lab were adapted for UvrC (**Figure 3.1** and **Appendix A**) [72, 84]. Immobilized metal affinity and gel filtration chromatography was performed under strict anaerobic conditions in an anaerobic chamber and using standard Schlenk line technique ([72, 84]. A more rapid concentration system located in a glove bag also greatly

aided in streamlining the purification process. During initial studies, concentration steps post-purification were accomplished aerobically at 4 °C by centrifugation (a common technique). In our case, this likely resulted in generation of oligomeric species *in situ* prior to freezing and storing. Because concentration steps could also be carried out anaerobically, we eliminated the risk of aggregates forming *in situ* after column purification due to oxidative degradation. The stability exhibited by UvrC over the course of the purification during 15+ hours at room temperature was also a great improvement, as compared to the instability in atmosphere at 4 °C. The expression and anaerobic purification strategy allowed for isolation of the UvrC fusion protein in high purity with the same broad and shallow absorption band centered at 410 nm and yellow-tan color characteristic of a [4Fe4S] cluster (**Figure 3.1**, Bottom Left) [17, 21, 38, 73]. Based on the ratio of absorbances at 410 and 280 nm, each purification yielded approximately 5 mg of the UvrC fusion protein per liter of liquid culture (5 grams of wet pellet) with 60-70% incorporation the [4Fe4S] metal center (**Figure 3.1**, Bottom Middle) [5, 11, 16, 17, 25, 37, 41, 42, 50–52, 56, 57, 64, 76, 80].

To characterize the nature of the Fe center further, we used the ferene colorimetric assay to quantify the amount of protein-bound Fe (**Figure 3.1**, Bottom Right) [16]. We find that UvrC coordinates on average 4.0 ± 0.3 Fe per cluster (about 3 Fe per protein), which is consistent with the sub-stoichiometric levels of [4Fe-4S] cluster incorporation seen with other repair and replication enzymes. A range from 2 to 4 Fe per protein has been reported and has been attributed to incomplete incorporation or loss of a labile Fe during the process of overexpression or purification, even when each step is completed anaerobically [3, 13, 28, 35, 48, 49, 60, 64, 83].

Comparison of the data from the aerobic and anaerobic purifications further demonstrates the improvement to the quality UvrC isolated, which can most readily be seen in the chromatogram from the size exclusion column, where the ratio of soluble:aggregated protein is much improved, suggesting increased yields. Aggregated protein and what we thought was soluble protein were not as easily separated under aerobic conditions, and the soluble protein displayed an earlier elution volume. Under anaerobic conditions, the separation between the aggregated protein (first peak) and soluble protein (aggregated peak) is greater (**Figure 3.1** Top Left and Middle and **Figure 3.2**, Left). While the UV-Vis absorption spectra of both proteins are similar, there is a small feature in the UV-Vis spectrum of aerobically-purified UvrC at 325 nm, which could be due to partially-degraded cluster in the $[3Fe4S]^{+}$ state (**Figure 3.2**, Middle) [38].

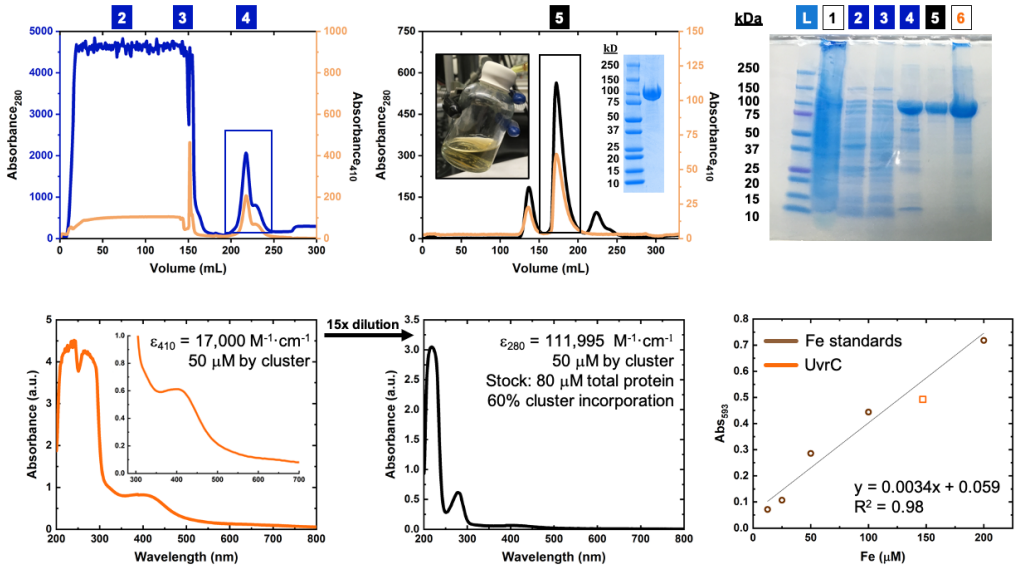

Figure 3.1 Anaerobic purification of UvrC.(*Top Left and Middle*) All purification steps were completed in a glove bag or using standard Schlenk line technique under a positive pressure of N_2 or Ar gas. UvrC is purified using affinity and gel filtration chromatography. Shown are representative chromatograms. Cell lysate is first loaded onto a 10 mL Histrap column, washed with 10% elution buffer to remove non-specifically bound debris, and then eluted with a linear gradient of elution buffer (Materials and Methods). The collected peak (boxed, dark blue) is then concentrated and further purified on a Superdex 200 column. The yellow and clear peak (boxed and pictured) are concentrated and stored in 250 µL aliquots at concentrations between 20 and 30 µM. (*Top Left*) After concentration, subfractions taken during purification analyzed by SDS-PAGE to assess purity. Labels with a blue background correspond to fractions taken from the Histrap column. The label with a black background corresponds to the fraction taken from the Superdex. L: Ladder; 1: Insoluble pellet (black box and text); 2: Histrap flow through; 3: Histrap 10% wash; 4: Collected Histrap fraction; 5: Collected Superdex fraction: 6: Concentrated UvrC (black box, orange text). (*Bottom Left and Middle*) UV-visible absorbance spectrum for purified UvrC shows a broad and shallow absorption band centered at 410 nm, which is characteristic of [4Fe4S] clusters. Also shown is an example of how percent incorporation is calculated using absorption maxima at 280 nm and 410 nm. (*Bottom Right*) A representative standard curve and data point from an independent trial of the ferene iron quantification assay is shown. All buffers are at pH 7.5. Lysis Buffer: 25 mM Tris-HCl, 0.5 M KCl, 10% v/v glycerol supplemented with 6-8 tablets of crushed cOmplete™ protease inhibitor cocktail tablets (Roche), DNAse (15 kU, Sigma), and DTT (1 mM); Nickel Elution Buffer: 25 mM Tris-HCl, 0.5 M KCl, 20% v/v glycerol, 0.5 M Imidazole, 1 mM DTT; Size Exclusion Buffer: 25 mM Tris-HCl, 0.5 M KCl, 20% v/v glycerol, 1 mM DTT.

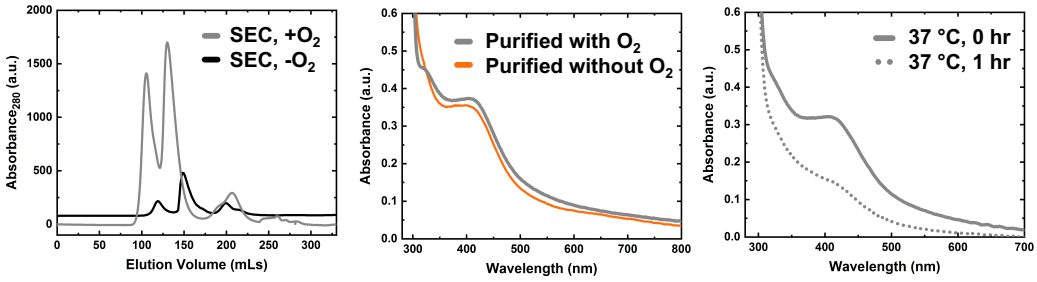

Figure 3.2 Comparison of the UvrC isolated aerobically and anaerobically. (*Left*) During an aerobic purification at 4 °C (from ~30 g wet pellet, gray), UvrC elutes at an earlier volume off of a prep grade size exclusion column than UvrC isolated during anaerobic purification (~10 gram wet pellet, black). The ratio of solube:aggregated protein is also greater for the anaerobic sample. Flow rates and buffer components for the aerobically-purified samples are the same, except size exclusion buffer does not contain DTT. (*Middle*) An extra shoulder centered near 325 nm (gray) can be seen for UvrC purified in atmosphere (both in UvrC buffer). (*Right*) As shown in Chapter 2, incubation of aerobically-purified UvrC at 37 °C results in near complete degradation of the cluster in 1 hour.

3.3.2 Oxidative Degradation of the UvrC-bound [4Fe4S] Cofactor Results in Protein Aggregation

To explore the oxidative degradation first seen for the [4Fe4S] cofactor (**Figure 3.2**, Right) and subsequent aggregation further, we incubated anaerobically-purified UvrC in aerobic UvrC buffer (25 mM Tris-HCl, 0.5 M KCl, 20% v/v glycerol) at 37 °C and monitored the absorption band at 410 nm. We find that on the timescale of a UvrC activity assay (1 hr), 20% of the cluster degraded after incubation at 37 °C, while complete degradation was observed after 4 hours (**Figure 3.3**, Top Left). The degradation here was slower than what we observed previously (1 hr vs. 4 hrs), possibly because UvrC isolated anaerobically is not already partially degraded. As seen previously, aggregation of UvrC followed oxidative degradation of the cofactor, which was monitored using an analytical size exclusion column more appropriate to the volume and amount of material used per incubation (**Figure 3.3**, Top Right). We further verified that the bleaching of the absorbance at 410 nm was due only to degradation of the [4Fe4S] center and not the peptide through gel analysis (**Figure 3.3**, Middle Left). Anaerobic incubation of holo UvrC at 37 °C in the absence of O_2 did not result in degradation of the [4Fe4S] cluster here either, further confirmation that the source of the degradation is due to O_2 (**Figure 3.3**, Middle Right). We also observe that binding to duplex DNA does not affect cluster

degradation (see below for studies of UvrC-DNA complexes) (**Figure 3.3**, Bottom Left). Using a standard curve, we determined that holo-UvrC elutes at a volume consistent with protein migrating in dimeric form (~ 220 kDa, assuming a globular protein migrating based on size rather than shape) (**Figure 3.3**, Bottom Right) [53, 69, 74]. The apo-UvrC species eluted at the void volume of the column would correspond to aggregrates that are >a pentamer in size.

As emphasized previously, metalloproteins can be challenging to handle, and oxidative degradation of the [4Fe4S] cofactor of UvrC was non-trivial to observe. As summarized in the previous chapter, our early studies were carried out with UvrC purified aerobically at 4 °C [22]. The protein was isolated from a peak that eluted after the void volume of the size exclusion column was yellow in color, and exhibited a temperature-dependent EPR signal, so it appeared that an aerobic purification at 4 °C was sufficient for isolating holoenzyme. The sensitivity to O_2 could have easily been overlooked. The straightforward time courses that demonstrated degradation of the [4Fe4S] cofactor in the presence of molecular oxygen after incubating at 37 °C for 1 hour (again, common incubation times and temperatures for an activity assay), were carried out at concentrations of protein orders of magnitude above (μM) what is commonly used in an activity assay (nM).

The significance of our observations and findings of other investigators regarding how [4Fe4S] cofactor in EndoIII, MutY, DinG, and UvrC are transformed by exposure to reactive species remains to be explored fully *in vitro* and *in vivo*. EndoIII, MutY, and DinG have not been reported to be similarly sensitive to O_2, and moreover, we have observed previously that EndoIII is not only highly soluble, but also stable at room temperature in atmosphere for many days [5, 10, 16]. EndoIII, homolog MutY, and DinG have furthermore been crystallized aerobically [10, 18, 19, 36, 76]. EndoIII does, however, react rapidly with another diatomic signaling molecule, NO, causing loss of one iron atom per cluster and formation of a mononuclear dinitrosyl iron complex and a dinuclear Roussin's red ester in the cluster binding domain [16]. Transformation of the iron center is reversible and does not affect global protein structure or DNA binding, but does shift the redox potential of the cluster and hinders enzymatic activity [16, 61]. DinG also reacts with NO and is inactivated, but surprisingly, is resistant to treatment with H_2O_2 [60]. Cellular responses mediated by sensing of reactive species by iron-sulfur transcription factors has been well-characterized, though in contrast, the specificity and responses of repair proteins to reactive species is not as fully understood [12, 31, 43]. Variations in the stability of the [4Fe4S] cofactor from repair proteins across different bacterial

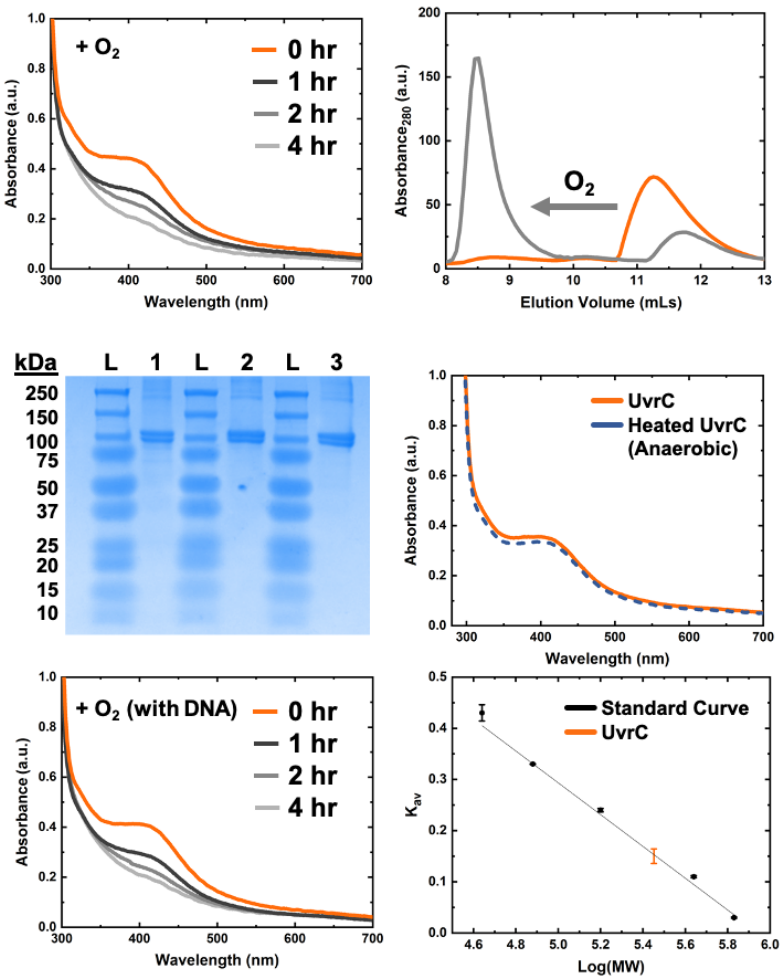

Figure 3.3 Degradation of the UvrC-bound [4Fe4S] cluster in the presence O_2. (*Top Left*) Incubation of UvrC at 37 °C in aerobic UvrC buffer (25 mM Tris-HCl, 0.5 M KCl, 20% v/v glycerol) resulted in the disappearance of the absorption band at 410 nm. Incubation for 1 hour (the timescale of an activity assay) led to 20% degradation. (*Top Right*) Holo-UvrC was examined by size exclusion chromatography in degassed buffer at room temperature. Holoenzyme (orange trace) eluted at a volume consistent with a dimer (see *Bottom Right*). Apoprotein (gray trace) arising from oxidative degradation eluted at the void volume, indicating that the apoprotein had formed species > 600 kDa. (*Middle Left*) Aerobic incubation does not result in degradation of peptide backbone of UvrC [65]. L: Ladder; Lane 1: Purified UvrC; Lane 2: Aerobically-degraded UvrC; Lane 3: Aerobically-degraded UvrC incubated with the WM 30mer. (*Middle Right*) The [4Fe4S] cluster of UvrC is stable during incubation at 37°C in the absence of O_2 over the course of 4 hours (blue dashed line). (*Bottom Left*) Binding to the duplexed 30-mer WM substrate does not slow the aerobic degradation of the [4Fe4S] cluster. (*Bottom Right*) Relative to a standard curve of elution volumes for globular proteins, UvrC elutes at a volume consistent with a protein that is a dimer. Elution volumes were measured in triplicate for each protein. Average elution volumes are shown, and the error bars represent the standard deviation.

species adapted to niche environments is also not fully appreciated [15, 27, 81, 82]. Exploring how UvrC and other DNA repair enzymes are involved in detecting changes in cellular environments and in the cellular response to endogenous and exogenous stressors (separate or related to their repair activities in the genome) is an area that warrants further investigation.

3.3.3 Holo-UvrC Is Redox Active

X-band electron paramagnetic resonance (EPR) spectroscopy was used to characterize the the [4Fe4S] center further. In the native state, we again saw a signal centered at g = 2.01, however, the intensity of the signal is significantly smaller compared to the spectrum taken aerobically (shown in Chapter 2), highlighting the improvements in sample quality for UvrC in anaerobic conditions. A small signal at g = 2.01 has been observed previously and found to be due to a small percentage of the native protein population in the $[3Fe4S]^{1+}$ state (with the rest of the population in the EPR-silent $[4Fe4S]^{2+}$ state) (**Figure 3.4**, Top) [6, 13, 28, 42, 48]. As discussed, two categories of protein-bound [4Fe4S] clusters are known: (i) ferredoxins which cycle between the 2+/1+ oxidization states and (ii) HiPIPs which cycle between the 3+/2+ oxidation states [21, 29, 38, 39]. To classify the nature of the [4Fe4S] cluster, UvrC was again treated with the oxidant potassium ferricyanide and immediately frozen in liquid N_2, which resulted in the appearance of a large and sharp signal at g = 2.01 [13, 28, 35, 49, 64, 83]. We assign this signal to a $[3Fe4S]^{1+}$ species derived from an oxidized $[4Fe4S]^{3+}$ cluster, indicating that UvrC accesses the 3+/2+ redox couple. Equivalent spectra have been observed for EndoIII and homologues, repair proteins with [4Fe4S] clusters that are generally substantially more stable under aerobic conditions [6]. A corresponding signal at g = 4.3 can also be observed after treatment with ferricyanide, suggestive of a ferric species in solution and consistent with the release of an iron atom from the $[4Fe4S]^{3+}$ species following oxidization [2, 26]. No clear evidence of the $[4Fe4S]^{3+}$ species, characterized by a g = 2.1, before Fe loss was apparent [21, 38, 73]. Taken together, these data demonstrate that UvrC resembles these other DNA repair proteins and coordinates a HiPIP-like [4Fe4S] cluster when bound to DNA.

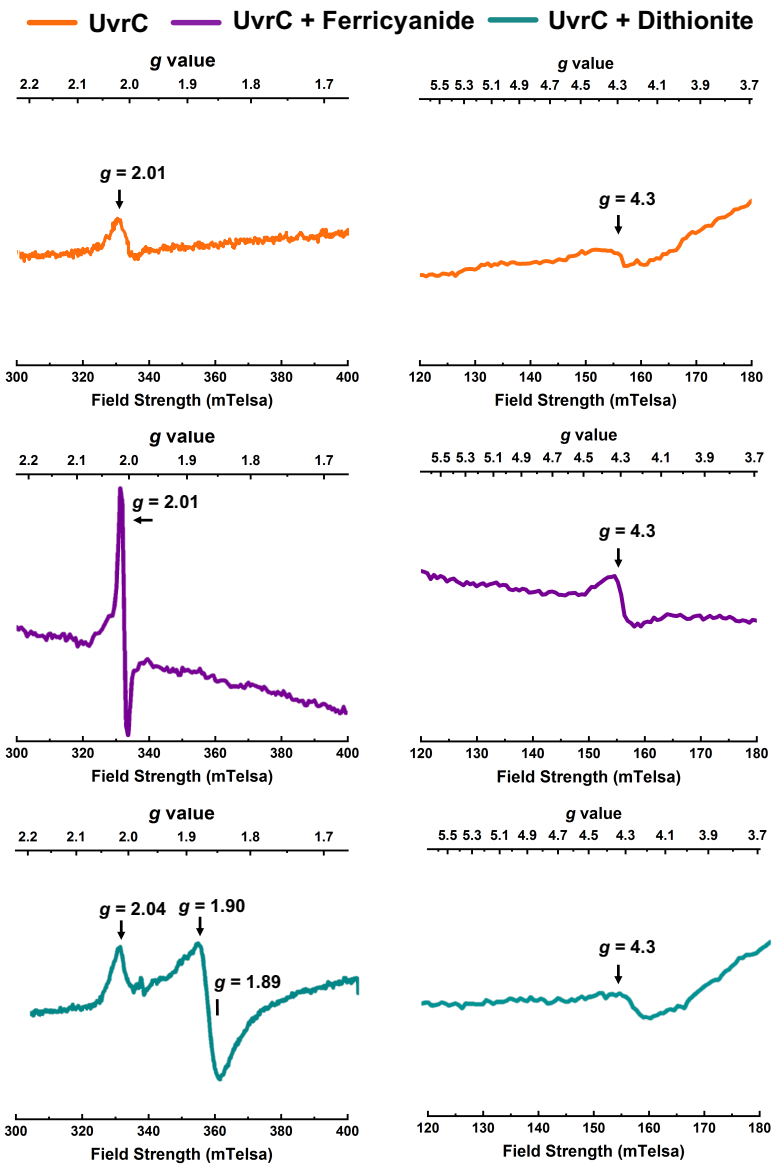

Figure 3.4 Anaerobic EPR. (*Top*) Using X band EPR spectroscopy, a small signal was observed for UvrC (orange) at $g = 2.01$, which is attributed to a small percentage of the protein population in the $[3Fe4S]^{1+}$ state. (*Middle*) A large and sharp signal was observed in the presence of ferricyanide (purple), at $g = 2.01$. This signal is attributed to the transformation of oxidized $[4Fe4S]^{3+}$ species to the $[3Fe4S]^{1+}$ species and release of ferric iron. A corresponding signal at $g = 4.3$ (*Middle Right*), characteristic of ferric iron species was seen upon oxidation which is not observed above the background signal for UvrC in the native state (*Top Right*). (*Bottom*) In the presence of dithionite, signals were also observed at $g = 2.04$, $g = 1.90$, and $g = 1.89$. This signal could be due to $4Fe4S]^{+}$ and/or degraded $[2Fe2S]^{+}$ species, which are difficult to distinguish through EPR [14, 26]. All spectra were taken in buffer containing 25 mM Tris, 0.5 M KCl, and 20% glycerol (v/v) at a pH of 7.5 (UvrC buffer). Spectra were taken with samples containing 10 μM UvrC by cluster, 50 μM ferricyanide, and 2 mM dithionite. EPR Conditions: 9.37 GHz, 10 K, 16 mW microwave power.

We also studied UvrC in the presence of dithionite, and again, saw signals at g = 2.04, 1.90, and 1.89. It is difficult to distinguish the $[4Fe4S]^+$ from the $[2Fe2S]^+$ species, which is not uncommon to observe for sensitive clusters ([14, 17, 26]). As it is unlikely that the UvrC-bound [4Fe4S] cofactor can access both the 3+/2+ and 2+/1+ couple, additional experiments combining EPR with Fe quantification and graphite electrochemistry could help in assigning the signals seen in the presence of chemical reductants and oxidants.

3.3.4 UvrC Independently Forms a Complex with DNA Duplexes

To continue characterizing UvrC in holo form, we returned to examining how UvrC interacts with radiolabeled, duplexed 30 base pair substrates using electrophoretic mobility shift assays (EMSAs) completed in an anaerobic chamber [16, 66, 67, 80]. Since the majority of the genome in the cell is comprised of non-damaged dsDNA through which redox signaling can occur, we were interested in how UvrC in its holo form interacts with WM duplexes as well as damaged substrates. We selected a fluorescein-modified substrate (F), which is considered to mimic damage caused by polycyclic aromatic hydrocarbons, natural substrates of the UvrABC system ([32], and references therein). Once formation of WM and F duplexes was confirmed with annealing titrations (see **Appendix A**), UvrC was incubated anaerobically with duplexed substrates at a high KCl concentration to avoid precipitation of UvrC (discussed in Chapter 2). Mixtures of UvrC and DNA did not appear cloudy, and no scattering was observed by UV-Vis (see (**Figure 3.3**, Bottom Left). Free and complexed DNA was resolved on a native gel that was pre-equilibrated in degassed running buffer. Band intensities were quantified, and the fraction of complexed DNA as a function of free UvrC concentration was fit to the Hill equation. UvrC was found to form high affinity complexes with duplexed substrates, with apparent dissociation constants of 100 ± 20 nM and 80 ± 30 nM for WM and F substrates, respectively (n = 3 independent trials) (see (**Figure 3.5**, Bottom Left). The complexes not only appear to be high affinity but also stable, even at the high KCl concentration used; band smearing was not observed over all three trials.

We note that the UvrC-DNA complex displayed a much lower mobility than free duplexes. Low mobility of UvrC on native gels has been seen previously (with and without DNA substrates) and has been attributed to the positive charge of UvrC (predicted pI of about 9) in neutral buffers, which would cause migration to the positive electrode to be unfavorable [45]. Low migration has also been attributed to precipitation of protein in the gel, but we do not observe precipitation in solution

[86]. However, Hill coefficients > 1 were found for both WM and F substrates, suggesting there is also some possibility of oligomerization upon binding to DNA. Low mobility in our system could therefore be explained through the predicted positive charge of UvrC or to formation of high molecular weight oligomers of UvrC on DNA. In any case, we conclude that holo-UvrC forms a high affinity complex with undamaged and damaged duplexed DNA.

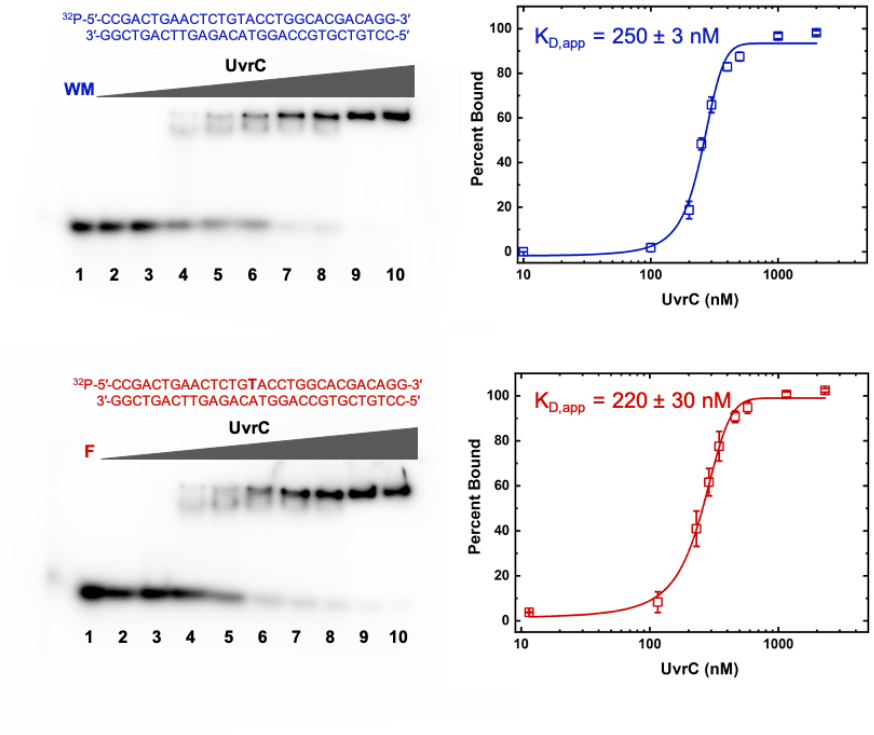

Figure 3.5 UvrC forms a complex with DNA substrates. UvrC was incubated with 30 bp DNA substrates in degassed UvrC buffer (25 mM Tris-HCl, 0.5 M KCl, 20% v/v glycerol). Free and complexed DNA were separated by native gel electrophoresis using degassed running buffer (25 mM Tris-HCl, 192 mM glycine, pH 8.3) in an anaerobic chamber in an atmosphere of N_2 with 2-4% H_2 at room temperature. Data from the gel shift assays indicate that UvrC forms a complex with both WM duplexes (*Top*) and a fluorescein-modified (F) substrate (*Bottom*) at a high affinity. Lane 1: DNA only (100 nM). Lanes 2-10: 10 nM to 2 μM UvrC by cluster with a constant duplex concentration of 100 nM. For each DNA substrate, binding data from three independent trials were fit using a Hill function and then the apparent dissociation constants were averaged (reported with the standard error of the mean). Hill coefficients were also found to be >1.

3.3.5 DNA Binding Does Not Lead to Independent Enzymatic Activity

Our observation that holo-UvrC forms complexes with dsDNA independently of other NER proteins led us to investigate if holo-UvrC also exhibited independent or nonspecific enzymatic activity, which has been observed previously [9, 47]. UvrC uniquely contains two independent active sites, a GIY-YIG motif in the N-terminal domain which is responsible for making the incision 3′ to the site of damage and a second active site which is a structurally-conserved RNase H-like domain in the C-terminal end of the protein that achieves incision 5′ to the damage site [34]. The 5′ and 3′ incisions can even be reconstituted *in vitro* with C-terminal and N-terminal truncation products of UvrC, respectively, which both exclude the Cys-rich region.

Standard activity assay conditions include Mg^{2+}, ATP, DTT (or another common reducing agent), and a KCl concentration of 0.1 M [33, 44, 65, 70, 78]. We first verified that buffer-exchanging UvrC into lower-salt buffer did not cause immediate destabilization of the protein. The UV-Vis spectrum indicated that [4Fe4S] cofactor was not lost in the process of buffer exchanging or when incubated at 37 °C (**Figure 3.6**, Top Left). Furthermore, size exclusion chromatography confirmed that UvrC in buffer containing 0.1 M KCl eluted at the same volume as UvrC in buffer containing 0.5 M KCl, confirming that the oligomeric state was unchanged during buffer exchange (**Figure 3.6**, Top Right). We also verified that UvrC exhibited a similar binding profile to dsDNA (both WM and F substrates) in buffer that contained 0.1 M KCl as in buffer containing 0.5 M KCl (**Figure 3.6**, Middle and Bottom).

We tested the activity of UvrC at multiple concentrations on the F substrate as well as the WM substrate as a control. Even up to a concentration of 1 μM UvrC by cluster (3:1 DNA:UvrC ratio), no evidence of substrate incision by UvrC under the conditions tested was observed. The absence of enzymatic activity in the presence of DNA binding suggests that a complicated set of factors controls UvrC activity, which appear to prevent spurious reactions from occurring even as UvrC is bound to dsDNA in holo form. How the [4Fe4S] cofactor is involved in such regulation remains to be determined. For other repair and replication proteins, the finely-tuned roles of the [4Fe4S] cofactor have been examined over many studies. These studies have been particularly informative for understanding how disruption of the [4Fe4S] cofactor inhibits subunit assembly (and therefore enzymatic activity) *or* enzymatic activity alone of the multisubunit B family replication enzymes, polymerases ϵ and δ, respectively [24, 48, 75]. In the context of the multisubunit exinuclease repair complex formed by UvrABC, we speculate that because the [4Fe4S] domain is

adjacent to the UvrBC interacting domain (see Chapter 2, **Figure 2.3**), the [4Fe4S] cluster may analogously be involved in the association of UvrC with other NER proteins or the overall activity of the exinuclease complex [20]. Other roles may also exist for the [4Fe4S] cluster of UvrC relevant for other repair pathways, one of which is possible to study because of the independent DNA binding activity of UvrC (*vide infra*).

3.3.6 UvrC Participates in DNA-mediated Charge Transport Chemistry

Our characterization of UvrC as a metalloprotein culminated with exploration of the DNA-bound redox chemistry under anaerobic conditions [4, 22, 23, 50, 55, 80]. With confirmation that UvrC forms complexes with WM duplexes, we prepared multiplex chips using a thiol-modified 30 bp WM substrate from EMSA experiments which formed self-assembled DNA monolayers on gold surfaces (**Figure 3.8**, Top Left). Prepared multiplex chips were taken into an anaerobic chamber and allowed to equilibrate in degassed UvrC electrochemistry buffer (25 mM Tris-HCl, 0.25 M KCl, 20% glycerol (v/v), 4 mM spermidine, and 0.5 mM EDTA at pH 7.5). After recording background buffer scans, UvrC was applied to DNA monolayers on the multiplex chip which resulted in appearance of a reversible, redox signal centered at a midpoint potential of 90 mV ± 0.03 vs. NHE, consistent with the redox activity observed by EPR (**Figure 3.8**, Top Right). The signal increased with time, suggesting that UvrC is a diffusive species at the monolayer [7]. Varying scan rate and quantifying the anodic and cathodic peak currents in a Randles−Sevcik analysis confirmed that the redox-active species on the electrode is indeed diffusive (**Figure 3.8**, Bottom) [5]. Thus we conclude that UvrC behaves like the other HiPIP-like repair and replication proteins we have studied that contain a [4Fe4S] cluster. UvrC is the fourth repair protein from *E. coli* and the sixth protein from Bacteria reported to do so [1, 3, 24]. Moreover, UvrC shares a DNA-bound redox potential with EndoIII, MutY, and DinG, the three other repair proteins from *E. coli* that are known to coordinate the redox-active [4Fe4S] cofactor.

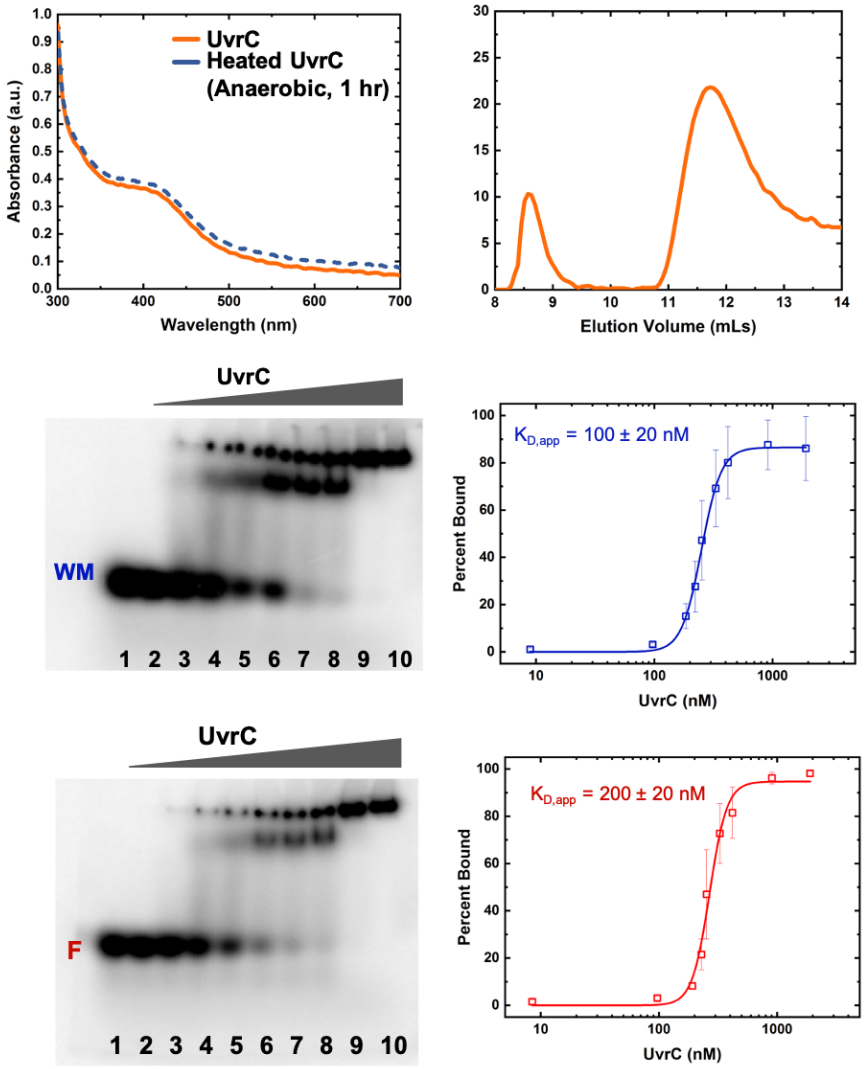

Figure 3.6 UvrC retains stability in low-salt buffer. (*Top*) Prior to an activity assay, UvrC was buffer-exchanged into low-salt activity buffer (25 mM Tris-HCl, 0.1 M KCl, 20% v/v glycerol). The UV-Vis spectrum (*Top Left*) and the size exclusion chromatogram (*Top Right*) indicate that the overall integrity of the [4Fe4S] cluster and the protein were not compromised by buffer exchanging UvrC into a low-salt environment. (*Middle*) The binding pattern of UvrC to duplexed WM and F (*Middle*) DNA substrates in low-salt activity buffer (with 0.1 M KCl) is comparable to the binding pattern of UvrC in high-salt UvrC buffer (with 0.5 M KCl). In the low-salt activity buffer, the apparent dissociation constants over three independent trials (reported with the standard error) are 100 ± 20 and 200 ± 20 nM for WM and F substrates, respectively. Hill coefficients were also found to be >1.

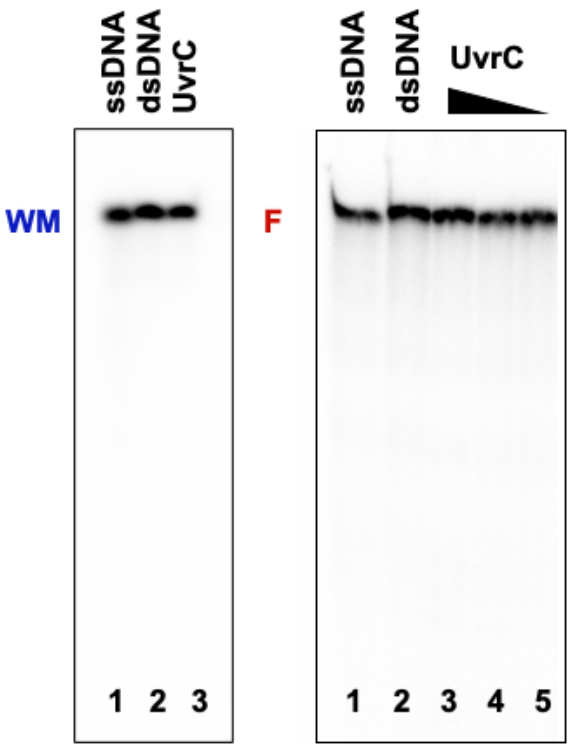

Figure 3.7 Activity assays. UvrC was incubated with WM or fluorescein-modified substrate (3 μM) at 37 °C in activity buffer containing 25 mM Tris, 0.1 M KCl, and 20% glycerol (v/v) at a pH of 7.5 in the presence of 10 mM Mg^{2+}, 10 mM ATP, and 1 mM DTT under anaerobic conditions. The reactions were resolved on a denaturing 20% urea gel, and incision of WM or damaged strands was not observed. (*Left*) Lane 1: ssDNA, Lane 2: dsDNA, Lane 3: 1 μM UvrC (by cluster). (*Right*) Lane 1: ssDNA; Lane 2: dsDNA; Lanes 3 - 5: 1 μM - 10 nM UvrC.

3.4 CONCLUSIONS

The data presented herein have demonstrated that UvrC coordinates a [4Fe4S] cluster that contributes to protein stability, undergoes oxidative degradation, facilitates substrate binding, and participates in DNA CT. With the discovery that UvrC is a [4Fe4S] enzyme, excision nucleases join the growing body of diverse repair and replication proteins known to bear the [4Fe4S] center. Excision nucleases are a small class of proteins, comprised of UvrC and a smaller protein Cho (UvrC homologue), found only in Bacteria and some Archaea. We predict that Cho, which is homologous to the N-terminal half of UvrC and contains the four conserved cysteine residues, may also coordinate a [4Fe4S] cluster [47, 54]. Other [4Fe4S] proteins may be identified once structural data becomes available for excision nucleases. We

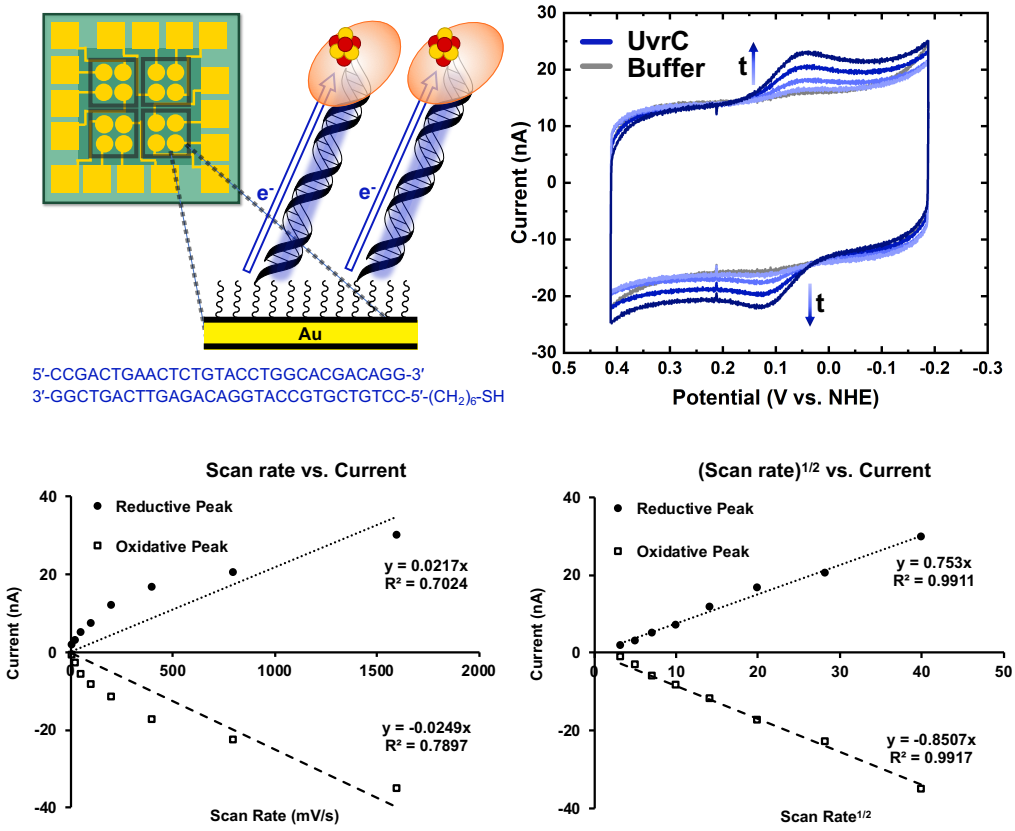

Figure 3.8 UvrC participates in DNA charge transport chemistry. (*Top Left*) Shown is a schematic of DNA-modified electrodes on multiplex chips. DNA duplexes are formed in monolayers through an alkane-thiol linker on gold multiplex chips with 16 independently-addressable electrodes [22, 23, 55]. (*Top Right*) All measurements were taken in an anaerobic chamber in degassed electrochemistry buffer (25 mM Tris-HCl, 0.25 M KCl, 20% glycerol (v/v), 4 mM spermidine, and 0.5 mM EDTA at pH 7.5). On DNA electrodes modified with a 30 bp WM substrate, UvrC (5 μM, 400 μL) is redox active at physiological potentials, exhibiting a reversible signal with a midpoint potential of 90 mV ± 0.03 vs. NHE. The initial signal (light blue) increases over time (1-3 hours) as protein diffuses to the monolayer surface. UvrC and all other [4Fe4S] repair proteins from *E. coli*, EndoIII, MutY, and DinG, share a DNA-bound potential which can facilitate redox sensing and signaling among different repair pathways *in vivo*. (*Bottom*) UvrC is diffusive on DNA monolayers. Scan rate was varied from 10 mV/s to 1600 mV/s, and the current at the anodic and cathodic peaks were quantified using software from CHI Instruments. A strong linear relationship between peak current and the square root of scan rate can be seen, indicating UvrC is diffusive (rather than adsorbed) on DNA monolayers.

also note that even though substrate processing by prokaryotic and eukaryotic NER machinery is similar, the proteins in each pathway that accomplish the repair are divergent. Even so, a [4Fe4S] protein has now been found in each system, UvrC and XPD (a SF2 5′→3′ helicase) in prokaryotic and eukaryotic NER, respectively. In a small set of archaeal species, both UvrC and XPD are encoded in the genome [85].

Continued study of UvrC both *in vitro* and *in vivo* will help further our understanding of the relationship between UvrC activity and its [4Fe4S] cofactor (**Figure 3.9**). In the cell, [FeS] cofactors are loaded by biogenesis machinery to recipient proteins in a series of regulated and controlled steps; thus, there is a putative relationship between pathways that include UvrC (and perhaps Cho) and iron-sulfur metabolism [20, 58, 62]. UvrC is part of NER, in both the global genomic and the transcription-coupled subpathways, and the nature of interactions between NER proteins with newly-synthesized apo-UvrC and loaded holo-UvrC remains to be examined. Recognition of structurally and chemically diverse lesions and the activity of protein complexes with apo and holo-UvrC on substrates also requires further examination. It is possible that the different forms of UvrC in the cell, apo, holo, and aggregated, may have different roles and are recognized differently by cellular components.

In its holo form, we expect that UvrC alone would be found in complex with DNA due to the high affinity of the complex observed here. When bound to DNA, UvrC can participate in a redox signaling network through DNA CT chemistry, which would serve as a means for crosstalk among repair pathways *in vivo*, allowing for rapid scanning of the genome for lesions [1, 3, 24]. This study certainly highlights how the enigmatic functions of UvrC, which have eluded understanding for many years, may be related to the [4Fe4S] cofactor. We expect that future studies which carefully monitor the [4Fe4S] cofactor will continue to unravel key aspects regarding the activity of UvrC *in vitro* and *in vivo*.

3.5 ACKNOWLEDGEMENTS

We are grateful to the NIH (5R35GM126904 to J.K.B.) and The Gordon and Betty Moore Foundation (to the Caltech Center for the Chemistry of Cellular Signaling) for their financial support. R.M.B.S. recognizes the National Science Foundation (NSF) for support through a Graduate Research Fellowship and the Center for Environmental Microbial Interactions (CEMI, Caltech) through a Pilot Grant. M.A.G. was an NIH predoctoral trainee (NIH/NRSA 5T32GM07616) and also a recipient of a CEMI Pilot Grant. The authors are especially grateful to Professor Douglas

Rees and the Rees group for use of their vacuum manifold for anaerobic purification of UvrC. In particular, we are grateful for Ailiena Maggiolo for her training and assistance. This work was also facilitated by use of the Caltech EPR facility which is supported by the NSF (NSF-1531940) and the Dow Next Generation Educator Fund. This research also utilized the Autoflex MALDI TOF mass spectrometer in the Caltech CCE Multiuser Mass Spectrometry Laboratory which is supported by the Dow Next Generation Educator Fund. Instruments in the Center for Molecular Medicine also facilitated this research.

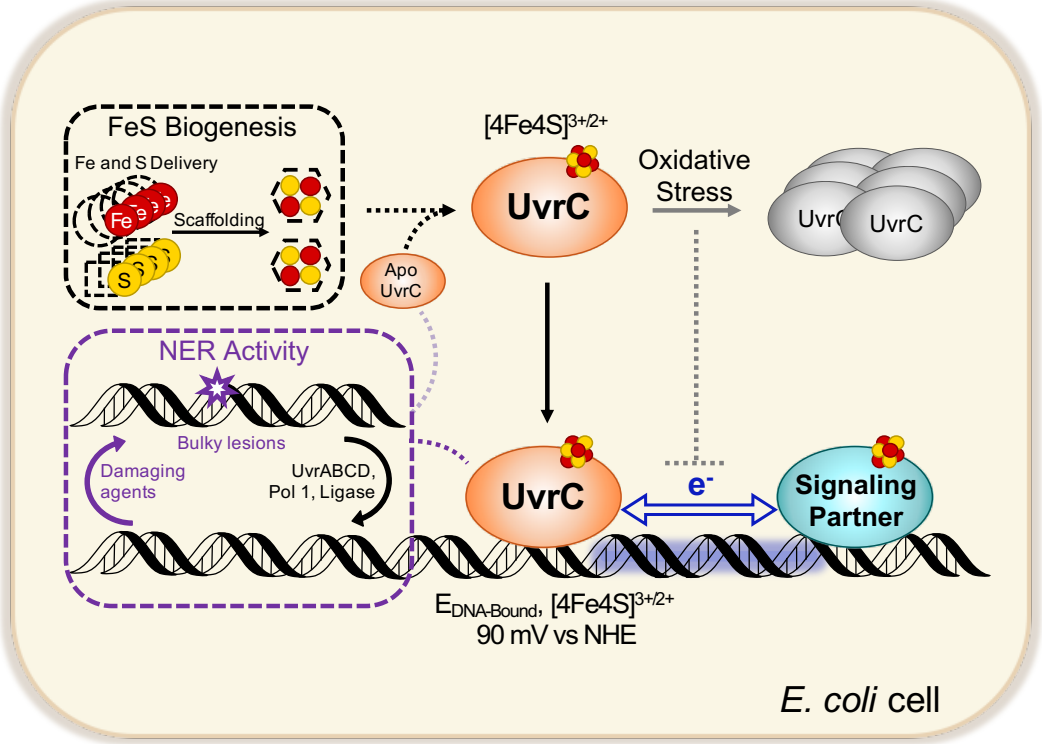

Figure 3.9 Implications for UvrC as a [4Fe4S] protein. Examination of UvrC in its holo form is likely to uncover many crucial details regarding the activity of UvrC *in vivo*. Connections between FeS biogenesis machinery and the NER pathway (dashed, black square and dashed, purple square), cellular functions of apo (orange oval), holo (orange oval and cofactor), and aggregated UvrC (gray ovals), the role of O_2 sensitivity (solid gray arrow), and DNA-mediated redox signaling with other repair pathways (solid blue, double headed arrow) remain to be explored.

3.6 Appendix A: Supplemental Purification Methods

Diagrams are taken from a combination of nitrogenase (where I shadowed Rees group members during training) and UvrC purifications. Dark brown solutions are nitrogenase, and light yellow/tan solutions are UvrC. Shown in **Figure 3.10** is a summary of the purification steps. See Materials and Methods for details specific to the UvrC purification.

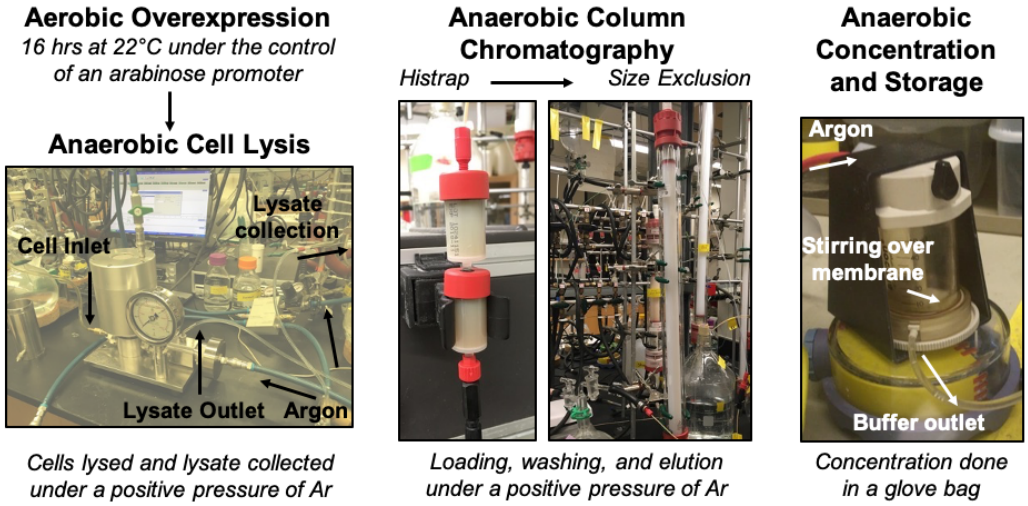

Figure 3.10 Expression and purification overview. (*Left*) Overexpression cells harboring MBP-UvrC are stored frozen until the day of purification, where they are thawed in a glove bag and then lysed using an Emusliflex under a positive pressure of argon. Lysed cells are centrifuged, purified over a Histrap column under a positive pressure of argon, concentrated in a glove bag, and then purified using size exclusion chromatography under a positive pressure of argon (*Middle*). Purified protein is concentrated once more, aliquoted, flash frozen, and stored until use.

3.6.1 Degassing Purification Buffers

3.6.1.1 Assembling the Cold Trap

A cold trap for the chosen manifold was prepared by submerging the cold trap in dry ice and ethanol in a dewar and placing a towel over the cold trap. A vacuum hose and a hose to the chosen manifold were connected to the cold trap, clamps were tightly screwed down, and the vacuum switch that is associated with the chosen manifold was turned on. The vacuum was checked for oil spurts or burning. Degassing of buffers proceeded when the pressure reached between 20 and 50 mbar (about 30

minutes).

3.6.1.2 Preparing Degassing Chambers

Columns were equilibrated in filtered ddH_2O the day before degassing, and buffers were made the day of the water equilibration. Round bottom flasks were chosen that could hold twice the volume of the buffer to degas along with adapters with stems that can reach just above the bottom of the flask (Tygon tubing adjusted as necessary) (**Figure 3.11**). The bottom of the adapter was lightly greased along with the valves, while checking the valves for too much grease (if grease gets onto a column, it can clog the column). Extra grease was removed with a pipe cleaner. The valves were secured with clips or a screw (depending on the design of the joint). A Keck clip was placed on the joint where the adapter meets the round bottom flask. The valve on the side of the adapter that is closest to the black rubber tubing was closed, and the valve on the other side with the glass-only connection was left open. The final assembly is shown in **Figure 3.11**.

3.6.1.3 Programming the Autocycler

At the chosen degassing manifold, the Schlenck line was opened to argon, and the bubbler was checked for gas flow. A rubber hose was connected to the degassing chamber, and the Autocycler was turned on. The Autocycler was switched to the Manual Mode and Argon settings. The Autocycler was programmed to pull vacuum for 7 min and refill with Ar for 2 min for 12 cycles. The Autocycler was switched to the Vac mode to make sure the lines were working; the bubbler should start bubbling and the pressure should lower on the pressure gauge. The Autocycler was switched back to Ar, and system was monitored until it returned to the starting pressure (the bubbler should stop bubbling vigorously). The Autocycler was placed on Auto, and the program was started. It is advisable to monitor a complete cycle to catch any malfunctions.

3.6.1.4 Cleaning Up

Buffers that needed to be left out overnight remained on the Schlenk line with the argon line open. Otherwise, the valve on the buffer going to the Schlenck and the Schlenk line were closed (finger tight). The Autocycler was placed on Manual, and the system was tested by placing it on vacuum and then back to argon. The

Autocycler and vacuum were turned off and the trap was released. The bubbler was monitored for leaks in the lines.

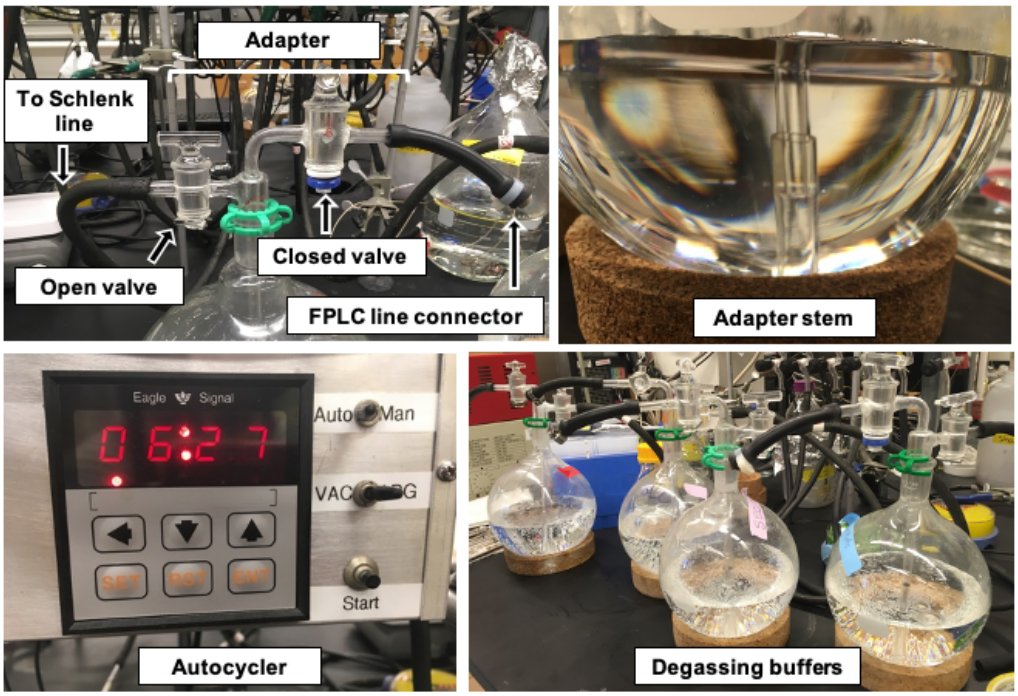

Figure 3.11 Degassing buffers. (*Top Left*) Buffers placed in round bottom flasks sealed with an adaptor that has a connection to a Schlenk line port and connection to an FPLC line (labeled). (*Top Right*) The stem of the adapter should reach near the bottom of the round bottom flask. (*Bottom Left*) The Autocycler which controls the degassing sequence. (*Bottom Right*) Buffers degassing in parallel.

3.6.2 Column Equilibration

The FPLC lines were washed with 20% ethanol and water. Columns were connected to the FPLC using the the drip-to-drip method by flowing water through the inlet and connecting the column to the FPLC lines (this is done to avoid introducing air into the lines). A flowing argon line was connected to a flask of degassed buffer and the valve to the line was opened. The inlet line was was opened and buffer was allowed to flow out. The drip-to-drip method was used again to connect the inlet line to the buffer adapter (the lines screw together). Buffer was flowed through the FPLC on the bypass position, then the buffer was flowed to the desired column position. Columns were equilibrated in the desired volume of buffer.

3.6.3 Emulsiflex Assembly

The Emulsiflex-C5 (Avestin) homogenizer was assembled in the orientation shown in **Figure 3.12**. The regulator was connected to a full argon tank and an argon line was connected to the lysis chamber (a click should be heard once the line is in place). The linet line was placed in 20% ethanol, while the outlet line was placed in the waste. The argon tank was opened, and the tank and outlet readings were verified to be at the appropriate pressures (marked in black on the regulator). The green gas valve on the Emulsiflex was turned 90 degrees, and the Emulsiflex was allowed to cycle three times on low pressure, and then the system was turned off by turning the green argon valve to the off position. The inlet was placed in water, and the cycling was repeated on low pressure again, then the pressure control knob was adjusted to allow the Emulsiflex to cycle three times at high pressure (25,000 psi). The system was returned to low pressure and allowed to cycle three times. The Emulsiflex was turned off, the argon tank was shut off, and then the Emulsiflex was turned back on to depressurize the system. The green valve was left in the position shown.

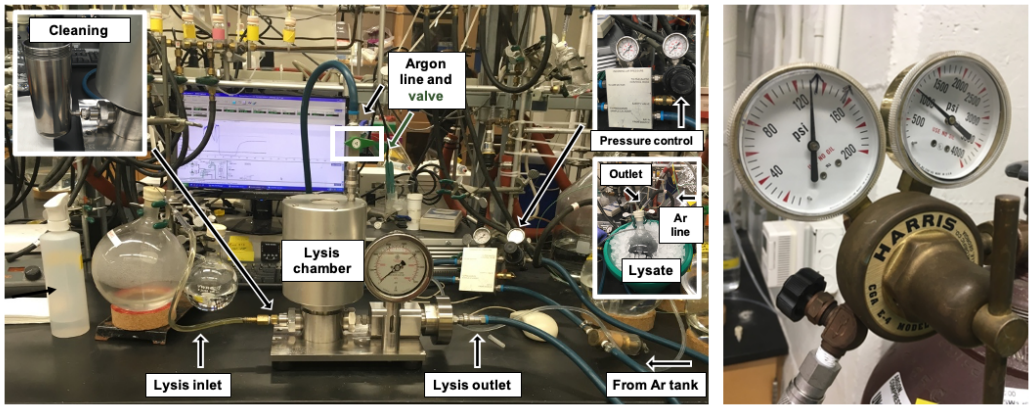

Figure 3.12 Emulsiflex assembly. Shown is the arrangement of the Emulsiflex instrument (*Left*) and the regulator for the argon tank (*Right*), which is connected to the Emulsiflex through blue hoses.

3.6.4 Cell Lysis

On the day of the purification, cell pellets were thawed on ice in a glove bag. While cells were thawing, a 100 mM solution of DTT was made in the glove bag in degassed lysis buffer. DTT was added to the stock lysis buffer to a final concentration of 1 mM. The remaining DTT was placed in a Wheaton vial and sealed with a rubber stopper. Cells were resuspended in Lysis Buffer (100 mL of buffer per 10 g of

wet pellet) that was supplemented on the day of the purification with 6-8 tablets of crushed cOmplete™ protease inhibitor cocktail tablets (Roche) and DNAse (15 kU, Sigma). Tablets were crushed with a glass stirring rod. A Dounce homogenizer was used to homogenize the resuspended cell slurry, using both the loose and the tight rods. Once the slurry was homogenized, the cell slurry was passed over a 100 μm nylon cell strainer (Corning) by pipetting and collected in a wide-mouth flask (the strainer sits in the flask). The filtered slurry was transferred to a round bottom flask which was then sealed with rubber stopper and tape. Lysis buffer was added to another flask and sealed.

The flask of lysis buffer was secured with a clamp and a Schlenck line port delivering argon was introduced to the flask through a needle that punctured the rubber stopper. The Emulsiflex was equilibrated in degassed lysis buffer as described above. After clamping the flask of lysate and placing it on ice, a Schlenck line port delivering argon was introduced. The Emulsiflex inlet (affixed with a long needle reaching to the bottom of the flask) was also introduced to the lysate. An empty flask with rubber stopper and argon line (on ice) was placed at the collection outlet. The outlet is also affixed with a long needle. Just prior to cell lysis, the argon line was closed to avoid overpressure in the collection flask; once collection was finished, the argon line was re-opened. Cells were lysed at high pressure (25,000 psi). Cells were allowed to cool before a second round of lysis. The lysate was brought into a glove bag, loaded into screw-cap polycarbonate vials with an O-ring, and centrifuged on a Sorvall™ RC 6 Plus Centrifuge (ThermoFisherScientific) at 13,000 rpm for 45 minutes at 4 °C. During centrifugation, the Emulsiflex was cleaned using lysis buffer (low and high pressure) and water (low pressure). An outside chamber was attached to the cell to inlet (see **Figure 3.12**, Top Left inset), filled with water, sealed with a screw cap (not shown), and another argon line was used to pressurize the cell. This was repeated a total of three times. The chamber was removed, the inlet line was reattached, and 20% ethanol was passed through the Emulsiflex (low pressure). The instrument was disassembled and returned to storage.

3.6.5 Column Chromatography

Prior to purification, DTT was added to all the buffers (**Figure 3.13**, Top Left). The bottle of DTT in the Wheaton vial was put on an argon line. A syringe with needle was prepared by aspirating out argon from the top head space of the DTT bottle, the syringe was emptied, more argon with some DTT solution was taken out, swirled around, and emptied. DTT solution was aspirated out once more, the adapter in

the buffer solution was unclipped, lifted quickly, DTT was added through the long needle, the needle was removed, the adapter was quickly put back in place, and the Keck clip was returned. Buffer with DTT was then applied to the columns.

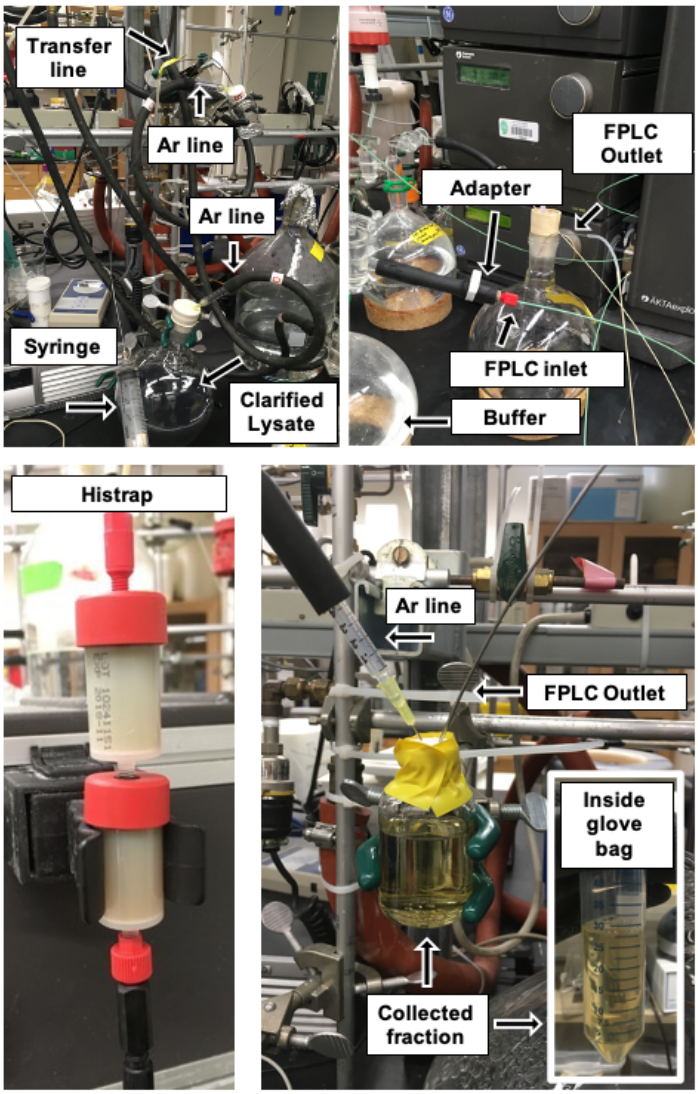

Figure 3.13 Purification on the Histrap column. (*Top*) Lysate is loaded onto the Histrap column using a transfer line connected to one of the buffer ports. (*Bottom*) Once the buffer port has been reconnected to the buffer line, the column was washed and protein was eluted and collected.

After centrifugation, supernatant was combined in the glove bag in a round bottom flask and covered with a rubber stopper. The flask was then placed on an argon line. A transfer line was prepared; the steps are similar to the steps required for preparing the syringe to add DTT, except that a thin piece of Tygon tubing with

another needle at the end is prepared. In the last step, the transfer line is place in the headspace of the lysate, and argon is allowed to flow out of the line. While argon was flowing out of the transfer line, the loading buffer valve closest to the FPLC adapter was closed (**Figure 3.13**, Top Right). The buffer line was unscrewed, and adaptors were taken off the end of the FPLC inlet line. Next, the needle in the headspace was pushed into the lysate and the Tygon tubing at the end was pinched to stop the flow of the lysate. Very slowly, the Tygon tubing was released and allowed to drip. While dripping, the FPLC line was inserted into the Tygon tubing without introducing any air into the line. After application of the lysate to the column, the buffer line was reconnected to the Lysis buffer line. The purification program was run as described in the Experimental Section, and fractions were collected in Wheaton vials that have been prepared with taped rubber stoppers in the glove bag. When collecting, the argon line was turned off to avoid overpressurizing.

An Ultracentrifugation Cell was assembled in the glove bag (**Figure 3.14**), and buffer was used to test the cell for leakage. The fractions from the Histrap column were concentrated to a volume less than 10 mLs (the recommended maximum volume for the Superdex 200). The concentrate was placed in a Wheaton vial, and a transfer line was prepared as above in order to load the concentrate onto the Superdex 200 column (**Figure 3.15**). The soluble fraction was collected, concentrated between 20-30 μM to avoid precipitation upon freezing, aliquoted in screw cap vials, then immediately flash frozen in liquid N_2 and stored at ≤ -80 °C.

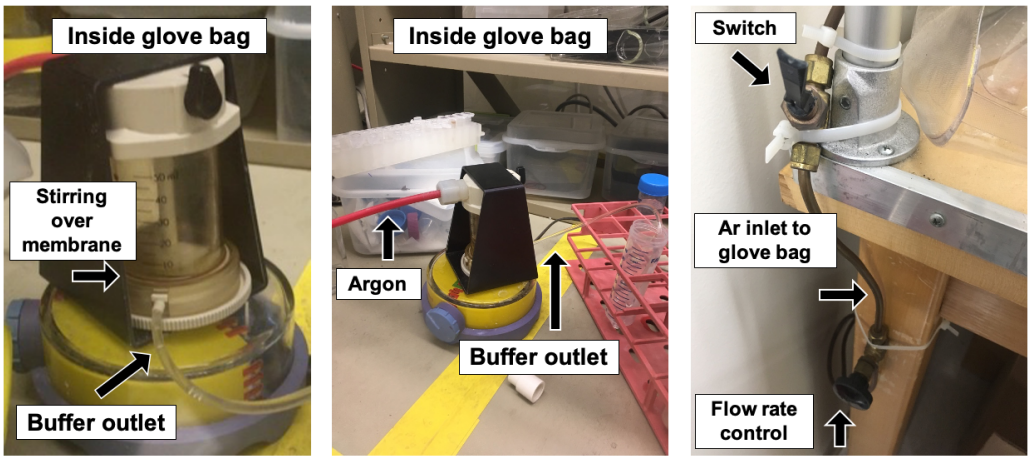

Figure 3.14 Anaerobic concentration. (*Left and Middle*) To assemble an Ultrafiltration Cell, a 30 kDa membrane was placed on a screw cap (attached to the buffer outlet), an O-ring was placed on top of the membrane, and the screw cap was connected to the concentrator cell. The cell was capped, the black switch on the cap was placed in the upright position, secured in place in a black brace, and placed over a stir plate. (*Right*) The cell was pressurized through an argon line.

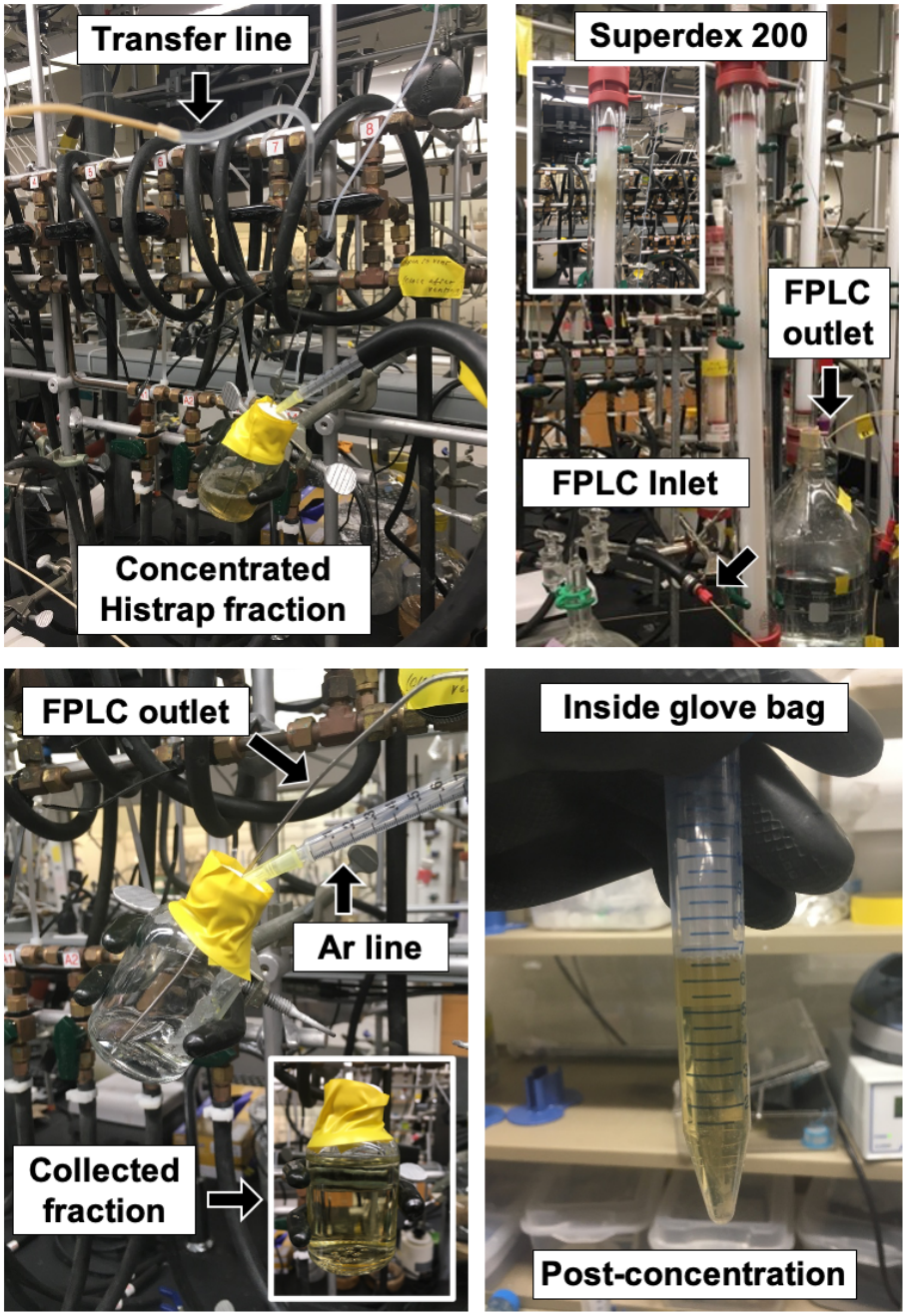

Figure 3.15 Purification on the Superdex 200 column. Concentrated fractions are loaded onto the Superdex 200 using a transfer line connected to one of the buffer ports. (*Top*) Once the buffer port has been reconnected to the buffer line, protein was eluted, collected, and concentrated (*Bottom*).

3.7 Appendix B: DNA substrates

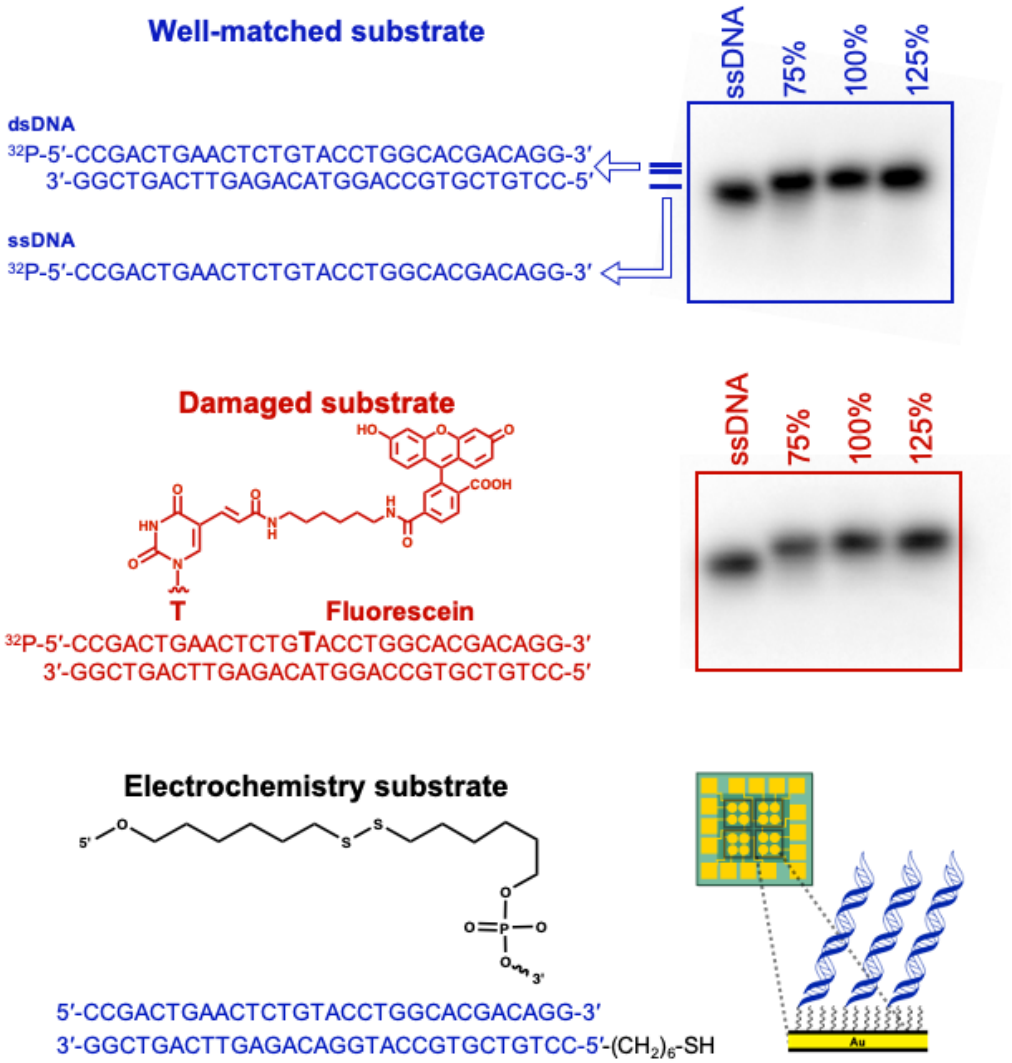

Figure 3.16 DNA substrates. DNA substrates used for gel shift assays (*Top and Middle*) and representative annealing titrations are shown. Separation of single and double can be seen and are labeled. The electrochemistry substrate is also shown (*Bottom*), along with a schematic of DNA monolayers.

References

[1] A. R. Arnold, M. A. Grodick, and J. K. Barton. DNA Charge Transport: From Chemical Principles to the Cell. *Cell Chemical Biology*, 23(1):183–197, 2016. ISSN 24519448. doi: 10.1016/j.chembiol.2015.11.010. URL http://dx.doi.org/10.1016/j.chembiol.2015.11.010.

[2] A. R. Arnold, A. Zhou, and J. K. Barton. Characterization of the DNA-Mediated Oxidation of Dps, A Bacterial Ferritin. *Journal of the American Chemical Society*, 138(35):11290–11298, 2016. ISSN 15205126. doi: 10.1021/jacs.6b06507.

[3] P. L. Bartels, E. O'Brien, and J. K. Barton. DNA signaling by iron-sulfur cluster proteins. In T. A. Rouault, editor, *Biochemistry, Biosynthesis and Human Diseases: Biochemistry, Biosynthesis, and Human Diseases*, volume 2, pages 405–423. De Gruyter, Berlin, Boston, 2017. ISBN 9783110479850. doi: 10.1515/9783110479850-015.

[4] P. L. Bartels, J. L. Stodola, P. M. Burgers, and J. K. Barton. A Redox Role for the [4Fe4S] Cluster of Yeast DNA Polymerase δ. *Journal of the American Chemical Society*, 139(50):18339–18348, 2017. ISSN 15205126. doi: 10.1021/jacs.7b10284.

[5] P. L. Bartels, A. Zhou, A. R. Arnold, N. N. Nuñez, F. N. Crespilho, S. S. David, and J. K. Barton. Electrochemistry of the [4Fe4S] Cluster in Base Excision Repair Proteins: Tuning the Redox Potential with DNA. *Langmuir*, 33(10):2523–2530, mar 2017. ISSN 15205827. doi: 10.1021/acs.langmuir.6b04581. URL http://dx.doi.org/10.1021/acs.langmuir.6b04581.

[6] A. K. Boal, E. Yavin, O. A. Lukianova, V. L. O'Shea, S. S. David, and J. K. Barton. DNA-bound redox activity of DNA repair glycosylases containing [4Fe-4S] clusters. *Biochemistry*, 44(23):8397–8407, 2005. ISSN 00062960. doi: 10.1021/bi047494n. URL http://pubs.acs.org/doi/abs/10.1021/bi047494n.

[7] E. M. Boon, A. L. Livingston, N. H. Chmiel, S. S. David, and J. K. Barton. DNA-mediated charge transport for DNA repair. *Proceedings of the National Academy of Sciences*, 100(22):12543–12547, 2003. ISSN 0027-8424. doi: 10.1073/pnas.2035257100. URL http://www.pnas.org/cgi/doi/10.1073/pnas.2035257100.

[8] S. E. Bowman, J. Bridwell-Rabb, and C. L. Drennan. Metalloprotein Crystallography: More than a Structure. *Accounts of Chemical Research*, 49(4):695–702, 2016. ISSN 15204898. doi: 10.1021/acs.accounts.5b00538.

[9] P. R. Caron and L. Grossman. Incision of damaged versus nondamaged DNA by the *Escherichia coli* UvrABC proteins. *Nucleic Acids Research*, 16(16):7855–7865, 1988. ISSN 03051048. doi: 10.1093/nar/16.16.7855.

[10] K. Cheng and D. B. Wigley. DNA translocation mechanism of an XPD family helicase. *eLife*, 7:e42400, 2018. ISSN 2050084X. doi: 10.7554/eLife.42400.

[11] N. H. Chmiel. Efficient recognition of substrates and substrate analogs by the adenine glycosylase MutY requires the C-terminal domain. *Nucleic Acids Research*, 29(2):553–564, 2001. doi: 10.1093/nar/29.2.553.

[12] J. C. Crack, J. Green, A. J. Thomson, and N. E. Brun. Iron-sulfur clusters as biological sensors: The chemistry of reactions with molecular oxygen and nitric oxide. *Accounts of Chemical Research*, 47(10):3196–3205, 2014. ISSN 15204898. doi: 10.1021/ar5002507.

[13] R. P. Cunningham, H. Asahara, J. F. Bank, C. P. Scholes, J. C. Salerno, K. Surerus, E. Miinck, J. McCracken, J. Peisach, and M. H. Emptage. Endonuclease III Is an Iron-Sulfur Protein. *Biochemistry*, 28(10):4450–4455, May 1989. ISSN 15204995. doi: 10.1021/bi00436a049. URL `http://dx.doi.org/10.1021/bi00436a049`.

[14] G. E. Cutsail, J. Telser, and B. M. Hoffman. Advanced paramagnetic resonance spectroscopies of iron-sulfur proteins: Electron nuclear double resonance (ENDOR) and electron spin echo envelope modulation (ESEEM). *Biochimica et Biophysica Acta - Molecular Cell Research*, 1853(6):1370–1394, 2015. ISSN 18792596. doi: 10.1016/j.bbamcr.2015.01.025.

[15] M. J. DellaVecchia, D. L. Croteau, M. Skorvaga, S. V. Dezhurov, O. I. Lavrik, and B. Van Houten. Analyzing the handoff of DNA from UvrA to UvrB utilizing DNA-protein photoaffinity labeling. *Journal of Biological Chemistry*, 279 (43):45245–45256, 2004. ISSN 00219258. doi: 10.1074/jbc.M408659200.

[16] L. A. Ekanger, P. H. Oyala, A. Moradian, M. J. Sweredoski, and J. K. Barton. Nitric Oxide Modulates Endonuclease III Redox Activity by a 800 mV Negative Shift upon [Fe4S4] Cluster Nitrosylation. *Journal of the American Chemical Society*, 140(37):11800–11810, Sep 2018. ISSN 0002-7863. doi: 10.1021/jacs.8b07362. URL `https://doi.org/10.1021/jacs.8b07362`.

[17] S. A. Freibert, B. D. Weiler, E. Bill, A. J. Pierik, U. Mühlenhoff, and R. Lill. Biochemical Reconstitution and Spectroscopic Analysis of Iron–Sulfur Proteins. *Methods in Enzymology*, 599:197–226, 2018. ISSN 15577988. doi: 10.1016/bs.mie.2017.11.034.

[18] J. C. Fromme and G. L. Verdine. Structure of a trapped endonuclease III-DNA covalent intermediate. *EMBO Journal*, 22(13):3461–3471, 2003. ISSN 02614189. doi: 10.1093/emboj/cdg311.

[19] J. C. Fromme, A. Banerjee, S. J. Huang, and G. L. Verdine. Structural basis for removal of adenine mispaired with 8-oxoguanine by MutY adenine DNA glycosylase. *Nature*, 427(6975):652–656, 2004. ISSN 14764660. doi: 10.1038/nature02306.

[20] J. O. Fuss, C. L. Tsai, J. P. Ishida, and J. A. Tainer. Emerging critical roles of Fe-S clusters in DNA replication and repair. *Biochimica et Biophysica Acta - Molecular Cell Research*, 1853(6):1253–1271, 2015. ISSN 18792596. doi: 10.1016/j.bbamcr.2015.01.018. URL http://dx.doi.org/10.1016/j.bbamcr.2015.01.018.

[21] H. B. Gray, E. I. Stiefel, J. S. Valentine, and I. Bertini. *Bioinorganic Chemistry*. University Books, 2006. ISBN 1891389432.

[22] M. A. Grodick. *DNA-mediated charge transport signaling within the cell*. PhD thesis, California Institute of Technology, 2016. URL https://resolver.caltech.edu/CaltechTHESIS:07192015-214603085.

[23] M. A. Grodick, H. M. Segal, T. J. Zwang, and J. K. Barton. DNA-mediated signaling by proteins with 4Fe-4S clusters is necessary for genomic integrity. *Journal of the American Chemical Society*, 136(17):6470–6478, 2014. ISSN 15205126. doi: 10.1021/ja501973c.

[24] M. A. Grodick, N. B. Muren, and J. K. Barton. DNA charge transport within the cell. *Biochemistry*, 54(4):962–973, 2015. ISSN 15204995. doi: 10.1021/bi501520w.

[25] Y. Ha, A. R. Arnold, N. N. Nuñez, P. L. Bartels, A. Zhou, S. S. David, J. K. Barton, B. Hedman, K. O. Hodgson, and E. I. Solomon. Sulfur K-Edge XAS Studies of the Effect of DNA Binding on the [Fe4S4] Site in EndoIII and MutY. *Journal of the American Chemical Society*, 139(33):11434–11442, 2017. ISSN 15205126. doi: 10.1021/jacs.7b03966.

[26] W. R. Hagen. EPR spectroscopy as a probe of metal centres in biological systems. *Dalton Transactions*, (37):4415–4434, 2006. ISSN 14779226. doi: 10.1039/b608163k.

[27] P. O. Hardy and G. Chaconas. The nucleotide excision repair system of borrelia burgdorferi is the sole pathway involved in repair of DNA damage by UV light. *Journal of Bacteriology*, 195(10):2220–2231, 2013. ISSN 00219193. doi: 10.1128/JB.00043-13.

[28] J. A. Hinks, M. C. Evans, Y. De Miguel, A. A. Sartori, J. Jiricny, and L. H. Pearl. An iron-sulfur cluster in the Family 4 uracil-DNA glycosylases. *Journal of Biological Chemistry*, 277(19):16936–16940, 2002. ISSN 00219258. doi: 10.1074/jbc.M200668200.

[29] R. H. Holm, P. Kennepohl, and E. I. Solomon. Structural and functional aspects of metal sites in biology. *Chemical Reviews*, 96(7):2239–2314, 1996. ISSN 00092665. doi: 10.1021/cr9500390.

[30] J. A. Imlay. Iron-sulphur clusters and the problem with oxygen. *Molecular Microbiology*, 59(4):1073–1082, 2006. ISSN 0950382X. doi: 10.1111/j.1365-2958.2006.05028.x.

[31] J. A. Imlay. Transcription Factors That Defend Bacteria Against Reactive Oxygen Species. *Annual Review of Microbiology*, 69(1):93–108, 2015. ISSN 0066-4227. doi: 10.1146/annurev-micro-091014-104322.

[32] M. Jaciuk, E. Nowak, K. Skowronek, A. Tañska, and M. Nowotny. Structure of UvrA nucleotide excision repair protein in complex with modified DNA. *Nature Structural and Molecular Biology*, 18(2):191–198, 2011. ISSN 15459993. doi: 10.1038/nsmb.1973.

[33] E. Karakas, J. J. Truglio, D. Croteau, B. Rhau, L. Wang, B. Van Houten, and C. Kisker. Structure of the C-terminal half of UvrC reveals an RNase H endonuclease domain with an Argonaute-like catalytic triad. *EMBO Journal*, 26(2):613–622, 2007. ISSN 14602075. doi: 10.1038/sj.emboj.7601497.

[34] C. Kisker, J. Kuper, and B. Van Houten. Prokaryotic nucleotide excision repair. *Cold Spring Harbor Perspectives in Biology*, 5(3):1–18, 2013. ISSN 19430264. doi: 10.1101/cshperspect.a012591.

[35] S. Klinge, J. Hirst, J. D. Maman, T. Krude, and L. Pellegrini. An iron-sulfur domain of the eukaryotic primase is essential for RNA primer synthesis. *Nature Structural and Molecular Biology*, 14(9):875–877, 2007. ISSN 15459993. doi: 10.1038/nsmb1288.

[36] C. F. Kuo, D. E. McRee, C. L. Fisher, S. F. O'Handley, R. P. Cunningham, and J. A. Tainer. Atomic structure of the DNA repair [4Fe-4S] enzyme endonuclease III. *Science*, 258(5081):434 LP – 440, oct 1992. URL `http://science.sciencemag.org/content/258/5081/434.abstract`.

[37] F. H. Lessner, M. E. Jennings, A. Hirata, E. C. Duin, and D. J. Lessner. Subunit D of RNA polymerase from Methanosarcina acetivorans contains two oxygen-labile [4Fe-4S] clusters: Implications for oxidant-dependent regulation of transcription. *Journal of Biological Chemistry*, 287(22):18510–18523, 2012. ISSN 00219258. doi: 10.1074/jbc.M111.331199.

[38] S. J. Lippard and J. M. Berg. *Principles of Bioinorganic Chemistry*. University Science Books, Mill Valley, CA, 1994. ISBN 0935702725.

[39] J. Liu, S. Chakraborty, P. Hosseinzadeh, Y. Yu, S. Tian, I. Petrik, A. Bhagi, and Y. Lu. Metalloproteins containing cytochrome, iron-sulfur, or copper redox centers. *Chemical Reviews*, 114(8):4366–4369, 2014. ISSN 15206890. doi: 10.1021/cr400479b.

[40] Z. Lu, R. Sethu, and J. A. Imlay. Endogenous superoxide is a key effector of the oxygen sensitivity of a model obligate anaerobe. *Proceedings of the National Academy of Sciences of the United States of America*, 115(14):E3266–E3275, 2018. ISSN 10916490. doi: 10.1073/pnas.1800120115.

[41] K. J. McDonnell, J. A. Chemler, P. L. Bartels, E. O'Brien, M. L. Marvin, J. Ortega, R. H. Stern, L. Raskin, G. M. Li, D. H. Sherman, J. K. Barton, and S. B. Gruber. A human MUTYH variant linking colonic polyposis to redox degradation of the [4Fe4S]2+cluster. *Nature Chemistry*, 10(8):873–880, 2018. ISSN 17554349. doi: 10.1038/s41557-018-0068-x. URL https://www.nature.com/articles/s41557-018-0068-x.

[42] T. E. Messick, N. H. Chmiel, M. P. Golinelli, M. R. Langer, L. Joshua-Tor, and S. S. David. Noncysteinyl coordination to the [4Fe-4S]2+ cluster of the DNA repair adenine glycosylase MutY introduced via site-directed mutagenesis. Structural characterization of an unusual histidinyl-coordinated cluster. *Biochemistry*, 41(12):3931–3942, 2002. ISSN 00062960. doi: 10.1021/bi012035x.

[43] E. L. Mettert and P. J. Kiley. Fe-S proteins that regulate gene expression. *Biochimica et Biophysica Acta - Molecular Cell Research*, 1853(6):1284–1293, 2015. ISSN 18792596. doi: 10.1016/j.bbamcr.2014.11.018.

[44] I. G. Minko, A. J. Kurtz, D. L. Croteau, B. Van Houten, T. M. Harris, and R. S. Lloyd. Initiation of repair of DNA - Polypeptide cross-links by the UvrABC nuclease. *Biochemistry*, 44(8):3000–3009, 2005. ISSN 00062960. doi: 10.1021/bi0478805.

[45] G. F. Moolenaar, M. Bazuine, I. C. Van Knippenberg, R. Visse, and N. Goosen. Characterization of the Escherichia coli damage-independent UvrBC endonuclease activity. *Journal of Biological Chemistry*, 273(52):34896–34903, 1998. ISSN 00219258. doi: 10.1074/jbc.273.52.34896.

[46] G. F. Moolenaar, V. Monaco, G. A. Van Der Marel, J. H. Van Boom, R. Visse, and N. Goosen. The effect of the DNA flanking the lesion on formation of the UvrB-DNA preincision complex. Mechanism for the UvrA-mediated loading of UvrB onto a DNA damaged site. *Journal of Biological Chemistry*, 275(11):8038–8043, 2000. ISSN 00219258. doi: 10.1074/jbc.275.11.8038.

[47] G. F. Moolenaar, L. Höglund, and N. Goosen. Clue to damage recognition by UvrB: Residues in the β-hairpin structure prevent binding to non-damaged DNA. *EMBO Journal*, 20(21):6140–6149, 2001. ISSN 02614189. doi: 10.1093/emboj/20.21.6140.

[48] D. J. A. Netz, C. M. Stith, M. Stümpfig, G. Köpf, D. Vogel, H. M. Genau, J. L. Stodola, R. Lill, P. M. J. Burgers, and A. J. Pierik. Eukaryotic DNA polymerases require an iron-sulfur cluster for the formation of active complexes. *Nature Chemical Biology*, 8(1):125–132, 2012. ISSN 1552-4450. doi: 10.1038/nchembio.721. URL http://www.nature.com/doifinder/10.1038/nchembio.721.

[49] I. Oberpichler, A. J. Pierik, J. Wesslowski, R. Pokorny, R. Rosen, M. Vugman, F. Zhang, O. Neubauer, E. Z. Ron, A. Batschauer, and T. Lamparter. A

photolyase-like protein from agrobacterium tumefaciens with an iron-sulfur cluster. *PLoS ONE*, 6(10), 2011. ISSN 19326203. doi: 10.1371/journal.pone.0026775.

[50] E. O'Brien, M. E. Holt, M. K. Thompson, L. E. Salay, A. C. Ehlinger, W. J. Chazin, and J. K. Barton. The [4Fe4S] cluster of human DNA primase functions as a redox switch using DNA charge transport. *Science*, 355(6327): eaag1789, Feb 2017. URL http://science.sciencemag.org/content/355/6327/eaag1789.abstract.

[51] E. O'Brien, M. E. Holt, L. E. Salay, W. J. Chazin, and J. K. Barton. Substrate Binding Regulates Redox Signaling in Human DNA Primase. *Journal of the American Chemical Society*, 140(49):17153–17162, 2018. ISSN 15205126. doi: 10.1021/jacs.8b09914.

[52] E. O'Brien, L. E. Salay, E. A. Epum, K. L. Friedman, W. J. Chazin, and J. K. Barton. Yeast require redox switching in DNA primase. *Proceedings of the National Academy of Sciences of the United States of America*, 115(52): 13186–13191, 2018. ISSN 10916490. doi: 10.1073/pnas.1810715115.

[53] D. K. Orren and A. Sancar. The (A)BC excinuclease of Escherichia coli has only the UvrB and UvrC subunits in the incision complex. *Proceedings of the National Academy of Sciences of the United States of America*, 86(14): 5237–5241, 1989. ISSN 00278424. doi: 10.1073/pnas.86.14.5237.

[54] A. V. Perera, J. B. Mendenhall, C. T. Courcelle, and J. Courcelle. Cho endonuclease functions during DNA interstrand cross-link repair in Escherichia coli. *Journal of Bacteriology*, 198(22):3099–3108, 2016. ISSN 10985530. doi: 10.1128/JB.00509-16.

[55] C. G. Pheeney, A. R. Arnold, M. A. Grodick, and J. K. Barton. Multiplexed electrochemistry of DNA-bound metalloproteins. *Journal of the American Chemical Society*, 135(32):11869–11878, 2013. ISSN 00027863. doi: 10.1021/ja4041779.

[56] S. Pokharel and J. L. Campbell. Cross talk between the nuclease and helicase activities of Dna2: Role of an essential iron-sulfur cluster domain. *Nucleic Acids Research*, 40(16):7821–7830, 2012. ISSN 03051048. doi: 10.1093/nar/gks534.

[57] S. L. Porello, S. D. Williams, H. Kuhn, M. L. Michaels, and S. S. David. Specific recognition of substrate analogs by the DNA mismatch repair enzyme MutY. *Journal of the American Chemical Society*, 118(44):10684–10692, 1996. ISSN 00027863. doi: 10.1021/ja9602206.

[58] S. Puig, L. Ramos-Alonso, A. M. Romero, and M. T. Martínez-Pastor. The elemental role of iron in DNA synthesis and repair. *Metallomics*, 9(11):1483–1500, 2017. ISSN 1756591X. doi: 10.1039/c7mt00116a.

[59] J. T. Reardon and A. Sancar. Purification and Characterization of Escherichia coli and Human Nucleotide Excision Repair Enzyme Systems. *Methods in Enzymology*, 408:189–213, 2006. ISSN 00766879. doi: 10.1016/S0076-6879(06)08012-8.

[60] B. Ren, X. Duan, and H. Ding. Redox control of the DNA damage-inducible protein DinG helicase activity via its iron-sulfur cluster. *Journal of Biological Chemistry*, 284(8):4829, 2009. ISSN 00219258. doi: 10.1074/jbc.M807943200.

[61] P. A. Rogers, L. Eide, A. Klungland, and H. Ding. Reversible inactivation of E. coli endonuclease III via modification of its [4Fe-4S] cluster by nitric oxide. *DNA Repair*, 2(7):809–817, 2003. ISSN 15687864. doi: 10.1016/S1568-7864(03)00065-X.

[62] T. A. Rouault. Mammalian iron-sulphur proteins: novel insights into biogenesis and function. *Nature Reviews Molecular Cell Biology*, 16(1):45–55, Jan 2015. ISSN 1471-0072. URL http://dx.doi.org/10.1038/nrm3909http://10.0.4.14/nrm3909.

[63] T. A. Rouault. Iron-sulfur proteins hiding in plain sight. *Nature Chemical Biology*, 11(7):442–445, 2015. ISSN 15524469. doi: 10.1038/nchembio.1843.

[64] J. Rudolf, V. Makrantoni, W. J. Ingledew, M. J. R. Stark, and M. F. White. The DNA Repair Helicases XPD and FancJ Have Essential Iron-Sulfur Domains. *Molecular Cell*, 23(6):801–808, 2006. ISSN 10972765. doi: 10.1016/j.molcel.2006.07.019.

[65] A. Sancar and W. D. Rupp. A novel repair enzyme: UVRABC excision nuclease of Escherichia coli cuts a DNA strand on both sides of the damaged region. *Cell*, 33(1):249–260, 1983. ISSN 00928674. doi: 10.1016/0092-8674(83)90354-9.

[66] K. N. Schaefer and J. K. Barton. DNA-mediated oxidation of p53. *Biochemistry*, 53(21):3467–3475, 2014. ISSN 15204995. doi: 10.1021/bi5003184.

[67] K. N. Schaefer, W. M. Geil, M. J. Sweredoski, A. Moradian, S. Hess, and J. K. Barton. Oxidation of p53 through DNA charge transport involves a network of disulfides within the DNA-binding domain. *Biochemistry*, 54(3):932–941, 2015. ISSN 15204995. doi: 10.1021/bi501424v.

[68] M. Senda and T. Senda. Anaerobic crystallization of proteins. *Biophysical Reviews*, 10(2):183–189, 2018. ISSN 18672469. doi: 10.1007/s12551-017-0345-8.

[69] S. Singh, G. E. Folkers, A. M. Bonvin, R. Boelens, R. Wechselberger, A. Niztayev, and R. Kaptein. Solution structure and DNA-binding properties of the C-terminal domain of UvrC from E. Coli. *EMBO Journal*, 21(22):6257–6266, 2002. ISSN 02614189. doi: 10.1093/emboj/cdf627.

[70] M. Skorvaga, K. Theis, B. S. Mandavilli, C. Kisker, and B. Van Houten. The β-hairpin motif of UvrB is essential for DNA binding, damage processing, and UvrC-mediated incisions. *Journal of Biological Chemistry*, 277(2):1553–1559, 2002. ISSN 00219258. doi: 10.1074/jbc.M108847200.

[71] J. D. Slinker, N. B. Muren, A. A. Gorodetsky, and J. K. Barton. Multiplexed DNA-modified electrodes. *Journal of the American Chemical Society*, 132(8): 2769–2774, 2010. ISSN 00027863. doi: 10.1021/ja909915m.

[72] T. Spatzal, K. A. Perez, O. Einsle, J. B. Howard, and D. C. Rees. Ligand binding to the FeMo-cofactor: Structures of CO-bound and reactivated nitrogenase. *Science*, 345(6204):1620 – 1623, Sep 2014. doi: 10.1126/science.1256679. URL http://science.sciencemag.org/content/345/6204/1620.abstract.

[73] W. V. Sweeney and J. C. Rabinowitz. Proteins Containing 4Fe-4S Clusters: An Overview. *Annual Review of Biochemistry*, 49(1):139–161, 1980. ISSN 0066-4154. doi: 10.1146/annurev.bi.49.070180.001035.

[74] M. S. Tang, M. Nazimiec, X. Ye, G. H. Iyer, J. Eveleigh, Y. Zheng, W. Zhou, and Y. Y. Tang. Two Forms of UvrC Protein with Different Double-stranded DNA Binding Affinities. *Journal of Biological Chemistry*, 276(6):3904–3910, 2001. ISSN 00219258. doi: 10.1074/jbc.M008538200.

[75] J. ter Beek, V. Parkash, G. O. Bylund, P. Osterman, A. E. Sauer-Eriksson, and E. Johansson. Structural evidence for an essential Fe–S cluster in the catalytic core domain of DNA polymerase ϵ. *Nucleic Acids Research*, 47(11): 5712–5722, Apr 2019. ISSN 0305-1048. doi: 10.1093/nar/gkz248. URL https://doi.org/10.1093/nar/gkz248.

[76] M. M. Thayer, H. Ahern, D. Xing, R. P. Cunningham, and J. a. Tainer. Novel DNA binding motifs in the DNA repair enzyme endonuclease III crystal structure. *The EMBO journal*, 14(16):4108–20, 1995. ISSN 0261-4189. URL http://www.pubmedcentral.nih.gov/articlerender.fcgi?artid=394490&tool=pmcentrez&rendertype=abstract.

[77] J. J. Truglio, B. Rhau, D. L. Croteau, L. Wang, M. Skorvaga, E. Karakas, M. J. DellaVecchia, H. Wang, B. Van Houten, and C. Kisker. Structural insights into the first incision reaction during nucleotide excision repair. *The EMBO journal*, 24(5):885–894, 2005. ISSN 0261-4189. doi: 10.1038/sj.emboj.7600568.

[78] J. J. Truglio, E. Karakas, B. Rhau, H. Wang, M. J. Dellavecchia, B. Van Houten, and C. Kisker. Structural basis for DNA recognition and processing by UvrB. *Nature Structural and Molecular Biology*, 13(4):360–364, 2006. ISSN 15459985. doi: 10.1038/nsmb1072.

[79] C. L. Tsai and J. A. Tainer. Robust Production, Crystallization, Structure Determination, and Analysis of [Fe–S] Proteins: Uncovering Control of Electron

Shuttling and Gating in the Respiratory Metabolism of Molybdopterin Guanine Dinucleotide Enzymes. *Methods in Enzymology*, 599:157–196, 2018. ISSN 15577988. doi: 10.1016/bs.mie.2017.11.006.

[80] E. C. M. Tse, T. J. Zwang, and J. K. Barton. The Oxidation State of [4Fe4S] Clusters Modulates the DNA-Binding Affinity of DNA Repair Proteins. *Journal of the American Chemical Society*, 139(36):12784–12792, Sep 2017. ISSN 0002-7863. doi: 10.1021/jacs.7b07230. URL http://dx.doi.org/10.1021/jacs.7b07230.

[81] A. Vaisman, J. P. McDonald, D. Huston, W. Kuban, L. Liu, B. Van Houten, and R. Woodgate. Removal of Misincorporated Ribonucleotides from Prokaryotic Genomes: An Unexpected Role for Nucleotide Excision Repair. *PLoS Genetics*, 9(11), 2013. ISSN 15537390. doi: 10.1371/journal.pgen.1003878.

[82] S. Van Der Veen and C. M. Tang. The BER necessities: The repair of DNA damage in human-adapted bacterial pathogens. *Nature Reviews Microbiology*, 13(2):83–94, 2015. ISSN 17401534. doi: 10.1038/nrmicro3391.

[83] B. E. Weiner, H. Huang, B. M. Dattilo, M. J. Nilges, E. Fanning, and W. J. Chazin. An iron-sulfur cluster in the C-terminal domain of the p58 subunit of human DNA primase. *Journal of Biological Chemistry*, 282(46):33444–33451, 2007. ISSN 00219258. doi: 10.1074/jbc.M705826200.

[84] B. B. Wenke, T. Spatzal, and D. C. Rees. Site-Specific Oxidation State Assignments of the Iron Atoms in the $[4Fe{:}4S]^{2+/1+/0}$ States of the Nitrogenase Fe-Protein. *Angewandte Chemie International Edition*, 58(12):3894–3897, mar 2019. ISSN 1433-7851. doi: 10.1002/anie.201813966. URL https://doi.org/10.1002/anie.201813966.

[85] M. F. White and T. Allers. DNA repair in the archaea-an emerging picture. *FEMS Microbiology Reviews*, 42(4):514–526, 2018. ISSN 15746976. doi: 10.1093/femsre/fuy020.

[86] N. Wirth, J. Gross, H. M. Roth, C. N. Buechner, C. Kisker, and I. Tessmer. Conservation and divergence in nucleotide excision repair lesion recognition. *Journal of Biological Chemistry*, 291(36):18932–18946, 2016. ISSN 1083351X. doi: 10.1074/jbc.M116.739425.

[87] A. Yan and P. J. Kiley. Chapter 42 Techniques to Isolate O2-Sensitive Proteins. [4Fe-4S]-FNR as an Example. In *Methods in Enzymology*, volume 463, pages 787–805. 2009. doi: 10.1016/S0076-6879(09)63042-1.

Chapter 4

APPROACHES FOR ISOLATION OF APO-UVRC

4.1 INTRODUCTION

Iron sulfur metal centers are versatile inorganic cofactors that serve many specialized functions in the cell, and identification of a general role for the [4Fe4S] center in repair and replication is ongoing [1, 2, 9, 24]. This is in contrast to other proteins involved in nucleic acid transactions, such as transcription factors, where transformations of [FeS] centers are involved in mounting rapid responses to reactive oxygen species, reactive nitrogen species, iron availability, and other changes in cellular environment ([5, 12, 15]). For repair and replication enzymes, one approach used to investigate the role of the cofactor has been to study variants with engineered or naturally-occurring mutations at coordinating cysteines, which disrupt cluster stability. Mutant studies have demonstrated that the cofactor is important for protein expression, protein stability, subunit assembly, enzymatic activity, and proficiency in redox signaling through DNA charge transport chemistry [6, 10, 11, 13, 14, 16, 20, 26, 30]. How mutations disrupt overall function appears to depend highly on the protein.

Cysteine mutants of the repair protein MutY and human homolog, MUTYH, have been well-studied in the literature. In a screen of MutY mutants, Golinelli *et al.* found that the extent to which each variant was affected by cysteine mutation (relative to WT) varied widely depending on which residue (ex. Cys192, Cys199, Cys202, or Cys208) was mutated and what mutation is chosen (ex. alaline, serine, or histidine) [10]. For example, the Cys199Ala mutant could not be studied due to complete abolishment of expression, while overexpression of the Cys199Ser mutant was greatly diminished. In contrast, overexpression and protein stability for the Cys199His mutant was comparable to WT protein, and a MutY truncate harboring the Cys199His mutation could even be crystallized [14]. Surprisingly though, both Cys199Ser and Cys199His exhibited WT repair activity, even though cluster loading and stability was affected (though not abolished). As described in Chapter 1, more recent work with a novel MUTYH germline variant, Cys306Trp (C306W) associated with early-onset, aggressive colon cancer, demonstrated that the Cys306Trp mutation was associated with diminished cluster loading, protein aggregation (reversible with β-mercaptoethanol and DTT), rapid degradation of the

[4Fe4S] cluster upon oxidation to the [3Fe-4S]$^{+1}$ species (as monitored using DNA-modified electrochemistry), as well as diminished substrate binding, redox signaling on DNA, and activity on damaged substrates [13].

As detailed in Chapter 1, the coordinating cysteines in other repair enzymes have also been found to be important for activity on damaged substrates, protein stability, and repair activity *in vivo* [19, 23, 25, 31]. As briefly mentioned in Chapter 3, coordinating cysteines were demonstrated to be important for eukaryotic replication polymerases, polymerase ϵ (leading strand, Pol ϵ) and polymerase δ (lagging strand, Pol δ) [16, 26]. Cysteine mutations did not interfere with assembly of the four subunits of Pol ϵ, but the mutations did abolish enzymatic activity [26]. In contrast, cysteine mutation did interfere with subunit assembly for Pol ϵ, thereby also interfering with enzymatic activity [16].

Incubation of WT protein with air-sensitive clusters in aerobic buffer is another commonly-used method to generate apo species of transcription factors [18, 21, 22]. Removal of the cofactor from holoenzyme through treating with chelators, low pH, or denaturation and refolding has also been used [8, 17, 20, 29]. These approaches are less widespread for repair and replication proteins, possibly due to yields and instability [8, 20]. Other iron sulfur proteins, such as radical SAM enzymes, can often be overexpressed and isolated in apo form (or even crystallized) and the holo form can be reconstituted *in vitro* where applicable [3, 7, 28]; this strategy has not been reported for repair and replication proteins.

For UvrC, we were interested in exploring the role of the cofactor further, in large part because we demonstrated that the air-sensitive cofactor is so integral for the stability of UvrC. The body of work on UvrC up until the discovery of the [4Fe4S] cluster was to our knowledge completed under aerobic conditions presumably with apo protein (and not just dilute protein) [27]. Studying holoenzyme in parallel with apo-UvrC would allow for a more direct comparison of our samples and the apo protein species that has likely been the subject of investigation in the majority of the bacterial NER literature. Such studies would also provide insight to what functions apo and holo-UvrC could occupy *in vivo*. Described here are the first attempts to generate and isolate soluble apo-UvrC through mutation of coordinating cysteines and through solubilization of aggregated product(s) after aerobic incubation. Overall, we found that disruption of the cofactor using the methods described leads to aggregation that is not easily reversible, further highlighting how important the cofactor is for UvrC. Discussed are implications of these preliminary results and recommendations for future investigations.

4.2 EXPERIMENTAL METHODS

4.2.1 General Procedures

General procedures are as described in Chapters 2 and 3.

4.2.2 Site Directed Mutagenesis

4.2.2.1 Primer Design and Primer Sequences

Site directed mutagenesis primers were designed according to the instructions that accompany Agilent's QuikChange site directed mutagenesis kits. The OligoAnalyzer (IDT), an online tool, was used to check sequences for stable hairpins and used to adjust the sequences to minimize hairpin formation. The sequences selected are given below for forward (F) and reverse (R) primers.

Cys154Ala

F 5′-CTACTGCAAAAGATTTTCCCCATTCGCCAGGCCGAAAATA-3′

R 5′-ACGCGAGCGATTGCGATAAACACTATTTTCGGCCTGGCG-3′

Cys166Ala

F 5′-GAAAATAGTGTTTATCGCAATCGCTCGCGTCCGGCCCTGCAA-3′

R 5′-GCCCTATCTGGTATTGCAGCGGCGGACGCGAGC-3′

Cys174Ala

F 5′-CTGCAATACCAGATAGGGCGCGCGCTGGGACCG-3′

R 5′-TCACTCACCAGTCCTTCAACGCACGGTCCCAGCGCGCGCCCT-3′

Cys178Ala

F 5′-GATAGGGCGCTGTCTGGGACCGGCAGTTGAAGG-3′

R 5′-GTATTCTTCTTCACTCACCAGTCCTTCAACTGCCGGTCCC-3′

4.2.2.2 Cys154Ala Plasmid

The QuikChange II-E Site-Directed Mutagenesis Kit was used to generate the Cys154Ala mutant. 50 ng of WT pBAD-UvrC plasmid and 125 ng of each primer was used. Temperature cycling was as follows: 1. 30 seconds at 95 °C; 2. 16 cycles of 30 seconds at 95 °C, 1 minute at 60 °C, and 10 minutes 68 °C; 3. a final extension according to the manufacturer's instructions. Once the amplification was complete, 30 U of Dpn I was added to the reaction mixture and then incubated for 3 hours at 37°C. Subsequent purification steps were completed using Qiagen kits. Plasmids were transformed into a vial of One Shot® TOP10 Electrocomp™ *E. coli* cells (Invitrogen) using a MicroPulser Electroporation Unit (Bio-Rad) with a 1.8 kV pulse. Cells were recovered by growing in 1 mL of SOC Media (Invitrogen) for 1

hour at 240 rpm at 37 °C. To an LB/Amp plate (50 mg/LB), 250 μL transformed cells were plated and grown at 37 °C overnight. Individual colonies were picked and grown in liquid cultures overnight as above, miniprepped using a Qiagen kit, and sequenced by Laragen. The sequence data was aligned to the sequence of WT UvrC using BLAST®n [4]. Samples containing the desired plasmids were transformed into TOP10 cells, grown, cell stocks were made with 25% glycerol, and cells were flash frozen in liquid N_2 before storing -80 °C.

4.2.2.3 Cys166Ala, Cys174Ala, and Cys178Ala Plasmids

The region around the Cys166, Cys174, and Cys178 is GC-rich, and we found that a mutagenesis protocol that included dimethyl sulfoxide was needed. The QuikChange II XL Site-Directed Mutagenesis Kit was used to generate the Cys166Ala, Cys174Ala, and Cys178Ala mutants. For the Cys166Ala, reaction 50 ng of WT pBAD-UvrC plasmid was used; for the Cys174Ala and Cys178Ala reactions, 10 ng of plasmid was used. 125 ng of each primer was used for all reactions. Temperature cycling was as follows: 1. 30 seconds at 95 °C; 2. 16 cycles of 30 seconds at 95 °C, 1 minute at 60 °C, and 10 minutes 68 °C; 3. a final extension according to the manufacturer's instructions. Once the amplification was complete, 10 U of Dpn I was added to the reaction mixture, then incubated for 2 hours at 37°C. Subsequent steps were completed as instructed by Qiagen. Plasmids were transformed and sequenced as above.

4.2.3 Induction Trials

Induction trials were completed as described in Chapter 2.

4.2.4 Overexpression and Purification of UvrC

Overexpression and purification was completed aerobically as described in Chapter 2.

4.2.5 Overexpression and Purification of Cys→Ala Mutants

Overexpression and purification was completed as described in Chapter 2. Purification was completed aerobically for all mutants and once anaerobically for Cys154Ala, as described in the methods Chapter 2 and Chapter 3, respectively.

4.2.6 Generation of Apo Protein During Aerobic Incubation

UvrC was incubated at concentrations between 15 and 20 μM in aerobic UvrC buffer (25 mM Tris-HCl, 0.5 M KCl, 20% v/v glycerol) at 37 °C that was either supplemented with DTT (at a concentration 100x of the cluster) during heating, treated with DTT after heating (at a concentration 1000x of the cluster), or supplemented with 0.05 % (v/v) Tween® 20 during heating. Products from heating were resolved on a Superdex 200 column in UvrC buffer, UvrC buffer containing 1 mM of DTT, or UvrC buffer containing 05 % (v/v) Tween® 20.

4.3 RESULTS AND DISCUSSION

4.3.1 Mutation of Coordinating Cysteines Leads to Destabilization of UvrC

To explore the site of coordination, we generated Cys→Ala mutations of the cysteine residues that are highly conserved at positions Cys154, Cys166, Cys174, and Cys178. Sequencing data confirmed that the intended mutations had been made on the UvrC expression vector (**Figure 4.1**). We found that the Cys154Ala and Cys166Ala mutants overexpress similarly to WT UvrC. In contrast, expression of the Cys174Ala and Cys178Ala mutants were not detectable in whole cell lysate (**Figure 4.2**, Top Right). The Cys154Ala and Cys166Ala mutants were purified aerobically (during the same time period that the experiments in Chapter 2 were completed), and the chromatograms from the size exclusion column are shown in **Figure 4.2**. Both Cys154Ala and Cys166Ala mutants eluted in the void volume as aggregates and were colorless. Once the anaerobic expression and purification system in Chapter 3 had been developed, attempts were made to purify Cys154Ala anaerobically; aggregation was also seen (data not shown). Attempts were also made to isolate any amount of the Cys174Ala and Cys178Ala mutants, but none could be harvested (data not shown).

For future studies, the position and type of mutation (alanine, serine, etc.) will likely require optimization, as expression of the Cys174Ala and Cys178Ala mutants were severely compromised while the Cys154Ala and Cys166Ala mutants aggregated. Purification of mutants may also require additional optimization, perhaps with the addition of reducing agents or detergents to assist in solubilizing the aggregates. Expression in the presence of UvrA and/or UvrB for stabilization may also aid in downstream isolation. Examination of other regulatory aspects of the cysteines ligating the [4Fe4S] cluster of UvrC will be fascinating to investigate, especially with regard to protein stability, subunit assembly, and enzymatic activity on damaged DNA substrates.

Figure 4.1 Sequencing data for the Cys→Ala mutants. The sequence of UvrC is shown aligned to sequencing data obtained from Laragen. The sequences were aligned using Blast®n.

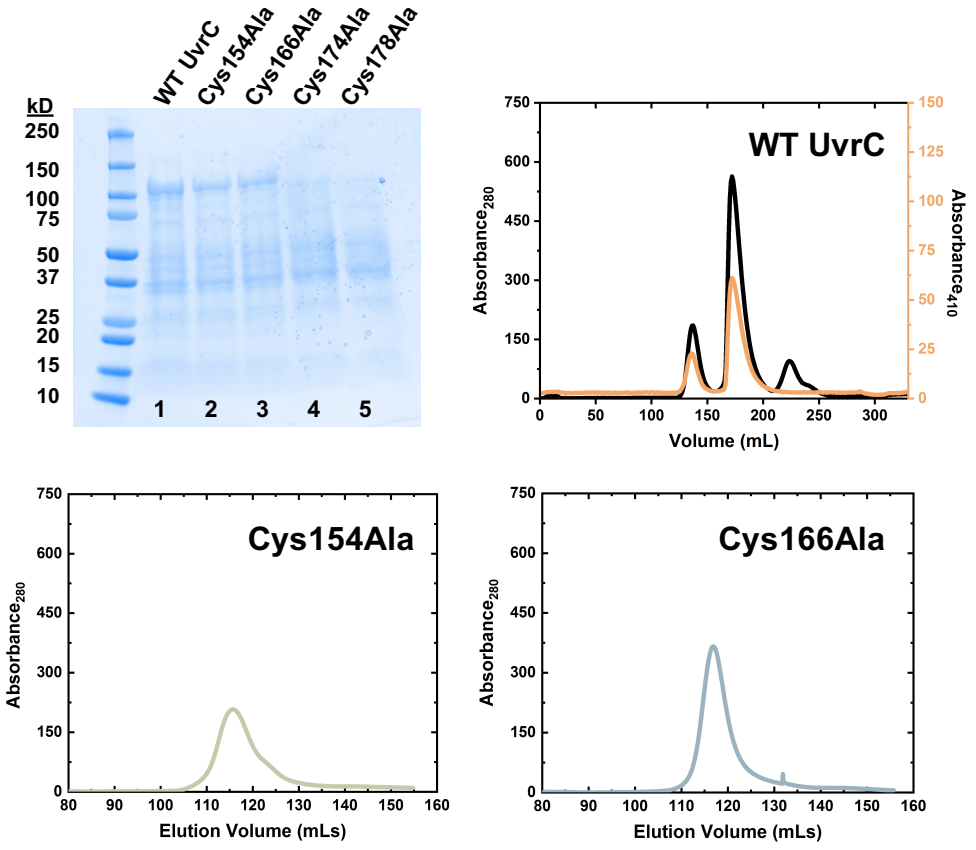

Figure 4.2 Expression and purification of Cys→Ala mutants of UvrC. (*Top Left*) The expression of Cys→Ala mutants was assessed by resolving whole cell lysate by SDS-PAGE. (*Top Right, Bottom Left, Bottom Right*) The purification chromatograms for WT UvrC, Cys154Ala, and Cys166Ala from the size exclusion column are shown.

4.3.2 Apo Species of UvrC Are Not Readily Solubilized

Since mutating coordinating cysteine residues did not readily provide a means to isolate soluble apo-UvrC, we briefly explored methods to generate soluble apo-UvrC following oxidative degradation. We have established that aggregation of apo-UvrC species occurs following degradation of the [4Fe4S] cofactor in aerobic conditions, and it is possible that the aggregates are formed through disulfide bonds and/or through association between hydrophobic surfaces that become exposed upon degradation of the cofactor. To test these possibilities, we first incubated UvrC at 37 ° in the presence of DTT (in 100x excess of the cluster) and used a Superdex 200 column to analyze the apo protein. We found that while DTT slowed the aerobic degradation of the [4Fe4S] cluster (not shown), incubation with DTT did not prevent aggregation (**Figure 4.3**, Left). All protein eluted at the void volume. Addition of a 1000-fold excess of DTT following aerobic incubation also did not result in solubilizing the aggregate (**Figure 4.3**, Middle). Similarly, aerobic incubation in mild detergent also did not yield soluble apo-UvrC (**Figure 4.3**, Right). Our initial work here further highlights how important the cluster is for UvrC stability and how investigations of apo-UvrC will need additional development. Future work may require other methods for removing the cofactor, such as use of other reducing agents, reducing agents in combination with detergents, chelators, or denaturing and refolding in order to remove the cofactor while preserving the solubility of UvrC.

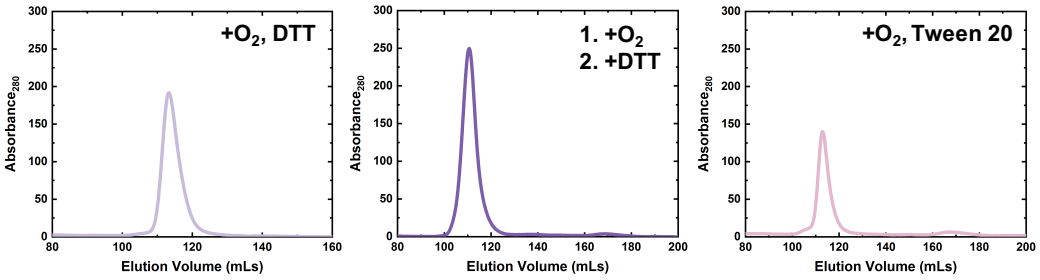

Figure 4.3 Incubation of apo-UvrC with DTT and Tween 20. Aerobic incubation with DTT (*Left*), DTT treatment after aerobic incubation (*Middle*), and aerobic incubation with Tween 20 (*Right*) are shown.

4.4 CONCLUSIONS

Overall, our observations support the assignment of Cys154, Cys166, Cys174, and Cys178 as coordinating residues. Understanding of the [4Fe4S] cofactor may

benefit from investigations of the other more moderately-conserved cysteine residues at positions 265, 398, and 413. However, because the sequences around these cysteines were not suggestive of a [4Fe4S] binding domain, they have not been an immediate focus. Understanding the role of the UvrC-bound [4Fe4S] cofactor in bacterial NER will benefit, however, from additional studies with solubilized cysteine mutants and/or solubilized apo protein. It will be particularly important to understand how the holoenzyme compares in function to the species of UvrC that has been previously studied in the literature. Other opportunities to reexamine the NER pathway and explore additional functionalities of the [4Fe4S] cluster have also emerged with the discovery that UvrC is a metalloprotein. One major area to revisit concerns the protein-protein interactions involved in facilitating formation of UvrABC protein complex(es). Direct comparison of holo and apo-UvrC would allow for determination of how the integrity of the cofactor may contribute to assembly of the full bacterial NER complex and activity on damaged substrates. Until now, UvrC has eluded understanding, and there are many new opportunities to study UvrC and the bacterial NER pathway anew in the context of the [4Fe4S] cofactor, which we predict will continue to lead to key insights for UvrC.

4.5 ACKNOWLEDGEMENTS

We thank two undergraduate researchers, Jianing (Jenny) He and Sirus K. Han, who assisted with studies of mutant proteins while they were students at Caltech. J.H. assisted in constructing the plasmids, and SKH assisted with aerobic purification of the mutants.

References

[1] A. R. Arnold, M. A. Grodick, and J. K. Barton. DNA Charge Transport: From Chemical Principles to the Cell. *Cell Chemical Biology*, 23(1):183–197, 2016. ISSN 24519448. doi: 10.1016/j.chembiol.2015.11.010. URL http://dx.doi.org/10.1016/j.chembiol.2015.11.010.

[2] P. L. Bartels, E. O'Brien, and J. K. Barton. DNA signaling by iron-sulfur cluster proteins. In T. A. Rouault, editor, *Biochemistry, Biosynthesis and Human Diseases: Biochemistry, Biosynthesis, and Human Diseases*, volume 2, pages 405–423. De Gruyter, Berlin, Boston, 2017. ISBN 9783110479850. doi: 10.1515/9783110479850-015.

[3] J. B. Broderick, B. R. Duffus, K. S. Duschene, and E. M. Shepard. Radical S-adenosylmethionine enzymes. *Chemical Reviews*, 114(8):4229–4317, 2014. ISSN 15206890. doi: 10.1021/cr4004709.

[4] N. R. Coordinators. Database resources of the National Center for Biotechnology Information. *Nucleic Acids Research*, 44 (D1):D7–D19, Jan 2016. ISSN 1362-4962. doi: 10.1093/nar/gkv1290. URL https://pubmed.ncbi.nlm.nih.gov/26615191https://www.ncbi.nlm.nih.gov/pmc/articles/PMC4702911/.

[5] J. C. Crack, J. Green, A. J. Thomson, and N. E. Brun. Iron-sulfur clusters as biological sensors: The chemistry of reactions with molecular oxygen and nitric oxide. *Accounts of Chemical Research*, 47(10):3196–3205, 2014. ISSN 15204898. doi: 10.1021/ar5002507.

[6] L. M. Engstrom, O. A. Partington, and S. S. David. An iron-sulfur cluster loop motif in the archaeoglobus fulgidus uracil-DNA glycosylase mediates efficient uracil recognition and removal. *Biochemistry*, 51(25):5187–5197, 2012. ISSN 00062960. doi: 10.1021/bi3000462.

[7] S. A. Freibert, B. D. Weiler, E. Bill, A. J. Pierik, U. Mühlenhoff, and R. Lill. Biochemical Reconstitution and Spectroscopic Analysis of Iron–Sulfur Proteins. *Methods in Enzymology*, 599:197–226, 2018. ISSN 15577988. doi: 10.1016/bs.mie.2017.11.034.

[8] W. Fu, S. O'Handley, R. P. Cunningham, and M. K. Johnson. The role of the iron-sulfur cluster in Escherichia coli endonuclease III. A resonance Raman study. *Journal of Biological Chemistry*, 267(23):16135–16137, 1992. ISSN 00219258.

[9] J. O. Fuss, C. L. Tsai, J. P. Ishida, and J. A. Tainer. Emerging critical roles of Fe-S clusters in DNA replication and repair. *Biochimica et Biophysica Acta - Molecular Cell Research*, 1853(6):1253–1271, 2015. ISSN 18792596. doi: 10.1016/j.bbamcr.2015.01.018. URL http://dx.doi.org/10.1016/j.bbamcr.2015.01.018.

[10] M. P. Golinelli, N. H. Chmiel, and S. S. David. Site-directed mutagenesis of the cysteine ligands to the [4Fe-4S] cluster of Escherichia coli MutY. *Biochemistry*, 38(22):6997–7007, jun 1999. ISSN 00062960. doi: 10.1021/bi982300n. URL https://doi.org/10.1021/bi982300n.

[11] D. Graf, J. Wesslowski, H. Ma, P. Scheerer, N. Krauß, I. Oberpichler, F. Zhang, and T. Lamparter. Key amino acids in the bacterial (6-4) photolyase PhrB from Agrobacterium fabrum. *PLoS ONE*, 10(10):e0140955, 2015. ISSN 19326203. doi: 10.1371/journal.pone.0140955.

[12] J. A. Imlay. Transcription Factors That Defend Bacteria Against Reactive Oxygen Species. *Annual Review of Microbiology*, 69(1):93–108, 2015. ISSN 0066-4227. doi: 10.1146/annurev-micro-091014-104322.

[13] K. J. McDonnell, J. A. Chemler, P. L. Bartels, E. O'Brien, M. L. Marvin, J. Ortega, R. H. Stern, L. Raskin, G. M. Li, D. H. Sherman, J. K. Barton, and S. B. Gruber. A human MUTYH variant linking colonic polyposis to redox degradation of the [4Fe4S]2+cluster. *Nature Chemistry*, 10(8):873–880, 2018. ISSN 17554349. doi: 10.1038/s41557-018-0068-x. URL https://www.nature.com/articles/s41557-018-0068-x.

[14] T. E. Messick, N. H. Chmiel, M. P. Golinelli, M. R. Langer, L. Joshua-Tor, and S. S. David. Noncysteinyl coordination to the [4Fe-4S]2+ cluster of the DNA repair adenine glycosylase MutY introduced via site-directed mutagenesis. Structural characterization of an unusual histidinyl-coordinated cluster. *Biochemistry*, 41(12):3931–3942, 2002. ISSN 00062960. doi: 10.1021/bi012035x.

[15] E. L. Mettert and P. J. Kiley. Fe-S proteins that regulate gene expression. *Biochimica et Biophysica Acta - Molecular Cell Research*, 1853(6):1284–1293, 2015. ISSN 18792596. doi: 10.1016/j.bbamcr.2014.11.018.

[16] D. J. A. Netz, C. M. Stith, M. Stümpfig, G. Köpf, D. Vogel, H. M. Genau, J. L. Stodola, R. Lill, P. M. J. Burgers, and A. J. Pierik. Eukaryotic DNA polymerases require an iron-sulfur cluster for the formation of active complexes. *Nature Chemical Biology*, 8(1):125–132, 2012. ISSN 1552-4450. doi: 10.1038/nchembio.721. URL http://www.nature.com/doifinder/10.1038/nchembio.721.

[17] K. Nishio and M. Nakai. Transfer of iron-sulfur cluster from NifU to apoferredoxin. *Journal of Biological Chemistry*, 275(30):22615–22618, 2000. ISSN 00219258. doi: 10.1074/jbc.C000279200.

[18] M. T. Pellicer Martinez, A. B. Martinez, J. C. Crack, J. D. Holmes, D. A. Svistunenko, A. W. B. Johnston, M. R. Cheesman, J. D. Todd, and N. E. Le Brun. Sensing iron availability via the fragile [4Fe–4S] cluster of the bacterial transcriptional repressor RirA. *Chemical Science*, 8(12):8451–8463,

2017. doi: 10.1039/C7SC02801F. URL http://dx.doi.org/10.1039/C7SC02801F.

[19] S. Pokharel and J. L. Campbell. Cross talk between the nuclease and helicase activities of Dna2: Role of an essential iron-sulfur cluster domain. *Nucleic Acids Research*, 40(16):7821–7830, 2012. ISSN 03051048. doi: 10.1093/nar/gks534.

[20] S. L. Porello, S. D. Williams, H. Kuhn, M. L. Michaels, and S. S. David. Specific recognition of substrate analogs by the DNA mismatch repair enzyme MutY. *Journal of the American Chemical Society*, 118(44):10684–10692, 1996. ISSN 00027863. doi: 10.1021/ja9602206.

[21] S. Rajagopalan, S. J. Teter, P. H. Zwart, R. G. Brennan, K. J. Phillips, and P. J. Kiley. Studies of IscR reveal a unique mechanism for metal-dependent regulation of DNA binding specificity. *Nature Structural and Molecular Biology*, 20(6):740–747, 2013. ISSN 15459993. doi: 10.1038/nsmb.2568.

[22] F. Reinhart, S. Achebach, T. Koch, and G. Unden. Reduced apo-fumarate nitrate reductase regulator (ApoFNR) as the major form of FNR in aerobically growing Escherichia coli. *Journal of Bacteriology*, 190(3):879–886, 2008. ISSN 00219193. doi: 10.1128/JB.01374-07.

[23] B. Ren, X. Duan, and H. Ding. Redox control of the DNA damage-inducible protein DinG helicase activity via its iron-sulfur cluster. *Journal of Biological Chemistry*, 284(8):4829, 2009. ISSN 00219258. doi: 10.1074/jbc.M807943200.

[24] T. A. Rouault. Iron-sulfur proteins hiding in plain sight. *Nature Chemical Biology*, 11(7):442–445, 2015. ISSN 15524469. doi: 10.1038/nchembio.1843.

[25] J. Rudolf, V. Makrantoni, W. J. Ingledew, M. J. R. Stark, and M. F. White. The DNA Repair Helicases XPD and FancJ Have Essential Iron-Sulfur Domains. *Molecular Cell*, 23(6):801–808, 2006. ISSN 10972765. doi: 10.1016/j.molcel.2006.07.019.

[26] J. ter Beek, V. Parkash, G. O. Bylund, P. Osterman, A. E. Sauer-Eriksson, and E. Johansson. Structural evidence for an essential Fe–S cluster in the catalytic core domain of DNA polymerase ϵ. *Nucleic Acids Research*, 47(11):5712–5722, Apr 2019. ISSN 0305-1048. doi: 10.1093/nar/gkz248. URL https://doi.org/10.1093/nar/gkz248.

[27] D. C. Thomas, M. Levy, and A. Sancar. Amplification and purification of UvrA, UvrB, and UvrC proteins of Escherichia coli. *Journal of Biological Chemistry*, 260(17):9875–9883, 1985. ISSN 00219258.

[28] J. L. Vey and C. L. Drennan. Structural insights into radical generation by the radical SAM superfamily. *Chemical Reviews*, 111(4):2487–2506, 2011. ISSN 00092665. doi: 10.1021/cr9002616.

[29] J. N. Vranish, W. K. Russell, L. E. Yu, R. M. Cox, D. H. Russell, and D. P. Barondeau. Fluorescent probes for tracking the transfer of iron-sulfur cluster and other metal cofactors in biosynthetic reaction pathways. *Journal of the American Chemical Society*, 137(1):390–398, 2015. ISSN 15205126. doi: 10.1021/ja510998s.

[30] B. E. Weiner, H. Huang, B. M. Dattilo, M. J. Nilges, E. Fanning, and W. J. Chazin. An iron-sulfur cluster in the C-terminal domain of the p58 subunit of human DNA primase. *Journal of Biological Chemistry*, 282(46):33444–33451, 2007. ISSN 00219258. doi: 10.1074/jbc.M705826200.

[31] J. T. P. Yeeles, R. Cammack, and M. S. Dillingham. An iron-sulfur cluster is essential for the binding of broken DNA by AddAB-type helicase-nucleases. *Journal of Biological Chemistry*, 284(12):7746–7755, 2009. ISSN 00219258. doi: 10.1074/jbc.M808526200.

Chapter 5

SUMMARY AND PERSPECTIVE

DNA repair and replication proteins that coordinate [4Fe4S] cofactors continue to offer rich areas for investigation, particularly regarding the roles of the metal cofactor. Seventeen years after the first protein-bound [4Fe4S] cluster was found associated with a repair glycosylase, SF2 helicases were the next family of repair proteins discovered to bind a [4Fe4S] center. Soon after, eukaryotic primases, helicase-nucleases, iron-sulfur bacterial cryptochromes and photolyases, eukaryotic B family polymerases, and the Cas4 exonuclease (part of CRISPR/Cas bacterial innate immunity) were all reported to coordinate a [4Fe4S] cluster. We and others expect that many more proteins involved in DNA transactions will continue to be discovered with iron sulfur cofactors, especially in light of more recent reports that have highlighted how some of these proteins require use of air-free techniques in order to isolate highly pure samples with intact metal centers. Continued collaboration with computational biologists in detecting unusual patterns in coordinating residues and in other motifs recognized by iron sulfur cluster biogenesis machinery will likely facilitate the acceleration of the discovery process. The multifunctional roles the [4Fe4S] cofactors occupy in contributing to protein or complex stability, substrate interactions, participating in redox signaling, and responding to changing cellular environments, requires considerably more attention and multidisciplinary investigation.

Through our work with UvrC, a repair enzyme in the Bacteria domain, we most recently have demonstrated that excision nucleases are also [4Fe4S] proteins. Our work began first with piecing together observations made separately in the literature of a cysteine-rich region at the N-terminus of UvrC and genetics assays in *E. coli* with another [4Fe4S] repair enzyme, DinG, that suggested redox signaling with nucleotide excision repair. In our early work with UvrC from *E. coli*, we screened new overexpression vectors and were able to isolate yellow protein with spectroscopic and redox properties supportive of the prediction that UvrC coordinated a [4Fe4S] cluster. Over time however, it became apparent that the cofactor degraded under aerobic conditions, which was a novel finding for a [4Fe4S] repair enzyme from *E. coli*.

After adapting anaerobic purification methods for nitrogenase, we were able to isolate UvrC with 60-70% cofactor incorporation. The [4Fe4S] cofactor is stable at room temperature in an anaerobic environment over the duration of purification and in subsequence experiments, but undergoes degradation in the presence of O_2 which results in formation of aggregated species. Mutation of coordinating cysteines - C154, C166, C174, and C178 - to alanine further demonstrated that UvrC is stabilized by the [4Fe4S] cofactor. In its holo form, UvrC also forms complexes with both well-matched and damaged duplex substrates independently of UvrA and UvrB and participates in DNA charge transport chemistry (DNA CT). Though UvrC independently associates with DNA duplexes, UvrC was not found to exhibit independent enzymatic activity on the damaged lesion under the conditions tested.

The discovery that UvrC coordinates a [4Fe4S] cofactor has also raised entirely new and important questions regarding the role of the protein in the cell. Another excision nuclease, Cho, a smaller protein that is homologous to the N-terminal region of UvrC, likely also coordinates a [4Fe4S] cofactor based on sequence similarity. Continued examination of UvrC (and perhaps Cho) in holo form both biochemically and structurally, along with UvrA and UvrB, will undoubtedly be important for elucidating the dynamics of complex assembly and activity on damaged substrates. Given how distinct our observations are for holo-UvrC from those in the literature, it is possible that holo-UvrC and apo-UvrC occupy completely different functionalities in the cell. The specificity of the UvrC-bound [4Fe4S] cofactor for reactivity with O_2, alone and in complex with UvrAB, and the degradation product(s) that form remains to be determined. There are some initial reports that the [4Fe4S] centers in repair proteins from *E. coli* can indeed be modified by ROS or RNS, affecting protein function. More extensive studies are needed with UvrC to establish if such reactivity could have a regulatory role related to cellular stress responses. Careful examination of the interplay between the integrity of the [4Fe4S] center and the stability of UvrC, UvrABC complex assembly, activity, and cellular recovery and growth will facilitate entirely new research directions on how the UvrABCD system acts in a large network of pathways that utilize the chemistry of [4Fe4S] cofactors to maintain and proliferate genomes.